

**"FINE-SGRAFFITO WARE", "AEGEAN WARE"
FROM ANAIA: AN ANALYTICAL APPROACH**

Meral BUDAK ÜNALER

**İzmir Institute of Technology
July, 2013**

**"FINE-SGRAFFITO WARE", "AEGEAN WARE"
FROM ANAIA: AN ANALYTICAL APPROACH**

**A Thesis Submitted to
the Graduate School of Engineering and Sciences of
İzmir Institute of Technology
in Partial Fulfillment of the Requirements for the Degree of**

**DOCTOR OF PHILOSOPHY
in Mechanical Engineering**

**by
Meral BUDAK ÜNALER**

**July 2013
İZMİR**

We approve the thesis of **Meral BUDAK ÜNALER**

Examining Committee Members:

Prof. Dr. Sedat AKKURT

Department of Mechanical Engineering, İzmir Institute of Technology

Prof. Dr. Metin TANOĞLU

Department of Mechanical Engineering, İzmir Institute of Technology

Assoc. Prof. Dr. Lale DOĞER

Department of History of Arts, Ege University

Prof. Dr. Mümtaz ÇOLAK

Department of Geology Engineering, Dokuz Eylül University

Assist. Prof. Dr. Engin ÖZÇİVİCİ

Department of Mechanical Engineering, İzmir Institute of Technology

11 July 2013

Prof. Dr. Sedat AKKURT

Supervisor, Department of Mechanical Engineering
İzmir Institute of Technology

Prof. Dr. Metin TANOĞLU
Head of the Department of
Mechanical Engineering

Prof. Dr. R. Tuğrul SENGER
Dean of the Graduate School of
Engineering and Sciences

ACKNOWLEDGMENTS

I would like to thank to my advisor, Prof. Dr. Sedat Akkurt for his support throughout the dissertation. His friendly manners and guidance are greatly appreciated. I would like to thank to Assoc.Prof.Dr.Lale Doęer about her polite and patient helps during this thesis. I would like to thank to Prof.Dr. Metin Tanoęlu for his guidance. I would like to thank to Prof.Dr. Zeynep Mercangöz for providing the archaeological samples. I would like to thank to Dr. Pavlos Koulouridakis for his technical support.

I would like to thank to workers of IZTECH Materials Research Center (IYTE-MAM) ; Mine Bahęeci, Duygu Oęuz Kılıę, Gökhan Erdoęan, Zehra Sinem Hortooęlu and Canan Güney for their kind and patient helps in the XRF, XRD and SEM analyses.

I would like to thank to my husband for his support, encouragement and patience during this work. Finally I would like to express my special thanks to my father, mother, sister, brother and Ilgın Tunęay for their constant encouragement, patience and support during this thesis.

ABSTRACT

“FINE-SGRAFFITO WARE”, “AEGEAN WARE” FROM ANAIA: AN ANALYTICAL APPROACH

Excavation in Byzantine castle, known as Kuşadası Kadıkalesi, Anaia provided ceramic finds which dates back to mid 12th and 13th century of Mid Byzantine period. These finds were produced as serial products. In first part of the thesis 47 samples with four different decoration repertoire; Fine Sgraffito, Incised-Sgraffito, Incised and Champlévé, were analyzed by Scanning Electron Microscope (SEM-EDX), X-Ray Diffraction (XRD) and X-Ray Fluorescence (XRF) methods, in order to identify the three distinct layers in cross sections: body, slip and glaze layers. Body was largely composed of SiO₂, Al₂O₃, CaO, Fe₂O₃, Na₂O and K₂O along with other less abundant elements. Slip had similar chemistry but with less Fe₂O₃. The glaze was composed mainly of lead oxide. Between the glaze and the slip some new well formed crystals of lead feldspar were found to precipitate in dimensions of roughly 10-50 µm. Statistical analysis tools like Hierarchical Clustering Analysis (HCA) and Principal Component Analysis (PCA) were used to see if any groupings were possible between the samples collected. Dendrograms indicated that these ceramics were made of two different types of clay. In second part of the thesis, replicate samples of earthenware pottery were manufactured in the laboratory to mimic the formation of the glazed pottery. Similar microstructural features were identified. Another HCA study was done to compare the Anaia samples with the literature. Dendrograms obtained showed some similarity. However, it was not possible to strongly and conclusively say that the two sample groups were related.

ÖZET

ANAIA'DAN "İNCE-SGRAFFİTO KAPLAR", "EGE KAPLARI": ANALİTİK BİR YAKLAŞIM

Kuşadası Kadıkalesi Anaia adı ile bilinen Bizans kalesinde yürütülen kazı çalışmasında Orta Bizans döneminin 12. yy ortası ile 13. yy aralığına tarihlendirilen seramik buluntuları ele geçmiştir. Tezin ilk kısmında İnce Sgraffito, Kazıma Sgraffito, Kazıma ve Champlevé teknikleri kullanılarak bezenmiş 47 seramik buluntunun Taramalı Elektron Mikroskobu (SEM-EDX), X-Işını Kırınımı (XRD), X-Işını Flöresansı (XRF) yöntemleri kullanılarak, kesitlerinde yer alan bünye, astar ve sır tabakaları karakterize edilmiştir. Bünye tabakası diğer elementlerle birlikte genel olarak SiO_2 , Al_2O_3 , CaO , Fe_2O_3 , Na_2O and K_2O içermektedir. Astar tabakası, bünye ile aynı kimyasal yapıya sahip olmakla birlikte daha az oranda demir içermektedir. Sır tabakası ise genel olarak yüksek oranda PbO içermektedir. Sır ve astar tabakaları arasında kabaca 10-50 μm boyutlarında kurşun feldispat kristalleri oluşmuşlardır. Buluntular Temel Bileşen Analizi (PCA) ve Hiyerarşik Kümeleme Analizi (HCA) yöntemleri kullanılarak sınıflandırılmışlardır. Sonuçlar bu seramiklerin iki farklı tip kil kullanılarak üretildiğini göstermiştir. Tezin ikinci kısmında sırlı seramik buluntuların benzerleri laboratuvar ortamında üretilmiştir. Üretilen örneklerde benzer mikroyapısal özellikler tespit edilmiştir. Anaia'dan ele geçen seramik buluntular ayrıca literatürdeki diğer örnekler ile Hiyerarşik Kümeleme Analizi (HCA) kullanılarak karşılaştırılmışlardır. Sonuçlara göre örnekler benzerlik göstermektedir, fakat kesin olarak birbirleriyle ilintili olduklarını söylemek mümkün değildir.

TABLE OF CONTENTS

LIST OF FIGURES	viii
LIST OF TABLES	ix
CHAPTER 1. INTRODUCTION	1
1.1. Background	1
1.2. Objectives.....	2
CHAPTER 2. LITERATURE REVIEW	3
2.1. Kuşadası Kadıkalesi/Anaia	3
2.2. History of Ceramics	4
2.3. Theory of Ceramics.....	5
2.4. Production Technology of Ceramics.....	9
2.4.1. Preparation of Ceramic Materials	9
2.4.2. Forming Techniques.....	11
2.4.3. Clay Drying	12
2.4.4. Conditions of Firing	13
2.4.5. Reactions During Firing.....	14
2.4.6. Firing Kilns	16
2.4.7. Surface Treatment	18
2.4.7.1. Slip	18
2.4.7.2. Glaze	19
2.5. Final Product Properties.....	23
2.6. Byzantine Ceramics	25
CHAPTER 3. MATERIALS AND METHODS	31
3.1. Archaeological Samples.....	31
3.1.1. Groups and Subgroups	32
3.1.2. Properties of Groups and Subgroups	45
3.2. Characterization Methods of Samples	46
3.3. Statistical Analysis of Samples	47

3.3.1. Hierarchical Cluster Analysis (HCA)	47
3.3.2. Principal Component Analysis (PCA)	52
CHAPTER 4. CHARACTERIZATION OF ARCHAEOLOGICAL SAMPLES	56
4.1. Optical Microscopy Analysis	56
4.2. X-Ray Diffraction (XRD) Analysis	65
4.3. Scanning Electron Microscope (SEM-EDX) Analysis	69
4.4. X-Ray Fluorescence (XRF) Analysis	94
4.5. Statistical Analysis	98
4.6. Archaeological and Stylistic Evaluation of Dendrograms	110
4.6.1. General Estimation of Dendrogram	115
4.6.2. General Archaeological Conclusion.....	117
4.6.3. Comparison of Anaia Samples with Archaeological Samples.....	118
4.6.4. General Interpretation and Discussion	123
CHAPTER 5. PRODUCTION AND CHARACTERIZATION OF REPLICATE SAMPLES	124
5.1. Production and Characterization of Replicate Samples with Clay Body ..	124
5.2. Production and Characterization of Replicate Samples with SiO ₂ Body ..	146
CHAPTER 6. GENERAL INTERPRETATION and DISCUSSION	150
CHAPTER 7. CONCLUSIONS	154
REFERENCES	155

LIST OF FIGURES

<u>Figure</u>	<u>Page</u>
Figure 2.1. Photograph of Kadikalesi/Anaia.....	3
Figure 2.2. Scanning electron microscope (SEM) image of kaolinite.....	7
Figure 2.3. Flowchart for raw material preparation	11
Figure 2.4. Moisture content effect on shrinkage and volume.....	12
Figure 2.5. Chart showing the reactions during firing process	14
Figure 2.6. Open Fire	16
Figure 2.7. Pit Kiln.....	17
Figure 2.8. Historical Closed Kiln	17
Figure 2.9. Deflocculant effect on viscosity	22
Figure 2.10. Microstructure of an typical ceramic.....	23
Figure 2.11. Fine Sgraffito ware	27
Figure 2.12. Incised-Sgraffito ware	27
Figure 2.13. Champlevé Ware	28
Figure 3.1. Intercluster distance for single, average and complete linkage.....	48
Figure 3.2. Group average clustering.....	51
Figure 3.3. Geometrical representation of principal component correlation	54
Figure 4.1. XRD pattern of sample 1.1.13	65
Figure 4.2. Body glaze comparison plot calculated with Equation 4.1	90
Figure 4.3. Scanning electron microscope (SEM) images of sample 1.5.1	91
Figure 4.4. EDX analysis of sample 1.5.1 depending on depth.....	93
Figure 4.5. A: PbO-Al ₂ O ₃ -SiO ₂ phase diagram (Temperatures in Kelvin); B: Anaia samples ternary diagram (showing the glaze composition).....	94
Figure 4.6. Grouping of samples according to body composition (determined by XRF method)	100
Figure 4.7. Grouping of samples according to slip composition (determined by EDX method).....	102
Figure 4.8. Grouping of samples according to glaze composition (determined by EDX method).....	104

Figure 4.9. Plot of first two principal components obtained PCA of chemical data of body layer obtained by XRF method. Statistical ellipses with 95% confidence level	105
Figure 4.10. Loading Plots of body layer, showing the effect of oxides on PC1 and PC2 values	106
Figure 4.11. Plot of first two principal components obtained PCA of chemical data of slip layer obtained by EDX method. Statistical ellipses with 95% confidence level	107
Figure 4.12. Loading plots of slip layer, showing the effect of oxides on PC1 and PC2 values	108
Figure 4.13. Plot of first two principal components obtained PCA of chemical data of glaze layer obtained by EDX method. Statistical ellipses with 95% confidence level	109
Figure 4.14. Loading plots of glaze layer, showing the effect of oxides on PC1 and PC2 values	110
Figure 4.15. Comparison of fine sgraffito decorated Anaia and Byzantine samples ..	121
Figure 4.16. Comparison of incised decorated Anaia samples with incised-sgraffito decorated Byzantine samples	122
Figure 4.17. Comparison of champlévé decorated Anaia and Byzantine samples	122
Figure 5.1. Plaster mold (a) and produced samples (b)	125
Figure 5.2. Crystals obtained at interface of S13 sample body and glaze part	144
Figure 5.3. SEM analysis results of sample at different magnifications.....	147
Figure 5.4. Line EDX analysis result of sample from glaze part(top) to body part(bottom)	147
Figure 5.5. Mapping analysis results of sample heat treated at 1600°C	148
Figure 5.6. Chemical compositions of crystal determined by EDX analysis	149

LIST OF TABLES

<u>Table</u>	<u>Page</u>
Table 2.1. Composition of body and slip parts of pottery sample characterized by EDX method	18
Table 3.1. Photographs of Group 1. Type 1 (scale bar is 5 cm)	32
Table 3.2. Photographs of Group 1. Type 2	35
Table 3.3. Photographs of Group 1. Type 3	36
Table 3.4. Photographs of Group 1. Type 4	38
Table 3.5. Photographs of Group 1. Type 5	39
Table 3.6. Photographs of Group 1. Type 6	39
Table 3.7. Photographs of Group 2	40
Table 3.8. Photographs of Group 3.....	41
Table 4.1. Optical microscopy images of samples	56
Table 4.2. Thicknesses of slip and glaze layers	64
Table 4.3. Mineralogical compositions and estimated firing temperatures of the samples	66
Table 4.4. SEM analysis results of samples (for 200X and 2500X magnifications)	69
Table 4.5. Chemical composition of the body layer of the samples determined by EDX method	83
Table 4.6. Chemical composition of the slip layer of the samples determined by EDX method	85
Table 4.7. Chemical composition of the glaze part of the samples determined by EDX method	87
Table 4.8. EDX analysis results of crystals (A and B) and glaze part (C)	92
Table 4.9. XRF Analysis results of body parts of samples. Major and minor elements are expressed in weight percent of oxides, trace elements in ppm	96
Table 4.10. Codes, decoration types and sources of Byzantine samples.....	118
Table 4.11. Codes and decoration types of Anaia samples	119
Table 4.12. Chemical composition of the samples as determined by WD-XRF method (Waksman and Wartburg 2006). Major and minor elements	

	are given in weight percent of oxides, trace elements are given in ppm.	120
Table 5.1.	Composition of Clay (Menemen) determined by XRF method	125
Table 5.2.	Amounts of oxides used in preparation of glaze layer	126
Table 5.3.	Photographs of samples	126
Table 5.4.	Amounts of oxides used in preparation of glaze layer	128
Table 5.5.	Photographs of samples	129
Table 5.6.	Chemical composition of Clay (K-244) determined by XRF method	131
Table 5.7.	Codes, contents and heat treatment procedures of samples.....	132
Table 5.8.	Photographs of produced samples	133
Table 5.9.	SEM analysis results of samples glazed with PbO	135
Table 5.10.	EDX analysis results of samples glazed with PbO	138
Table 5.11.	SEM analysis results of samples glazed with PbO+SiO ₂ (PbO:SiO ₂ , 9:1).....	140
Table 5.12.	EDX analysis results of samples glazed with PbO+SiO ₂ (PbO:SiO ₂ , 9:1)	140
Table 5.13.	SEM analysis results of samples glazed with PbO+Clay(K-244) (PbO:Clay, 9:1).....	141
Table 5.14.	EDX analysis results of samples glazed with PbO+Clay(K-244) (PbO:Clay).....	143
Table 5.15.	EDX analysis of results of spectrums.....	145
Table 5.16.	Formula of the crystals obtained at interface.....	146

CHAPTER 1

INTRODUCTION

1.1. Background

The term archaeology is generally used for a special part of the historic sciences. Archaeology tries to reconstruct the culture and history of past societies, especially of those on which no or poor written sources exist. Archaeology, in its broadest sense, studies a past material culture. In detail it is like a puzzle of very different aspects that is fitted together to a picture of the past. Archaeology today uses a whole variety of methods and tools such as survey and excavation, environmental analysis with pollen or glacial records, paleobotany and paleozoology, scientific and historical dating methods, historic and iconographic sources, models that have been developed from sociology and ethnology, archaeological experiments and material analysis of found artefacts. The use of methods borrowed from the natural sciences is nowadays subsumed under the term archaeometry (Gebhard 2003).

Material analysis plays a dominant role in archaeometry. The results will be different according to the application of different methods. The application of only one method is often not enough, and only the application of different methods may result in a detailed view of the objects. Material analysis has two main topics: the characterization of the material of which objects consist, and the characterization of the technical treatment or the manufacturing of the objects. The first provides information about the provenance of the material, while the latter helps to reconstruct ancient techniques. The provenance of an object or its raw material can give information about resources, trade contacts and economic systems. The ancient techniques used in a culture can be a main argument in the discussion of the level of civilization culture. In most cases, highly developed techniques only appear in complex, structured social systems, because experiments and communication between different crafts result in technical progress.

The application of scientific analysis in the second half of the 20th century has brought a new light into archaeology. Today, the material analysis is an integral part of

the archaeological work. The secret of success in such interdisciplinary studies has always been a very close collaboration between the archaeologists and scientists. It is therefore necessary that both be familiar with the principles of the methods used (Gebhard 2003).

1.2. Objectives

This thesis focuses on the characterization of pottery samples collected from Kuşadası Kadıkalesi/Anaia excavation together with production and characterization of replicate samples. Another purpose of this study is to see if raw ceramics can be classified based on their compositions. Statistical tool will be used for this purpose. Data will also be compared with literature.

CHAPTER 2

LITERATURE REVIEW

2.1. Kuşadası Kadıkalesi/Anaia

In the south of Kuşadası, a fortress referred to Kadıkalesi that first appeared on the maps of Kiepert and Philippson in the 19th century has been presenting important archaeological contexts for the history of Western Anatolia with systematic excavations since 2001 (Figure 2.1). Kadıkalesi is located on a proto-historic mound and it protected the harbour of Anaia an ancient town known from historical sources. From the findings, it can be deduced that the fortress not only protected the harbour but it was also used for international trade, as demonstrated by a monastery complex and surrounding tombs with ceramic, glass, metal and jewellery production within its walls. Only a very small part of this large fortress has been excavated but the wide range of findings and their quality provides evidence of a life that was different.



Figure 2.1. Photograph of Kadıkalesi/Anaia
(Source: <http://www.kadikalesianaia.org/kazilar.html>)

2.2. History of Ceramics

The earliest fired ceramic products which have been discovered are the figures from Czechoslovakia, and that dates back 24000 years. Fired clay vessels were first produced about 10000 years ago in the near east. These vessels were fired at relatively low temperatures and they were undecorated. By 6400 B.C pottery making was a well developed craft. The produced wares were coated with clay suspension. Polishing was applied to the surface and resulted in the formation of the less porous and the more attractive surface. Wares were decorated with incised lines. By the applications of pigments, black and red decorations were obtained (Kingery and Vandiver 1986). In Mesopotamia during the Halaf Period at 5500 B.C these techniques were used for production of polychrome wares. Clay suspensions were applied as paint before firing. Red decoration was obtained when the ware was fired in oxidizing atmosphere, black decoration was made by firing in reducing atmosphere (Kingery and Vandiver 1986).

During late fourth and third millennia the use of developed technology was common. Technology was based on controlling the kiln atmosphere during firing. It was perfected on Attic black on-red ware (Kingery and Vandiver 1986).

Quantity production of ceramics began in the 4th millennium B.C in Near East. Extensive use of potter's wheel, fired earthenware molds and specialized ceramic production were widespread (Kingery and Vandiver 1986).

From the early production through Roman times, earthenware in different sizes, shapes and styles was made everywhere. There were periods when the shape was important, others when geometric designs predominated. The first definitely new ceramic body composition, which was evolved in Egypt and Mesopotamia in 4500 B.C., is called Egyptian faience. The objective accomplished by the development of Egyptian faience was the preparation of a white body to serve as a ground for beautiful clear blue. The aim to produce a white ground for colored decoration underlies many of the important technological developments in ceramics. The simplest solution was the application of white clay slip over body as was done in Near East in the 9th and 10th centuries A.D., perhaps in response to the white porcelains that began to be imported from china during T'ang Dynasty (618-906 A.D.) (Kingery and Vandiver 1986).

The first Chinese glazes appeared during later Shang Dynasty (1027-771 B.C). They had high lime content and appreciable quantities of alkali and iron which lowers the melting temperature (Kingery and Vandiver 1986).

Successful glazes became extensively used in the Near East rather later than in China, because of the low firing temperatures on which the technology was based. Alkaline glazes were used on clay bodies beginning about 2300 B.C. Lead-alkali glazes were used on Near Eastern pottery in the beginning of 500 B.C., but lead glazes for vessels did not become widespread until the Roman era (Kingery and Vandiver 1986).

The 9th century A.D Islamic discovery of overglaze painting with metallic lusters on a tin opacified white glaze ground introduced development in nature of pottery decoration. Techniques for production of the opaque white tin glaze as a ground for overpainting, first with luster and then with other enamels spread throughout Spain to Italy, then to all of Europe where “majolica” became dominant form of European luxury pottery (Kingery and Vandiver 1986).

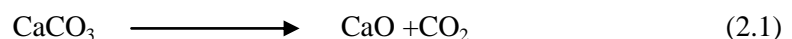
During the 16th and 17th centuries, majolica manufacture, known as faience, was the principal luxury ceramic in Europe. By the early 18th century, Chinese porcelain, Islamic faience and Near Eastern porcelain, were began to be manufactured in Europe. Ceramic developments became part of the chemical and industrial revolutions of the 18th century Europe (Kingery and Vandiver 1986).

2.3. Theory of Ceramics

Ceramic raw materials are composed of mainly clay and the associated materials. Clay helps to obtain plasticity which provides ability to form objects. Clays are classified as primary and secondary clays according to the location from which they are extracted. Primary clays are formed on the place of their parent rocks and are not carried either by wind or water. The deposits of primary clays are coarse grained and nonplastic. Primary clays are relatively pure and free from contamination with nonclay minerals. Most kaolins are primary clays (Rhodes 1973). Secondary clay is a type of clay that is carried from the place of the original parent rock. This type of clay is generally carried by water and wind. Secondary are much more widespread than primary clays. Carriage by water has an important effect on clay. The action of water in streams tends to grind up clay into smaller particle size. When the water of stream

begins to slow down, some of the material which it carries will settle out. The coarser particles settle first, leaving the fine particles suspended in water. When water reaches a lake or sea very small particles of clay sink to the bottom. Carried clays are composed of a variety of materials, such as iron, mica, quartz and other impurities (Rhodes 1973).

Impurities and inclusions in clay body have an important role in drying and firing. Inclusions may be naturally present in clay or may be added by potter as temper. There are three kinds of inclusions: calcium, feldspar and quartz. They have important roles in melting and fusion during firing. The most common and abundant inclusion in most ceramic bodies is quartz (SiO_2). Quartz is the earth's most stable and abundant natural mineral and is composed of SiO_4 tetrahedrons. These tetrahedrons are arranged in a spiral structure. Quartz is an important component of the ceramic body. It has an important role in determination of the structural properties (shrinkage, porosity, strength) of clay bodies. Quartz reduces firing shrinkage. It may also decrease the fired strength due to its alpha beta conversion. Second important category of inclusions in ceramic bodies is feldspar. Feldspar is an alumino-silicate. Calcium, sodium and potassium, are also present in feldspars in differing proportions. These elements are responsible for the division of the feldspars into lime feldspars, soda-lime feldspars and alkali feldspars. Feldspars are used as fluxes. Feldspars have relatively low melting point ($990\text{-}1050^\circ\text{C}$), they are highly viscous on melting and form thick liquid. Their very fine particles enhance their readiness to fuse. Due to these properties, the finely ground feldspars contribute melting. The net result is a dense body with reduced porosity. Owing to the high viscosity of the melt they cool to form a glass. Third important group of minerals in pottery is the calcium. Calcium occurs in various forms of calcium carbonate (CaCO_3), such as calcite, gypsum and limestone. Lime or calcium may occur naturally in clays, these clays are classified as calcareous. Calcium carbonate decomposes around 870°C during firing.



When calcareous clays are fired to 850°C or above and cooled a problem occurs in pottery. CaO is hygroscopic, it absorbs atmospheric moisture, forms quicklime and releases heat. This is accompanied by volume expansion that produces stresses in clay body, causing cracking. This situation is important when the lime particles in clay are very large. Rehydration of the lime reduces the strength of fired ware.

Most of the major clay minerals or mineral groups fall into category of layered silicates or phyllosilicates. The phyllosilicates, as also known as layered silicates, consist of regular ordering of layers of silica and alumina. Differences in the arrangement of these layers and substitution of various cations for the aluminum cause the formation of three major groups. The first group is composed from two-layer clays (kaolinites and halloysites), which have one layer of silica tetrahedrons and one layer of alumina octahedrons in their structure. A second group is composed of three-layer clays (smectites), which have one layer of alumina octahedrons sandwiched between two sheets of silica tetrahedrons in their structure. The third group is the mixed-layer clays (chlorite group), which have alternating layers of different types stacked on top of each other (Rice 1987).

Kaolinite is generally high in alumina which often exists in ratio of two to one with silica. The mineral is described by the idealized formula $\text{Al}_2\text{O}_3 \cdot 2\text{SiO}_2 \cdot 2\text{H}_2\text{O}$ and has an average chemical composition of 39.4% alumina, 46.6 % silica and 13.9 % water (Rice 1987, Velde 1992).

Kaolinite particles usually formed from flat hexagonal plates of moderate to large size ranging in diameter from 0.3 μm to 0.01 mm and approximately 0.05 μm thick (Figure 2.2). Their two-layer silica-alumina structure include relatively strong bond, providing little possibility for cation substitutions in the structure. Therefore the properties and composition of kaolinites are relatively constant (Rice 1987).

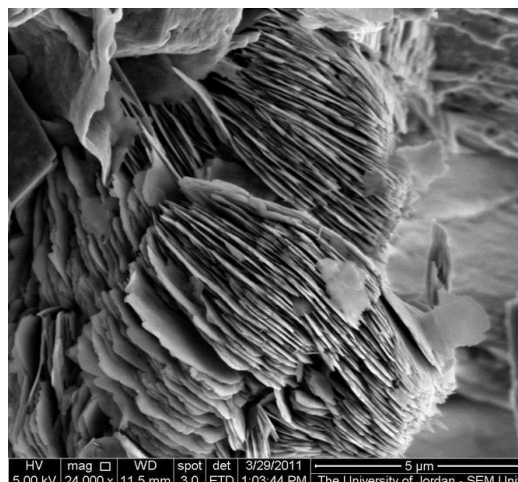


Figure 2.2. Scanning electron microscope (SEM) image of kaolinite (Source: <http://www.fei.com/resources/image-gallery/kaolinite-clay-2659.aspx>)

Halloysite is the second major mineral category in the two-layer group. Halloysite has some disorders in the stacking of its silica and alumina layers therefore include more water in the mineral structure (Rice 1987, Velde 1992, Grimshaw 1971).

The smectite clay group is one of the two categories of the clay minerals having a three layer structure. Smectites, composed of two sheets of silica tetrahedrons separated by an intermediate layer of alumina octahedrons, are joined by loose bonds. Therefore water molecules and atoms of a variety of elements can easily penetrate the spaces between these unit layers. Smectites have a higher ratio of silica to alumina (on the order of four to one) and more of the alkali metal elements (lithium, sodium, potassium, rubidium and cesium) chemically. Because of their lower alumina content, smectites are less refractory and more fusible than kaolin clays. The theoretical composition of smectite is 66.7% silica, 28.3% alumina and 5% water (Rice 1987, Velde 1992, Grimshaw 1971).

Smectite particles are thin and flat, and they do not have the regular hexagonal shape of kaolinite crystals. The particles of smectites are considerably smaller than kaolinite particles. Due to their small particle size, smectite clays are usually very plastic and sticky. Also fineness of smectite particles provide them the colloidal characteristic and their open lattice structure makes them useful for paints or slips.(Rice 1987).

The second major group of the three-layer clays is the illite group. Illite clay minerals have structures similar to smectites and micas. In the illite clay, about one-sixth of the silicon is replaced by aluminum, causing to a charge deficiency that is balanced chiefly by potassium (K^{1+}) but also by Mg^{2+} , Ca^{2+} and H^{1+} . This charge deficiency is primarily in the outer silica layers of the unit structure and therefore close to the surface, rather than in the interior alumina layer as it is in smectites. Therefore the illite clays are nonexpanding. Illite mineral particles occur in poorly defined flakes of very small sizes, but they are larger and thicker than smectites, with diameters ranging between 0.1 μm and 0.3 μm (Velde 1992, Grimshaw 1971). The fineness of these illite clays makes them useful for pottery slips. Slips on two famous categories of archaeological pottery, Greek black-figure ware and Arretine/Samian ware, have been manufactured from illite clays (Rice 1987).

2.4. Production Technology of Ceramics

2.4.1. Preparation of Ceramic Materials

The raw materials used by traditional potters generally require treatment before usage. The clay is often excavated from a pit, a field or a quarry as chunks. Transportation of dry clay is easier than wet clay. In order to obtain finer material these dry chunks of clay must be crushed, ground and sieved, the coarser fractions and impurities must be removed (Druc and Velde 1999).

Another technique used for purification of clay is Levigation. In this process clay is thrown into large tanks, larger inclusions settle down and finer particles are separated by remaining in suspension. Roman levigation tanks were very big with 10000 gallon capacity. In order to decant clays from levigation tanks smaller installations were also used. During this process inclusions like calcite can be removed, which could lead to problems in firing process (Henderson 2000).

Clay is composed from different constituents, which determines its properties during drying and firing processes. Different materials can also be added to clays in order to improve their properties (Henderson 2000).

In archaeological literature *Temper* is sometimes referred as a binder which has the effect of strengthening the body. Generally plastic clay is binder but non-plastic clays weaken the body. In spite of this disadvantage temper is used in body structure, because it simplifies the uniform drying, prevents shrinkage, reduces the strain and decreases the risk of cracking (Shephard 1956).

Primitive potters were used wide range of materials as tempers. Tempers can be organic or inorganic material, sands were most abundant material used as temper. Grog, small fragments of pot, were also used. Different kinds of rocks like andasites, diorites, trachytes and basalts and various organic materials were also used as tempers. Inorganic tempers include sponge spicules, shell, (quartz) sand, limestone, basalt, sandstone and volcanic ash. (Shepard 1956).

The materials, which occur naturally or can be added as tempers, include quartz, mica, calcite and shell. The distinction between the use of temper and natural occurrence of the same material in clay used can be made by determination of amount, shape and size of material in structure (Henderson 2000).

The temper is pre-treated before mixing with clay. Pre-treatment procedure will change according to the nature of temper. Mineral temper is crushed in a stamp mill or with hard tool. It is then ground and in order to separate coarser fraction and unwanted inclusions, sieved. Some materials such as rocks and shells can be heat treated in order to facilitate their crushing. Concerning shells, heat treatment process also prevents further material expansion which would be destructive during firing process. Other materials such as chaff, straw, cotton balls can be chopped, tree bark can be reduced to ashes, grog and bones can be ground and sieved before mixing to clay (Druc and Velde 1999). After the preparation of clay and tempers, they are mixed together with water and kneaded in order to obtain homogenized paste (Figure 2.3). Foot treating and wedging are other physical techniques applied in preparation for elimination of air from structure, increment of homogenization of moisture and inclusions and production of workable clay. Kneading process allows the complete mixing of raw materials therefore it is very important. If the homogenization process applied poorly air pockets are present in structure of fired product. These air pockets are sign of incomplete kneading, they can decrease the body strength and increase breakage during firing. Kneading is applied by foot or by hand on a flat surface. Wedging process is cutting the clay with wire and pressing it together repeatedly. Foot treating is the same with the kneading process but it is applied for the large quantities of clays. These preparation techniques improve the plasticity and help for successful firing of pot (Henderson 2000, Druc and Velde 1999). Preparation procedures modify the characteristics of original materials used in the production of ceramics (Druc and Velde 1999).

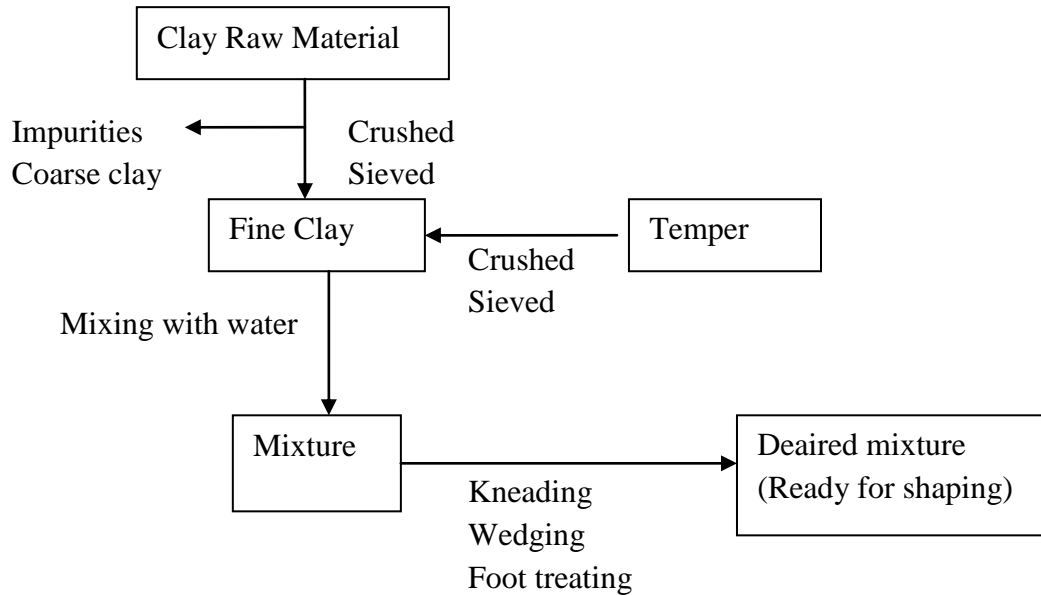


Figure 2.3. Flowchart for raw material preparation
(Source: Druc and Velde 1999)

2.4.2. Forming Techniques

There are wide range of methods used in forming process of potteries. Occasionally different methods are used for different parts of potteries. In primary method lump of clay is modeled by pinching, beating or drawing by using paddle and anvil, pressed into a mold, builded up from coils and thrown on a wheel. This technique converts the shapeless clay into basic shape. In the second technique basic shape is modified by scraping, trimming and beating by using a paddle and anvil. The forming techniques provide information about the technological advances of a society which produced the ware (Tite 1999, Druc and Velde 1999).

2.4.3. Clay Drying

Different factors have effects on clay drying, such as the humidity of environment, temperature of drying and amount of water in clay (Henderson 2000). Adsorbed water, that surrounds the clay platelets, starts to evaporate when the drying process of pottery starts. Therefore the clay platelets move towards each other until they

touch to each other, this motion causes the increment of density of clay and shrinkage of the entire mass. Amount of the drying shrinkage depends on the size of clay particles and amount of water in the structure (Figure 2.4). After the evaporation of water from structure all clay platelets are in contact and drying shrinkage is complete. This point is called as leather hard (Rhodes 1973). Pottery is not totally dry yet, for this reason it is not too hard, however strong enough for polishing and decoration applications without deformation. Surface decorations, like engraving, on pottery are generally applied at this stage (Druc and Velde 1999, Kingery and Vandiver 1986). Portion of water in clay, which was added in order to provide plasticity, is held in pores and requires longer time for evaporation. Decrement of particle size of clay causes the formation of finer pores in the structure, therefore longer time is required for evaporation of water. Pore water is generally replaced by air. After the removal of all pore water, contraction is finished (Druc and Velde 1999).

Drying speed is an important parameter for pottery. In the course of fast drying water evaporates from the surface of pot faster than interior. Consequently the surface of pottery contracts faster than interior. This condition causes the compression of surface, which can produce the cracks. The water in mineral lattice of clay is lost when the pottery is heat treated (Henderson 2000).

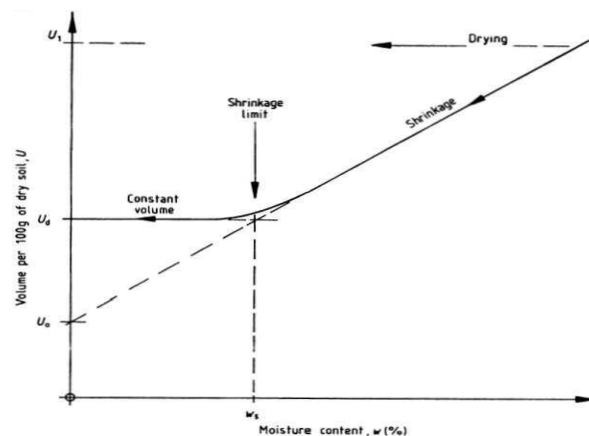


Figure 2.4. Moisture content effect on shrinkage and volume
(Source: British Standard, BS 1377-2:1990)

Grog is an already fired and ground clay material with fine particle size, therefore grog undergoes no further shrinkage. Addition of grog to the structure of clay body causes the decrement of total shrinkage. Flint and feldspar are the other materials which decrease the shrinkage and promote rapid drying (Kingery and Vandiver 1986).

2.4.4. Conditions of Firing

There are three important factors that affect the changes taking place in a pot during firing process:

1. Duration of firing
2. Temperature of firing
3. The atmosphere in kiln

All these factors must be considered together, because the change of one factor has effects on others. Duration of firing is a very important factor and composed from three stages. These stages are; temperature rising period (heating), duration at maximum temperature, and temperature falling period (cooling). Firing temperature can change during the different parts of firing cycle, determination of duration time at maximum temperature is very important (Henderson 2000).

Firing atmosphere is a very important factor on color, hardness, shrinkage and porosity of pottery. Firing atmosphere is defined as the balance of oxygen, carbon dioxide and carbon monoxide during firing process. Oxygen predominates in oxidizing atmosphere, however in reducing atmosphere oxygen is deficient, carbon dioxide and carbon monoxide predominate in kiln (Henderson 2000).

Oxidizing atmosphere is obtained in free burning kiln, which changes the state of iron in clay body. During the firing process if the maximum temperature is not reached, fuel does not give complete ignition, combustion is not completed, therefore reducing atmosphere is created in kiln, which causes the blackening. This gives reduced state to iron in the clay body. Color of clay remain in its initial state do not turn to reddish color. High degree of incomplete combustion forms the deposit of fuel gasses and solids on surface of ceramic kiln. These are reduced state of matter in firing process. The color of clays with organic constituents does not change. If high state of reduction is attained on surface of pottery, deposits of black organic particles will be formed on the surface (Velde and Druc 1999).

2.4.5. Reactions During Firing

Water between clay platelets serves as lubricant and evaporates during drying process and leaves 30-50 % volume empty space in the structure. Consequently unfired ware is weak and permeable. During firing process, final bit of moisture in pores evaporates, clay decomposes and evolves more water vapor. Meanwhile some of the organic materials in structure of clay body vaporizes, when the time and conditions are appropriate hydrocarbons and residuals in the structure burn and disappear. Firing process must be carried out slowly and with plenty of air in order to complete these processes (Kingery and Vandiver 1986).

During firing process each clay mineral behaves in a unique way and also many clay bodies, depending on their constituents, behave distinctively. This variability is the result of chemical composition of the clay materials and inclusions. Furthermore it is affected by the time, temperature and atmosphere during firing process (Rice 1987). Changes that take place in clay body can be showed are displayed in Figure 2.5.

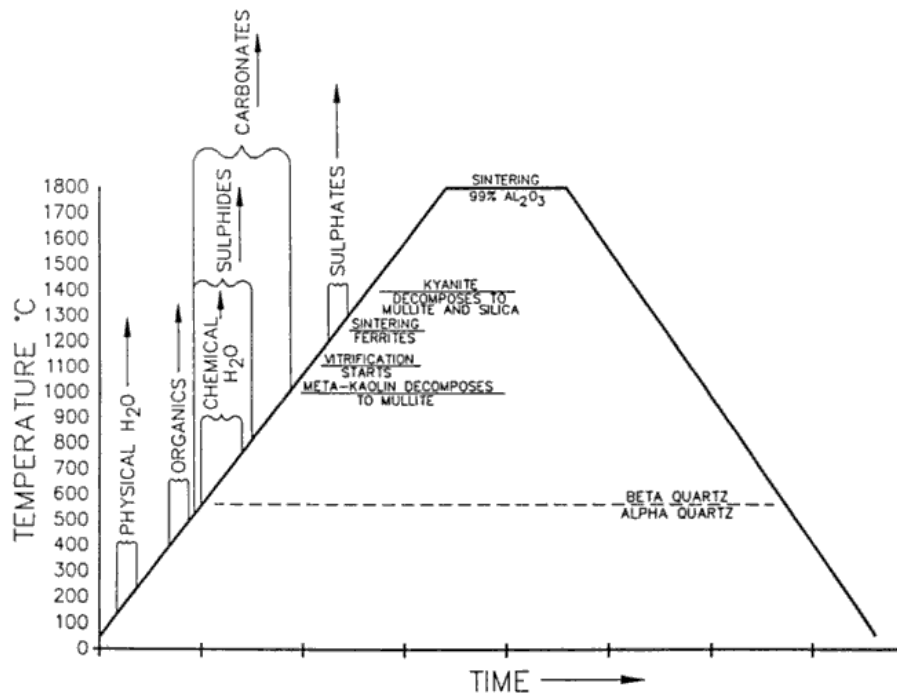


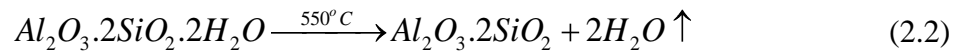
Figure 2.5. Chart showing the reactions during firing process

Variations that takes place during heating in clay body can be outlined as (Rice 1987):

-Room temperature to 200°C: During this phase of heating adsorbed water is lost from the clay. In this phase there is little or no shrinkage.

-200-400°C: Organic materials present in the clay starts to oxidize at these low temperatures. During the oxidation process organic materials migrate from interior to exterior parts of pottery causes the blackening of surface before driven off as CO₂.

-450-600°C: Chemically combined lattice water in structure of clay is removed. Kaolin is transformed to metakaolin phase with inconsiderable shrinkage and appreciable increment in porosity. Water loss and shrinkage are more slow for smectite and illite minerals.

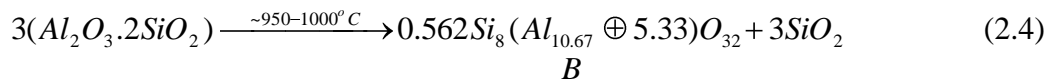
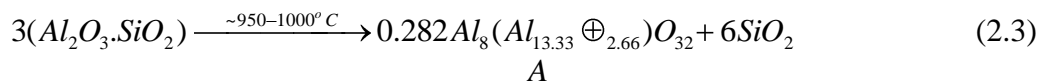


-573±5°C: Quartz is transformed from alpha to beta form

-750-850°C: Organic materials in the structure of clay body are burned. Removal of lattice water from the clay minerals causes the loose of characteristic crystalline structure of smectites and kaolins. Calcium carbonate is dissociates, and converted to quick lime.

-867-870 °C: Beta quartz converts to tridymite.

-950°C: At this temperature the structure of most smectites and kaolins is irreversibly lost. Spinel is a compound produced by the breakdown of metakaolin.

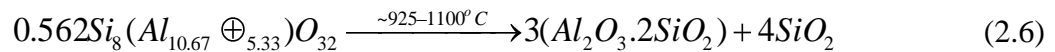
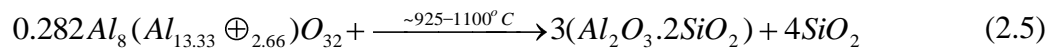


⊕: Vacancy

A: γ-Alumina type phase

B: Aluminosilicate spinel

-1050-1200°C: Spinel converts to needle like crystals of mullite in this temperature range and feldspar starts to melt.



-Above 1200 °C: The tridymite changes to cristobalite and silliminate, kyanite and cordierite form as high temperature mineral phases (Rice 1987).

These reactions are depend on the firing conditions and the properties of raw materials used in the production of pottery.

2.4.6. Firing Kilns

Firing temperature, atmosphere and duration are important parameters in firing process. Color, durability and permeability of potteries are affected by these parameters. Firing temperature and atmosphere depend on the type of firing. There are three main types of firing: open fires, semi-open structures (pit kilns) and closed structures. The products obtained are influenced by the performance and limitations of firing (Velde and Druc 1999, Rice 1987).

The simplest type is an open fire (Figure 2.6). It is the easiest firing method in terms of time investment and location, no structure is needed. The potter can fire a few pots in an open field. Open fires are found in domestic production (Velde and Druc 1999, Rice 1987).



Figure 2.6. Open Fire

(Source:<http://www.crownstudio.co.uk/graham%20taylor%20prehistoric%20pottery.html>)

Pit kilns are used in domestic production (Figure 2.7). They provide production of larger numbers of ceramic ware with a better quality. Firing atmosphere can be controlled in these kilns and more wares can be fired at the same time (Velde and Druc 1999, Rice 1987). Open firing tend to be short-lived and relatively low temperatures of 800-900°C are achieved during firing (Henderson 2000). The most important difference between pit kilns and open fire is that the pit kilns are enclosed by walls. The walls allow to reach higher temperatures in pit kilns than open fire (Shepard 1956).

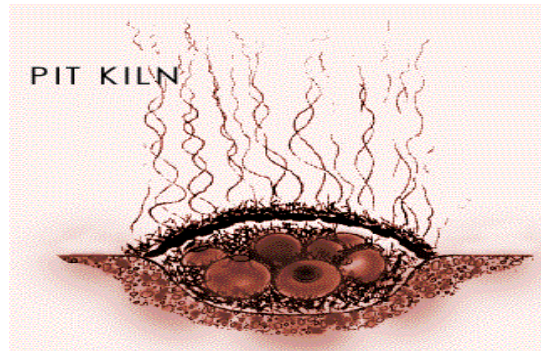


Figure 2.7.Pit Kiln
(Source: <http://seco.glendale.edu/~rkibler/kilns.html>)

Closed kilns are used for mass production (Figure 2.8). Better quality ware can be produced, because higher temperatures are reached in closed kilns (Velde and Druc 1999, Rice 1987). Temperature in this type of kilns can reach to 1300°C. Atmosphere is controlled as well as heating rate. The heating and cooling periods are much longer than open fires and pit kilns and whole firing process can take days (Shepard 1956).

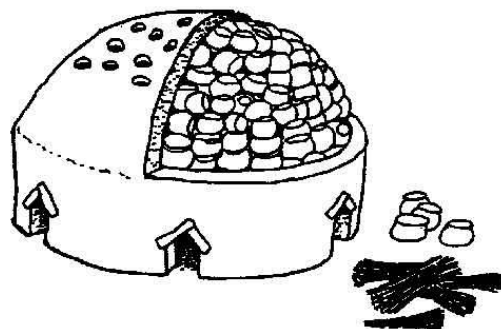


Figure 2.8.Historical Closed Kiln
(Source: <http://www.caroun.com/Research/Craft/PrimitivePotteryKilns.html>)

2.4.7. Surface Treatment

Potteries are subjected to a range of surface treatments. These treatments serve as decoration and reduces the permeability of the potteries to liquids. They provide nice visual effect and hide the surface marks left by the manufacturing process. Used surface treatments include plastic decoration such as impressed or incised patterns, burnishing, application of slip or mineral pigments and post-firing treatment with an organic coating called glaze (Shepard 1956, Rice 1987, Druc and Velde 1999).

2.4.7.1. Slip

Slip is a layer, composed of clay rich material and applied in a very liquid state to the air-dried ceramic body. Slip and body parts have similar compositions (Table 2.1).

Table 2.1. Composition of body and slip parts of pottery sample characterized by EDX method

Sample Part	SiO ₂	PbO ₂	Al ₂ O ₃	K ₂ O	Na ₂ O	MgO	CaO	Fe ₂ O ₃	TiO ₂
Slip	53.61	17.03	18.41	3.40	1.34	1.12	3.49	0.1	1.60
Body	49.88	5.98	18.83	3.19	2.43	3.30	6.15	9.07	1.18

Ceramic is usually dipped into the clay water mixture of the slip. The dryness of the ceramic extracts water from the slip which concentrates the clay particles on the surface of the unfired ceramic core, making a sort of clay cake on the surface. This clay cake does not drop, adhere fine to the ceramic after firing process. The objective of usage of slip is to cover the surface of ceramic and hide the defects. Slip has a strong tendency to loose its structure before the core of the ceramic, therefore it has covering effect. The slip becomes glassy or hard while the ceramic maintains its strength. In ceramic production adherence of slip to core is a very important technological step. During firing process clay rich slip diffuses into surface of ceramic and its thickness changes from several micro-meters to a millimeter or more (Druc and Velde 1999, Shepard 1956).

2.4.7.2. Glaze

Glazes are prepared from fused silicate mixtures, they are thin continuous coatings applied on clay wares and ceramics for protection, marking, sealing or decoration objectives. Glazes are glasses in their chemical and physical nature (Parmelee 1973). Origin of glazing date back to Egyptians to the 12000 BC. Earliest objects were vitreous layer coated steatite, containing 85% silica. During the 3rd millennium B.C glazed objects have been introduced from Egypt to the Crete and Aegean Islands. Neither Romans nor Greeks pay attention to Egyptian type of glaze, they developed very thin varnish-like terra sigillata. Place and time of discovery of lead glazes are not known and did not originated in any country. Lead glazes are used in Europe until 15th century.

Glaze is a thin layer of glass that has been fused onto a ceramic surface. Glaze is composed of three parts:

1. Network formers: The most common network former is the silica (SiO_2).
2. Network modifiers: Network formers can be used directly in the production of glasses but they are unsuitable for glazes. Silica melting point is above the 1700°C , therefore fused silica is not practical for usage. The highest temperatures achieved in traditional kilns was around 1100°C . In order to produce glaze at these low temperatures fluxes or network modifiers must be added to system. Common fluxes are lead, calcium, magnesium, potassium and sodium.
3. Intermediaries: Stronger glazes are produced by addition of intermediaries, such as alumina. (Rye 1981) Alumina (Al_2O_3) is used to increase viscosity of the glaze and give stability to glaze on the pottery, which allows the glaze to have a broader firing range (Daly 1995).

Glazes have compositions similar to glasses. The main difference between glasses and glaze is alumina content in their structure. Alumina added to glazes in order to render them less fluid at high temperatures, therefore they do not flow down the pottery wall. Glazes adds strength to the ware, provide non-absorbent, hard, impermeable and easily cleaned surface, allow variety of surface textures and colors. Glazes are usually applied by dipping, pouring, painting or spraying methods. Glazes

may be colored or opaque, contain tiny or visible crystals. Glaze may be applied on a raw body or fired body (Rice 1987, Kingery and Vandiver 1986).

The glazes are characterized by 40-50 percent porosity and during firing the first changes consist of burning out any organic material, decomposing clays and carbonates, and sintering the glaze particles together to reduce pore volume. Next there is the formation of a continuous glassy phase within the bubbles left from the pores and formed by decomposition of carbonates, clays, mica and feldspar. These bubbles work to the surface and break, forming pits, which then smooth out under the influence of surface tension. Gradually the remainder of ingredients dissolve and there often is a reaction between the glaze and the body. Glazes that look smooth often have a number of shallow pits on the surface. A long firing time and nonporous body are needed to obtain a good surface (Kingery and Vandiver 1986).

An important condition of the glaze composition is that it should fit the body, its thermal contraction should be same as the body or slightly less than it. Adhesion of glaze on body layer is very important. Glaze will flake off when the adhesion of glaze is poor or fit is too bad. If contraction of glaze is higher than the body, glaze has to be stretched out in order to match the body (Rado 1988). Tensile stresses in stretched out glaze causes cracks in the structure. If the contraction of glaze is less than the body, it is forced into further contraction, this situation produces compressive stresses in glaze structure. Glaze is more strong in compression than in tension, which causes the increment of overall strength of ware (Kingery and Vandiver 1986). When the compressive stresses become too great, glaze tends to rise of the body and produces cracks (Kingery and Vandiver 1986).

Glaze can be applied to unfired or single fired clay objects, but typically two firings are used. The first firing of clay body is applied at temperatures of 900-1000°C, and called as bisque or biscuit firing. The ware is then cooled, glaze is applied and clay object is refired. The bisque firing produces stronger pieces suitable for dipping in glaze and decoration, allows pieces to undergo firing shrinkage and leaves the body porous enough for better adherence of glaze (Rice 1987).

Glazes are classified according to their firing temperatures. Glazes fired below 1150-1200°C are classified as low temperature glazes, above 1200-1250°C are classified as high temperature glazes. Low temperature glazes are composed of alkaline or lead. High temperature glazes composed of feldspars or alkaline earth minerals such as dolomite, barium carbonate and calcium carbonate. The low temperature glazes can be

applied on high fired bodies however high temperature glazes can be applied on low fired bodies due to danger of deformation and overfiring (Rice 1987, Velde and Druc 1999).

Lead glazes are composed of lead compounds and silica. They are prepared as water suspension and applied over the body. Depending on the composition lead glazes melts at temperatures between 700°C and 1000°C. Medieval lead glaze contain 40-60% wt PbO, 2-3% wt Na₂O+K₂O and alumina content ranging between 2-7% wt. Lead glazes were used extensively in Roman and Byzantine worlds.

Usage of lead oxide in traditional glazes are based on several reasons. Lead oxide is strong flux, allows the glaze mature at lower temperatures than their leadless equivalents. Lead oxide allows maturing of glaze over a wider firing range. Lead oxide reveal high index of refraction and low surface tension, resulting in brilliant and smooth glaze surface. Lead oxide resists crystallization of glaze. There is a disadvantage of lead oxide, it is poisonous. In order to avoid lead poisoning appropriate precautions must be taken. It is caused by eating soluble lead compounds, the disease is very difficult to determine since the symptoms are similar to other illnesses (Eppler and Eppler 1998, Parmelee 1973). If the lead glazes are not formulated properly, they release lead into solution when they are subjected to acidic material. If such glazes are in contact with food, they may cause the lead poisoning (Eppler and Eppler 1998, Parmelee 1973).

Glazes are generally designed to have smooth, reflective and bright surfaces. When the surface of glaze is like mirror at the firing temperature, bubbles in the glaze shrink on cooling, forms small dimples which damage the flatness of surface. If the cooling procedure is slow tridymite or cristobalite crystals are formed at glaze surface, which causes the formation of rough surface with reduced transparency (Kingery and Vandiver 1986).

Viscosity of glaze can be reduced by the addition of materials called as deflocculant. (Figure 2.9). Deflocculants causes the formation of thinner glaze layer, even though it contains the same amount of water and dry material. Most of the deflocculants neutralizes the charges on particles, therefore the particles do not attract each other thus the dispersion of particles are controlled.

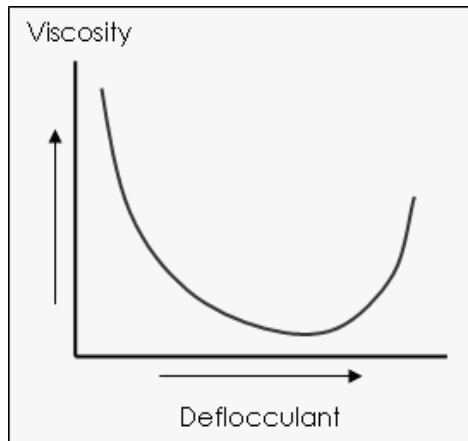


Figure 2.9. Deflocculant effect on viscosity
(Source:http://digitalfire.com/4sight/education/deflocculants_a_detailed_overview_324.html)

Glazes can be used in order to color the surface, mask the clay body of ceramic or for protection of colors below their surface when they are transparent (Velde and Druc 1999).

Lead glazes have advantages and disadvantages when they are compared with alkali glazes. In alkali glazes plant ash is used, its soluble in water. High lead glazes can be prepared as suspension of lead compound and silica, which causes the reduction of cost in terms of fuel and time. Alkali glazes have higher thermal expansion coefficient than the lead glazes. Lead glazes are cheaper and their production of them are easier than alkali glazes.

2.5. Final Product Properties

Pottery analysis generally focuses on the properties as its capability to contain liquids, to carry loads, to resist heating and cooling cycles, which affects the original use of pottery. These thermal, mechanical and physical properties provide information about the nature of raw materials, usage and manufacture of vessel (Velde and Druc 1999).

Internal structure of ceramics, arrangement of atoms within the components of a ceramic and arrangement of these components with respect to each other, affect the properties related to their usage. Pottery can be defined as a material composed of more than one phase Phases in ceramics include glassy material, pores and individual grains (Figure 2.10). In ceramics, microstructure is defined as the complex arrangement of phases. Microstructure is mostly discussed in terms of structure, composition, texture and surface characteristics. In low fired pottery, raw materials, manufacturing technique and phase changes are the factors which determines the microstructure. In high fired pottery equilibrium relations between phases, changes resulting from vitrification and formation of high temperature minerals are important in determination of microstructure (Rice 1987).

Microstructural properties determines the use related properties of pottery. Porosity, strength and hardness are most important properties for traditional pottery samples. All ceramic materials have pores or void spaces in their structures. Pores in the structure of ceramics affects properties such as conductivity, strength, resistance to chemical and mechanical erosion (Rice 1987).

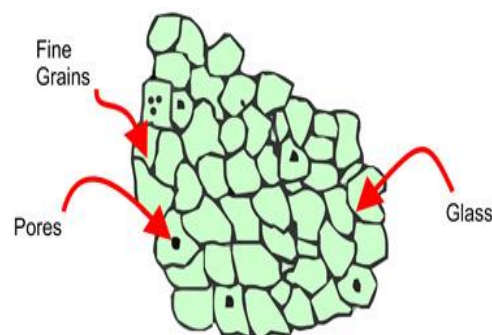


Figure 2.10. Microstructure of an typical ceramic.
(Source: <http://www.azom.com/article.aspx?ArticleID=5697>)

Additional important use related properties of ceramic is its durability or resistance to mechanical stresses during usage. Strength and hardness are the two closely related performance properties of fired ceramics. Determination of hardness provides information about the durability and serviceability of ceramic materials. Hardness has many meanings, including resistance to crushing, abrasion, scratching and penetration. Although the strength and hardness refer to resistance of material to mechanical deformation, there is difference between them. Hardness denotes deformations affecting the surface, whereas the strength is a measure of response stresses including the whole body (Rice 1987).

Hardness of clay is affected by firing temperature. It increases with the temperature of firing. Hardness is also affected by the firing atmosphere. Usage of reducing atmosphere hardens the fired pottery. Microstructural features influencing hardness include grain size and porosity of fired piece. Nonporous and finer grained materials are generally harder. Slip and glaze applications on surface also increase the hardness (Rice 1987).

The strength of fired ceramic depends on many properties such as composition and particle size of clay, texture of paste, production technique, thermal cycle during production, drying and firing conditions. Finer clay particles easily adhere to each other during firing. The fluxes determine the nature of bond formed between particles, and temperature of bond formation. Texture is affected by size, shape and amount of non-plastic inclusions which is the main reason of variation in pottery strength. Strength can be defined in different ways, generally in terms of its resistance to various stresses without fracturing, deformation and rupture (Grimshaw 1971, Shepard 1956).

There are six types of stress which affect the ceramic body. These are: shear, compressive, tensile, transverse, impact and torsional. Different methods can be used in order to measure response of materials to these stresses. Then the strength of material can be calculated (Rice 1987, Shepard 1956).

2.6. Byzantine Ceramics

Roman Empire is divided into two parts by 400 AD, Western Roman Empire formally ended in 5th century but the Byzantine Empire (Eastern Roman Empire) survived until 1453. Byzantine Empire with capital city at Constantinople, played central role in political, religious, cultural and economic area throughout the European Middle Ages (Dark 2001, Lemerle 2004).

Although the study of pottery plays important role in the Western Roman Empire archaeology, archaeologists have neglected the Byzantine pottery. Byzantine people used a lot of pottery in their life. Coarse-ware vessels were used for cooking and storage, Fine-ware vessels were made for table use or display. Round-bottomed amphore were used as container for transportation of goods or for storage (Dark 2001).

Early Byzantine coarse-wares include cooking pots, cups, candle-sticks, flasks, domed or saucer-shaped lids, bowls, jars, lamps, jugs with wide variety of shapes. Some of these shapes were produced in same fabrics with different finish from Early Byzantine fine-wares, but others produced in fabrics containing larger mineral inclusions. These coarse wares had plain surfaces, but sometimes burnished, polished, slipped or decorated with incised horizontal or slanting lines (Dark 2001).

Roman traditions continued in Early Byzantine coarse-wares, without main changes in decoration, shape or fabric. Middle Byzantine coarse-wares continued this pattern of overall continuity with changes in details of vessel form and decoration. After 13th century important changes in coarse-ware manufacture have occurred. Middle Byzantine coarse-wares were replaced by grey and red fabrics in Constantinople after mid 13th century. Although the shapes of wares remained similar, these potteries were technically in poor quality. Because of these differences the coarse-ware production in Constantinople was disrupted, ceramics were less extensively used and new vessel shapes popularized (Dark 2001).

Byzantine fine-wares showed different pattern of development. Most of the Byzantine settlements used fine-ware pottery, which were much more closely datable than the coarse-wares. Fine-wares give information about the Byzantine cultural and political history and provide a way of dating (Dark 2001).

The fine wares produced in the 5th, 6th and 7th centuries fine-wares composed of unglazed red-slipped wares and unglazed painted vessels were used as table pottery that

are suitable for dining and display. This group has limited range of decorative styles and shapes additionally was in red color. In 5th century fine-wares were red slipped and unglazed vessels with red fabrics but in 7th century fine-wares were white or pink fabrics covered with glaze. The date and place of Byzantine glazed pottery production is unknown. The glazed pottery that became the standard fine-ware of the middle Byzantine Empire was glazed white ware. These wares have characteristic pink or white color and are decorated with incised or painted designs (Dark 2001).

Fine-wares called as 'red' fabrics are first used in the 12th century. Important innovation in Byzantine pottery was the development of new decoration type called as *Sgraffito* (Dark 2001). In this decoration desired motif engraved on the light-colored or white surface by the craftsman with a stylus. The act of engraving uncover the red surface of clay and the engraved lines stand out against the white field formed by slip, by this way decoration is created. This decoration technique, that is known as *Sgraffito*, from the Italian verb *sgraffiare* (engrave), was the major technique used in Byzantine pottery. The glaze layer determined the final appearance of pattern engraved through the slip. Archaeological evidences have propose that firing was applied twice, before and after application of glaze, to Byzantine pottery with decoration. First firing transformed the clay body of the vase into pottery, second firing liquefied the glaze and it adhered to surface of the pottery like a skin (Papanikola-Bakirtzi 1999).

The first phase of Byzantine sgraffito-decorated pottery is characterized by usage of different colors of glaze on exterior and interior parts of the same vessel. These vessels are called as *Duochrome Sgraffito Ware*. Pale yellow or mid-green colored glazes are used for these wares.

These vessels are generally flat plates with decoration engraved into red body with a stylus through the white or cream slip. Thin incisions are left unfilled but look as darker lines against the paler slipped body. *Fine Sgraffito Ware* (Figure 2.11) has similar properties with *Duochrome Sgraffito Ware*. The difference between these two wares is the exterior glaze color. Exterior surface of *Duochrome Sgraffito Ware* is covered with glaze in different color (Dark 2001, Papanikola-Bakirtzi 1999).



Figure 2.11. Fine Sgraffito ware
(Source: Papanikola-Bakirtzi 1999)

The next development during the 12th century was the usage of broader incision for Byzantine sgraffito pottery. These vessels were called as *Incised Sgraffito Ware* (Figure 2.12) and they began with vessels that resemble Fine Sgraffito Ware in their decoration but employ broader line (Dark 2001).

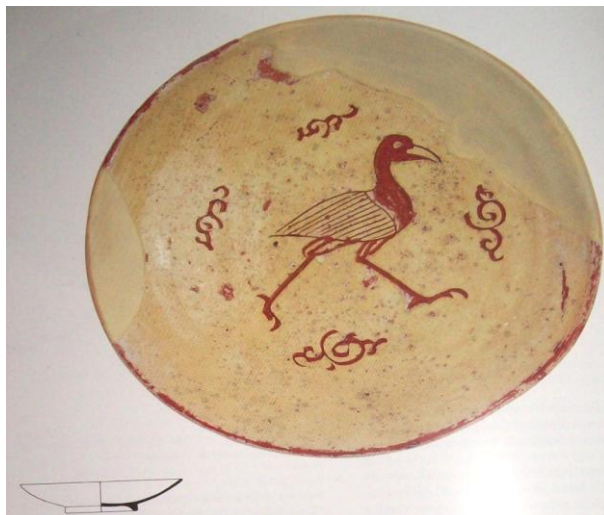


Figure 2.12. Incised-Sgraffito ware
(Source: Papanikola-Bakirtzi 1999)

Another twelfth century innovation was the *Champlevé Ware* (Figure 2.13), where portions of the slip were removed to show whole areas of the fabric below the glaze. These wares may also be related to *Incised Sgraffito Ware* (Dark 2001).



Figure 2.13. Chamlevé Ware
(Source: Papanikola-Bakirtzi 1999)

There are three main phases in production of Middle Byzantine fine-wares. In the first phase both white-wares and red wares were manufactured. In the second phase the glazed white wares were used. In third phase, starts at the beginning of 12th century, Sgraffito wares, white wares and imitations of white wares were produced (Dark 2001).

Late Byzantine ceramic period have a different ceramic signature like Middle Byzantine and Early Byzantine periods. In this period limited range of glazed pottery were produced. Sgraffito, chamlevé and slip painted decoration were used for these wares. Most common form of fine-ware vessel was bowls which replaced the plates. Glazed ceramic tiles were no longer produced. Late Byzantine glazes were darker, more vitreous and glossier than the Middle Byzantine period samples. In Late Byzantine period, dark green and bright ochre or gold yellow colors were used instead of the pale yellows or apple greens of Middle Byzantine period. The red and polychrome painting left. Marbled glazes, generally were used on Middle Byzantine white wares, also disappeared. Usage of combination of different colors in glazes were common. Late Byzantine fine-wares represent the last phase of Byzantine ceramic tradition (Dark 2001).

Analysis of ceramics have important role in archaeological descriptions. In an archaeological excavation ceramic finds provides important information about a previously existed society and culture. Obtained information is used in dating the sites, establishing chronology, identification of the social and economic patterns and determination of relationships within a community (Grimshaw 1971).

Pottery analysis is generally used in determination of the properties that affects the original usage of product, its capacity to contain liquids, to carry loads, to resist heating and cooling cycles. These mechanical, chemical and thermal properties provide information about usage of pottery, production type, and nature of raw materials (Rice 2005).

Phases in ceramics are composed of pores, individual grains and glassy material. The relationships among the phases are important. Because they change constantly with the chemical and physical state of the ceramic during firing and cooling. In order to determine the number, amount and composition of all phases present in the structure of ceramics phase, diagrams are used (McHale 1994, McHale 1998).

Complex arrangement of these phases in a ceramic is defined as its microstructure. Microstructure describes the internal arrangement of amorphous and crystalline materials, pores and boundaries between them. Microstructure is generally defined in terms of texture, structure, composition and surface characteristics. Composition refers to nature of crystalline and non-crystalline phases and pores. Texture depends on the shape, size and orientation of phases, and structure refers to the arrangement of phases (Rice 2005).

Primary determinants of microstructure in low-fired pottery are the raw materials, production technique, and phase changes during firing. However in high-fired ceramics, high temperature mineral formation, changes resulting from vitrification and equilibrium relations between phases are more important. The porosity, hardness and strength of ceramics are affected by its microstructural characteristics (Lahlil et.al. 2008, Buxeda et al. 2001, Tite et al. 2001).

The behavior of a clay material under conditions of temperature changes and at a series of uniform temperature is important, because heat is a significant component in production and in many applications of ceramics. Thermal properties of ceramic are important in initial heat treatment of clay and in the use of the fired products with heat. Thermal behavior of ceramics are determined by thermal conductivity and thermal expansion coefficients of them (Rice 2005, Hein et al. 2008, Roberts 1963).

Archaeological ceramics are characterized according to their mechanical, structural and thermal properties but more commonly used techniques focus on chemical and mineralogical constituents of the ceramic (Rice 2005).

Mineralogical analysis of the pottery is done to determine its mineralogical components, both in the clay matrix and in the coarser particulate part. The most

common techniques are based on optical characteristics of minerals visible under microscope (petrography), their behavior when bombarded by X-rays (x-ray diffraction) and their behavior when heated (thermal analyses) (Isphording 1974, Eiland and Williams 2001, Sciau et al.2006, Ion et al. 2009, Papadopoulou et al.2006, Moropoulou et al. 1995, Hein and Kilikoglou 2007, Rathossi et al. 2004, Grifa et al. 2009).

Determination of chemical composition of a ceramic material is an analytically important objective. Determination of chemical composition of a ceramic can provide important information on its origin and fabrication, although chemical data do not determine the sources of elements in the body or relation to each other. Therefore chemical analysis and mineralogical study together give optimal characterization (Rice 2005, Feliu et al. 2004, Fermo et al. 2008, Hill 2004, Casellato et al. 2007, Chen 2006).

Different type of measurements can be used in determination of the quantity of chemical elements in a sample including weight of the compounds formed, volume of solutions used and wavelength and intensity of radiation absorbed or emitted. Most of the methods used in analyzing pottery are optical emission spectroscopy, X-ray fluorescence, electron microprobe, neutron activation analysis and X-ray photoelectron spectroscopy, atomic absorption, Mössbauer spectroscopy and infrared spectroscopy (Ramos et al. 2002, Pillay et al.2000, Padilla et al. 2006, Shoval and Beck 2005, Benedetto et al. 2005, Froh 2004, Wagner et al. 2000, Tsolakidou and Kilikoglou 2002, Filho et al. 2005, Bower et al. 1975).

CHAPTER 3

MATERIALS AND METHODS

3.1. Archaeological Samples

Kadıkalesi is located in the south coast of Kuşadası and a cultural property of Byzantine Empire. The castle was constructed in 13th century. Excavation which continues in Kadıkalesi, provides glazed and unglazed ceramic finds, especially the faulty production remnants of glazed ceramic finds, and enables the information that the Kadıkalesi was one of the local workshops of West Anatolia and Greece, and its products was following after the products of Constantinople, which was started to drop in after the 12th century. Finds excavated from Kadıkalesi provides glazed ceramics which includes fine sgraffito pot samples that may be imported from important centers like Constantinople and Corinth. (Mercangöz. and Doğer 2009).

The glazed samples excavated from Kadıkalesi includes red and white body table pots which dates back to 12th and 13th century. Red body import ceramics, which is famous in Middle Byzantine period harbor cities and Pelagos, Skopelos, Kumluca Göçük Burun shipwrecks, provide rich finds at Kadıkalesi.





Fine Sgraffito, Incised-Sgraffito, Incised and Champlevé style dishes and pots obtained from this excavation, have differences with respect to their outer surface application and body structure. According to these differences samples were classified into groups and subgroups.

The most important criteria in decision of groups and subgroups were the outer surface applications and the changes observed by eye and hand magnifier, owing to the similarities obtained in samples' special forms and glaze properties. In this work the subgroups will be compared with main groups, main groups will be compared with each other to determine relation between them.

3.1.1. Groups and Subgroups









The samples collected from Kadikalesi are classified according to their morphological typology by Assoc. Prof. Lale Doğer in Department of History of Arts at Ege University. Photographs of samples' face and back sides are presented in Table 3.1-10.

Table 3.1. Photographs of Group 1. Type 1 (scale bar is 5 cm)

1.1.1		
Champlevé (Aegean Type)		
1.1.2		
Incised-Sgaffito		







(cont. on next page)

Tablo 3.1 (cont.)

1.1.3		
Champlevé (Aegean Type)		
1.1.4		
Incised		
1.1.6		
Incised		
1.1.7		
Incised (Aegean Type)		

(cont. on next page)

Tablo 3.1 (cont.)

1.1.8		
Incised		
1.1.10		
Incised-Sgraffito		
1.1.13		
Fine Sgraffito		

(cont. on next page)

Table 3.2. Photographs of Group 1. Type 2

















1.2.1		
Incised-Sgraffito		
1.2.2		
Incised		
1.2.3		
Fine Sgraffito		
1.2.5		
Champlévé(Aegean Type)		

Table 3.3. Photographs of Group 1. Type 3

1.3.1		
Monochrome Plain Ware		
1.3.3		
Fine Sgraffito		
1.3.4		
Champlevé (Aegean Type)		
1.3.5		
Fine Sgraffito		

(cont. on next page)

Tablo 3.3 (cont.)







1.3.6		
Incised		
1.3.8		
Champlevé(Aegean Type)		
1.3.9		
Incised(Aegean Type)		

Table 3.4. Photographs of Group 1. Type 4










1.4.4		
Fine Sgraffito		
1.4.6		
Incised		
1.4.10		
Fine Sgraffito		
1.4.11		
Champlevé (Aegean Type)		

Table 3.5. Photographs of Group 1. Type 5

1.5.1		
Incised(Aegean Type)		
1.5.2		
Champlévé(Aegean Type)		

Table 3.6. Photographs of Group 1. Type 6

1.6.2		
Fine Sgraffito		
1.6.3		
Fine Sgraffito		

(cont. on next page)

Tablo 3.6 (cont.)





1.6.4		
Champlevé(Aegean Type)		

Table 3.7. Photographs of Group 2









2.2		
Fine Sgraffito		
2.3		
Incised (Aegean Type)		

Table 3.8. Photographs of Group 3

3.1		
Fine Sgraffito		
3.2		
Fine Sgraffito		
3.5		
Incised(Aegean Type)		
3.6		
Fine Sgraffito		









(cont. on next page)

Table 3.8 (cont.)

3.8		
Incised (Aegean Type)		
3.10		
Incised(Aegean Type)		
3.11		
Fine Sgraffito		
3.13		
Incised-Sgraffito		









(cont. on next page)

Table 3.8 (cont.)

3.14		
Fine Sgraffito		
3.17		
Incised		
3.18		
Incised(Aegean Type)		
3.19		
Incised-Sgraffito		

(cont. on next page)

Table 3.8 (cont.)

3.21		
Incised(Aegean Type)		
3.22		
Incised-Sgraffito		
3.24		
Champlevé (Aegean Type)		
3.25		
Incised(Aegean Type)		

3.1.2. Properties of Groups and Subgroups

Body structure identification of the samples are determined by Assoc. Prof. Dr. Lale Doğer, by naked eye.

Group 1:

Contains Fine Sgraffito, Incised Sgraffito, Incised and Champlevé style open pot finds with single color glaze and without decoration. Body has moderate strength and contains intensely lime particles. Big cavities and fine channels are seen in structure due to lime cracks. In general red body color is at Munsell 2.5 YR 5/8-6/8 ile 5 YR 5/6-7/6-7/8 values. Group has subgroups according to outer surface operations.

Group 1. Type 1(1.1.1,1.1.2,1.1.3,1.1.4,1.1.6,1.1.7,1.1.8,1.1.10,1.1.13)

The outer surface rims have white-cream color slip. Transparent yellow or green color glaze covers the whole surface including the base part. Due to the application of glaze without slip the outer surface have brown or jade-like brown appearance.

Group 1. Type 2(1.2.1,1.2.2,1.2.3,1.2.5)

The outer surface rims have white-cream color slip. Transparent colorless or yellow color glaze was applied irregularly to surface including the base part. Glazed parts have bright brown, unglazed parts have matte brown appearance.

Group 1. Type 3(1.3.1,1.3.3,1.3.4,1.3.5,1.3.6,1.3.8,1.3.9)

The outer surface rims have white-cream color slip. Outer surface, including the base, have ireegularly applied white-cream color slip. Rims has thicker slip layer. The whole surface is covered with transparent, yellow or green glaze.

Group 1. Type 4(1.4.4,1.4.6,1.4.10,1.4.11)

The outer surface, including the base, has thick layer of white-cream color slip and transparent or yellow color glaze.

Group 1. Type 5(1.5.1,1.5.2)

Finds are the samples of the Incised and Champlevé type decoration. Even though the outer surface of samples are damaged, there is residual of glaze on the joint of the body and base except the underside of the base part.

Group 1. Type 6(1.6.2,1.6.3,1.6.4)

Samples generally have Incised type decoration, inner and outer surfaces of them have different color of glaze. Rim or body parts of limited number of samples, with fine sgraffito decoration, have white color slip and yellow or green color glaze.

Group 2: (2.2,2.3)

The samples have Incised-sgraffito or fine-sgraffito decoration. Body have mica mineral and includes white and black particles. The body color is in worth of 2.5 YR 6/8 and yellow glaze is in worth of 2.5 YR 8.4.

Group 3: (3.1,3.2,3.5,3.6,3.8,3.10,3.11,3.13,3.14,3.17,3.18,3.19,3.21,3.22,3.24,3.25)

This group contains Fine Sgraffito, Incised-Sgraffito, Incised (Aegean Type) and Champlevé (Aegean Type) style decorated open ware finds. The body of the samples has small pebbles, lime particles and high porosity. The color of the body is in worth of 5 YR 5/6-6/6-6/8, and small quantities are in the worth of 2.5 YR 5/6-6/8. The outer surface is covered with thin and non-intensive layer of white slip. The slip at rim part is thicker and the glaze is applied only to rim part of the samples.

3.2. Characterization Methods of Samples

The chemical characterization of pottery samples provide identification of pottery types or groups separation of local and transported products. Properties of raw material used in production of pottery is a chemical footprint characteristic of provenance area (Gliozzo et al 2008, Zuckerman et al. 2010).

Optical microscopy analysis is performed with high performance Leica DM 500 stereo microscope, with maximum magnification of 80X.

Mineralogical characteristics of body part of samples are determined by X-Ray Diffraction (XRD) method. Analysis is performed with Philips X'pert Pro Diffractometer by using CuK α radiation, the diffraction angle (2θ) ranged between 4-70 $^{\circ}$ to obtain the diffractogram.

Microstructural and chemical properties of body, slip and glaze parts of samples are determined by Scanning Electron Microscopy (SEM)analysis by using Philips XL-30S FEG and FEI Quanta 250 FEG instruments. Equipped with X-Ray Energy Dispersive System (EDS).

Chemical composition of body part of samples are determined by X-Ray Fluorescence (XRF) spectroscopy. Standard ceramic (South African SRM MINTEK SARM 69) was run alongside the samples in order to check precision and consistency of measurements.

3.3. Statistical Analysis of Samples

Chemical data obtained from XRD and XRF analyses are statistically processed in order to determine similarities, differences and possible classification of samples. Chemical composition values of samples are standardized in order to compensate the differences between minor and trace elements. Principal component analyses (PCA) and hierarchical clustering analyses (HCA) are employed by usage of SPSS 16.0 statistical software.

3.3.1. Hierarchical Cluster Analysis (HCA)

Hierarchical cluster analysis is a general approach to cluster analysis. In hierarchical cluster analysis aim is to group the close objects together. Important characteristic of this analysis is calculations of distance measures between objects, and between clusters are repeated once objects begin to be grouped into clusters (Baxter 1994). Hierarchical clustering methods proceed either as a series of successive division or a series of successive mergers. Agglomerative hierarchical methods begins with individual objects. Initially there are as many clusters as objects. The most similar objects are first grouped and these initial groups are merged according to their similarities. As the similarity decreases all subgroups are merged into single cluster (Johnson and Wichern 1992). Divisive hierarchical methods work on contrary direction. Initial group of objects is divided into two subgroups such that the objects in one subgroup are far from the objects in the other. These subgroups are then subdivided into dissimilar subgroups. The process proceeds until there are as many subgroups as objects, where each object forms a group. The results of both agglomerative and divisive methods can be displayed in the form of two dimensional diagram called as Dendrogram (Johnson and Wichern 1992).

Cluster analysis is type of multivariate analysis and application steps are;

1. raw or log-transformed (to base 10) data are standardized.
2. dis-similarity between objects is measured by Euclidean distance
3. objects are clustered by different linkage methods (Baxter 1994).

Linkage methods are suitable for clustering items, as well as variables. There are four types of linkage methods; average linkage, complete linkage, single linkage, and Ward's Method (Johnson and Wichern 1992) (Figure 3.1).

Searching the data for a structure of grouping is an important investigation technique. Groupings can provide information for identification of relationships and outliers. Clustering or grouping is different from classification procedure. Classification is related to known number of groups. Objective in classification is to determine new description of these groups. Cluster analysis is a simple technique, no assumptions are made about the structure and number of groups. Grouping is done according to similarities or dissimilarities (Johnson and Wichern 1992).

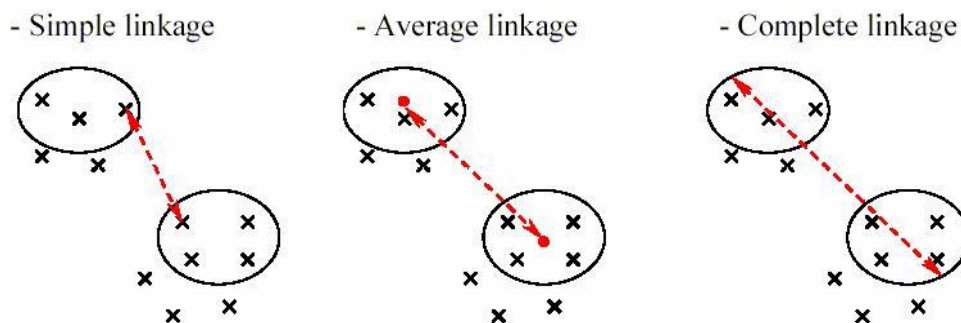


Figure 3.1. Intercluster distance for single, average and complete linkage
(Source: <http://compbio.pbworks.com/f/linkages.JPG>)

The steps in agglomerative hierarchical clustering algorithm for grouping N objects are (Johnson and Wichern 1992);

1. Start with N clusters, each containing a single entity and an $N \times N$ symmetric matrix distances (or similarities) D .
2. Search the distance matrix for the nearest (most similar) pair of clusters. Let the distance between most similar clusters X and Y be d_{xy} .
3. Merge clusters X and Y . Label the newly formed clusters (XY). Update the entries in the distance matrix by;
 - a. Deleting the rows and columns corresponding to clusters X and Y
 - b. Adding a row and column giving the distances between clusters (XY) and remaining clusters.
4. Repeat steps 2 and 3 a total of $N-1$ times. All objects will be in single cluster at termination of algorithm. Record the identity of clusters that are merged and distances and similarities at which the mergers take place (Johnson and Wichern 1992).

Some modifications are applied to data before multivariate methods. These modifications involve transformation or standardization of data. Transformation is generally applied in order to provide data with normal distribution. Standardization gives the variables equal weight. Two methods are different, standardization are applied by equation (Everitt 1993);

$$z_i = (x_i - \bar{x})/s \quad (3.1)$$

Logarithmic transformation are applied by equation (Everitt 1993);

$$y_{ij} = \log(x_{ij}) \quad (3.2)$$

Logarithmic transformation, transforms the data to a normal distribution.

Construction of simple group structure from complex data requires measurement of similarity or closeness. In similarity measurement there are important considerations. These considerations include the scales of measurement (ratio, interval, ordinal, nominal) or nature of variables (continuous, binary, discrete). Proximity is usually indicated by some sort of distances when items are clusters. Euclidean distance is often preferred for clustering (Johnson and Wichern 1992, Krzanowski 1993). Euclidean distance is calculated by the equation in order to determine similarity.

(3.3)

Clustering algorithms are classified into four groups;

1. Single Linkage Clustering

In single linkage clustering (or nearest neighbor) two clusters are combined that contain the two individuals having greatest similarity (Baxter 1994, Everitt 1993, Shennan 1997).

The inputs to a single linkage algorithm can be similarities or distances between pairs of objects. Groups are formed from individual entities by combining nearest neighbors. Nearest neighbors means largest similarity or smallest distance. Smallest distance in $D = \{d_{ik}\}$ and combine the corresponding objects, U and V, to obtain cluster (UV) and any other cluster W are computed by;

$$d_{(uv)w} = \min\{d_{uw}, d_{vw}\} \quad (3.4)$$

The quantities d_{uw} and d_{vw} are distances between the nearest neighbor of clusters U and W and clusters V and W. Graphical representation of single linkage clustering

can be done in the form of dendrogram or tree diagram. The branches in the tree represent cluster (Johnson and Wichern 1992).

2. Complete Linkage Clustering:

The *complete linkage* or furthest neighbour clustering method is the opposite of single linkage. In this method similarity between two clusters is defined by the pair of individuals (one from each cluster) that are least similar. At any stage of this method the most similar clusters are joined (Baxter 1994, Everitt 1993, Shennan 1997, Massart and Kauffman 1989).

Complete-linkage clustering progress in much the same manner as single linkage, with one important exception. At each stage similarity (distance) between clusters is determined by the similarity (distance) between two elements one from each cluster that are most distant. Complete-linkage clustering ensures that all items are in a cluster (Johnson and Wichern 1992).

The general agglomerative algorithm again initiate with finding minimum entry in $D = \{d_{ik}\}$ and joining the corresponding objects, such as U and V to get cluster (UV) . For step 3 in general algorithm the distances between (UV) and any other cluster W are computed by

$$d_{(UV)W} = \max \{d_{uw}, d_{vw}\} \quad (3.5)$$

d_{uw} and d_{vw} are the distances between the most far members of clusters U and W and clusters V and W (Johnson and Wichern 1992).

3. Group Average Clustering

Similarity or dissimilarity between groups is described as the arithmetic average of similarities between pairs of members (Johnson and Wichern 1992) by using equation;

$$\frac{\sum_{i=1}^n \sum_{j=1}^n S_{ij}}{n_i n_j} \quad (3.6)$$

Where S_{ij} is similarity between a member of group i and a member of group j , n_i : Number of individuals in group i , n_j : Number of individuals in group j .

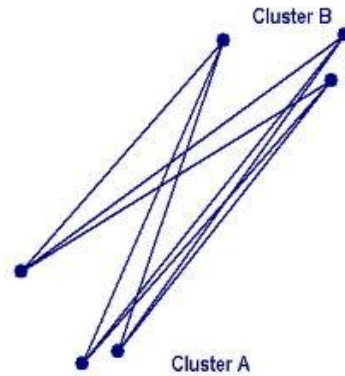


Figure 3.2. Group average clustering

(Source:http://nocweba.ntu.edu.sg/medmine/MICA/manual/Manual_hierclust_files)

In this method the distance between two clusters is described as the average distance between all pairs of items where one member of a pair belongs to each cluster (Figure 3.2). Input to the average-linkage algorithm may be similarities or distances and the method can be used to group objects. The average linkage algorithm progresses in the manner of the general algorithm. Distance matrix $D=\{d_{ik}\}$ is investigated in order to find nearest objects, U and V . These objects are combined to form the cluster (UV) . For step 3 of the general algorithm, the distances between (UV) and any other cluster W are determined by:

$$d_{(uv)w} = \frac{\sum_i \sum_k (d_{ik})}{N_{(uv)} N_w} \quad (3.7)$$

d_{ik} : distance between object i in the cluster (UV) and object k in the cluster W , $N_{(uv)}$ and N_w are the number of objects in (UV) and W (Johnson and Wichern 1992).

4. Ward's Hierarchical Clustering

Ward proposed a clustering procedure trying to form partitions P_n, P_{n-1}, \dots, P_1 in a manner which minimizes the loss related with each grouping and to quantify that loss in a form that is readily interpretable. In the analysis at each step union of every pair of clusters are considered. The two clusters whose fusion caused the minimum increment in information loss are combined. In Ward's method information loss is defined in terms of error sum of squares (ESS) criterion (Everitt 1983, Shennan 1997).

$$ESS = \sum_{i=1}^n (X_i - \bar{X})^2 \quad (3.8)$$

\bar{X} : Mean value

In Ward's method measure of the amount of variability (S) within a cluster is defined as (Everitt 1983);

$$S = \sum_i \sum_k (y_{ik} - \tilde{y}_k)^2 \quad (3.9)$$

\tilde{y}_k : mean of the k'th variable in the cluster.

Linkage methods are important hierarchical procedures. Linkage methods are suitable for clustering items as well as variables (Johnson and Wichern 1992, Everitt 1983). Dendrograms are useful technique to understand and to construct relationships between samples collected from historical sites. They are widely used in the literature for grouping purposes (Zhang et al.2002, Kilikoglou et al.1991, Sena et al.1995, Mirti et al. 1999, Barone 2005). Cluster analysis is the most widely applied multivariate method in archaeology, it is not a single method, and it is a general term for a wide range of techniques. In archaeology the most common use is to classify a set of individuals into subgroups such that individuals within a group are similar to each other and different from individuals in other groups (Baxter 1994).

3.3.2. Principal Component Analysis (PCA)

Principal components analysis is a data transformation technique. If a number of variables is measured, each variable will have a variance. Generally these variables will be associated with each other. The data set as a whole will have a total variance which is the sum of the individual variances. Each variable measured is an axis, or dimension of variability (Daultrey 1976). In principal components analysis the data are transformed to describe the same amount of variability, the total variance, with the same number of axes, the number of variables, but in such a way that:

- the first axis accounts for as much of the total variance as possible
- the second axis accounts for as much of the remaining variance as possible that is uncorrelated with the first axis
- the third axis accounts for as much of the total variance remaining after accounted by the first two axes.

There is no correlation between new axes or dimensions. They are weighted with respect to the amount of total variance which they define. Generally this causes the

formation of a few large axes accounting for most of the total variance. Larger number of small axes accounts for very small amounts of the total variance. These small axes are generally neglected from other considerations. Therefore the data set with P correlated variable converted to data set with M uncorrelated axes or principal components. Value of M is usually less than P . If further analysis is planned, having data with M uncorrelated axes is very important property. (Daultrey 1976, Shennan 1997).

Principal Component Analysis (PCA) have important functions (Daultrey 1976);

1. It provides helpful information about the relationships of variables.
2. It provides information about the relationships between units.
3. It suggests main brief trends, if there are any, within the data and determines which variables are involved in these trends.
4. It transforms the data with very large percentage of variation in a large number of variables to a data with smaller number of variables.
5. This transformation produces new variables which are uncorrelated with each other.

These properties make PCA more useful than cluster analysis. In PCA variables and cases are dealt with together, also variation in data are not involved, separated into different independent dimensions, for this reason easier to understand (Shennan 1997).

Principal component analysis depends on intercorrelation of data set. If P variables are not correlated with any other, there exist a set of uncorrelated axes and principal component analysis can't be performed. If two variables are correlated, the contours of equiprobability are elliptic, ellipse is defined by two vectors or axes (Daultrey 1976).

Geometrical presentation of principal components correlations are done by graphical methods (Figure 3.3.). Whether variables can be imagined as vectors with equal lengths, that arise from common origin, their relations can be represented in terms of angular distance between them (Shennan 1997).,

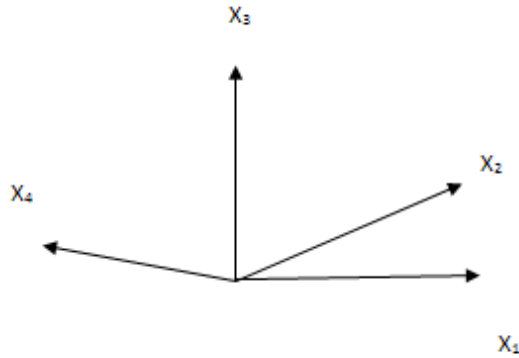


Figure 3.3. Geometrical representation of principal component correlation
(Source: Shennan 1997)

In figure four variables represented as a line with a direction, starting from common origin. In terms of pictorial representation, x_1 and x_2 are closely interrelated and neither is very closely related to x_3 , although x_2 is closer to it than x_1 , finally x_4 is more or less diametrically opposed to x_1 and x_2 and more or less unrelated to x_3 . The size of the angles can be directly related to the values of the correlation coefficients, these correspond to the cosines of the angles concerned. When two variables are perfectly correlated the angle between them is 0. In such a case the value of the correlation coefficient is 1, the cosine of angle is 0. (Shennan 1997).

In principle component analyses the variance of a linear combination of the variables are tried to be maximized. Principal components are concerned only with the core structure of a single sample of observations on p variables. The first principal component is the linear combination with the maximal variance, for a dimension along which the observations are maximally separated or spread out. The second principal component is the linear combination with maximal variance in a direction orthogonal to the first principal component (Rencher 2002).

Principal component analysis deals with a single sample of n observation vectors y_1, y_2, \dots, y_n that form a group of points in a p -dimensional space. Principal component analysis can be applied to any distribution of y , but it will be easier to visualize geometrically if the group of points is ellipsoidal. If the variables y_1, y_2, \dots, y_p in y are correlated, the ellipsoidal group of points is not oriented parallel to any of the axes represented by y_1, y_2, \dots, y_p . The natural axes of the group of points (the axes of the ellipsoid) with origin at \bar{y} , the mean vector of y_1, y_2, \dots, y_n is tried to be find. This is done by translating the origin to \bar{y} and then rotating the axes. After rotation so that the axes

become natural axes of the ellipsoid, the new variables (principal components) will be uncorrelated. The axes can be rotated by multiplying each y_i , by an orthogonal matrix \mathbf{A} .

$$z_i = \mathbf{A}y_i \quad (3.10)$$

thus an orthogonal matrix transforms y_i to a point z_i that is the same distance from the origin, and the axes are effectively rotated. Finding the axes of the ellipsoids is equivalent to finding the orthogonal matrix \mathbf{A} that rotates the axes to line up with the natural extensions of the group of points so that the new variables (principal components) z_1, z_2, \dots, z_p in $\mathbf{z} = \mathbf{A}\mathbf{y}$ are uncorrelated. Sample covariance matrix of \mathbf{z} , $\mathbf{S}_z = \mathbf{A}\mathbf{S}$ is going to be diagonal: (Rencher 2002).

$$\mathbf{S}_z = \mathbf{A}\mathbf{S}\mathbf{A}' = \begin{pmatrix} s_{z_1}^2 & 0 & \dots & 0 \\ 0 & s_{z_2}^2 & \dots & 0 \\ \vdots & \vdots & \dots & \vdots \\ 0 & 0 & \dots & s_{z_p}^2 \end{pmatrix}, \quad (3.11)$$

\mathbf{S} is the sample covariance matrix of y_1, y_2, \dots, y_n , by $\mathbf{S}\mathbf{C} = \mathbf{D} = \text{diag}(\lambda_1, \lambda_2, \lambda_1, \dots, \lambda_p)$ where the λ_i 's are eigenvalues of \mathbf{S} and \mathbf{C} is an orthogonal matrix whose columns are normalized eigenvectors of \mathbf{S} . The orthogonal matrix \mathbf{A} that diagonalizes \mathbf{S} is the transpose of the matrix \mathbf{C} :

$$\mathbf{A} = \mathbf{C}' = \begin{pmatrix} a'_1 \\ a'_2 \\ \vdots \\ a'_p \end{pmatrix}, \quad (3.12)$$

Where a_i is the i th normalized eigenvector of \mathbf{S} . The principal components are the transformed variables $z_1 = \dots, z_1 = \dots, \dots, z_p = \dots$, in $\mathbf{z} = \mathbf{A}\mathbf{y}$.

For every square matrix \mathbf{A} , a scalar λ and a non zero vector \mathbf{x} can be found such that

$$\mathbf{A}\mathbf{x} = \lambda\mathbf{x} \quad (3.13)$$

λ is called an eigenvalue of \mathbf{A} and \mathbf{x} is an eigenvector of \mathbf{A} corresponding to λ . The eigenvectors of an $n \times n$ symmetric matrix \mathbf{A} is mutually orthogonal. It follows that if the n eigenvectors of \mathbf{A} are normalized and inserted as columns of matrix $\mathbf{C} = (\mathbf{x}_1, \mathbf{x}_2, \dots, \mathbf{x}_n)$ then \mathbf{C} is orthogonal (Rencher 2002).



CHAPTER 4

Characterization of Archaeological Samples

4.1. Optical Microscopy Analysis

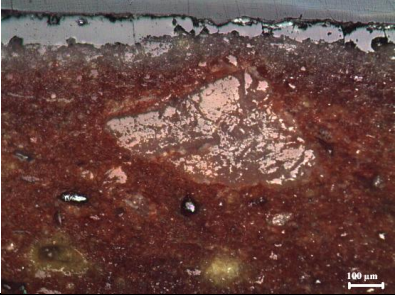
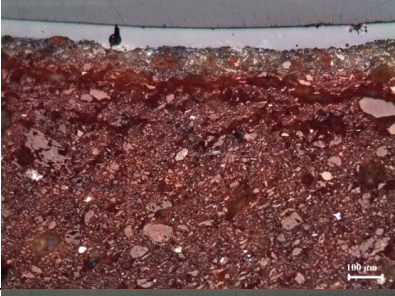
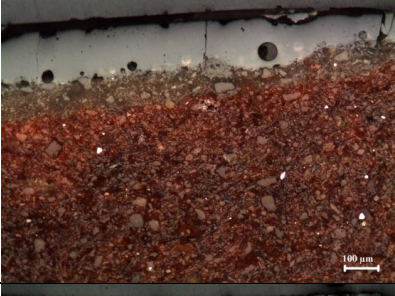


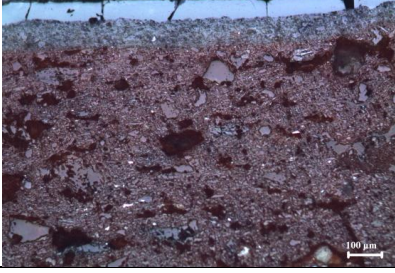
Optical microscopy analysis is performed by Leica DM 500 instrument. Investigated samples' codes, slip and glaze heights and glaze/slip ratio are given in Table 4.1. Thickness of slip and glaze parts were determined according to the optical image results.

Table 4.1. Optical microscopy images of samples

Codes	Optical Images	Slip Thickness (μm)	Glaze Thickness (μm)	Glaze/Slip Ratio
1.1.1.		67	90	1.3
1.1.2		34	80	2.4

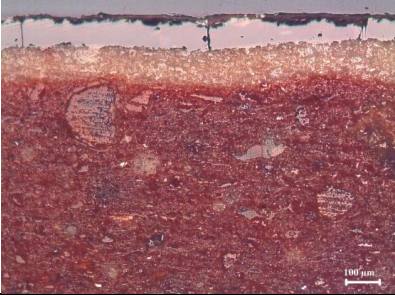
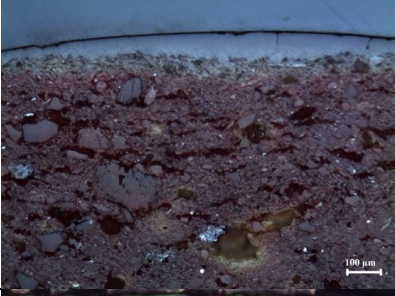

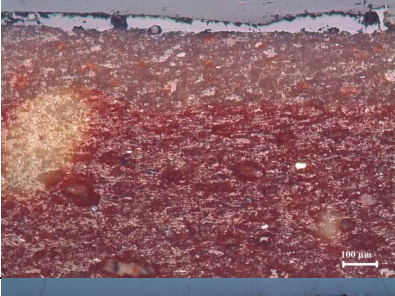


(cont. on next page)

Table 4.1 (cont.)

1.1.3		84	100	1.2
1.1.4		115	109	0.9
1.1.6		183	255	1.4
1.1.7		344	138	0.4
1.1.8		124	189	1.5
1.1.10		154	147	1.0


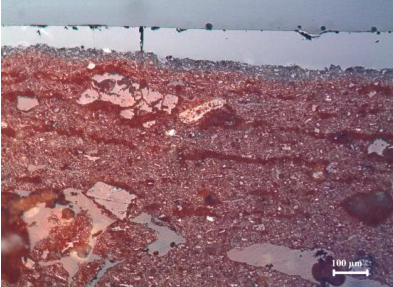
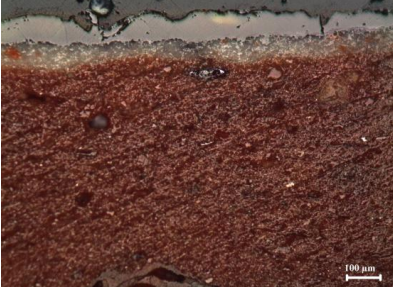

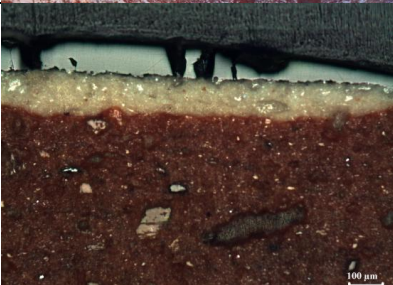

(cont. on next page)

Table 4.1 (cont.)

1.1.13		213	199	0.9
1.2.1		96	148	1.5
1.2.2.		54	125	2.3
1.2.3		444	90	0.2
1.2.5		87	270	3.1
1.3.1		145	141	1.0

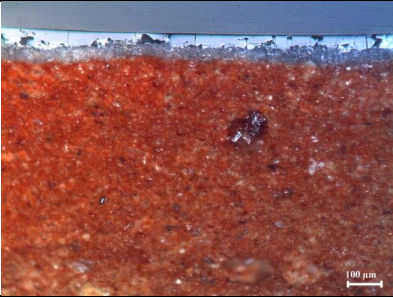
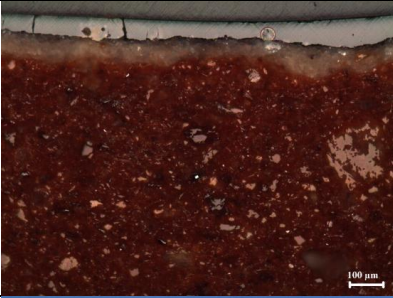

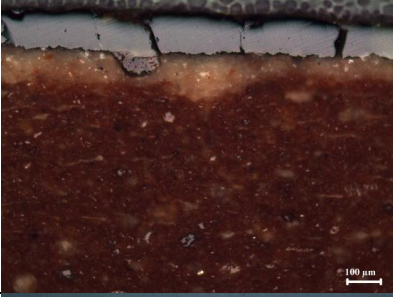
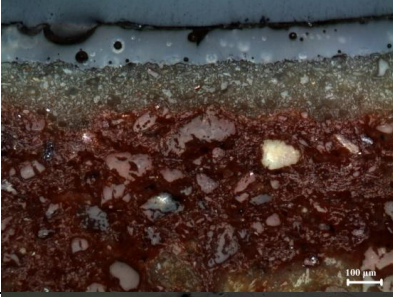
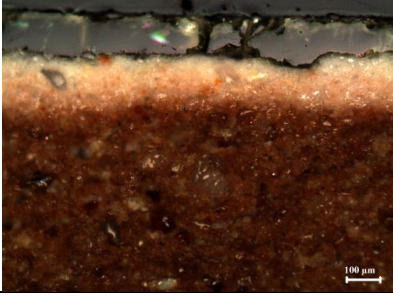
(cont. on next page)

Table 4.1 (cont.)

1.3.3		203	200	1.0
1.3.4		68	160	2.4
1.3.5.		123	175	1.4
1.3.6		98	165	1.7
1.3.8.		204	184	0.9
1.3.9		406	187	0.5


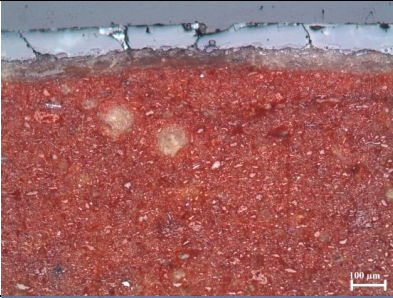
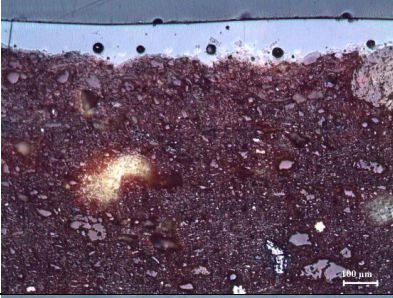
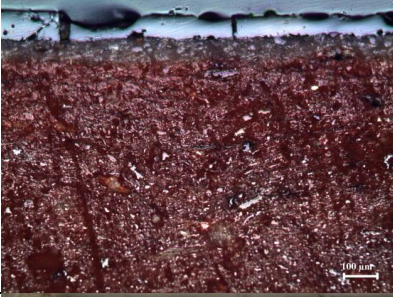

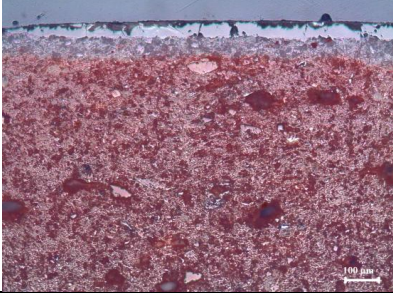
(cont. on next page)

Table 4.1 (cont.)

1.4.4		120	113	0.9
1.4.6		169	104	0.6
1.4.10		146	159	1.1
1.4.11		129	188	1.5
1.5.1		322	177	0.5
1.5.2		250	230	0.9

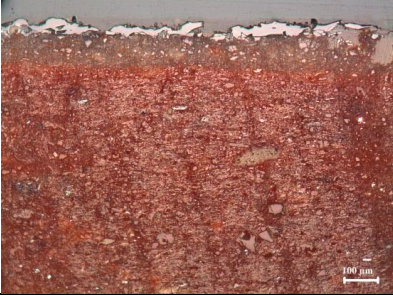
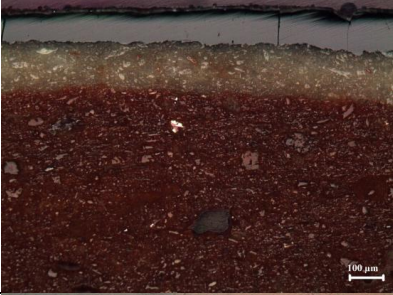
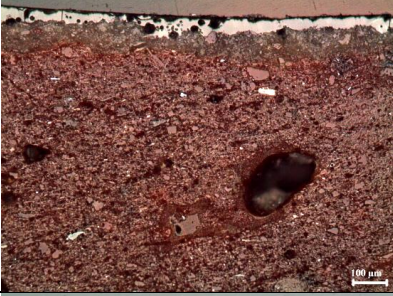

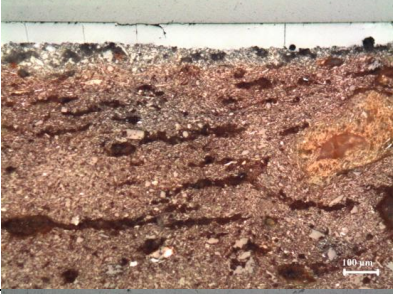
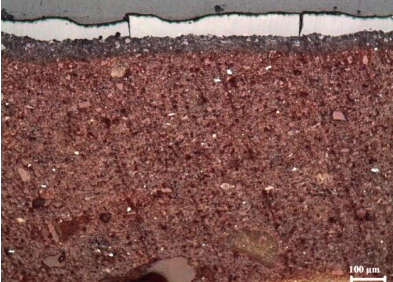
(cont. on next page)

Table 4.1 (cont.)

1.6.2.		78	101	1.3
1.6.3		113	229	2.0
1.6.4		162	159	1.0
2.2		130	115	0.9
2.3		143	112	0.8
3.1		118	83	0.7




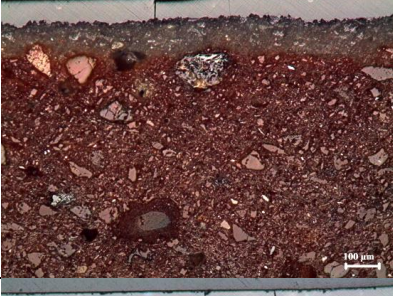


(cont. on next page)

Table 4.1 (cont.)

3.2		172	83	0.5
3.5.		280	164	0.6
3.6		144	69	0.5
3.8		154	88	0.6
3.10		128	125	1.0
3.11		106	132	1.2

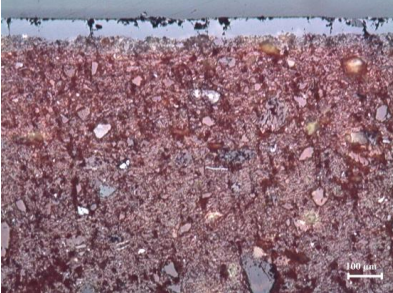
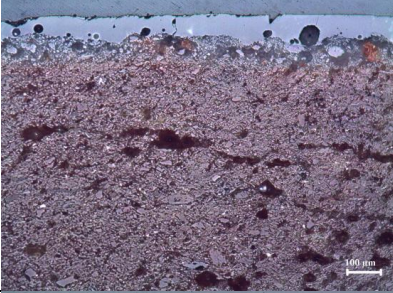
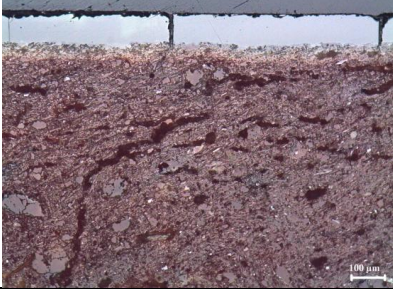
(cont. on next page)

Table 4.1 (cont.)

3.13		108	83	0.8
3.14		189	132	0.7
3.17		135	63	0.5
3.18		186	129	0.7
3.19		103	91	0.9
3.21		148	144	1.0

(cont. on next page)

Table 4.1 (cont.)

3.22		86	197	2.3
3.24		135	143	1.1
3.25		93	172	1.8

Glaze and slip layer thicknesses were measured from reflected light optical micrographs that were obtained in cross polars. In cross polars mode of the microscope these bossy, slip and glaze layers are clearly visible. It is difficult to separate these layers on SEM micrographs even in BSE mode which shows different chemistries in different areas in different greyscales. Results of measurements are given in Table 4.2.

Table 4.2. Thicknesses of slip and glaze layers

Group No.	Glaze/Slip Ratio	Slip Layer Thicknesses (μm)				Glaze Layer Thicknesses (μm)			
		Range	Mean	Median	Std.Dev.	Range	Mean	Median	Std.Dev.
1	0.2-3.1	34-444	163	129	103	80-255	159	159	50
2	0.8	143	-	-	-	112	-	-	-
3	0.5-2.3	86-280	143	135	48	63-197	119	127	40
Decoration type	Glaze/Slip Ratio	Slip Layer Thicknesses (μm)				Glaze Layer Thicknesses (μm)			
		Range	Mean	Median	Std.Dev.	Range	Mean	Median	Std.Dev.
Champlevé	0.9-3.1	67-204	132	129	64	90-270	169	160	57
Incised	0.5-2.3	54-406	182	146	101	63-255	146	141	46
Incised-Sgraffito	0.8-2.4	34-154	96	69	43	83-197	131	90	50
Fine Sgraffito	0.2-2	78-444	167	145	89	69-229	134	123	51

Considering the results Group 1 samples had the highest slip and glaze average thickness values and glaze/slip ratios compared to Groups 2 and 3. As per the decoration style, incised samples had the highest average slip thicknesses while incised-sgraffito samples had the lowest average slip thickness. This was expected because these techniques involve coarse tool tips and fine tool tips, respectively, for the incision of the surface during decoration (Papanikola-Bakirtzi 1999). Incised-sgraffito samples had average glaze height values close to those of fine sgraffito samples. Champlévé samples had the highest average glaze height value compared to others.

4.2. X-Ray Diffraction (XRD) Analysis

Mineralogical characterization of the body layers of the samples were done by XRD analysis via the usage of Philips X'pert Pro Diffractometer. Cu K α radiation was used for analysis. Determined mineralogical compositions of samples are given in Table 4.3 together with the estimated firing temperatures. The XRD pattern of the representative sample 1.1.13 is given in Figure 4.1. Mineralogical compositions and estimated firing temperatures of samples are given in Table 4.3.

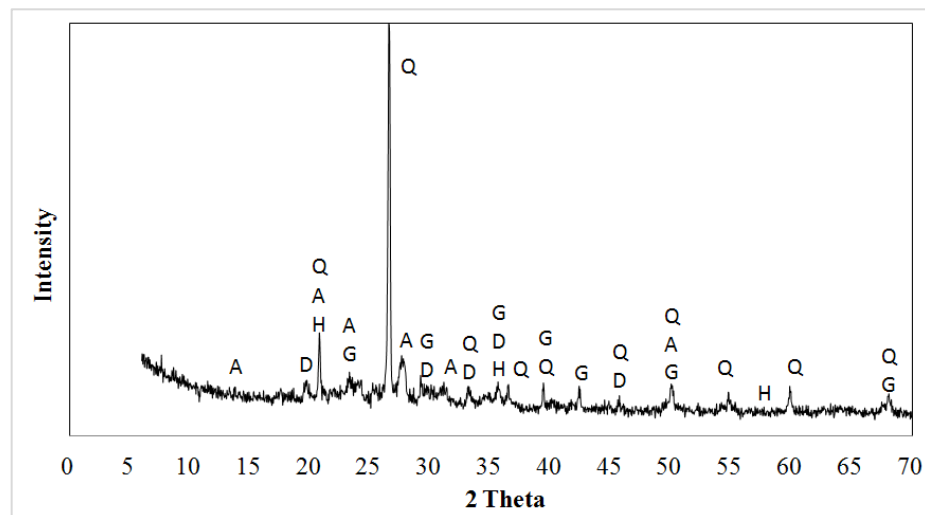


Figure 4.1. XRD pattern of sample 1.1.13

Table 4.3. Mineralogical compositions and estimated firing temperatures of the samples

Codes	Mineralogical Composition	Temperatures
1.1.1	Albite, Quartz, Diopside, Gehlenite, Hematite	800-900°C
1.1.2	Albite, Quartz, Diopside, Gehlenite, Muscovite	800-900°C
1.1.3	Albite, Quartz, Diopside, Muscovite	800-900°C
1.1.4	Albite, Quartz, Diopside, Gehlenite,	800-900°C
1.1.6	Albite, Quartz, Gehlenite	800-900°C
1.1.7	Albite, Quartz, Diopside, Gehlenite, Muscovite	800-900°C
1.1.8	Albite, Quartz, Diopside, Gehlenite	800-900°C
1.1.10	Albite, Quartz, Wollastonite, Gehlenite	800-900°C
1.1.13	Albite, Quartz, Diopside, Gehlenite, Hematite	800-900°C
1.2.1	Albite, Quartz, Diopside, Muscovite	800-900°C
1.2.2	Albite, Quartz, Muscovite	<900°C
1.2.3	Albite, Quartz, Hematite	>800°C
1.2.5	Albite, Quartz, Diopside	800-900°C
1.3.1	Albite, Quartz, Diopside	800-900°C
1.3.3	Albite, , Quartz, Diopside	800-900°C
1.3.4	Albite, Quartz, Diopside, Muscovite, Wollastonite	800-900°C
1.3.5	Albite, Quartz, Diopside	800-900°C
1.3.6	Albite, Quartz, Hematite, Muscovite	800-900°C
1.3.8	Albite, Quartz, Gehlenite	800-900°C
1.3.9	Albite, Quartz, Gehlenite, Muscovite, Wollastonite	800-900°C
1.4.4	Albite, Quartz, Microcline	800-900°C
1.4.6	Albite, Quartz, Gehlenite, Muscovite	800-900°C
1.4.11	Albite, Quartz, Diopside, Muscovite	800-900°C
1.5.1	Albite, Quartz, Diopside, Muscovite	800-900°C
1.5.2	Albite, Quartz, Muscovite, Hematite, Diopside	800-900°C
1.6.2	Albite, Quartz, Diopside	800-900°C
1.6.3	Albite, Quartz, Diopside	800-900°C
1.6.4	Albite, Quartz, Diopside	800-900°C
2.2	Albite, Quartz, Muscovite, Hematite	800-900°C
2.3	Albite, Quartz, Muscovite, Gehlenite	800-900°C

(cont. on next page)

Table 4.3 (cont.)

3.1	Albite, Quartz, Muscovite	<900°C
3.2	Albite, Quartz, Muscovite, Gehlenite	800-900°C
3.5	Albite, Quartz, Diopside, Gehlenite, Wollastonite,	800-900°C
3.6	Albite, Quartz, Diopside	800-900°C
3.8	Albite, Quartz, Diopside, Gehlenite	800-900°C
3.10	Albite, Quartz, Muscovite, Diopside	800-900°C
3.11	Albite, Quartz, Muscovite, Gehlenite,	800-900°C
3.13	Albite, Quartz, Diopside	800-900°C
3.14	Albite, Quartz, Wollastonite	800-900°C
3.17	Albite, Quartz, Diopside, Muscovite, Wollastonite	800-900°C
3.18	Albite, Quartz, Muscovite, Gehlenite	800-900°C
3.19	Albite, Quartz, Diopside, Hematite	800-900°C
3.21	Albite, Quartz, Diopside, Wollastonite, Orthoclase	800-900°C
3.22	Albite, Quartz, Diopside	800-900°C
3.24	Albite, Quartz, Muscovite, Gehlenite	800-900°C
3.25	Albite, Quartz, Diopside, Muscovite, Wollastonite	800-900°C

Quartz is generally the most abundant mineral phase followed by albite, mica (muscovite), diopside, wollastonite, gehlenite and dolomite. The presence of mica is reported here solely because it was identified as such in XRD analysis search-match software. The more explicit identification of the correct mineral needs further petrographic tests via thin section samples which was not performed in this thesis. Such a study would require an expertise in optical mineralogy which the author lacks. Groups were identified according to their morphological typology as well as the mineralogical properties. Groups 1 and 3 contain feldspar albite and quartz, followed by lesser amounts of diopside and muscovite while in some samples gehlenite, wollastonite and hematite were also found. Group 2 contains albite, quartz and muscovite followed by gehlenite and hematite while no diopside or wollastonite were observed. Hematite is detected in a few samples in this group.

Firing is the most important step in pottery production (See Section 2.4.5). Each of the raw materials in pottery has a function. Clay, for example, provides plasticity which makes shaping possible. Quartz provides the skeleton to the ceramic object which

provides stability of the shape at both high and low temperatures. Alkali containing minerals like feldspar provide the fluxing agents that help obtain partial vitrification necessary for mechanical strength. During firing with increment of temperature micro textural relationship between the paste matrix and the minerals changes. Endothermic and exothermic transformations occur in clay matrix, in mineral phases and at the interface of minerals and clay matrix (Riccardi et al. 1999). Transformations depends on the particle size, chemistry and mineralogical properties of clay raw material and tempers, firing temperature, soaking time and kiln atmosphere (Cultrone et al.2011). Unlike modern ceramics, these historical ceramics are not fired to high enough temperatures to achieve a high degree of vitrification. These are generally porous ceramics with loosely bonded phases.

Mineralogical composition of samples are related to mineralogical properties of the raw material, tempers added to samples and newly formed minerals during firing process (Ortega et al. 2010). Minerals observed in each sample group can be compared with data from the literature to predict the firing temperatures (Cultrone et al. 2001, Maritan et al. 2005, Maritan et al 2006, Jordan et al. 2009, Trindade et al. 2009, Tschegg et al. 2009).

During firing process for carbonate rich samples, decomposition of calcite in clay matrix occurs between 600-850°C, presence of calcite in the structure is the sign of temperature lower than 850°C (Ortega et al. 2010). This reaction depends on the grain size and chemistry of carbonates (Tschegg et al. 2009). CaO produced from this reaction reacts with free silica and alumina derived from the decomposition of illite minerals and composes the gehlenite at temperatures higher than 800°C (Ortega et al. 2010). Gehlenite, wollastonite and diopside are the main minerals formed newly during firing process of ceramics (Buxeda and Garrigos 1999). Calcareous structure of ceramics produces the gehlenite, wollastonite and diopside during firing procedure (Heimann and Maggetti 1979). Gehlenite and wollastonite which are stable at 800-900°C, are classified as intermediate compounds (Traoré et al. 2000) and breakdown to form anorthite at temperatures higher than 950°C (Rathossi 2004, Cultrone et al. 2001). Formation of pyroxenes, like diopside, starts at quartz-dolomite interface at 800-900°C (İssi et al.2011). Muscovite starts to break down in the range of 900-1000°C (Grimshaw 1971). Formation of high temperature minerals depends on the type of clay minerals, their particle size distribution, amount of calcite and period of firing process (Charalambous et al. 2010).

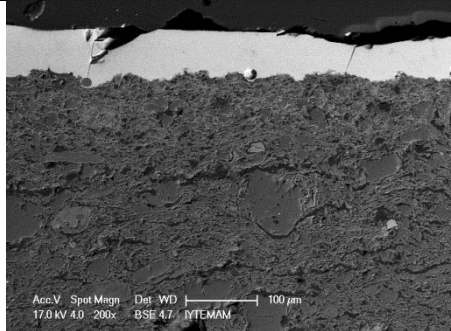
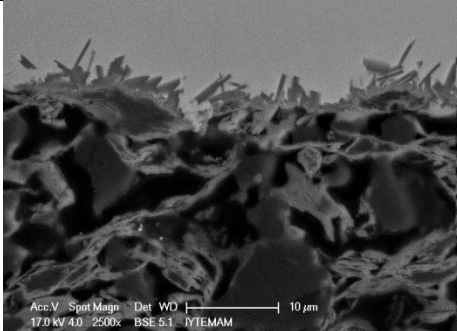
Hematite was detected in structure of a few samples. This is related with the occurrence of hematite in small particle size or poorly crystallized phase. The size of iron oxide crystals in ceramics depends on the firing temperature, firing atmosphere and amount of calcite in the structure of sample (Gangas et al., 1976; Maniatis et al., 1981, 1983). During the firing process with oxidizing atmosphere, destruction of initial clay minerals causes an increment of the amount of calcium aluminosilicates that incorporate ferric ions provided from clay lattice or from iron oxides. This reaction causes the decrement of the amount and size of ferric oxide (Maniatis et al., 1981, 1983; Wagner and Wagner, 2004).

XRD analysis which represent the minerals in the structure serves as indicator of the temperature ranges reached by the samples. According to the XRD analysis of the samples firing temperatures of the samples were predicted to be in the range of 800-900°C.

4.3. Scanning Electron Microscope (SEM-EDX) Analysis

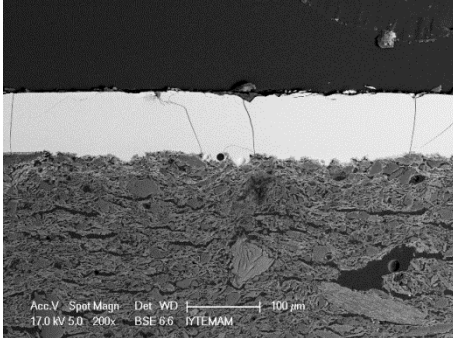
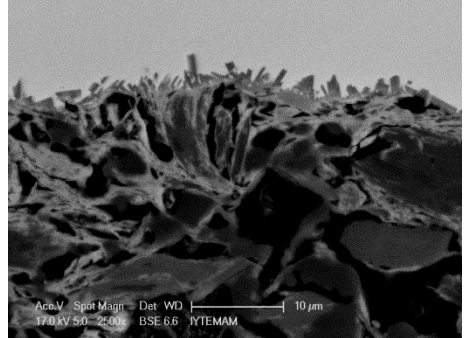
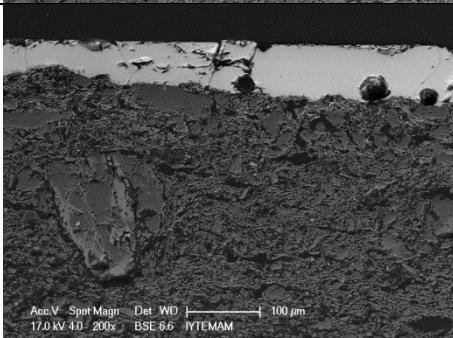
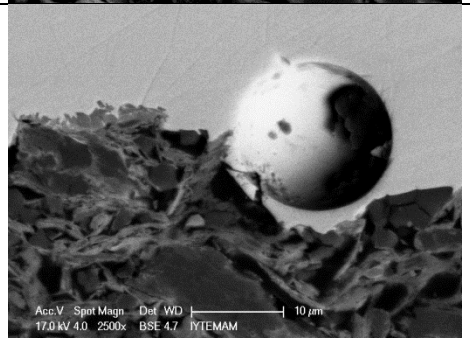
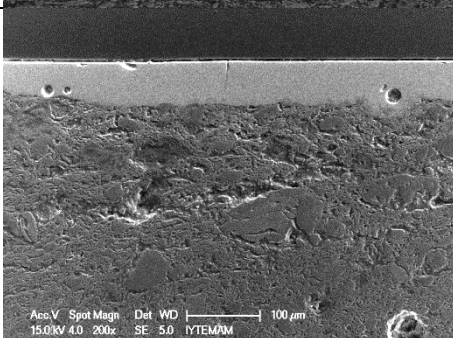
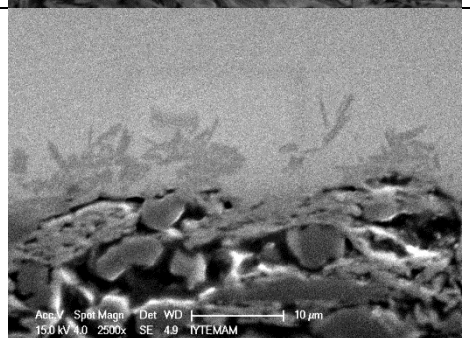
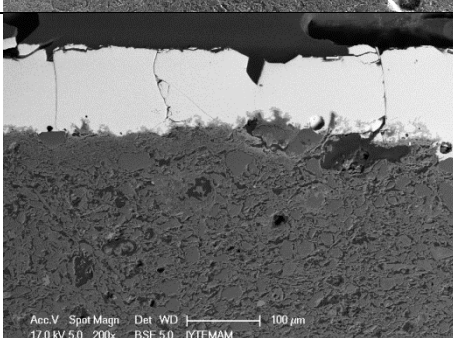
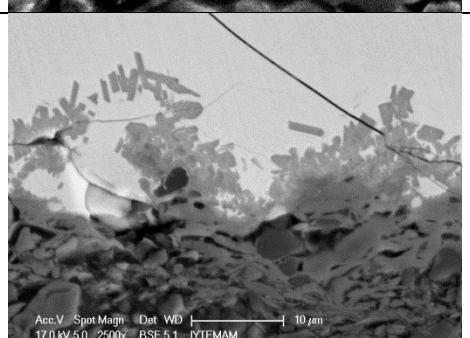
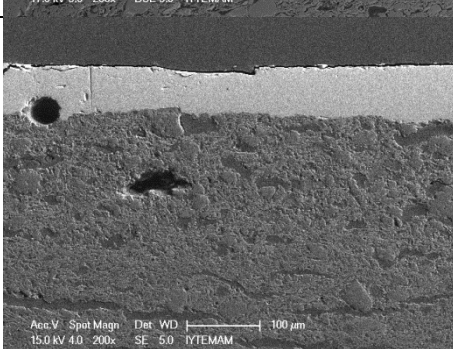
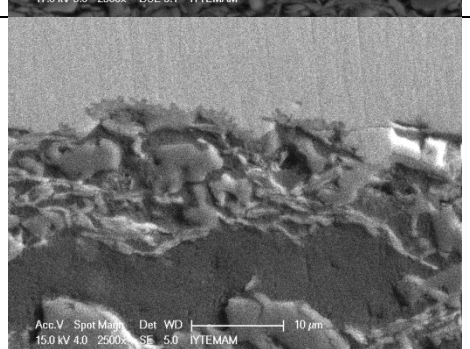
Microtexture and chemical composition of samples were determined by using the back-scattered electron image mode of low vacuum Scanning Electron Microscope (SEM) and the Energy Dispersive X-ray Technique (EDX), results are given in Table 4.4. SEM analysis were carried on polished samples after gold coating.

Table 4.4. SEM analysis results of samples (for 200X and 2500X magnifications)

Codes	200x	2500X
1.1.1		

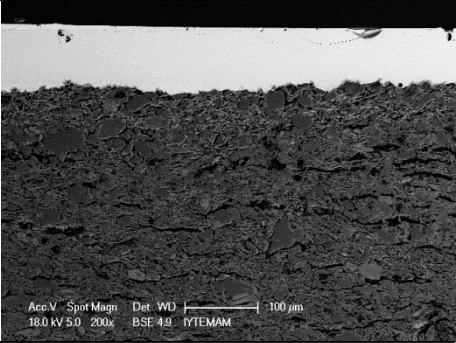
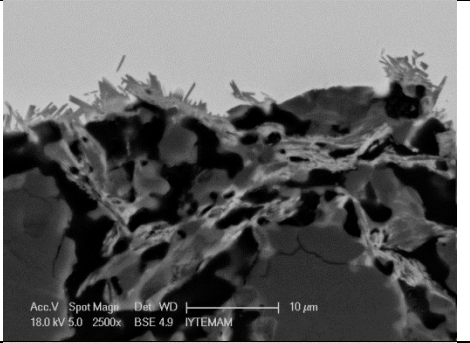
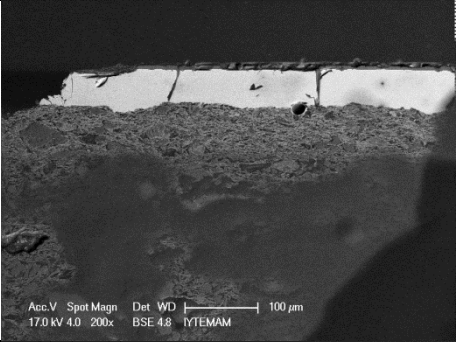
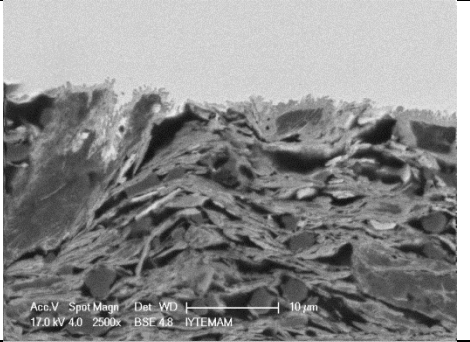
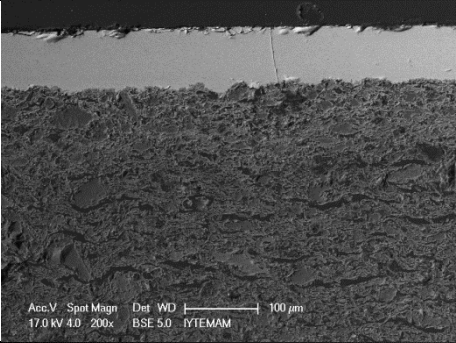
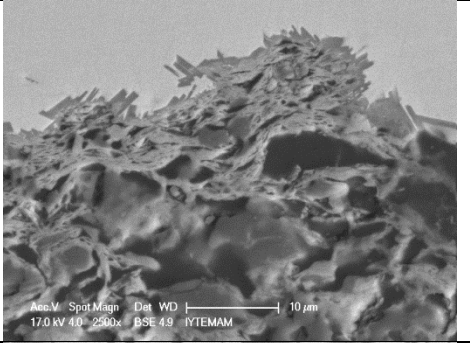
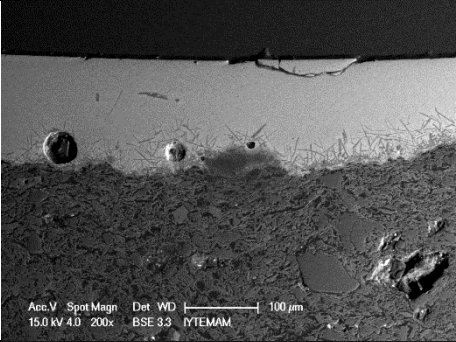
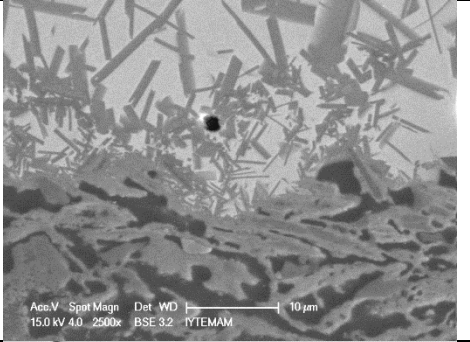
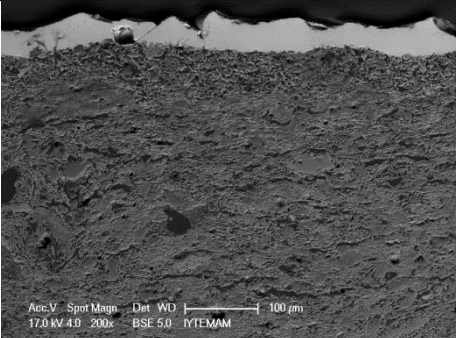
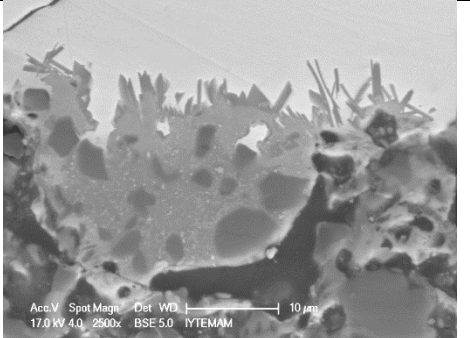
(cont. on next page)

Table 4.4 (cont.)

1.1.2	 <p>Acc.V Spot Magn Det WD 100 μm 17.0 kV 5.0 200x BSE 6.6 IYTEMAM</p>	 <p>Acc.V Spot Magn Det WD 10 μm 17.0 kV 5.0 2500x BSE 6.6 IYTEMAM</p>
1.1.3	 <p>Acc.V Spot Magn Det WD 100 μm 17.0 kV 4.0 200x BSE 6.6 IYTEMAM</p>	 <p>Acc.V Spot Magn Det WD 10 μm 17.0 kV 4.0 2500x BSE 4.7 IYTEMAM</p>
1.1.4	 <p>Acc.V Spot Magn Det WD 100 μm 15.0 kV 4.0 200x SE 5.0 IYTEMAM</p>	 <p>Acc.V Spot Magn Det WD 10 μm 15.0 kV 4.0 2500x SE 4.9 IYTEMAM</p>
1.1.6	 <p>Acc.V Spot Magn Det WD 100 μm 17.0 kV 5.0 200x BSE 5.0 IYTEMAM</p>	 <p>Acc.V Spot Magn Det WD 10 μm 17.0 kV 5.0 2500x BSE 6.1 IYTEMAM</p>
1.1.7	 <p>Acc.V Spot Magn Det WD 100 μm 15.0 kV 4.0 200x SE 5.0 IYTEMAM</p>	 <p>Acc.V Spot Magn Det WD 10 μm 15.0 kV 4.0 2500x SE 5.0 IYTEMAM</p>

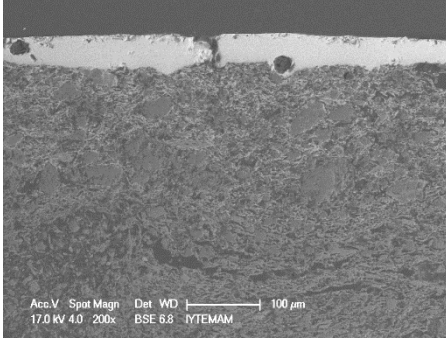
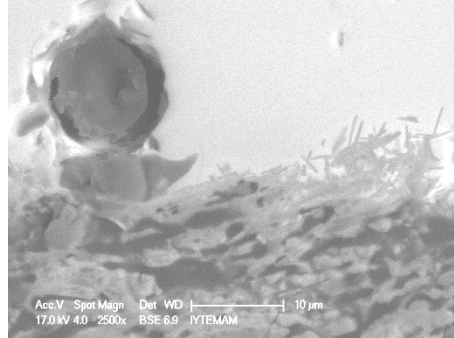
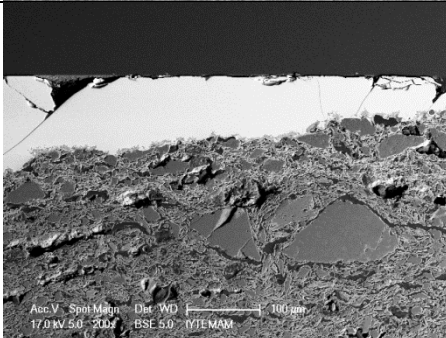
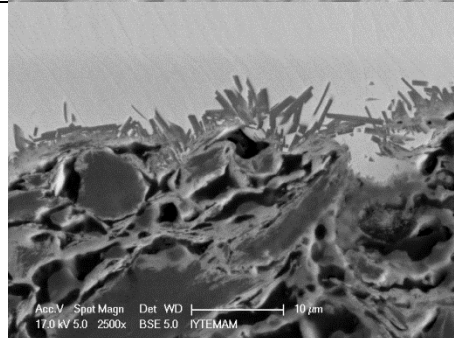

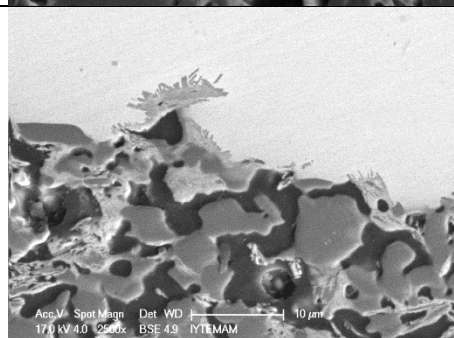
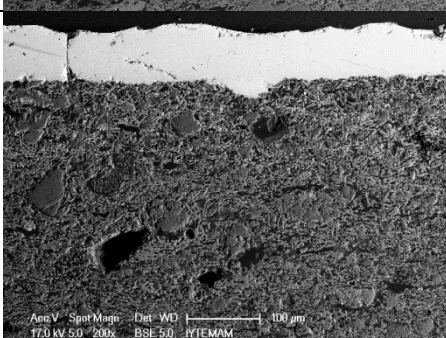
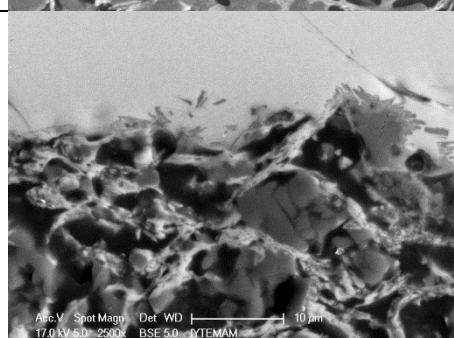
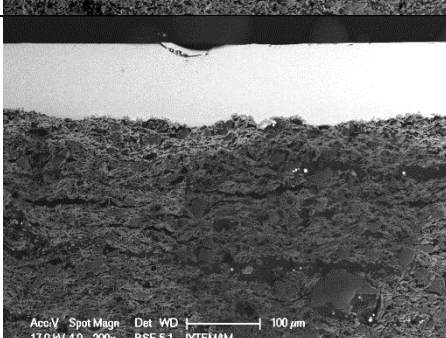
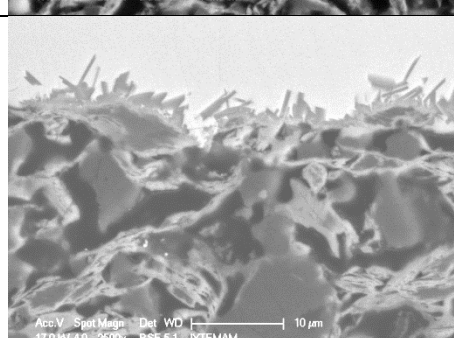
(cont. on next page)

Table 4.4 (cont.)

<p>1.1.8</p>		
<p>1.1.10</p>		
<p>1.1.13</p>		
<p>1.2.1</p>		
<p>1.2.2</p>		

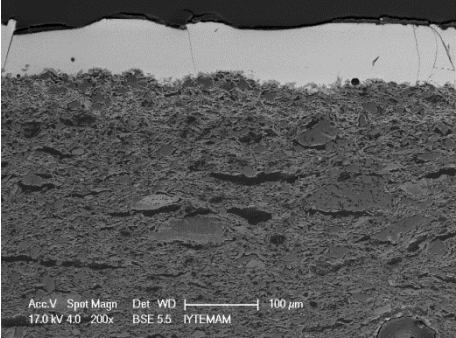
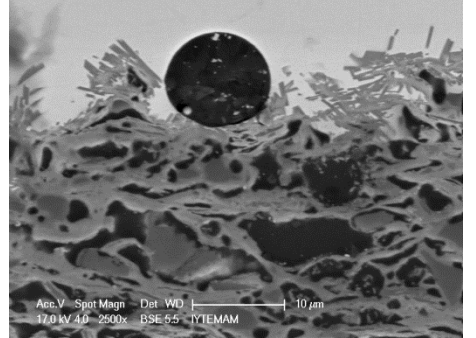
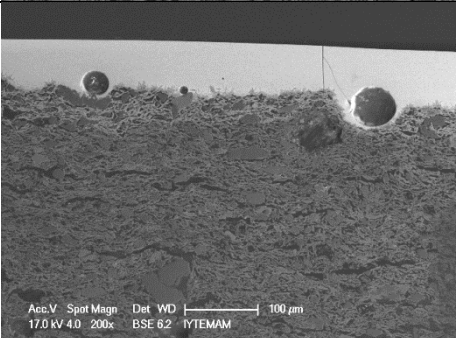
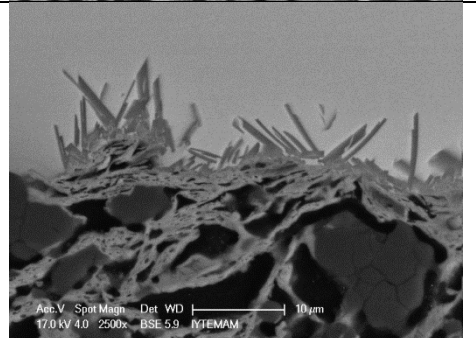
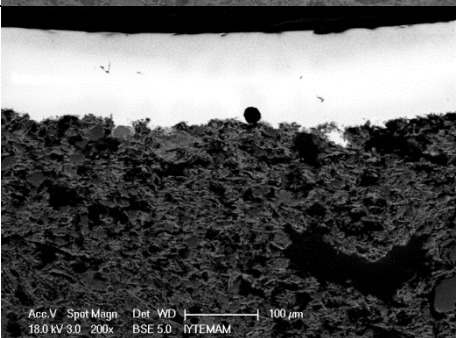
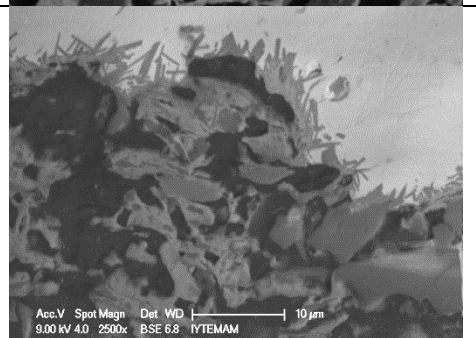
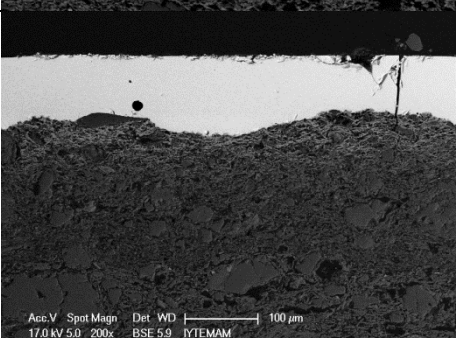
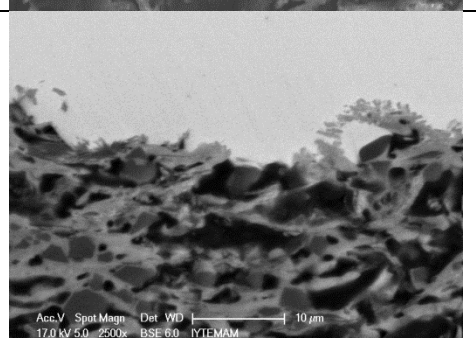
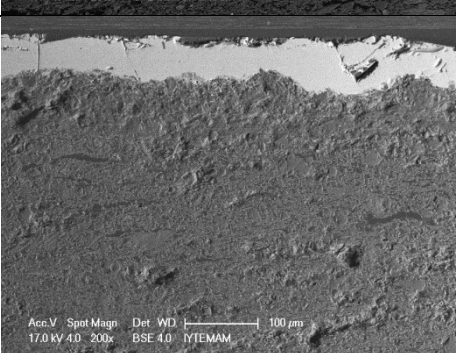
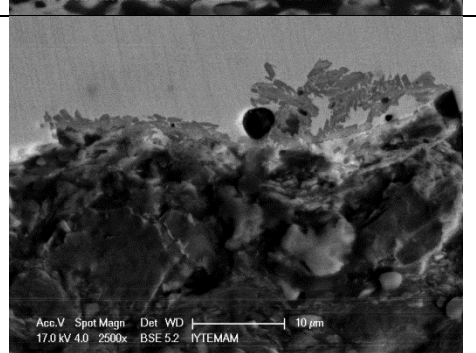
(cont. on next page)

Table 4.4 (cont.)

1.2.3		
1.2.5		
1.3.1		
1.3.3		
1.3.4		

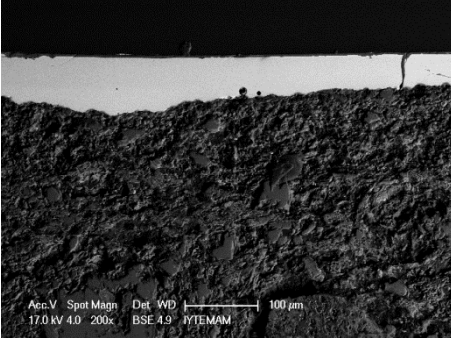
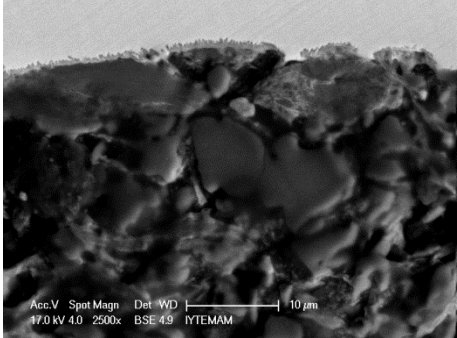
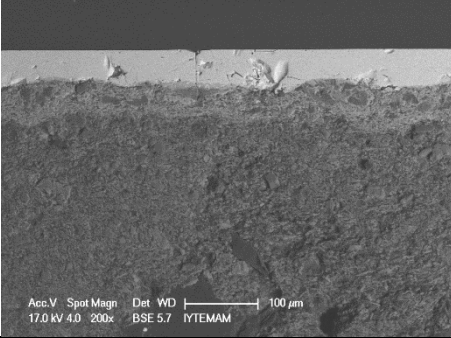
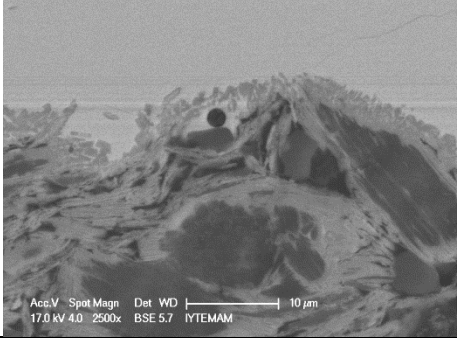
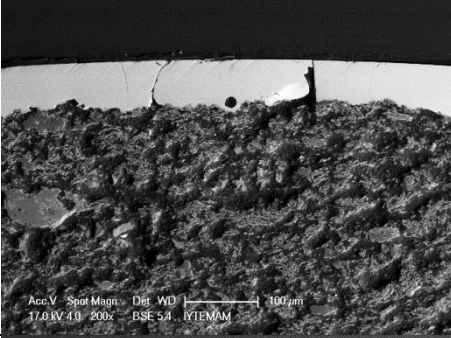
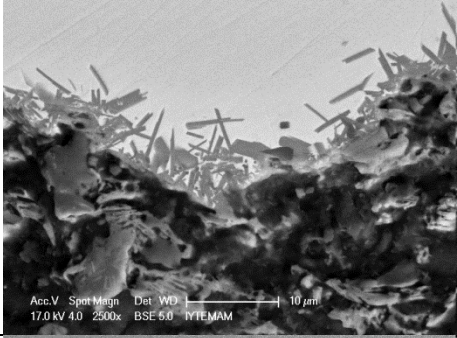
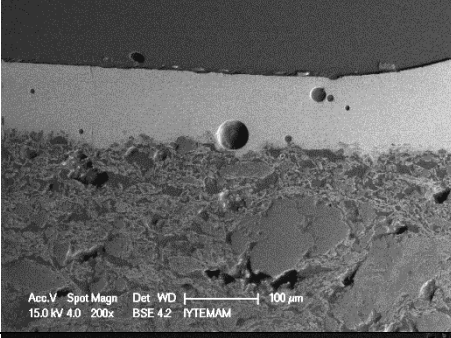
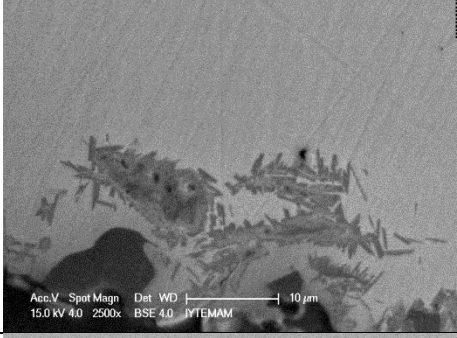
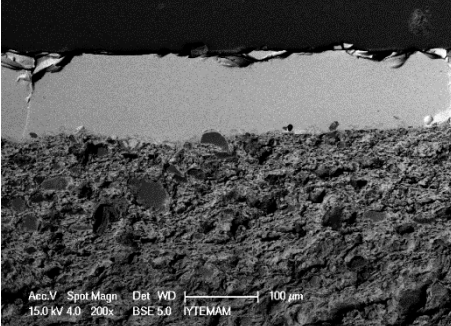
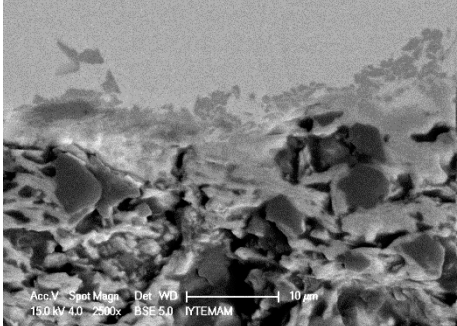
(cont. on next page)

Table 4.4 (cont.)

1.3.5	 <p>Acc.V Spot Magn Det WD 100 μm 17.0 kV 4.0 200x BSE 5.5 IYTEMAM</p>	 <p>Acc.V Spot Magn Det WD 10 μm 17.0 kV 4.0 2500x BSE 5.5 IYTEMAM</p>
1.3.6	 <p>Acc.V Spot Magn Det WD 100 μm 17.0 kV 4.0 200x BSE 6.2 IYTEMAM</p>	 <p>Acc.V Spot Magn Det WD 10 μm 17.0 kV 4.0 2500x BSE 5.9 IYTEMAM</p>
1.3.8	 <p>Acc.V Spot Magn Det WD 100 μm 18.0 kV 3.0 200x BSE 5.0 IYTEMAM</p>	 <p>Acc.V Spot Magn Det WD 10 μm 9.00 kV 4.0 2500x BSE 6.8 IYTEMAM</p>
1.3.9	 <p>Acc.V Spot Magn Det WD 100 μm 17.0 kV 5.0 200x BSE 5.9 IYTEMAM</p>	 <p>Acc.V Spot Magn Det WD 10 μm 17.0 kV 5.0 2500x BSE 6.0 IYTEMAM</p>
1.4.4	 <p>Acc.V Spot Magn Det WD 100 μm 17.0 kV 4.0 200x BSE 4.0 IYTEMAM</p>	 <p>Acc.V Spot Magn Det WD 10 μm 17.0 kV 4.0 2500x BSE 5.2 IYTEMAM</p>

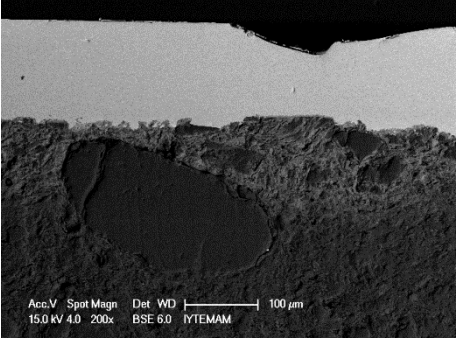
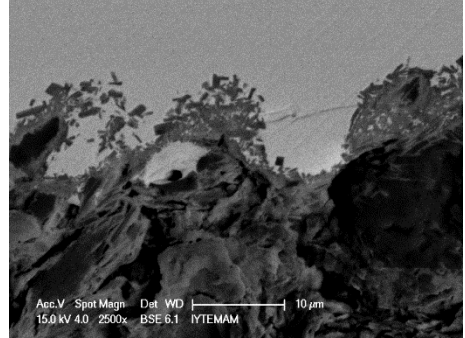
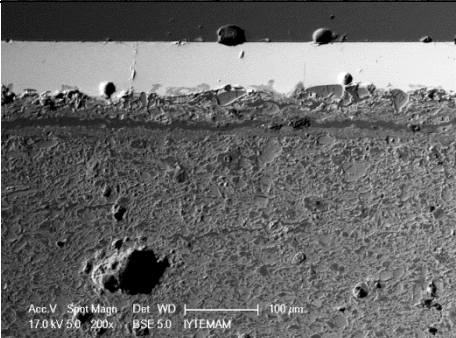
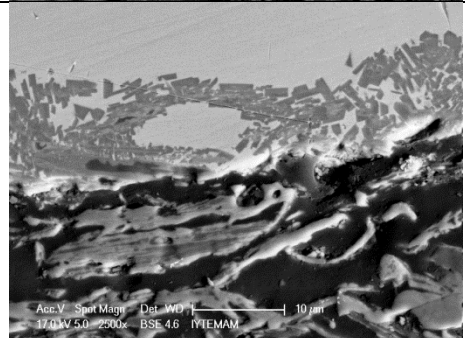
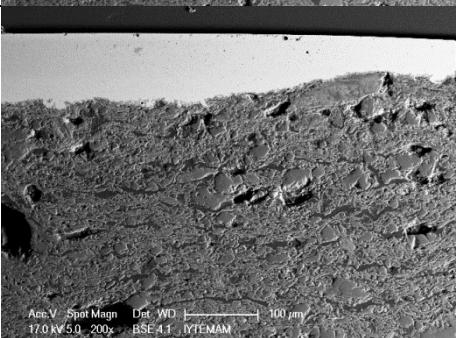
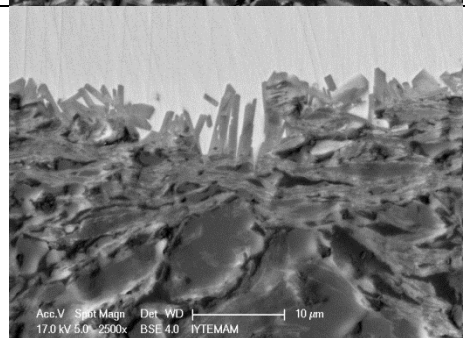
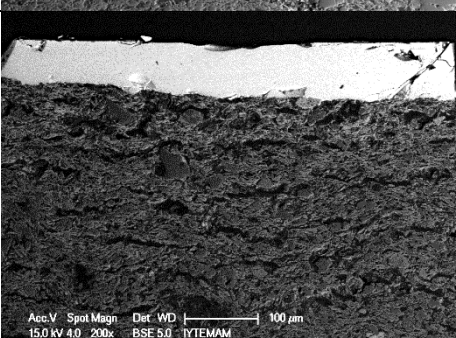
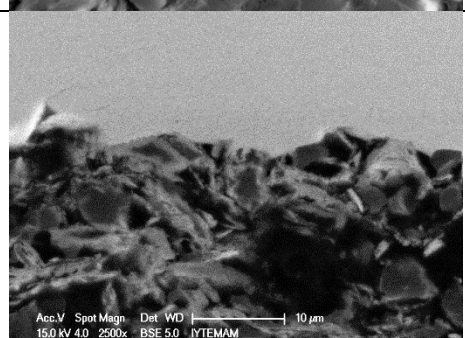
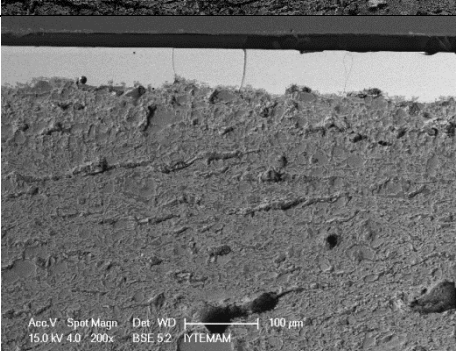
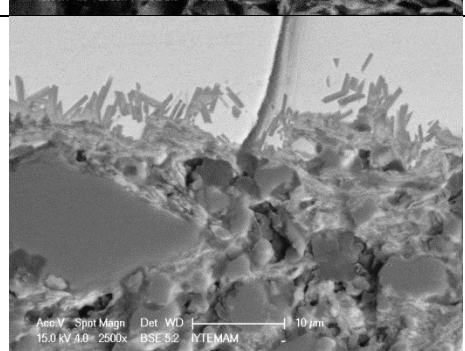
(cont. on next page)

Table 4.4 (cont.)

<p>1.4.6</p>	 <p>Acc.V Spot Magn Det WD 100 μm 17.0 kV 4.0 200x BSE 4.9 IYTEMAM</p>	 <p>Acc.V Spot Magn Det WD 10 μm 17.0 kV 4.0 2500x BSE 4.9 IYTEMAM</p>
<p>1.4.10</p>	 <p>Acc.V Spot Magn Det WD 100 μm 17.0 kV 4.0 200x BSE 5.7 IYTEMAM</p>	 <p>Acc.V Spot Magn Det WD 10 μm 17.0 kV 4.0 2500x BSE 5.7 IYTEMAM</p>
<p>1.4.11</p>	 <p>Acc.V Spot Magn Det WD 100 μm 17.0 kV 4.0 200x BSE 5.4 IYTEMAM</p>	 <p>Acc.V Spot Magn Det WD 10 μm 17.0 kV 4.0 2500x BSE 6.0 IYTEMAM</p>
<p>1.5.1</p>	 <p>Acc.V Spot Magn Det WD 100 μm 15.0 kV 4.0 200x BSE 4.2 IYTEMAM</p>	 <p>Acc.V Spot Magn Det WD 10 μm 15.0 kV 4.0 2500x BSE 4.0 IYTEMAM</p>
<p>1.5.2</p>	 <p>Acc.V Spot Magn Det WD 100 μm 15.0 kV 4.0 200x BSE 5.0 IYTEMAM</p>	 <p>Acc.V Spot Magn Det WD 10 μm 15.0 kV 4.0 2500x BSE 5.0 IYTEMAM</p>

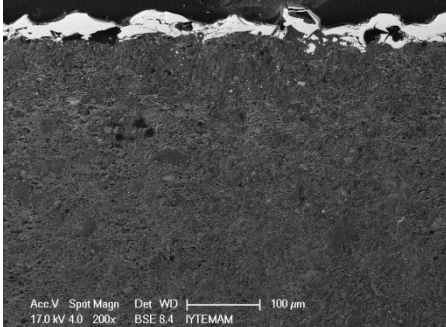
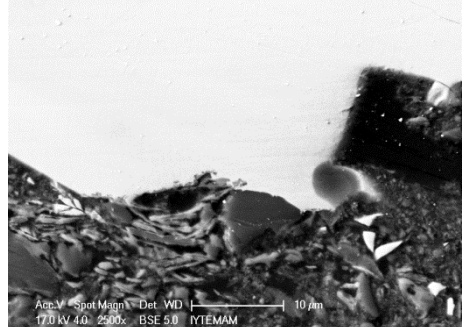
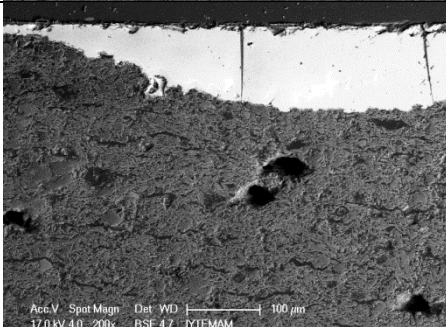
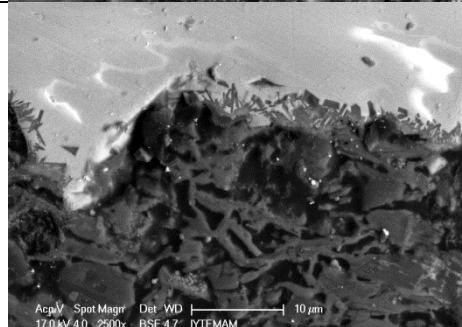
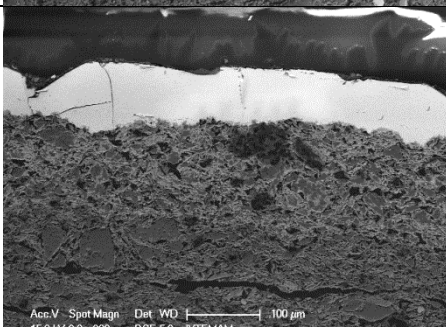
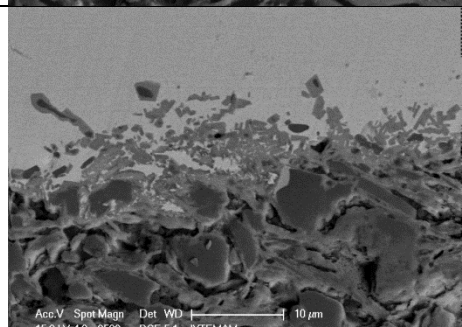
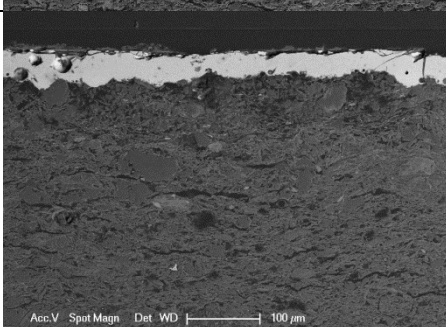
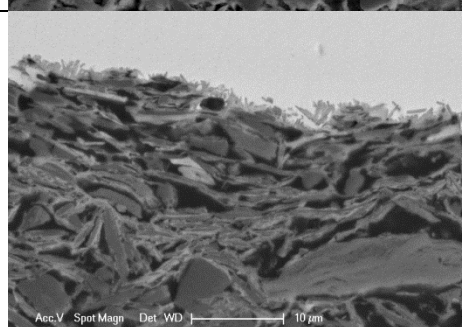
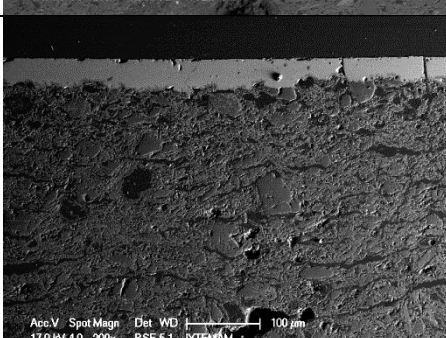
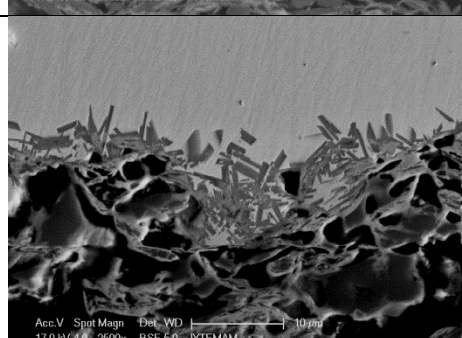
(cont. on next page)

Table 4.4 (cont.)

1.6.2	 <p>Acc.V Spot Magn Det WD 100 μm 15.0 kV 4.0 200x BSE 6.0 IYTEMAM</p>	 <p>Acc.V Spot Magn Det WD 10 μm 15.0 kV 4.0 2500x BSE 6.1 IYTEMAM</p>
1.6.3	 <p>Acc.V Spot Magn Det WD 100 μm 17.0 kV 5.0 200x BSE 5.0 IYTEMAM</p>	 <p>Acc.V Spot Magn Det WD 10 μm 17.0 kV 5.0 2500x BSE 4.6 IYTEMAM</p>
1.6.4	 <p>Acc.V Spot Magn Det WD 100 μm 17.0 kV 5.0 200x BSE 4.1 IYTEMAM</p>	 <p>Acc.V Spot Magn Det WD 10 μm 17.0 kV 5.0 2500x BSE 4.0 IYTEMAM</p>
2.2	 <p>Acc.V Spot Magn Det WD 100 μm 15.0 kV 4.0 200x BSE 5.0 IYTEMAM</p>	 <p>Acc.V Spot Magn Det WD 10 μm 15.0 kV 4.0 2500x BSE 5.0 IYTEMAM</p>
2.3	 <p>Acc.V Spot Magn Det WD 100 μm 15.0 kV 4.0 200x BSE 5.2 IYTEMAM</p>	 <p>Acc.V Spot Magn Det WD 10 μm 15.0 kV 4.0 2500x BSE 5.2 IYTEMAM</p>

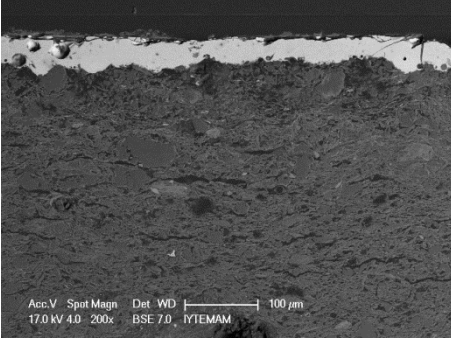
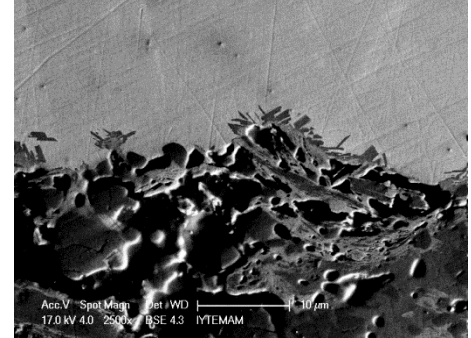
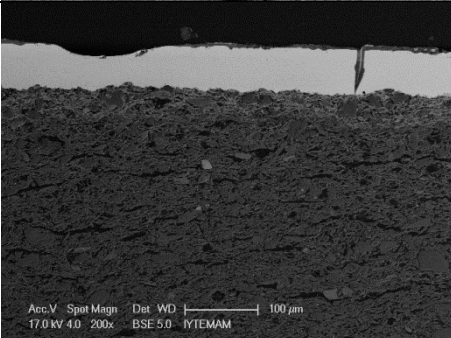
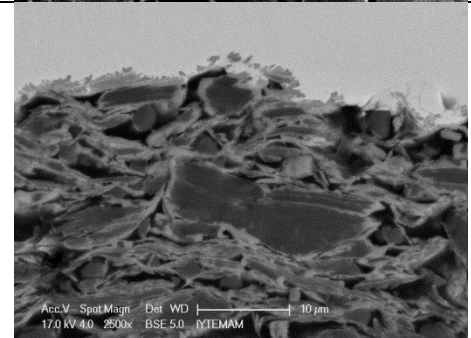
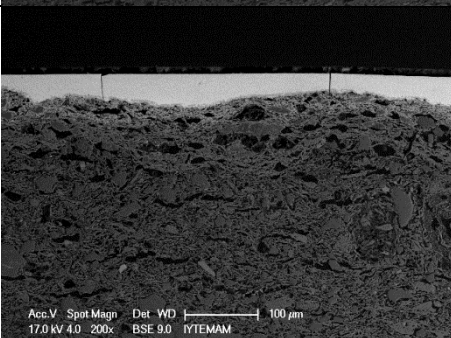
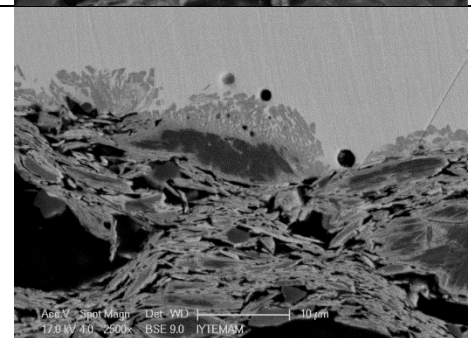
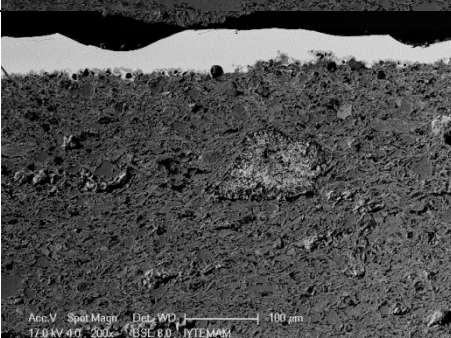
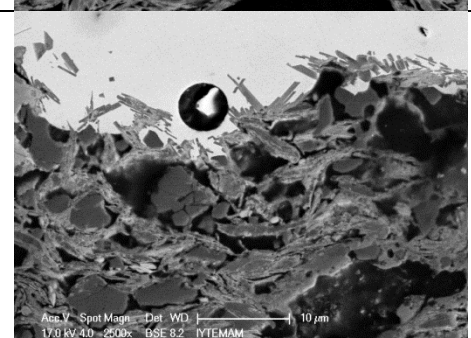
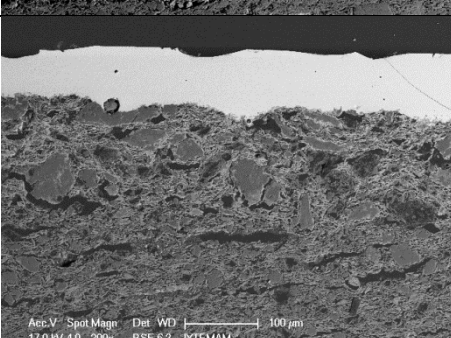
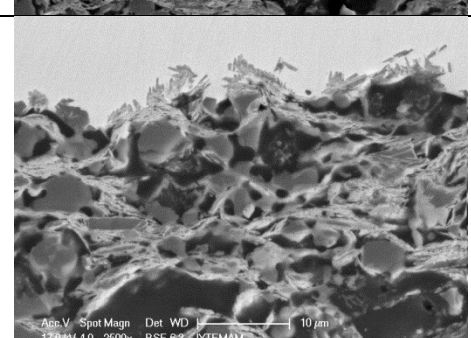
(cont. on next page)

Table 4.4 (cont.)

<p>3.1</p>	 <p>Acc.V Spot Magn Det WD 100 μm 17.0 kV 4.0 200x BSE 8.4 IYTEMAM</p>	 <p>Acc.V Spot Magn Det WD 10 μm 17.0 kV 4.0 2500x BSE 5.0 IYTEMAM</p>
<p>3.2</p>	 <p>Acc.V Spot Magn Det WD 100 μm 17.0 kV 4.0 200x BSE 4.7 IYTEMAM</p>	 <p>Acc.V Spot Magn Det WD 10 μm 17.0 kV 4.0 2500x BSE 4.7 IYTEMAM</p>
<p>3.5</p>	 <p>Acc.V Spot Magn Det WD 100 μm 15.0 kV 3.0 200x BSE 5.2 IYTEMAM</p>	 <p>Acc.V Spot Magn Det WD 10 μm 15.0 kV 4.0 2500x BSE 5.1 IYTEMAM</p>
<p>3.6</p>	 <p>Acc.V Spot Magn Det WD 100 μm 17.0 kV 4.0 200x BSE 7.0 IYTEMAM</p>	 <p>Acc.V Spot Magn Det WD 10 μm 17.0 kV 4.0 2500x BSE 7.0 IYTEMAM</p>
<p>3.8</p>	 <p>Acc.V Spot Magn Det WD 100 μm 17.0 kV 4.0 200x BSE 5.1 IYTEMAM</p>	 <p>Acc.V Spot Magn Det WD 10 μm 17.0 kV 4.0 2500x BSE 5.0 IYTEMAM</p>

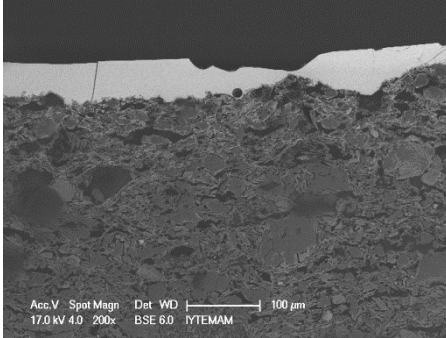
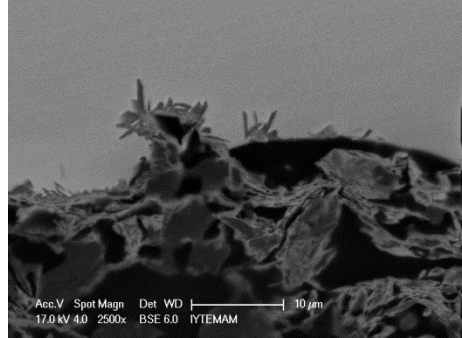
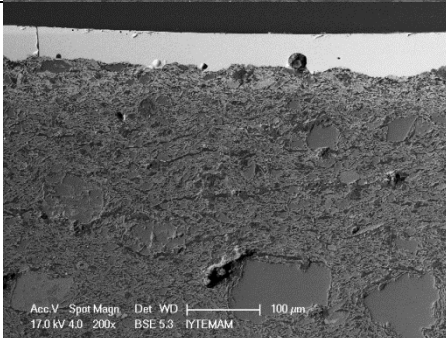
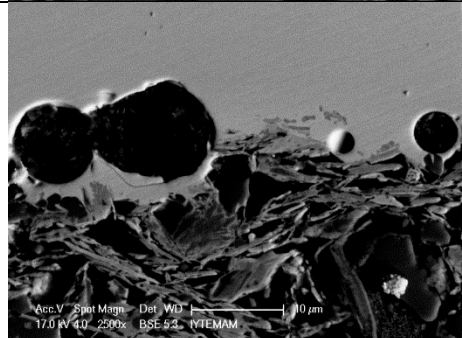
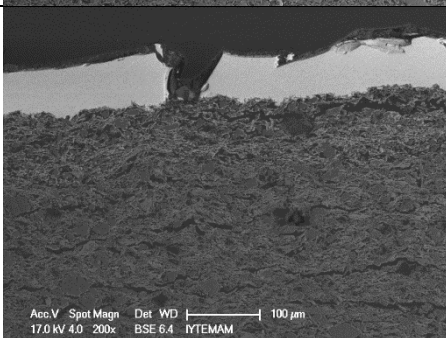
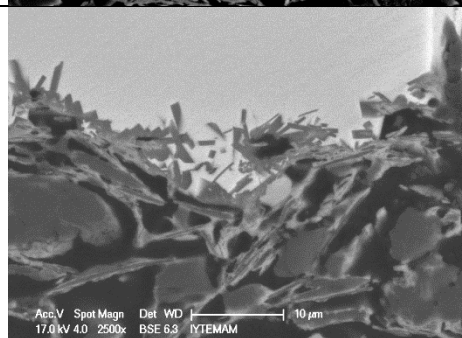
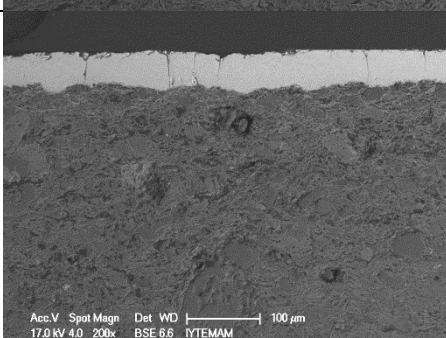
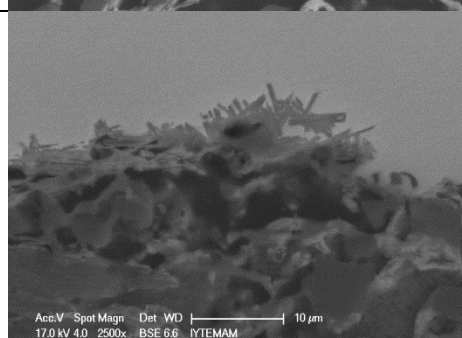
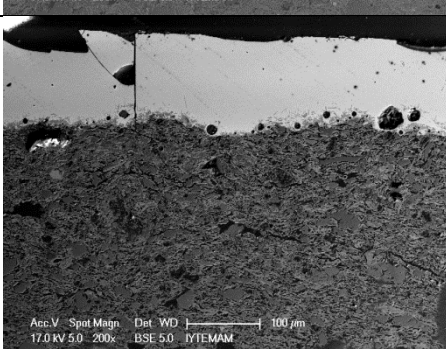
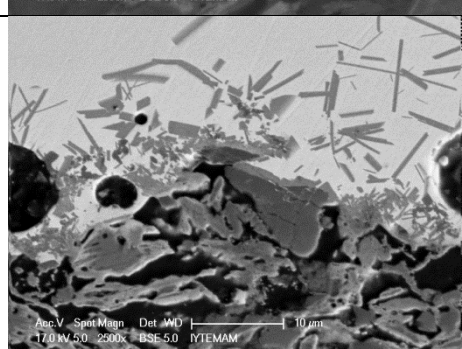
(cont. on next page)

Table 4.4 (cont.)

3.10	 <p>Acc.V Spot Magn Det WD 100 μm 17.0 kV 4.0 200x BSE 7.0 IYTEMAM</p>	 <p>Acc.V Spot Magn Det WD 10 μm 17.0 kV 4.0 2500x BSE 4.3 IYTEMAM</p>
3.11	 <p>Acc.V Spot Magn Det WD 100 μm 17.0 kV 4.0 200x BSE 5.0 IYTEMAM</p>	 <p>Acc.V Spot Magn Det WD 10 μm 17.0 kV 4.0 2500x BSE 5.0 IYTEMAM</p>
3.13	 <p>Acc.V Spot Magn Det WD 100 μm 17.0 kV 4.0 200x BSE 9.0 IYTEMAM</p>	 <p>Acc.V Spot Magn Det WD 10 μm 17.0 kV 4.0 2500x BSE 9.0 IYTEMAM</p>
3.14	 <p>Acc.V Spot Magn Det WD 100 μm 17.0 kV 4.0 200x BSE 8.0 IYTEMAM</p>	 <p>Acc.V Spot Magn Det WD 10 μm 17.0 kV 4.0 2500x BSE 8.2 IYTEMAM</p>
3.17	 <p>Acc.V Spot Magn Det WD 100 μm 17.0 kV 4.0 200x BSE 6.3 IYTEMAM</p>	 <p>Acc.V Spot Magn Det WD 10 μm 17.0 kV 4.0 2500x BSE 6.3 IYTEMAM</p>

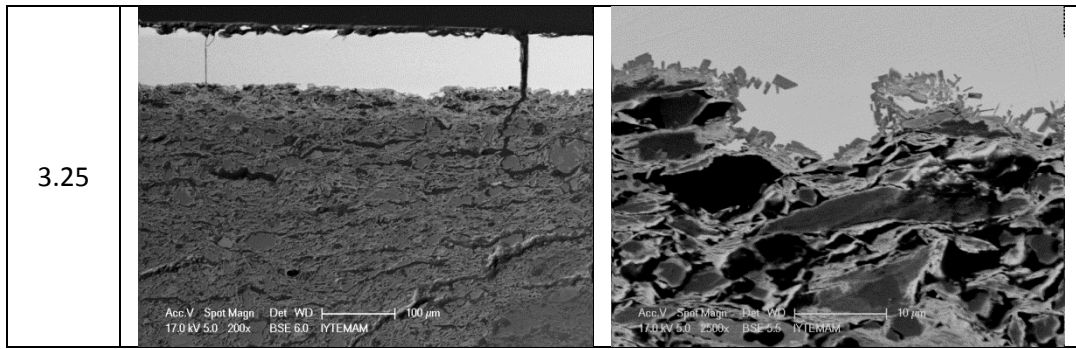
(cont. on next page)

Table 4.4 (cont.)

3.18	 <p>Acc.V Spot Magn Det WD 100 μm 17.0 kV 4.0 200x BSE 6.0 IYTEMAM</p>	 <p>Acc.V Spot Magn Det WD 10 μm 17.0 kV 4.0 2500x BSE 6.0 IYTEMAM</p>
3.19	 <p>Acc.V Spot Magn Det WD 100 μm 17.0 kV 4.0 200x BSE 5.3 IYTEMAM</p>	 <p>Acc.V Spot Magn Det WD 10 μm 17.0 kV 4.0 2500x BSE 5.3 IYTEMAM</p>
3.21	 <p>Acc.V Spot Magn Det WD 100 μm 17.0 kV 4.0 200x BSE 6.4 IYTEMAM</p>	 <p>Acc.V Spot Magn Det WD 10 μm 17.0 kV 4.0 2500x BSE 6.3 IYTEMAM</p>
3.22	 <p>Acc.V Spot Magn Det WD 100 μm 17.0 kV 4.0 200x BSE 6.6 IYTEMAM</p>	 <p>Acc.V Spot Magn Det WD 10 μm 17.0 kV 4.0 2500x BSE 6.6 IYTEMAM</p>
3.24	 <p>Acc.V Spot Magn Det WD 100 μm 17.0 kV 5.0 200x BSE 5.0 IYTEMAM</p>	 <p>Acc.V Spot Magn Det WD 10 μm 17.0 kV 5.0 2500x BSE 5.0 IYTEMAM</p>

(cont. on next page)

Table 4.4 (cont.)



Due to high lead content, glaze layer had a high BSE yield. Some of the samples had cracks and bubbles in their glaze part. Existence of bubbles in the glaze can be related to viscosity of the glaze and the occurrence of gas-forming-reactions in the body. Lead oxide, in addition to its low melting point, acts as flux in the structure of glaze. Samples with few bubbles have high PbO content and high fluidity which allows gas bubbles to escape during firing. A high proportion of bubbles are observed in viscous glazes with low lead oxide amount (Maltoni et al.2012). Bubbles observed in the glaze layer can mainly be attributed to released carbon dioxide during decomposition of calcite in calcareous bodies during firing process (Saad 2002). The interface between the slip and the body layers was difficult to determine in SEM images due to the similarities the composition of clay. During the firing process interaction between body and glaze layers produces an interaction layer. This reaction depends on many factors like firing temperature, porosity, composition of glaze and body layers, firing atmosphere, firing duration (Tite et al. 1998, Molera et al. 1998). Diffusion of elements from body to glaze and glaze to body layers takes place while new crystals are formed at this interaction zone (Tite et al. 1998). According to SEM results all samples had this interaction zone in changing thicknesses.

Chemical composition of body, slip and glaze layers of samples are determined by EDX method. Measurements are taken from three areas and the results are given as average values. Body parts of the samples are composed mainly from silica (34-62 %wt) (Table 4.5). Silica is the most abundant mineral in all traditional ceramics. These Byzantine ceramics are no exception. Silica ends up in clay because the two minerals coexist in nature and also during weathering they are always observed together. Byzantine ceramists were probably not interested in adding more quartz to clay like their modern counterparts. Al₂O₃ concentration ranges between 12-20 %wt,

Fe_2O_3 concentration ranges between 0-7 %wt, alkali concentrations were in the ranges of 1- 4 % by weight for Na_2O and K_2O . During firing alkalis can act as fluxes and can support the vitrification and sintering if the temperatures are high enough to allow these reactions. But the XRD results in the Section 4.2 indicated the presence of feldspatic minerals in these samples, meaning that the firing temperatures were not high enough to exploit the binding ability of most of the feldspatic minerals in the body. Some minor melting may have occurred though, due to the multicomponent mixtures of these minerals that provide very low melting temperatures in ternary, quaternary or even quinary eutectic compositions. Sufficient strength could therefore be developed via partial vitrification provided from such mixtures. MgO content ranges between 1 to 5 % by weight, TiO_2 and P_2O_5 concentrations range from 0-2 %wt and 0-1.5 %wt. High MgO content of samples can be related to the usage of Mg-rich pyroxene, high Na_2O and K_2O content can be related to high feldspar content of these samples. PbO_2 in the structure of body (PbO 1-8 %wt) resulted from the diffusion of Pb from glaze.

As listed in Table 4.6, slip layers of the samples were composed mainly of silica (29-54 %wt), alumina (11-23 %wt except the sample 1.6.3), alkalis (Na_2O 0-4 %wt and K_2O 1-5 %wt), magnesia (1-5 %wt) and lead oxide (PbO 3-24 %wt). High content of MgO can be related with the usage of Mg-rich pyroxenes in the structure. Lead oxide concentration of the slip part was higher than the body part due to diffusion of lead oxide from glaze to slip part during firing process. ZrO_2 content of sample 1.6.3 was very high (17 %wt) compared to the other samples. Zirconium oxide is generally added to glazes in order to render it opaque but this is a modern practice developed after World War I in 1910's during which the supply of the otherwise regularly used SnO_2 was scarce (Rhodes 1973). It was therefore surprising to observe Zr in the EDS analysis of the slip. Information in the literature suggested that the clay used for slip layer may perhaps be of marine origin (Pollard and Heron 2008) In marine environment clay sometimes is enriched in some elements like zirconium. Further evidence is definitely needed to confirm this hypothesis.

Glaze parts of the samples had a high amount of lead oxide (37-56%wt) with significant amount of silica (15-34 %wt) and some alumina (3-9 %wt) (Table 4.7). Alkali content of glazes were less than 4 %wt ($\text{Na}_2\text{O}+\text{K}_2\text{O}$). Copper and iron were observed in large amounts in some of the glaze samples (CuO 0-23 %wt and Fe_2O_3 0-2 %wt).

EDX analysis given in Table 4.5-6-7 indicated that regardless of the decoration type and group, all samples had similar glaze, slip and body compositions with the exception of the CuO content. For the green glazed samples CuO content was found to be high as expected (Molera et al. 1999, Molera et al. 1997, Hatcher et al. 1994).

Considering the body and the slip layers, elemental composition results (Table 4.5-4.6) showed that the body layer was richer in silica, iron oxide and calcium oxide, and the slip layer was richer in aluminum oxide and potassium oxide. Decline of SiO₂ and increment of Al₂O₃ in the slip part was probably related with the removal of coarse quartz particles and usage of fine-grained clay minerals in the slip (Papachristodoulou et al. 2010, Tite et al.1982). Also it could be understood from the selection of more appropriate clay, which was different from the clay that was used in production of body part (Mirti and David 2001). Calcium concentration in slip part was decreased compared to body part, in order to enhance quality. Because the carbonate grains can modify the alignment of clay platelets parallel to surface of the ware, and may conduce to formation of high-temperature alkaline earth aluminosilicates (Maniatis et al. 1981, Papachristodoulou et al. 2010). Iron content of body layer was higher than the slip layer, ranging between 0-7 %wt (average concentration 3.6% wt) for body and 0-4 %wt (average concentration 1.5 %wt) for slip (except samples 1.4.10 and 1.6.2). In order to prevent red or black coloration of coating, iron content of the slip layer was purposefully kept at low levels (Mirti and Davit 2001). The same finding was made in this thesis. Iron contents of all slip samples (average 1.5 % wt) were lower than those of the body samples (3.6 % wt) with only few exceptions.

The glaze was found to be poorer in SiO₂, Al₂O₃ and alkali oxide content than the body and slip layers. PbO content of the glazes were naturally very high. CuO and Fe₂O₃ were the colorants used in the glazes. Green color of lead glazes is generally related with the presence of Cu⁺² or Fe²⁺ in the glaze while yellow to brown colors are associated with the presence of Fe (Molera et al. 1999, Molera et al. 1997, Hatcher et al. 1994). According to the EDX analysis results, copper oxide content of the green glazes was very high (3.5 and 1.6.2). Therefore, the green and yellow colors of glazes were related with the copper and iron oxides, respectively.

Ancient glazes can be classified into three groups, alkali glazes, lead-alkali glazes and high lead glazes. Alkali glazes contain silica and alkali oxides (Na₂O 10-18 %wt, K₂O 3-5 %wt), lead-alkali glazes contain lead oxide (20-40 %wt), alkali oxide (5-12 %wt) and high lead glazes contain a high amount of lead oxide (45-60 %wt)

along with little alkali oxide of less than 2 %wt (Pace et al.2008). According to EDX analysis results all the samples studied in this thesis were covered with high lead glazes.

The glazes in this study contained significant amount of Al₂O₃ (average 6.7% wt). Source of alumina is important, it can be added to the glaze suspension in the form of clay or can diffuse from the body during firing (Tite et al.1998, Molera et al. 1997). Glaze makers may have the knowledge of advantage of alumina addition to glaze. Viscosity of the glaze can be controlled by the addition of alumina (Saad 2002). Tables 4.5-4.6-4.7 list the compositions of the body, slip and glaze layers of all the samples studied in this thesis.

There are two methods for the production of lead glazes. In the first method, lead oxide is applied to non-calcareous clay bodies, while in the second method, lead oxide is mixed with silica and applied to calcareous clay bodies (Tite et al. 1998, Walton and Tite 2010). In the first method, glaze is formed by reaction of lead oxide with clay body, in the second method, lead oxide reacts with silica in order to form glaze which will then interact with the body. According to Hurst and Freestone (1996) the two methods can be distinguished by Equation 4.1.

$$C_i^* = \frac{C_i * 100}{\sum_{i=1}^N C_i - (C_{PbO} + C_{CuO})} \quad (4.1)$$

This equation provides the calculation of the concentration of oxides in the glaze composition. The concentration of oxides in the glaze other than PbO can be plotted against their concentrations in the body to figure out if the glaze has any additive apart from PbO (Figure 4.2). The diagonal line in Figure 4.2 indicates the line along which the non-PbO oxides are equally concentrated in the body and in the glaze. Lead oxide, silica, alumina and other oxide concentrations should remain constant through the thickness of glaze. When the glaze is prepared from a mixture of lead oxide and silica, the calculated silica content of the glaze should be higher than the measured silica content in the body (Walton 2004, Benedetto et al.2004). As can be seen from Figure 4.2, all samples are produced with the usage of only lead oxide because all compositions marked in the Figure 4.2 lie below or on the diagonal.

Table 4.5. Chemical composition of the body layer of the samples determined by EDX method

Wt%	SiO ₂	Al ₂ O ₃	MgO	PbO ₂	Fe ₂ O ₃	Na ₂ O	CaO	SrO	ZrO ₂	ZnO	K ₂ O	SnO ₂	P ₂ O ₅	BaO	TiO ₂	La ₂ O ₃	Ce ₂ O ₃	V ₂ O ₅	Cr ₂ O ₃	MnO	Rb ₂ O	NiO	CuO
1.1.1	43.7	18.5	3.6	3.8	3.6	2.4	3.4	3.4	3.7	1.1	2.8	2.1	0.2	0.6	1.0	1.6	1.0	0.7	0.6	0.6	0.1	0.9	0.68
1.1.2	41.7	17.2	4.0	4.7	3.8	2.4	4.8	2.7	3.3	1.5	2.5	1.5	0.2	0.9	0.6	1.4	0.8	0.8	0.6	0.8	1.8	0.7	1.36
1.1.3	43.4	16.3	3.8	3.6	3.0	2.8	3.2	3.8	3.7	1.2	2.3	2.3	0.5	1.4	0.7	2.2	1.2	0.8	0.8	0.9	0.2	0.9	1.04
1.1.4	43.6	13.8	3.0	3.3	5.6	1.8	3.9	6.6	4.4	0.7	2.8	2.0	0.0	0.1	1.2	1.5	1.1	0.6	0.7	0.8	0.0	1.3	1.45
1.1.6	55.3	12.0	2.7	2.2	2.8	1.1	3.1	8.7	3.2	2.1	1.6	1.2	0.6	0.4	0.5	0.6	0.4	0.2	0.2	0.2	0.0	0.5	0.53
1.1.7	44.7	17.2	3.3	2.0	6.4	1.7	4.2	6.1	4.2	0.8	2.9	1.3	0.0	0.4	0.7	0.5	0.0	0.3	0.4	0.7	0.0	0.9	1.28
1.1.8	48.7	15.4	3.3	2.9	3.3	1.9	3.5	8.4	2.8	1.6	2.2	1.4	0.5	0.4	0.5	0.8	0.4	0.3	0.2	0.4	0.0	0.5	0.58
1.1.10	52.3	13.9	3.9	3.5	0.3	3.4	1.5	6.9	4.2	1.9	1.4	1.6	0.8	0.3	0.5	1.1	0.9	0.6	0.3	0.4	0.0	0.1	0.00
1.1.13	42.0	17.0	3.4	2.3	3.8	2.3	3.7	8.2	3.0	0.4	2.7	2.2	0.1	1.3	0.6	1.8	1.0	0.8	0.7	0.8	0.0	1.0	1.07
1.2.1	49.3	13.9	2.8	2.9	3.8	2.2	3.9	9.4	3.3	0.3	2.4	1.7	0.0	0.4	0.7	0.9	0.5	0.2	0.3	0.3	0.0	0.5	0.51
1.2.2	41.7	17.2	4.0	4.7	3.8	2.4	4.8	2.7	3.3	1.5	2.5	1.5	0.2	0.9	0.6	1.4	0.8	0.8	0.6	0.8	1.8	0.7	1.36
1.2.3	41.6	16.8	3.0	2.7	4.8	1.7	4.2	7.5	2.2	1.3	3.0	2.2	0.4	0.5	1.0	2.0	1.1	0.8	0.8	0.8	0.0	0.8	0.94
1.2.5	49.8	15.6	3.7	1.5	4.0	1.6	2.8	9.1	3.7	2.0	2.4	1.1	0.0	0.0	0.5	0.4	0.0	0.0	0.1	0.3	0.0	0.5	0.85
1.3.1	45.1	18.4	4.7	3.5	0.7	3.7	1.8	5.5	5.4	2.1	1.6	1.9	0.0	0.7	0.6	1.5	0.8	0.7	0.4	0.5	0.0	0.3	0.09
1.3.3	41.7	15.0	3.4	3.2	4.4	2.0	3.7	8.5	5.0	1.0	2.5	2.0	0.0	0.4	0.8	1.5	0.8	0.6	0.5	0.8	0.0	0.9	1.15
1.3.4	47.8	17.1	3.0	5.1	5.4	1.5	4.1	5.5	1.2	0.7	3.1	1.2	0.1	0.7	0.4	0.8	0.0	0.4	0.2	0.3	0.0	0.7	0.75
1.3.5	42.0	18.4	4.3	3.2	2.8	2.4	2.8	3.0	3.8	2.1	2.6	1.9	0.2	1.3	0.8	1.6	1.0	0.7	0.8	0.9	1.8	0.9	0.91
1.3.6	44.3	14.4	2.9	3.2	3.4	1.2	3.8	8.5	2.3	1.1	2.8	2.4	0.8	1.0	1.0	1.8	1.2	1.1	0.9	1.0	0.0	0.5	0.51
1.3.8	45.7	17.8	3.0	3.8	5.2	1.8	4.2	6.3	0.8	0.9	3.5	1.4	0.7	0.3	1.0	0.7	0.4	0.3	0.3	0.3	0.6	0.6	0.44
1.3.9	46.5	13.0	3.0	2.4	4.5	1.8	3.1	8.4	3.2	1.0	2.6	2.2	0.2	0.4	0.9	1.8	1.1	0.7	0.7	0.8	0.0	0.7	1.02
1.4.4	44.6	17.9	3.0	2.5	6.0	1.7	4.1	6.6	1.8	0.4	3.3	1.8	0.3	0.2	1.1	1.2	0.8	0.4	0.4	0.5	0.0	0.5	0.67
1.4.6.	46.4	14.5	2.6	2.4	4.3	1.5	4.9	7.2	1.8	0.7	2.8	2.5	0.6	0.4	1.1	1.3	1.3	0.8	0.8	0.8	0.0	0.6	0.57
1.4.10	43.4	17.2	3.1	2.3	5.2	1.7	3.8	6.0	2.4	0.7	3.0	2.1	0.2	0.3	2.0	1.7	1.2	0.7	0.7	0.7	0.0	0.8	0.80
1.4.11	44.0	14.9	2.9	7.5	2.7	1.9	6.0	7.6	1.3	1.0	2.6	1.1	0.9	0.7	0.5	1.2	0.8	0.6	0.4	0.5	0.0	0.7	0.31

(cont. on next page)

Table 4.5 (cont.)

Wt%	SiO ₂	Al ₂ O ₃	MgO	PbO ₂	Fe ₂ O ₃	Na ₂ O	CaO	SrO	ZrO ₂	ZnO	K ₂ O	SnO ₂	P ₂ O ₅	BaO	TiO ₂	La ₂ O ₃	Ce ₂ O ₃	V ₂ O ₅	Cr ₂ O ₃	MnO	Rb ₂ O	NiO	CuO
1.5.1	62.5	15.4	1.6	6.0	4.3	1.9	3.3	0.0	0.0	0.2	3.5	0.2	0.1	0.1	0.4	0.1	0.0	0.1	0.0	0.0	0.0	0.1	0.03
1.5.2	46.0	15.1	3.1	2.5	5.5	2.3	4.2	6.4	4.3	0.4	2.8	1.3	0.0	0.6	0.7	0.7	0.7	0.4	0.4	0.6	0.0	0.9	1.15
1.6.2	48.2	19.7	4.2	1.2	5.6	1.8	4.1	4.9	0.7	0.8	3.4	1.2	1.5	0.1	0.8	0.5	0.3	0.3	0.3	0.2	0.0	0.2	0.15
1.6.3	39.9	16.1	4.1	2.9	2.9	2.1	6.5	8.6	6.2	1.8	1.9	1.3	0.0	0.8	0.4	0.9	0.6	0.3	0.4	0.5	0.0	0.9	0.88
1.6.4	45.6	15.0	3.1	3.2	4.3	2.3	3.3	7.1	3.6	0.4	2.6	1.8	0.0	0.3	1.1	1.8	1.2	0.5	0.6	0.7	0.0	0.7	0.78
2.2.	43.0	15.4	2.9	2.9	6.1	1.8	3.6	5.6	4.1	0.3	3.1	2.0	0.0	0.4	1.2	1.8	1.4	0.7	0.7	0.8	0.0	1.0	1.22
2.3	41.7	17.3	3.6	3.7	3.4	2.7	2.8	8.4	4.1	0.4	2.5	1.7	0.0	0.8	0.8	1.6	0.5	0.7	0.6	0.7	0.0	0.8	1.33
3.1	34.7	18.1	4.8	4.2	0.1	3.8	1.9	5.2	4.6	3.2	1.5	2.1	0.6	0.2	0.5	1.1	1.0	0.4	0.3	0.2	11.4	0.0	0.00
3.2	41.8	17.9	3.8	2.9	2.6	2.4	2.8	5.3	2.7	2.7	2.1	1.2	0.4	0.4	0.6	0.6	0.4	0.5	0.2	0.4	6.8	0.6	0.76
3.5	52.4	10.4	1.3	1.0	7.0	0.6	9.8	3.0	0.3	0.2	4.1	0.9	0.5	0.4	0.9	0.6	0.4	0.4	0.1	0.8	0.0	1.1	3.93
3.6	40.1	17.4	3.6	3.9	3.5	2.4	4.0	5.5	3.8	1.3	2.7	2.0	0.0	1.0	0.7	2.1	1.1	0.8	0.8	0.9	0.1	1.0	1.23
3.8	47.4	16.7	2.6	3.6	2.7	2.2	3.8	7.6	1.8	0.5	2.8	1.9	1.1	0.0	1.1	1.0	1.4	0.8	0.7	0.4	0.0	0.0	0.00
3.10	48.0	17.9	4.5	4.4	0.0	2.8	0.7	8.9	6.1	3.3	0.9	1.7	0.9	0.0	0.0	0.0	0.0	0.0	0.0	0.0	0.0	0.0	0.00
3.11	43.2	17.3	3.3	3.5	4.7	1.9	3.6	5.8	2.7	1.1	3.1	2.0	0.0	1.1	0.7	1.7	0.6	0.7	0.6	0.7	0.1	0.8	1.06
3.13	42.4	14.5	5.4	2.9	1.4	1.2	3.5	7.7	2.7	2.5	2.1	1.9	0.9	0.7	0.9	2.0	1.1	0.7	0.6	0.5	4.2	0.3	0.00
3.14	40.8	17.1	4.3	3.1	0.5	2.2	2.0	7.4	3.1	3.2	1.9	2.4	1.0	1.3	0.4	1.0	1.5	0.4	0.4	0.2	5.7	0.1	0.00
3.17	44.2	18.8	3.6	4.3	3.4	2.4	2.8	5.4	3.0	1.0	2.6	1.6	0.2	0.3	0.8	0.9	1.0	0.6	0.7	0.7	0.0	0.7	0.92
3.18	49.0	15.7	3.1	3.5	4.2	1.9	4.0	4.3	1.7	1.4	2.9	1.2	0.8	0.7	0.6	1.0	0.8	0.6	0.5	0.5	0.0	0.8	0.73
3.19	46.0	18.9	4.2	3.5	0.8	3.6	2.3	5.1	4.8	0.8	2.1	2.2	0.2	0.3	1.0	1.2	0.7	0.9	0.6	0.6	0.0	0.1	0.13
3.21	46.5	16.8	3.2	2.8	5.2	1.6	4.7	5.8	3.0	1.0	2.8	1.6	0.0	0.5	1.0	0.8	0.7	0.6	0.4	0.4	0.0	0.4	0.42
3.22	43.6	14.2	3.0	2.6	5.1	2.0	9.1	6.1	2.2	0.8	2.4	1.7	0.2	0.1	0.8	1.2	0.6	0.5	0.6	0.7	0.0	1.1	1.30
3.24	42.3	17.1	4.6	5.1	0.3	2.8	1.7	5.3	6.9	2.9	1.6	2.5	0.0	1.3	0.5	1.9	1.0	0.7	0.7	0.6	0.3	0.0	0.00
3.25	48.8	15.3	3.9	2.9	1.3	2.5	2.7	6.3	3.8	1.2	1.9	1.8	0.3	0.7	0.8	1.4	0.8	0.6	0.6	0.4	0.3	0.9	0.89

Table 4.6. Chemical composition of the slip layer of the samples determined by EDX method

Wt%	SiO ₂	Al ₂ O ₃	MgO	PbO ₂	Fe ₂ O ₃	Na ₂ O	CaO	SrO	ZrO ₂	ZnO	K ₂ O	SnO ₂	P ₂ O ₅	BaO	TiO ₂	La ₂ O ₃	Ce ₂ O ₃	V ₂ O ₅	Cr ₂ O ₃	MnO	Rb ₂ O	NiO	CuO
1.1.1	41.9	21.3	3.5	10.1	3.9	2.4	2.9	3.6	2.8	1.4	2.7	0.5	0.0	0.0	0.4	0.3	0.1	0.1	0.2	0.2	0.0	0.6	1.0
1.1.2	42.2	19.1	2.6	8.8	3.8	2.0	3.0	6.9	2.4	0.3	3.1	1.0	0.0	0.4	0.7	0.8	0.5	0.4	0.3	0.3	0.0	0.6	0.9
1.1.3	54.2	15.2	1.9	9.3	0.7	2.0	1.3	4.0	3.6	1.6	2.0	0.3	0.0	0.8	0.1	0.2	0.2	0.2	0.3	0.3	0.0	0.7	1.2
1.1.4	42.7	14.7	1.5	16.8	1.3	1.8	1.5	7.1	3.9	0.4	2.2	0.9	0.0	0.6	0.3	0.8	0.5	0.2	0.2	0.3	0.0	0.7	1.6
1.1.6	54.5	18.5	1.9	5.3	1.1	0.8	0.8	8.5	2.8	2.0	1.7	0.8	0.1	0.2	0.3	0.2	0.1	0.2	0.0	0.0	0.0	0.1	0.3
1.1.7	48.3	12.1	1.9	12.4	1.2	1.6	1.0	7.4	4.6	0.5	2.8	1.1	0.0	0.2	0.5	0.8	0.5	0.2	0.4	0.3	0.0	1.2	1.1
1.1.8	53.9	14.2	1.8	5.9	0.6	1.4	2.6	8.8	2.6	1.5	2.4	1.0	0.2	0.3	0.2	0.4	0.4	0.3	0.3	0.3	0.0	0.4	0.6
1.1.10	42.0	20.2	2.5	14.3	0.7	2.9	0.4	6.0	3.6	1.4	1.7	1.1	0.0	0.2	0.3	0.9	0.4	0.4	0.3	0.2	0.0	0.3	0.3
1.1.13	35.6	21.6	1.8	18.6	1.2	2.0	0.9	6.6	2.5	0.6	2.6	1.1	0.2	0.5	0.5	0.5	0.5	0.5	0.3	0.4	0.0	0.6	1.1
1.2.1	43.0	19.6	1.9	7.5	1.6	1.9	5.9	8.3	3.1	0.7	1.6	0.9	0.0	0.0	0.7	0.4	0.4	0.4	0.4	0.3	0.0	0.5	0.9
1.2.2	54.3	15.2	2.8	7.0	1.3	2.0	2.6	2.9	3.0	2.0	2.4	0.6	0.1	0.0	0.2	0.4	0.6	0.4	0.3	0.1	0.7	0.5	0.7
1.2.3	37.2	19.2	2.3	17.6	1.4	1.4	0.7	7.5	2.7	1.0	2.9	1.0	0.0	0.6	0.4	0.5	0.0	0.3	0.4	0.5	0.0	0.5	1.9
1.2.5	51.4	12.4	1.8	13.2	0.3	0.9	0.4	9.5	3.5	2.2	2.1	1.0	0.0	0.1	0.1	0.0	0.1	0.0	0.0	0.1	0.0	0.3	0.5
1.3.1	53.9	13.5	3.5	8.3	0.6	4.0	0.5	5.8	4.3	1.8	1.6	0.0	0.0	0.6	0.1	0.2	0.3	0.4	0.3	0.3	0.2	0.3	0.0
1.3.3	51.1	12.0	1.9	10.1	1.0	1.7	1.7	9.2	4.6	0.6	2.4	1.0	0.0	0.5	0.2	0.3	0.1	0.2	0.2	0.2	0.0	0.6	0.6
1.3.4	47.0	15.7	2.4	11.9	0.3	2.7	0.8	6.7	2.8	1.2	1.6	1.2	0.7	0.4	0.5	1.5	1.1	0.6	0.6	0.4	0.0	0.0	0.0
1.3.5	46.4	18.0	2.2	16.8	0.8	1.9	0.5	3.1	3.5	2.0	2.0	0.0	0.0	0.0	0.2	0.3	0.1	0.1	0.1	0.1	0.7	0.5	0.7
1.3.6	47.3	13.5	1.5	12.3	1.0	1.1	1.2	7.5	1.9	0.8	2.8	1.2	0.4	0.8	0.4	1.2	0.2	1.1	0.7	0.9	0.0	1.5	0.8
1.3.8	44.5	16.5	2.5	11.9	3.3	1.9	3.2	5.8	0.5	1.3	3.3	0.6	0.8	0.1	0.9	0.1	0.1	0.3	0.3	0.4	0.1	0.6	1.2
1.3.9	48.6	15.0	1.5	13.2	0.8	1.2	0.7	9.0	2.6	1.6	1.8	0.7	0.0	0.3	0.2	0.2	0.4	0.2	0.2	0.3	0.0	0.6	1.0
1.4.4	34.7	18.7	1.6	23.7	1.4	1.1	0.7	6.2	2.0	0.8	1.4	1.1	0.1	0.1	0.7	1.2	0.7	0.6	0.8	0.5	0.0	0.8	1.1
1.4.6	53.6	9.9	1.5	6.2	1.1	1.1	5.0	8.3	0.4	0.8	2.3	1.5	1.3	0.9	1.2	1.4	0.5	0.8	0.5	0.6	0.0	0.6	0.4
1.4.10	40.6	20.0	4.6	6.1	6.3	2.0	2.5	6.3	1.4	0.7	3.3	0.9	0.2	0.3	0.5	1.0	0.5	0.4	0.4	0.5	0.0	0.7	0.7
1.4.11	36.3	14.3	3.6	9.4	2.9	1.9	6.9	6.6	1.6	1.8	2.2	2.0	1.5	0.2	1.2	1.5	2.1	1.2	1.1	1.0	0.0	0.7	0.0

(cont. on next page)

Table 4.6 (cont.)

Wt%	SiO ₂	Al ₂ O ₃	MgO	PbO ₂	Fe ₂ O ₃	Na ₂ O	CaO	SrO	ZrO ₂	ZnO	K ₂ O	SnO ₂	P ₂ O ₅	BaO	TiO ₂	La ₂ O ₃	Ce ₂ O ₃	V ₂ O ₅	Cr ₂ O ₃	MnO	Rb ₂ O	NiO	CuO
1.5.1	54.7	13.6	2.2	20.6	1.5	1.9	1.9	0.0	0.1	0.2	2.5	0.2	0.0	0.2	0.1	0.2	0.1	0.1	0.0	0.1	0.0	0.0	0.0
1.5.2	41.9	10.5	1.2	19.9	1.6	1.2	0.7	6.7	3.9	0.8	1.3	0.8	0.0	1.0	0.3	1.5	0.8	0.6	0.6	1.0	0.0	1.7	1.9
1.6.2	33.3	23.3	1.4	2.6	8.5	0.6	1.3	2.8	0.3	0.6	3.1	1.3	0.9	0.8	1.6	1.5	1.6	0.9	0.9	1.1	0.7	3.8	7.2
1.6.3	3.9	7.1	6.3	11.5	2.8	3.8	3.8	5.7	16.6	4.3	1.8	5.0	0.0	3.1	1.4	4.6	1.8	1.8	1.6	1.9	6.2	2.3	2.8
1.6.4	44.8	20.1	1.6	12.6	0.9	2.1	0.4	7.7	2.8	0.1	3.4	0.9	0.0	0.4	0.1	0.4	0.1	0.3	0.3	0.1	0.0	0.4	0.5
2.2	49.8	14.3	1.5	17.2	0.7	1.2	0.7	6.4	3.6	0.6	2.1	0.4	0.0	0.0	0.1	0.1	0.1	0.0	0.2	0.1	0.0	0.3	0.4
2.3	50.1	13.1	1.9	11.7	0.7	2.0	0.9	9.6	3.2	0.4	2.1	0.3	0.0	0.7	0.1	0.6	0.1	0.2	0.2	0.2	0.0	0.8	1.1
3.1	28.7	22.7	3.4	8.8	0.0	3.7	0.6	5.1	5.9	4.9	1.4	1.6	0.2	0.3	0.1	0.3	0.5	0.2	0.0	0.0	11.6	0.0	0.0
3.2	40.9	18.9	2.2	7.8	0.9	2.3	1.3	5.0	2.3	2.5	2.4	1.1	0.2	0.6	0.3	0.7	0.4	0.2	0.2	0.1	8.9	0.4	0.6
3.5	41.4	14.4	0.5	16.8	3.1	0.3	2.6	4.9	0.4	0.2	4.5	1.2	0.3	0.0	2.2	0.4	0.3	0.2	0.4	0.3	0.3	0.9	4.4
3.6	45.0	19.1	3.2	8.2	3.2	2.1	1.7	5.5	2.9	1.2	2.5	0.9	0.0	0.2	0.3	0.6	0.3	0.3	0.3	0.4	0.0	0.9	1.3
3.8	39.5	17.9	1.1	17.8	0.6	1.2	2.6	6.1	1.8	0.6	2.4	1.4	0.4	0.4	0.7	1.5	1.2	0.7	1.0	0.6	0.0	0.2	0.4
3.10	45.8	17.9	2.3	7.9	0.0	2.9	0.4	10.9	2.9	2.4	1.9	1.3	3.4	0.0	0.0	0.0	0.0	0.0	0.0	0.0	0.0	0.0	0.0
3.11	48.2	17.3	1.5	12.4	1.7	1.6	0.8	5.7	2.5	0.7	1.8	0.7	0.0	1.1	0.1	0.4	0.2	0.4	0.4	0.4	0.0	0.8	1.2
3.13	34.6	18.1	1.8	19.2	0.9	1.0	0.4	6.4	2.0	2.9	2.0	0.6	0.6	0.9	0.1	0.5	0.4	0.6	0.4	0.5	4.7	0.6	0.6
3.14	44.9	18.9	2.4	8.6	0.6	1.8	1.1	6.8	2.8	2.4	1.9	1.0	0.1	0.5	0.3	0.4	0.2	0.6	0.1	0.3	3.8	0.4	0.1
3.17	50.8	15.7	1.7	13.7	0.7	1.5	1.9	5.1	2.2	1.3	2.0	0.8	0.1	0.2	0.2	0.4	0.2	0.1	0.2	0.2	0.0	0.2	0.8
3.18	46.1	16.8	1.6	11.0	1.1	2.1	2.8	4.6	2.5	0.6	2.2	1.1	0.4	0.8	0.3	1.3	0.8	0.4	0.7	0.7	0.0	1.1	1.1
3.19	42.5	16.4	2.9	17.3	0.5	2.5	0.8	5.0	4.1	1.6	1.0	1.0	0.0	0.6	0.3	1.5	0.7	0.5	0.4	0.4	0.0	0.0	0.0
3.21	44.4	15.7	1.6	16.3	1.3	1.6	0.9	6.6	2.4	0.7	4.4	0.5	0.0	0.2	0.2	0.5	0.2	0.3	0.4	0.3	0.0	0.4	1.1
3.22	46.6	16.9	1.2	14.4	1.0	1.8	1.2	6.1	2.2	0.6	3.4	0.9	0.0	0.7	0.3	0.4	0.0	0.3	0.3	0.4	0.0	0.7	0.5
3.24	41.9	20.8	5.1	7.9	0.2	2.9	1.9	6.0	5.2	3.0	1.6	1.2	0.0	0.4	0.2	0.1	0.3	0.2	0.0	0.2	0.5	0.3	0.1
3.25	43.6	18.2	2.1	14.0	0.8	1.9	1.9	6.2	3.2	1.3	2.2	0.5	0.2	0.0	0.3	0.3	0.4	0.3	0.2	0.2	0.4	0.8	1.0

Table 4.7. Chemical composition of the glaze part of the samples determined by EDX method

Wt%	SiO ₂	Al ₂ O ₃	MgO	PbO ₂	Fe ₂ O ₃	Na ₂ O	CaO	SrO	ZrO ₂	ZnO	K ₂ O	SnO ₂	P ₂ O ₅	BaO	TiO ₂	La ₂ O ₃	Ce ₂ O ₃	V ₂ O ₅	Cr ₂ O ₃	MnO	Rb ₂ O	NiO	CuO
1.1.1	22.5	7.9	2.6	50.1	1.8	1.4	1.5	4.0	3.1	1.3	0.5	0.4	0.2	0.2	0.2	0.5	0.1	0.3	0.1	0.1	0.6	0.3	0.5
1.1.2	21.7	6.3	1.8	49.9	1.7	1.3	0.8	5.7	3.3	0.8	0.6	0.6	0.0	0.5	0.4	1.1	0.6	0.5	0.3	0.5	0.0	0.8	0.8
1.1.3	28.2	7.1	2.2	43.5	1.4	1.9	1.0	4.3	3.2	0.8	0.9	0.6	0.0	0.1	0.4	0.6	0.5	0.4	0.4	0.5	0.4	0.7	1.0
1.1.4	26.1	8.1	2.0	43.2	1.4	1.2	1.4	6.1	3.9	0.7	0.6	0.6	0.0	0.4	0.4	0.8	0.5	0.3	0.2	0.7	0.0	0.4	1.0
1.1.6	22.7	7.6	2.2	49.8	0.9	1.0	0.4	5.8	3.2	1.8	0.3	0.2	0.1	0.3	0.2	0.6	0.5	0.3	0.3	0.4	0.0	0.7	0.9
1.1.7	19.3	5.0	1.9	51.4	1.9	1.0	1.2	5.5	3.8	1.0	0.5	0.3	0.0	0.8	0.2	1.2	0.3	0.6	0.4	0.8	0.0	1.1	1.9
1.1.8	23.2	6.5	2.3	49.6	0.8	0.7	0.8	5.9	2.8	2.5	0.6	0.7	0.4	0.2	0.2	0.5	0.4	0.2	0.3	0.3	0.0	0.4	0.7
1.1.10	22.8	6.2	2.8	48.6	0.7	1.8	0.5	5.4	3.7	2.3	0.3	0.6	0.0	0.1	0.4	0.7	0.6	0.4	0.7	0.4	0.0	0.5	0.5
1.1.13	21.7	6.6	2.0	49.7	1.0	1.4	0.9	5.9	3.0	1.2	0.6	0.8	0.1	0.5	0.4	0.4	0.4	0.4	0.4	0.5	0.0	0.7	1.6
1.2.1	25.5	9.0	2.3	39.8	2.2	1.8	2.2	6.8	3.1	0.6	1.1	1.1	0.0	0.0	0.7	0.6	0.8	0.3	0.5	0.4	0.0	0.6	0.8
1.2.2	28.1	8.0	2.6	42.8	1.2	1.9	1.4	4.0	2.8	1.1	0.9	0.6	0.2	0.3	0.1	0.7	0.6	0.1	0.2	0.3	0.6	0.8	0.7
1.2.3	30.8	6.7	2.1	40.6	1.7	1.3	1.1	5.9	2.3	0.6	1.3	0.8	0.0	0.6	0.3	0.9	0.6	0.3	0.3	0.4	0.0	0.7	0.9
1.2.5	22.3	6.8	2.6	48.6	1.3	1.2	1.0	6.3	3.6	2.1	0.4	0.4	0.0	0.0	0.3	0.3	0.3	0.4	0.2	0.3	0.0	0.6	1.3
1.3.1	27.2	8.3	3.4	38.8	0.7	3.2	0.7	5.0	3.8	1.7	0.6	0.9	0.2	0.8	0.3	0.6	0.2	0.7	0.5	0.5	0.3	0.9	0.7
1.3.3	27.0	6.0	2.1	45.1	1.2	1.1	0.7	6.8	3.8	1.3	0.6	0.5	0.0	0.3	0.3	0.2	0.6	0.1	0.2	0.4	0.0	0.8	1.0
1.3.4	25.6	8.6	2.7	41.7	1.2	2.1	0.6	5.6	2.9	1.0	0.6	0.8	0.2	0.9	0.1	1.2	0.7	0.4	0.3	0.6	0.0	1.2	1.1
1.3.5	21.2	7.7	2.4	48.8	1.1	1.2	1.0	3.7	3.1	1.9	0.5	0.4	0.0	0.7	0.1	1.0	0.3	0.3	0.5	0.6	1.0	0.8	1.4
1.3.6	25.9	7.6	1.4	38.1	2.1	0.9	0.9	5.4	2.1	0.8	1.2	1.3	0.1	0.5	0.8	2.0	1.3	1.1	1.1	1.0	0.0	1.9	2.6
1.3.8	21.6	7.2	2.9	50.2	0.6	1.7	0.8	5.4	1.5	2.3	0.4	0.5	0.9	0.3	0.2	0.8	0.5	0.2	0.3	0.1	0.9	0.3	0.6
1.3.9	22.0	4.9	2.1	51.6	1.2	0.7	0.8	5.8	3.4	2.1	0.3	0.4	0.1	0.0	0.4	0.5	0.6	0.4	0.3	0.5	0.0	0.9	1.1
1.4.4	24.3	4.5	1.7	52.9	0.9	0.9	0.4	5.6	2.2	0.8	0.3	0.5	0.3	1.0	0.0	0.8	0.3	0.5	0.5	0.5	0.0	0.7	0.4
1.4.6	24.5	3.5	1.5	49.7	1.3	0.7	0.9	5.2	1.9	0.8	0.4	0.6	0.6	1.0	0.5	0.9	0.8	0.9	0.8	0.7	0.0	1.4	1.4
1.4.10	19.9	5.0	2.1	51.7	1.8	1.3	1.2	5.1	2.9	0.9	0.6	1.0	0.1	0.3	0.6	1.1	0.7	0.7	0.6	0.5	0.0	0.8	1.2

(cont. on next page)

Table 4.7 (cont.)

Wt%	SiO ₂	Al ₂ O ₃	MgO	PbO ₂	Fe ₂ O ₃	Na ₂ O	CaO	SrO	ZrO ₂	ZnO	K ₂ O	SnO ₂	P ₂ O ₅	BaO	TiO ₂	La ₂ O ₃	Ce ₂ O ₃	V ₂ O ₅	Cr ₂ O ₃	MnO	Rb ₂ O	NiO	CuO	
1.4.11	24.7	6.6	1.9	44.7	1.9	0.8	1.6	5.5	1.8	1.1	0.7	0.4	0.7	0.4	0.5	0.9	0.5	0.6	0.6	0.8	0.0	1.2	1.9	
1.5.1	33.6	7.2	1.0	52.7	0.9	1.0	1.5	0.0	0.5	0.0	1.0	0.0	0.1	0.2	0.1	0.2	0.0	0.0	0.0	0.0	0.0	0.0	0.0	0.1
1.5.2	23.3	7.8	1.9	47.2	1.4	1.0	0.9	5.5	4.2	1.1	0.3	0.5	0.0	0.2	0.3	0.5	0.8	0.4	0.3	0.6	0.0	0.9	1.0	
1.6.2	18.4	2.9	0.8	55.6	0.8	0.4	0.4	3.7	1.3	0.4	0.3	0.1	0.5	0.5	0.1	0.3	0.4	0.0	0.1	0.2	0.1	1.4	11.2	
1.6.3	22.1	6.8	2.2	47.2	0.6	1.5	0.4	6.9	4.9	1.8	0.3	0.8	0.0	0.2	0.4	0.5	0.4	0.2	0.2	0.6	0.4	0.9	0.9	
1.6.4	19.7	6.7	2.3	51.1	1.3	1.2	1.0	5.8	3.8	1.4	0.4	0.6	0.0	0.3	0.5	0.8	0.8	0.4	0.4	0.4	0.0	0.4	0.8	
2.2	25.3	4.3	1.7	50.9	1.0	0.8	0.7	5.4	3.8	0.9	0.4	0.4	0.0	0.0	0.4	0.7	0.7	0.4	0.6	0.2	0.0	0.7	0.6	
2.3	21.5	7.0	2.3	47.9	1.0	1.5	0.8	6.1	3.7	1.2	0.4	0.6	0.0	0.0	0.5	1.2	0.5	0.4	0.5	0.5	0.0	1.0	1.2	
3.1	18.4	6.8	3.3	47.1	0.9	2.5	0.5	3.7	3.5	2.1	0.4	0.7	0.2	0.3	0.4	0.7	0.8	0.3	0.5	0.6	5.5	0.6	0.3	
3.2	17.8	5.4	2.3	50.4	1.2	1.5	0.6	5.5	2.2	1.8	0.4	0.8	0.3	1.0	0.3	0.8	0.6	0.4	0.5	0.6	3.4	1.2	1.2	
3.5.	15.3	3.3	0.7	43.0	2.1	0.3	1.0	3.0	1.4	0.7	0.3	0.7	0.3	0.2	0.5	0.7	0.5	0.4	0.5	0.5	0.2	1.3	23.3	
3.6	20.2	5.0	2.2	52.7	1.1	1.2	1.0	5.1	3.4	1.4	0.3	0.5	0.0	0.5	0.3	0.9	0.5	0.3	0.6	0.6	0.4	1.0	0.8	
3.8	31.9	8.4	3.2	37.3	0.0	2.0	0.6	7.7	4.0	2.5	0.8	0.5	0.5	0.3	0.2	0.0	0.2	0.0	0.0	0.0	0.0	0.0	0.0	
3.10	23.0	6.5	1.4	41.9	1.6	0.8	1.9	5.9	2.0	1.0	0.8	1.3	0.3	0.0	0.9	2.3	2.0	0.7	1.0	1.1	0.0	1.7	1.8	
3.11	21.2	3.7	1.9	53.5	1.0	1.3	0.5	4.6	2.8	1.2	0.3	0.4	0.2	0.5	0.3	1.0	0.7	0.4	0.4	0.4	0.8	1.1	1.8	
3.13	24.0	7.8	2.6	41.2	0.9	0.7	0.6	5.6	2.1	2.7	0.4	0.5	0.8	0.0	0.5	0.2	0.9	0.5	0.6	0.8	3.5	1.4	1.6	
3.14	23.1	6.6	2.6	42.8	0.9	1.1	0.7	6.1	3.0	3.0	0.4	0.0	0.6	0.4	0.2	1.2	0.6	0.8	0.7	0.6	2.6	1.0	1.0	
3.17	23.8	7.0	2.0	48.4	1.1	1.1	1.2	4.9	2.5	1.5	0.4	0.5	0.3	0.4	0.3	0.6	0.3	0.3	0.6	0.5	0.0	0.9	1.4	
3.18	23.9	7.0	1.9	47.3	1.4	1.6	1.4	5.0	2.3	1.1	0.6	0.5	0.2	0.7	0.2	0.8	0.4	0.4	0.5	0.7	0.0	0.9	1.2	
3.19	24.9	7.2	3.1	45.9	0.7	1.1	0.6	5.0	3.7	3.3	0.1	0.4	0.1	0.0	0.3	0.4	0.4	0.6	0.4	0.6	0.3	0.5	0.5	
3.21	21.4	6.3	1.9	50.8	1.1	1.4	1.0	5.3	2.9	0.9	0.7	0.4	0.2	0.7	0.4	0.7	0.1	0.4	0.5	0.4	0.3	0.9	1.2	
3.22	28.3	7.4	1.7	44.3	1.6	1.6	1.3	5.0	2.4	0.4	1.2	0.2	0.1	0.7	0.3	0.3	0.3	0.4	0.3	0.5	0.0	0.8	1.0	

(cont. on next page)

Table 4.7 (cont.)

Wt%	SiO₂	Al₂O₃	MgO	PbO₂	Fe₂O₃	Na₂O	CaO	SrO	ZrO₂	ZnO	K₂O	SnO₂	P₂O₅	BaO	TiO₂	La₂O₃	Ce₂O₃	V₂O₅	Cr₂O₃	MnO	Rb₂O	NiO	CuO
3.24	25.0	8.5	3.4	44.3	0.3	2.1	1.0	5.7	4.2	1.8	0.4	0.6	0.0	0.7	0.1	0.3	0.0	0.3	0.1	0.1	0.6	0.1	0.3
3.25	21.3	7.5	3.2	46.9	0.4	2.1	0.5	5.5	5.0	2.6	0.4	0.9	0.0	0.3	0.3	0.6	0.1	0.5	0.4	0.5	0.5	0.1	0.3

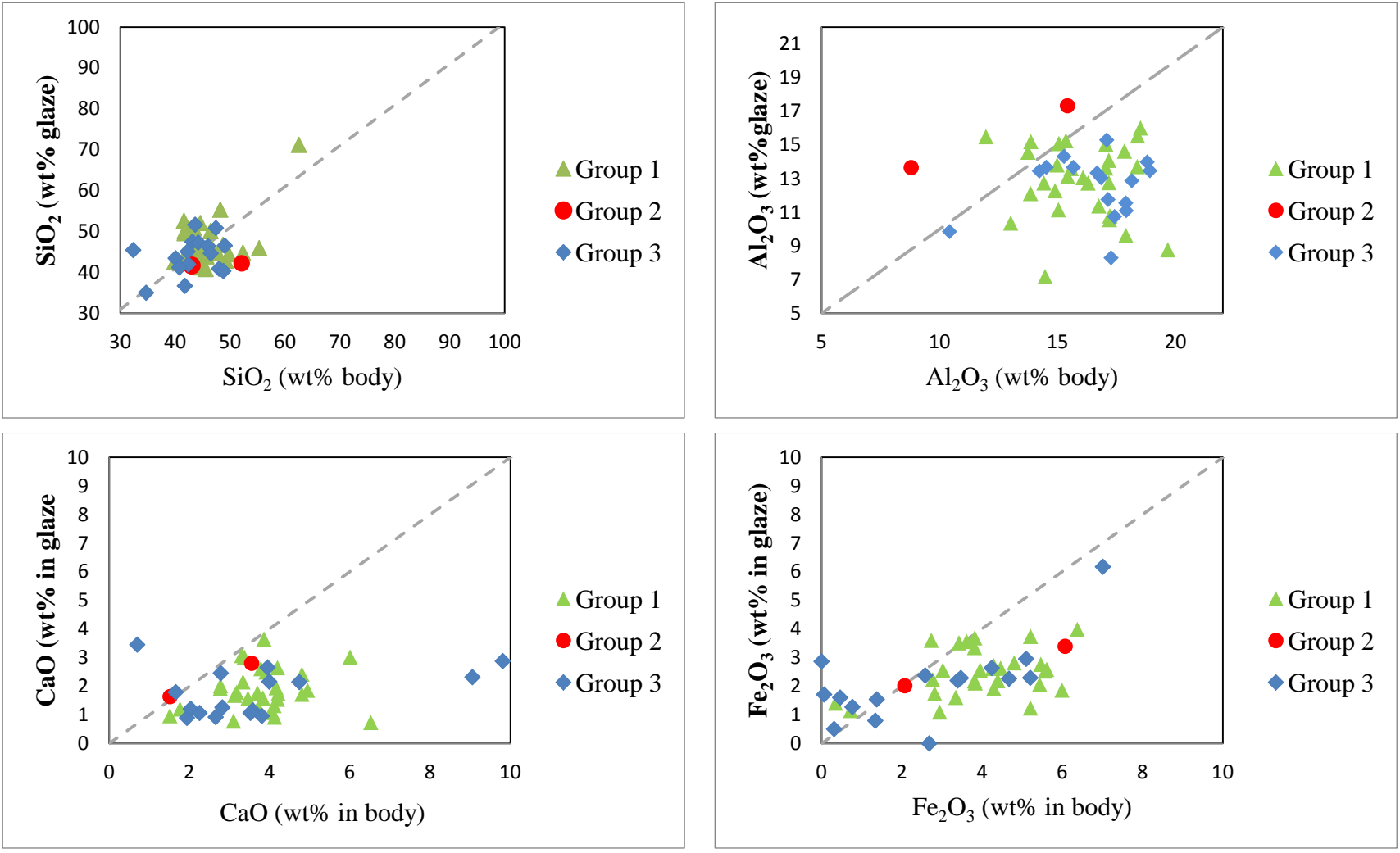


Figure 4.2. Body glaze comparison plot calculated with Equation 4.1

During heat treatment the glaze melts and lead in the structure of glaze reacts with the clay minerals in the body. These minerals diffuse into the glaze and in the counter direction lead oxide diffuses into the ceramic body during heat treatment. Alumina and potassium are very important in diffusion, because they lead to the formation of an interface layer composed of precipitated crystals of lead feldspar between the body and the glaze. The small crystallites of lead-potassium feldspars ((K,Pb)AlSi₃O₈) are also reported in the literature to form in such interfaces (Molera et al. 2001). Considering this information sample 1.5.1 was investigated by SEM-EDX method in detail (Figure 4.3).

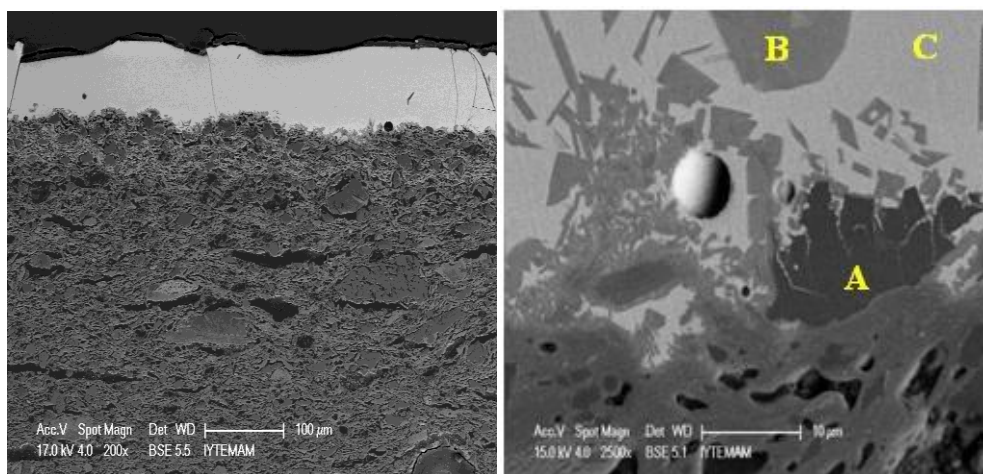


Figure 4.3. Scanning electron microscope (SEM) images of sample 1.5.1

Chemical composition (Table 4.8) and chemical formula of crystals at body-glaze interface, and glaze part is determined by EDX analysis. If thermodynamic equilibrium had been established the chemical potentials of each component would have to be equal in all phases. But the distribution of the elements in different phases still reflects upon these chemical potentials even though thermal equilibrium is not yet completely established.

Table 4.8. EDX analysis results of crystals (A and B) and glaze part (C)

Oxides	A	B	C	Oxides	A	B	C
ZnO	0.77	0.76	2.31	CaO	0.75	0.54	0.10
Na ₂ O	2.64	2.36	1.14	BaO	1.02	0.47	0
MgO	2.88	1.84	1.46	TiO ₂	0.47	0.37	0.7
Al ₂ O ₃	16.94	15.56	7.76	La ₂ O ₃	1.53	0.99	1.61
SiO ₂	41.54	29.5	20.47	Ce ₂ O ₃	1.36	0	0.58
SrO	10.43	8.47	7.05	V ₂ O ₅	0.78	0.62	1.45
P ₂ O ₅	0	0	0	Cr ₂ O ₃	0.75	0.54	1.07
ZrO ₂	3.27	3.46	4.09	MnO	1.02	0.24	1.13
PbO ₂	3.48	24.59	38.12	Fe ₂ O ₃	1.32	1.13	1.91
K ₂ O	6.66	2.00	0.8	NiO	1.15	0.89	2.18
SnO ₂	3.20	1.55	1.29	CuO	1.44	2.75	2.72

Part A and Part B are lead feldspar crystals and the chemical formula of them are Part A: $K_{1.4}Na_{0.5}Pb_{0.7}Si_{4.8}O_8$, Part B: $K_{0.5}Na_{0.5}Pb_{6.3}Si_4O_8$ and Part C is glaze with the chemical formula of P_8AS_2 ($Pb_8AlSi_2O_5$).

In order to determine compositional changes from glaze to body part, sample 1.5.1 is investigated by EDX method along a line from glaze exterior to inside the body (Figure 4.4).

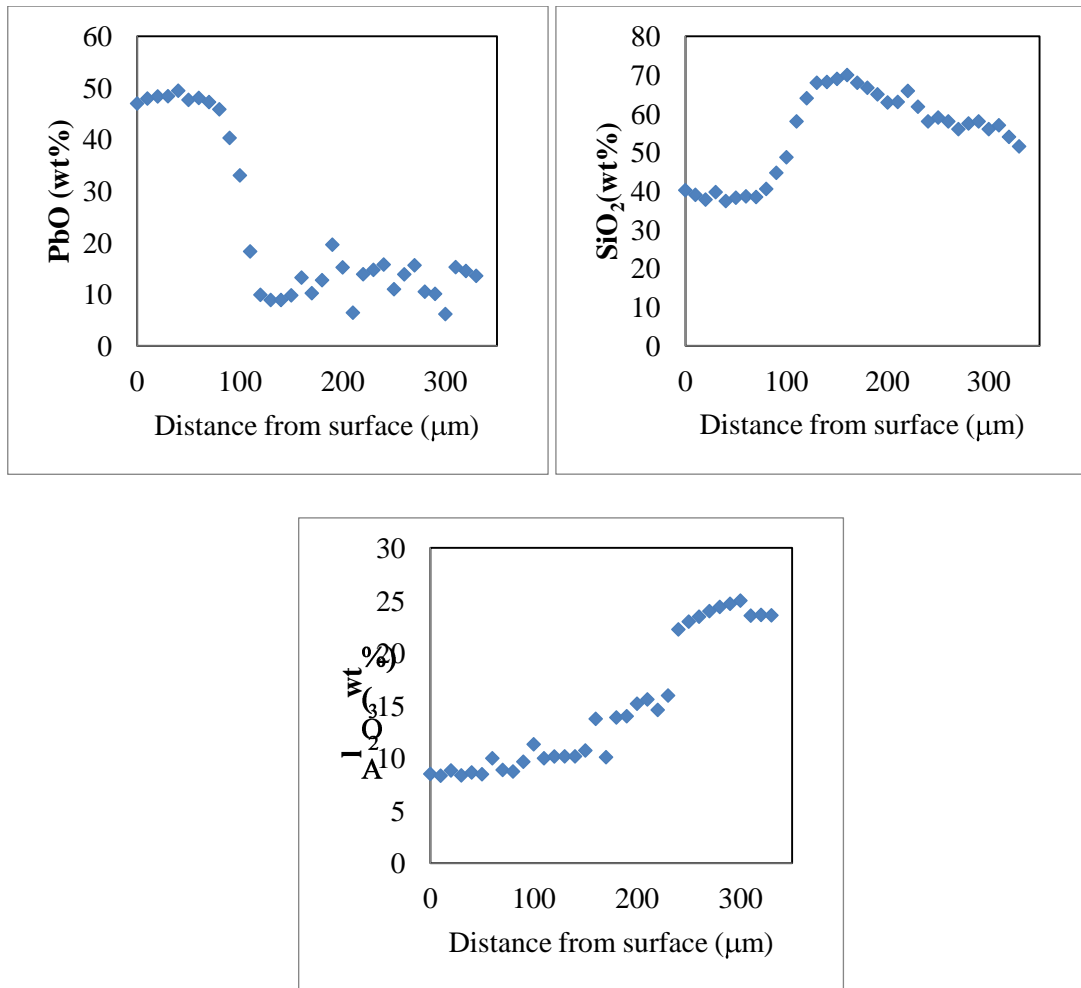


Figure 4.4. EDX analysis of sample 1.5.1 depending on depth

PbO₂ concentration decreases, SiO₂ and Al₂O₃ concentration increases along the line. Lead oxide, silica and alumina contents stay constant through the thickness of the glaze layer, which can be the evidence of the usage of only lead oxide in the production of glaze of sample 1.5.1.

Chemical compositions of the glaze are used in order to estimate the firing temperature. Ternary diagram (PbO-Al₂O₃-SiO₂) of the glaze layer of samples is given in Figure 4.5.

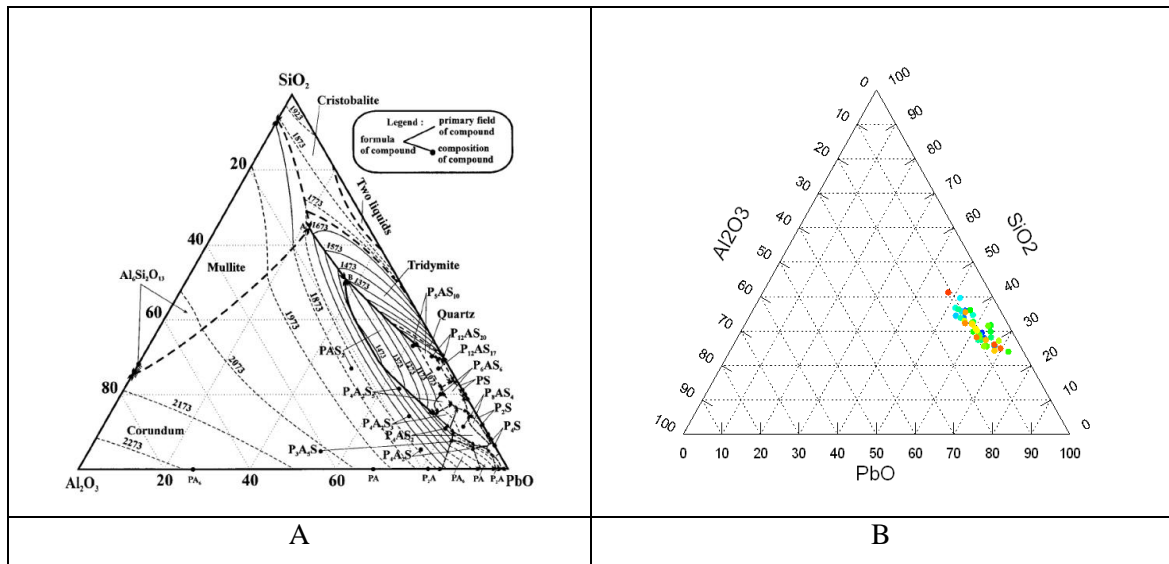


Figure 4.5. A: PbO-Al₂O₃-SiO₂ phase diagram (Temperatures in Kelvin); B: Anaia samples ternary diagram (showing the glaze composition)

Considering the PbO-Al₂O₃-SiO₂ phase diagram Anaia samples are probably heat treated at temperatures smaller than 1117 K(900°C) which are compatible with the XRD analysis results.

4.4. X-Ray Fluorescence (XRF) Analysis

Source of clay and other materials used in the production affects strongly the chemical composition of ceramic samples. Trace element concentrations reflect the geological variety of the samples (Hein et al. 2004, Padilla et al. 2006).

The chemical composition of body part of samples as determined by XRF method are given in Table 4.9. Body part of samples are composed mainly from silica (26-72 %wt). Concentration of silica is due to the presence of various amounts of quartz derived from the clay. Al₂O₃ concentration ranges between 5-39 %wt, Fe₂O₃ concentration ranges between 0-14 %wt. Alkalis have moderate concentrations (0-3 %wt Na₂O, 0-10 %wt K₂O). During firing alkalis can act as fluxes and can lead to vitrification and sintering (Mirti and David 2001). MgO content ranges between 0-10 %wt., TiO₂ and P₂O₅ concentrations range between 0-1 %wt.

High MgO content of sample (3.25) can be related to use of Mg-rich pyroxene. Highest Na₂O and K₂O content can be related to high feldspar content of these samples. PbO₂ in the body possibly resulted from diffusion from glaze.

Clays can be classified according to their CaO and flux (K_2O , Fe_2O_3 , CaO, MgO and TiO_2) concentrations. Clays containing CaO greater than 6% wt are classified as calcareous and those with lower than 6% wt are regarded as non-calcareous (Maniatis and Tite 1981). Clays containing flux (K_2O , Fe_2O_3 , CaO, MgO and TiO_2) lower than 9% wt are classified as low refractory, if these elements are higher than 9% wt they are classified as highly refractory (Maniatis and Tite 1981).

Samples 1.1.1 (Aegean Type Champlevé), 1.1.8 (Aegean Type Incised), 1.1.10 (Incised-Sgraffito), 1.1.13 (Fine Sgraffito), 1.2.1 (Incised-Sgraffito), 1.2.2 (Incised), 1.2.3 (Fine Sgraffito), 1.3.3 (Fine Sgraffito), 1.4.4 (Fine Sgraffito), 1.4.10 (Fine Sgraffito), 1.6.3 (Fine Sgraffito), 1.6.4 (Aegean Type Champlevé), 3.1 (Fine Sgraffito), 3.5 (Aegean Type Incised), 3.11 (Fine Sgraffito), 3.13 (Incised-Sgraffito), 3.17 (Incised), 3.22 (Incised-Sgraffito) and 3.24 (Aegean Type Champlevé) are classified as calcareous samples. Decoration type have no effect on the usage of calcareous clay in production of samples. Considering the flux (K_2O , Fe_2O_3 , CaO, MgO and TiO_2) content all samples are classified as refractory.

XRF analysis results are used in statistical treatment of samples. Samples are grouped with Hierarchical Clustering and Principal Component Analysis.

Table 4.9. XRF Analysis results of body parts of samples. Major and minor elements are expressed in weight percent of oxides, trace elements in ppm

Codes	Na ₂ O	MgO	Al ₂ O ₃	SiO ₂	P ₂ O ₅	K ₂ O	CaO	TiO ₂	MnO	Fe ₂ O ₃	Cu	V	Cr	Ni	Zn	Rb	Sr	Zr	Ba	La	Ce	Pb
	Weight Percent											ppm										
1.1.1	0.02	0.01	34.29	26.32	0.64	9.60	7.60	1.18	3.99	13.17	6135	431	31	21	4388	5	457	5	1873	1779	42	12497
1.1.2	2.10	2.53	18.87	58.13	0.20	4.32	5.07	0.92	0.24	6.52	1017	134	34	56	174	81	109	110	747	137	45	7233
1.1.3	2.10	2.53	18.87	58.13	0.20	4.32	5.07	0.92	0.24	6.52	1017	134	34	56	174	81	109	110	747	137	45	7233
1.1.4	2.10	2.35	18.12	59.12	0.20	4.22	5.49	0.94	0.23	6.33	311	120	35	56	206	93	140	173	798	118	46	5924
1.1.6	0.98	1.02	14.57	68.92	0.30	2.96	4.24	0.88	0.21	5.48	1325	106	35	24	222	130	175	341	619	103	47	487
1.1.7	1.97	2.58	19.99	56.67	0.18	4.64	5.29	0.95	0.25	6.91	712	156	34	40	208	149	121	156	808	34	46	2469
1.1.8	0.02	0.01	22.01	51.76	0.27	5.72	6.58	1.13	1.05	9.70	2403	189	32	22	1130	60	151	5	1442	374	43	9744
1.1.10	0.53	0.01	19.40	57.78	0.25	5.00	6.40	1.08	0.61	8.25	1560	191	32	22	543	141	169	5	1136	312	43	1864
1.1.13	0.02	0.01	22.69	51.01	0.40	6.03	6.40	1.17	1.33	9.95	1348	153	31	21	1553	77	217	5	1460	514	41	3418
1.2.1	1.97	2.14	17.27	57.35	0.24	3.86	8.11	0.87	0.23	5.95	1218	101	35	23	169	6	146	142	757	84	46	15687
1.2.2	0.03	0.01	38.73	18.80	0.78	9.14	8.47	1.29	5.06	14.06	8557	163	40	27	9658	37	766	7	1598	3382	6275	969
1.2.3	0.02	0.01	30.15	32.34	0.60	8.25	7.72	1.13	3.13	11.97	9178	342	34	23	2995	6	125	6	1706	1808	45	25012
1.2.5	1.81	1.86	17.55	60.83	0.30	4.18	5.66	0.89	0.23	6.16	704	125	35	44	210	130	113	119	761	86	46	2174
1.3.1	1.84	1.66	18.18	59.54	0.24	4.18	5.50	0.93	0.27	6.52	642	128	34	25	217	64	112	97	817	113	46	8121
1.3.3	1.09	0.01	20.03	54.68	0.24	5.20	7.13	1.03	0.55	8.77	1677	178	41	28	502	88	165	7	1029	206	55	7334
1.3.4	1.86	2.32	19.42	57.05	0.16	4.44	5.65	0.91	0.23	6.74	1052	143	35	43	177	81	115	100	798	34	46	8209
1.3.5	0.02	0.01	21.27	54.38	0.26	5.80	5.96	1.12	0.71	9.84	979	137	36	27	716	153	156	6	1327	297	47	1701
1.3.8	0.86	0.01	20.27	57.15	0.24	5.17	5.52	1.05	0.50	8.38	852	182	34	23	393	122	122	6	1102	167	46	4568
1.3.9	1.99	2.27	18.13	60.18	0.20	4.01	5.79	0.91	0.24	6.00	391	125	34	37	205	133	119	145	756	90	46	351
1.4.4	2.03	2.36	19.78	55.95	0.19	4.48	6.00	0.92	0.24	6.66	1026	142	34	50	174	69	125	85	821	129	45	9816
1.4.10	2.12	2.47	20.05	56.07	0.22	4.67	6.12	0.95	0.24	6.81	251	138	34	44	225	175	138	118	810	34	45	342
1.4.11	1.93	2.24	18.76	57.72	0.20	4.33	6.00	0.90	0.22	6.53	850	143	35	36	219	87	127	122	776	98	46	7878
1.5.1	2.06	2.17	16.60	62.01	0.20	3.92	5.53	0.89	0.23	5.88	474	96	35	34	226	118	243	222	778	283	47	1804

(cont. on next page)

Table 4.9 (cont.)

Codes	Na ₂ O	MgO	Al ₂ O ₃	SiO ₂	P ₂ O ₅	K ₂ O	CaO	TiO ₂	MnO	Fe ₂ O ₃	Cu	V	Cr	Ni	Zn	Rb	Sr	Zr	Ba	La	Ce	Pb
	Weight Percent										ppm											
1.5.2	2.09	2.35	17.79	59.52	0.27	4.23	5.64	0.92	0.23	6.13	575	113	34	41	190	113	140	1534	796	49	46	3296
1.6.2	2.01	3.59	20.46	52.58	0.79	5.26	6.07	0.95	0.23	7.54	1219	165	36	52	273	180	368	125	1472	35	50	426
1.6.3	1.27	2.14	17.41	53.68	0.28	3.98	13.40	0.93	0.21	6.34	699	129	35	24	228	157	294	175	668	85	46	376
1.6.4	0.05	0.02	20.49	52.36	0.36	5.48	8.64	1.08	0.98	9.15	3783	190	77	52	1008	74	243	13	1311	421	102	4775
2.2	2.02	2.20	19.13	57.78	0.65	4.47	5.64	0.92	0.24	6.58	1030	128	34	44	210	161	123	123	794	46	45	369
2.3	1.90	2.16	20.18	56.36	0.21	4.83	5.34	0.98	0.27	7.45	458	152	33	50	252	186	137	97	882	93	44	387
3.1	1.50	1.13	19.55	56.10	0.28	4.87	7.15	1.01	0.34	7.61	1006	139	33	42	282	155	151	70	934	205	44	948
3.2	1.27	0.26	20.34	57.27	0.20	5.11	5.38	1.06	0.40	8.30	1092	153	32	46	366	183	128	61	1030	159	43	74
3.5	1.06	0.01	19.54	57.25	0.23	4.99	5.38	1.07	0.49	8.25	1649	131	32	26	399	66	146	5	1071	258	43	11884
3.6	1.27	0.01	20.07	55.75	0.25	5.36	6.14	1.07	0.56	8.68	653	182	41	28	462	116	162	7	1010	263	55	4687
3.8	2.25	2.24	17.81	59.16	0.20	4.04	5.82	0.92	0.24	6.18	937	135	34	37	189	60	127	180	760	87	45	7674
3.1	2.01	2.31	19.77	56.87	0.18	4.71	5.65	0.94	0.23	6.88	1116	146	35	65	208	168	121	133	782	86	46	952
3.11	1.74	1.29	20.12	55.66	0.18	4.92	6.38	1.03	0.31	7.87	842	178	31	54	287	179	146	94	836	148	42	1507
3.13	1.48	4.17	16.63	58.33	0.22	4.17	6.94	0.95	0.20	6.18	1037	120	41	216	185	118	230	139	678	82	45	3553
3.14	1.41	0.15	19.66	57.78	0.21	5.04	5.85	1.04	0.39	8.10	620	178	33	23	384	171	138	53	943	191	44	186
3.17	0.02	0.01	23.81	44.21	0.40	6.41	10.45	1.11	1.47	10.52	6560	178	35	24	2596	127	309	6	1397	745	47	1092
3.18	2.09	2.01	17.59	60.31	0.27	4.10	5.85	0.95	0.34	6.16	390	132	35	56	257	156	145	214	820	59	46	455
3.19	1.61	0.98	19.64	57.43	0.22	4.94	5.35	1.03	0.42	7.99	511	153	33	44	363	180	191	104	1011	203	44	488
3.21	1.97	2.24	19.78	57.79	0.18	4.57	5.03	0.96	0.24	6.93	498	143	34	52	219	182	116	136	808	65	46	148
3.22	1.76	1.96	17.50	56.42	0.19	4.06	9.94	0.84	0.24	6.10	703	127	35	25	206	75	180	127	1055	35	47	6339
3.24	2.05	2.46	19.84	55.95	0.19	4.60	6.12	0.93	0.23	6.88	335	130	35	41	207	126	136	87	807	103	47	4699
3.25	2.88	10.25	4.86	71.63	0.52	0.19	0.10	0.04	0.06	0.08	72150	9	13	168	1032	2	2	2	158	148	72	576

4.5. Statistical Analysis

SPSS 16.0 package were used for statistical calculations. Chemical compositions of samples are used in hierarchical cluster analysis calculations. Hierarchical cluster analysis classifies samples into groups and the results are represented as dendrogram showing the relationship between samples. From the resulting dendrogram (Figure 4.6-4.7-4.8), it is obtained by the Ward's method as grouping rule according to the Euclidian distance, samples subdivided into two main groups according to their body, glaze and slip concentrations.

The resulting dendrogram structure is quite complex (Figure 4.6), samples from group 1-2-3 with different decoration types grouped in one cluster. These samples were supposed to share the different origin considering the visual examination.

Samples are grouped into two main groups according to their chemical composition of body layer determined by XRF method.

Samples in Group A have the SiO₂ content in the range of 44-72% wt, Al₂O₃ in the range of 5-24 %wt, MgO in the range 0-10 %wt, Na₂O in the range of 0-3 %wt, K₂O in the range of 0-6 %wt, Fe₂O₃ in the range of 0-11 %wt, CaO in the range of 0-13 %wt.

Considering the trace elements Cu in the range of 251-6560 ppm, V in the range of 9-191 ppm, Cr in the range of 13-77 ppm, Ni in the range of 21-216 ppm, Zn in the range of 174-2596 ppm, Rb in the range of 2-183 ppm, Sr in the range of 2-369 ppm, Zr in the range of 2-1564 ppm, Ba in the range of 158-1472 ppm, La in the range of 34-745 ppm, Ce in the range of 41-102 ppm, Pb in the range of 74-15687 ppm.

Samples in Group B have SiO₂ content in the range of 19-32%wt, Al₂O₃ in the range of 30-39%wt, MgO 0.009-0.011%wt, Na₂O in the range of 0.021-0.026%wt, K₂O in the range of 8-10%wt, Fe₂O₃ in the range of 12-14%wt, CaO in the range of 7-8%wt.

Considering the trace elements Cu in the range of 6135-9178 ppm, V in the range of 163-431ppm, Cr in the range of 31-40 ppm, Ni in the range of 21-27 ppm, Zn in the range of 2995-9658 ppm, Rb in the range of 5-37ppm, Sr in the range of 125-766 ppm, Zr in the range of 5-7 ppm, Ba in the range of 1598-1873 ppm, La in the range of 1779-3382 ppm, Ce in the range of 42-6275 ppm, Pb in the range of 969-25012 ppm.

Group A can be separated from Group B with its higher SiO₂, Al₂O₃, MgO, Na₂O, Cr, Ni, Rb, Zr contents and lower Cu, V, Zn, Sr, Ba, La, Ce, Pb contents. Clay

used in the production of these two groups may have been collected from different sources or may be produced by mixture of different clays.

Dendrogram using Ward Method

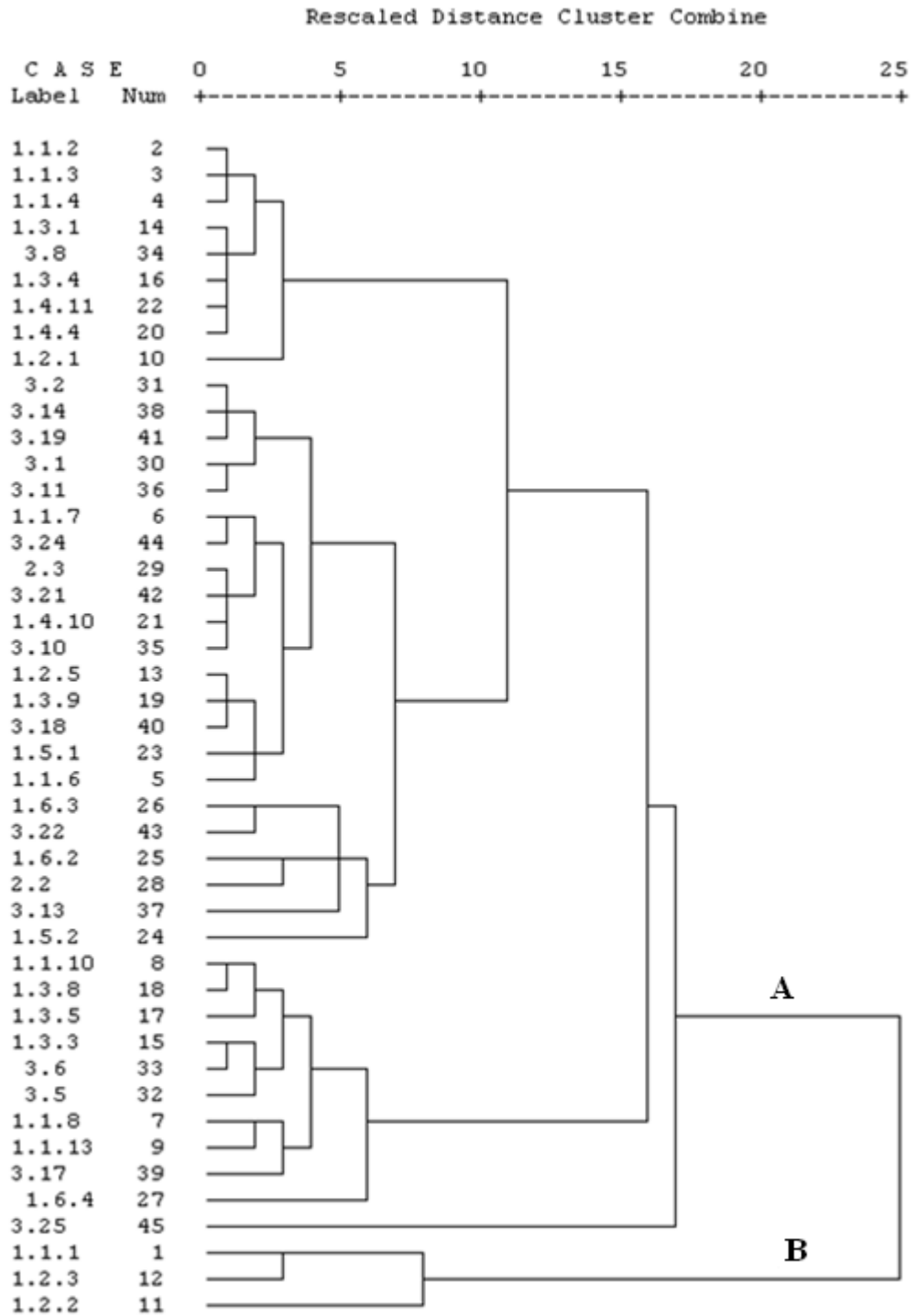


Figure 4.6. Grouping of samples according to body composition (determined by XRF method)

Samples grouped in to two main groups according to its slip composition determined by EDX method (Figure 4.7).

Samples in Group C have the SiO₂ content in the range of 29-55 %wt, Al₂O₃ in the range of 12-22 %wt, MgO in the range 1-5 %wt, Na₂O in the range of 1-4 %wt, K₂O in the range of 0-1 %wt, Fe₂O₃ in the range of 1-10 %wt, CaO in the range of 0-3 %wt.

Samples in Group D have SiO₂ content in the range of 33-54 %wt, Al₂O₃ in the range of 7-20 %wt, MgO 1-5 %wt, Na₂O in the range of 1-2 %wt, K₂O in the range of 3-5 %wt, Fe₂O₃ in the range of 1-9 %wt, CaO in the range of 1-7 %wt.

Samples from Group C have the similar SiO₂, Al₂O₃, MgO, Fe₂O₃ composition compared to Group D samples, Group C separated from Group D with its higher Na₂O and lower K₂O, CaO composition values. Tempers could be added to structure of Group D, or clay used in production of slip layer of two groups can be products of different sources.

Dendrogram using Ward Method

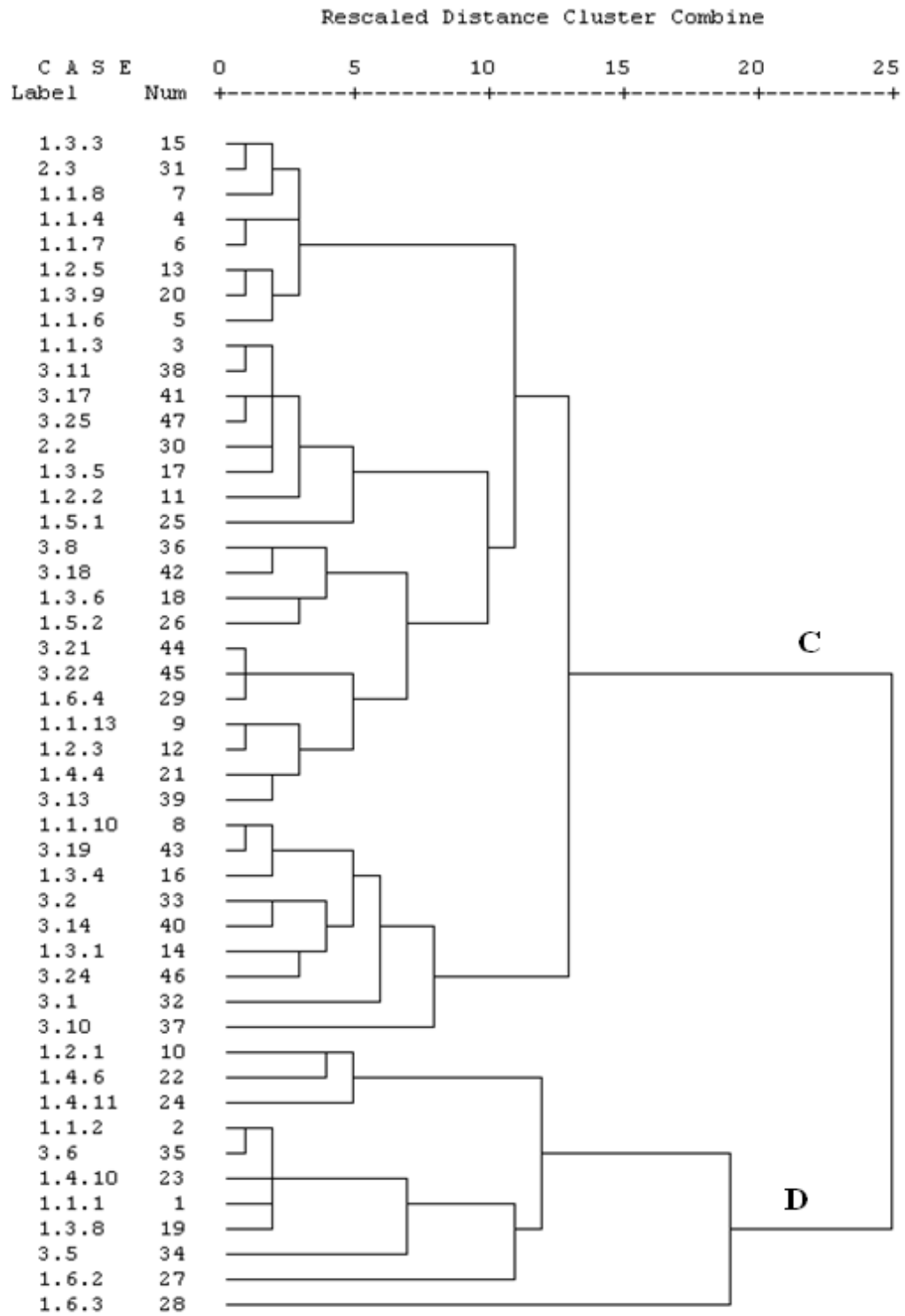


Figure 4.7. Grouping of samples according to slip composition (determined by EDX method)

Samples grouped in to two main groups according to its glaze composition determined by EDX method (Figure 4.8).

Samples in Group E have the PbO_2 content in the range of 37-56 %wt, SiO_2 in the range of 18-34 %wt, Al_2O_3 in the range of 3-9 %wt, MgO in the range 1-3 %wt, Na_2O in the range of 0-3 %wt, K_2O in the range of 0-1 %wt, Fe_2O_3 in the range of 0-2 %wt, CaO in the range of 0-1 %wt, CuO in the range of 0-23 %wt. Samples in Group F have PbO_2 content in the range of 38-47 %wt, SiO_2 in the range of 18-26 %wt, Al_2O_3 in the range of 7-8 %wt, MgO 1-3 %wt, Na_2O in the range of 1-3 %wt, K_2O in the range of 0-1 %wt, Fe_2O_3 in the range of 1-2 %wt, CaO in the range of 0-1 %wt, CuO in the range of 0-3 %wt.

Group E can be separated from Group F with its higher SiO_2 , PbO_2 and CuO composition. Group E can be the product of different workshop or could be produced with different recipe from the rest of the samples in same workshop.

Dendrogram using Ward Method

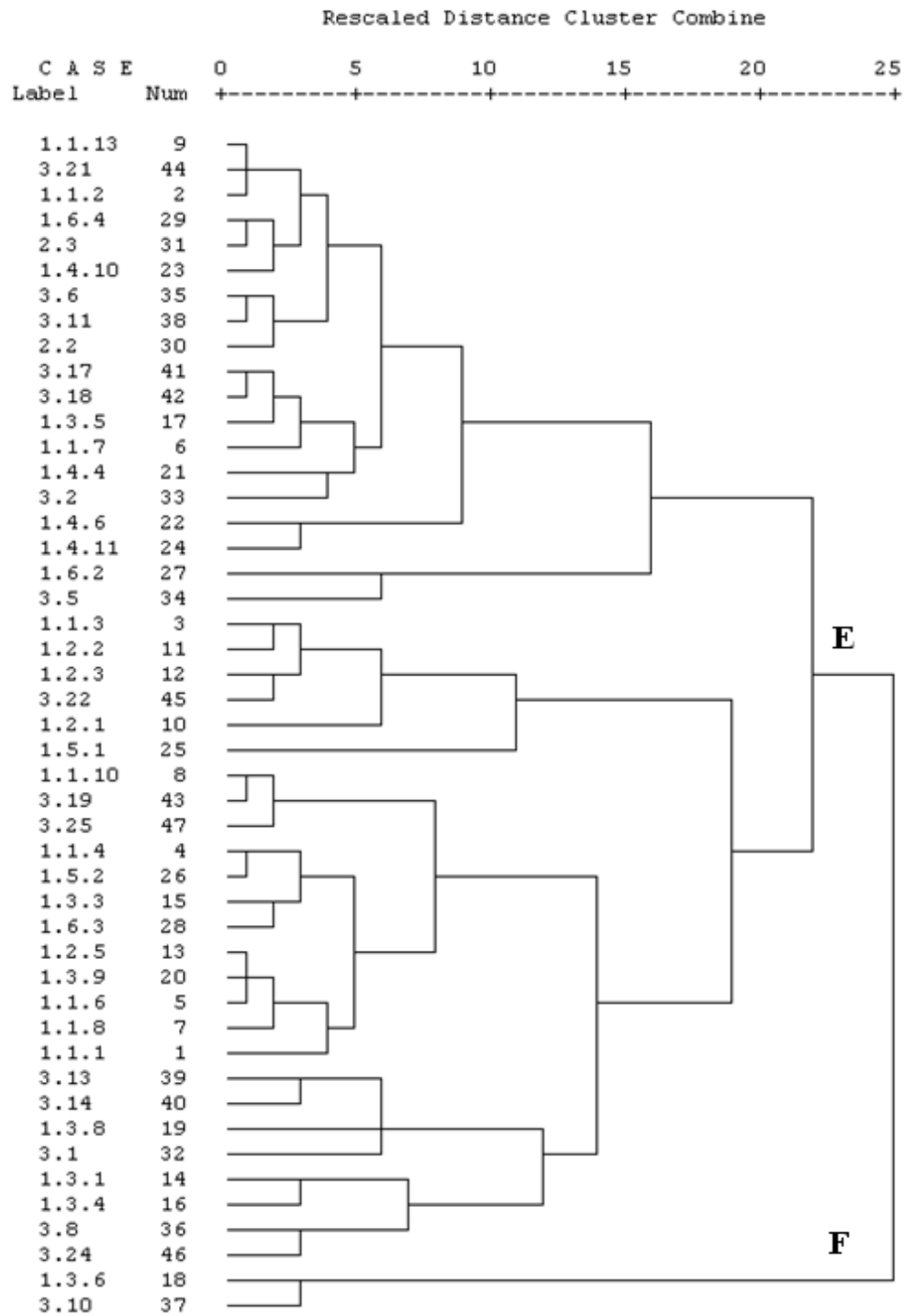


Figure 4.8. Grouping of samples according to glaze composition (determined by EDX method)

The Principal component analysis is the second method used to examine graphically the grouping pattern of samples. First two principal component describe generally most of the total variance, they are used generally in description of provenance of samples (Zhu et al. 2004). Loadings plot give information about the effect of elemental and oxide variables on first two principal components. High positive correlation between the oxides is denoted by small angles between vectors, right angles meaning no correlation and inverse correlations are denoted by angles close to 180° (Neff 1994).

Principal component analysis (46*23 data matrix) and Loading Plots of body, slip and glaze layers are given in Figures 4.9 to 4.14. The ellipses represent group membership assuming the 95% confidence limit.

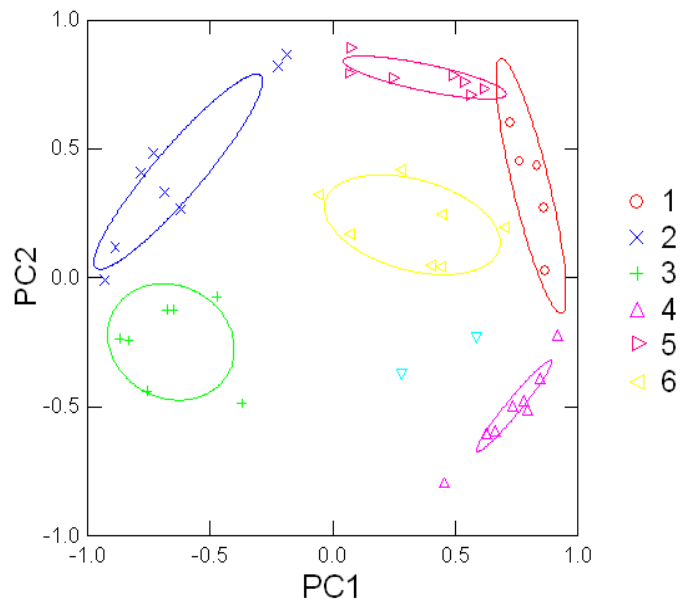


Figure 4.9. Plot of first two principal components obtained PCA of chemical data of body layer obtained by XRF method. Statistical ellipses with 95% confidence level

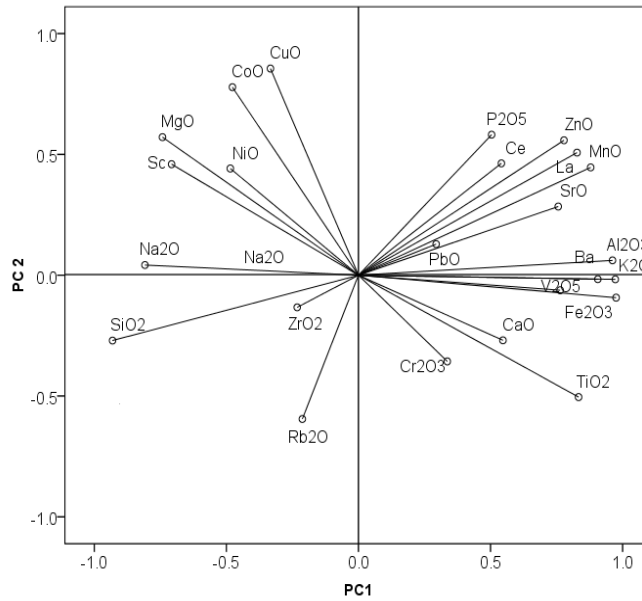


Figure 4.10. Loading Plots of body layer, showing the effect of oxides on PC1 and PC2 values

Principal component analysis of body part of samples shows that first two principal component (PC) account for 44% of the total variance in the data set (Figure 24). Score plot of first two principal components reveals that samples separated into 6 main groups. Samples in Group 1 are 3.18, 1.1.7, 1.3.9, 1.2.5, 3.24, Group 2 are 3.14, 3.2, 1.1.0, 1.3.5, 1.3.8, 3.6, 3.17, 1.1.13, Group 3 are 1.2.2, 1.1.8, 1.3.3, 1.6.4, 1.1.1, 1.2.3, Group 4 are 1.1.4, 1.1.3, 1.4.11, 1.1.2, 1.3.4, 3.8, 1.3.1, 1.4.4, 1.2.1, Group 5 are 3.19, 3.1, 3.11, 2.3, 1.4.10, 3.10, 3.21, Group 6 are 2.2, 1.1.6, 1.5.1, 1.6.3, 1.5.2, 3.13, 1.6.2. Groups are determined according to %95 confidence ellipses. Groups have samples with different decoration types. Groups' main chemical compositions are similar, differences are found from the trace element compositions. Group 1 samples have the lowest La content, Group 2 samples have the lowest Ni and Zr concentration, Group 3 samples have the highest Cu, V, Zn, Sr, Ba, La, Ce, Pb and lowest Rb concentration, Group 5 samples have the lowest Ce concentration, Group 6 samples have the highest Zr content.

Positive PC1 dominated by Fe_2O_3 , K_2O , Al_2O_3 , deficiency of Fe_2O_3 , K_2O , Al_2O_3 results in negative PC1 values (Figure 25). Negative PC1 is dominated by SiO_2 and Na_2O or SiO_2 and Na_2O deficiency results in positive PC1 values. Strong effect towards positive PC2 is caused by CuO and CoO content, negative PC2 values are related with Rb_2O content.

Tempers are the non-plastic materials, improves the workability of clay, allows the evaporation of water smoothly, minimizes shrinkage and prevents cracking, Quartz, limestone, shells, volcanic ash or crushed pots have been used as temper by potters (Papachristodoulou et al. 2006, Neff et al.1988). Addition of tempers causes the large deviations in Si, Ca and Na concentration but dilute the concentration of trace elements (Neff et al.1988). Concentration of these elements are very low compared to clay, large deviations caused by addition of tempers can cause the problems in distinguishing the local or imported potteries (Hall et al. 2002). Instead of addition of tempers mixture of two or more clay may be practiced in order to obtain desired properties in ceramic body (Neff et al.1988).

Except the Group 3 samples, all groups have similar Al_2O_3 and SiO_2 concentration. Group 3 could be produced by clays from different source or different recipe could be used in production of this group. CaO concentration of all samples are similar, these samples could be produced by using calcareous clays or by adding the calcite temper to clay.

Principal component analysis of slip layer of samples shows that first two principal component (PC) account for 35 % of the total variance in the data set (Figure 4.11).

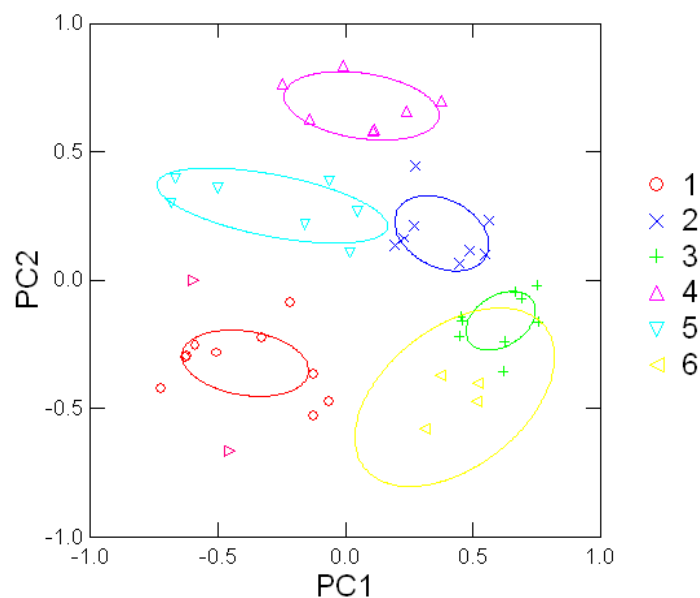


Figure 4.11. Plot of first two principal components obtained PCA of chemical data of slip layer obtained by EDX method. Statistical ellipses with 95% confidence level

Slip Groups are 1.3.8, 1.1.2, 1.2.1, 3.18, 1.6.2, 1.1.8, 3.8, 3.5, 1.4.11, Group 2 samples are 3.19, 1.1.6, 1.3.4, 3.10, 3.13, 1.1.13, 1.6.4, 3.11, Group 3 samples are 1.2.3, 1.2.5, 2.2, 1.4.4, 3.22, 1.3.9, 3.21, 2.3, 1.1.4, Group 4 samples are 3.1, 3.24, 3.2, 1.3.1, 3.14, 1.3.5, 1.1.10, Group 5 samples are 1.1.1, 1.2.2, 3.6, 1.1.3, 1.5.1, 3.17, 3.25, Group 6 samples are 1.3.3, 1.5.2, 1.3.6, 1.1.7. Groups are determined according to %95 confidence ellipses. Groups have samples with different decoration types.

Group 1 samples have the highest Fe_2O_3 , CaO , TiO_2 , Ce_2O_3 , V_2O_5 , Cr_2O_3 , NiO , CuO content. Group 2 samples have the highest Al_2O_3 , BaO , Group 3 samples have the highest PbO_2 , SrO content. Group 4 samples have the NaO , ZrO_2 and ZnO , Rb_2O , Group 5 samples have the highest SiO_2 content, Group 6 samples have the highest La_2O_3 and MnO content.

Slip compositions of samples have uniform profiles, there is no big differences between them, therefore the slip layer used on these ceramic samples could be produced from local clays.

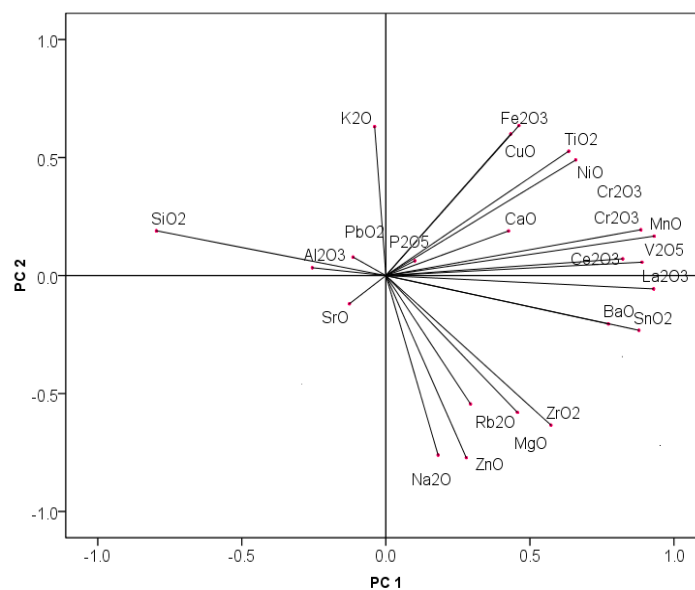


Figure 4.12. Loading plots of slip layer, showing the effect of oxides on PC1 and PC2 values

Positive PC1 is dominated by La_2O_3 , V_2O_5 , MnO , SnO_2 content (Figure 4.12). Negative PC1 is dominated by SiO_2 content. SiO_2 deficiency results in positive PC1 values. Strong effect towards positive PC2 is caused by K_2O and PbO_2 content, negative PC2 values are related with Na_2O and ZnO content.

Principal component analysis of glaze part of samples shows that first two principal component(PC) account for 64% of the total variance in the data set (Figure 4.13).

Samples in Group 1 are 1.3.8, 3.1, 1.2.5, 1.1.8, Group 2 are 1.6.4, 2.3, 3.6, 3.11, 2.2, 3.2, 3.13, 3.14, Group 3 are 1.4.10, 1.1.7, 1.4.4, 1.4.6, 1.6.2, 3.5, Group 4 are 3.18, 1.4.11, 1.2.3, 3.22, 1.2.1, 1.5.1, Group 5 are 1.1.3, 1.2.2, 1.1.4, 1.1.1, 1.3.1, 1.3.4, Group 6 are 1.1.13, 3.21, 1.1.2, 3.17, 1.3.5, 1.5.2, 1.3.6, 3.10, Group 7 are 1.1.10, 3.19, 3.25, 1.6.3, 1.1.6. Groups are determined according to %95 confidence ellipses. Groups have samples with different decoration types.

Group 1 samples have the highest P_2O_5 , Rb_2O , Group 2 samples have the lowest SnO_2 , Rb_2O content, Group 3 samples have the PbO_2 , BaO , NiO , CuO content, Group 4 samples have the highest SiO_2 , Fe_2O_3 , CaO , K_2O content, Group 5 samples have the highest Al_2O_3 , Na_2O content, Group 6 samples have the highest SnO_2 , TiO_2 , La_2O_3 , Ce_2O_3 , V_2O_5 , Cr_2O_3 , MnO content, Group 7 samples have the highest SrO , ZrO_2 , ZnO content. Group 3 sample with high amount of PbO_2 , CuO may resulted from the application of different production recipe or this group can be the product of different workshop.

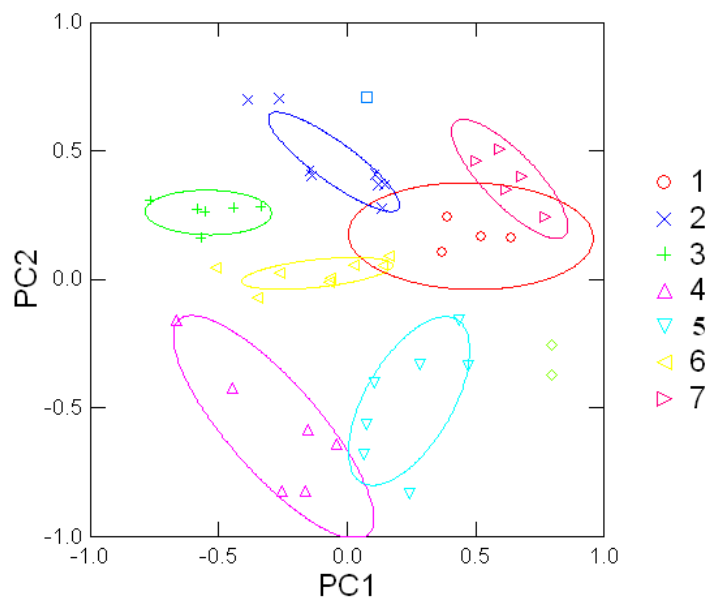


Figure 4.13. Plot of first two principal components obtained PCA of chemical data of glaze layer obtained by EDX method. Statistical ellipses with 95% confidence level

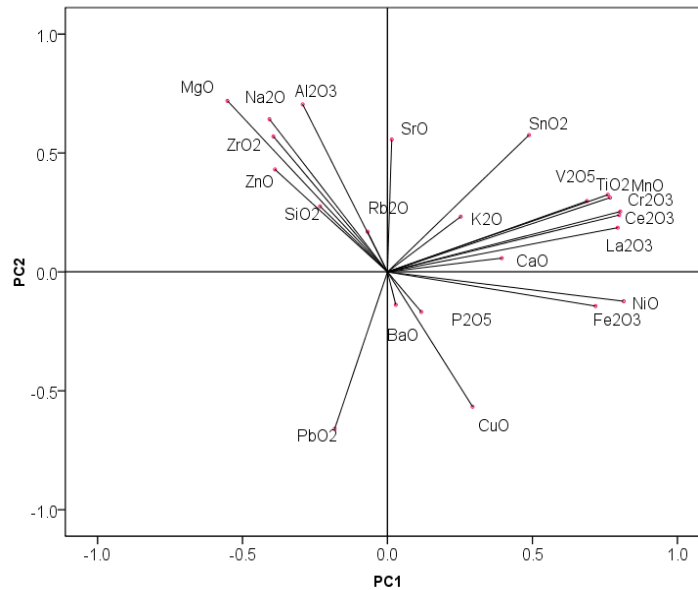


Figure 4.14. Loading plots of glaze layer, showing the effect of oxides on PC1 and PC2 values

Positive PC1 is dominated by Ce_2O_3 , Cr_2O_3 , La_2O_3 , NiO and Fe_2O_3 content. Negative PC1 is dominated by MgO content (Figure 4.14). Strong effect towards positive PC2 is caused by SrO and Al_2O_3 content, negative PC2 values are related with PbO_2 and CuO content.

4.6. Archaeological and Stylistic Evaluation of Dendrograms

Classification of samples according to their decoration types instead of body composition causes difficulties in distinguishing samples coming from same provenance and in understanding of their production and distribution scale.

In this study prior to analysis, ignoring decoration techniques valid according to current classification of Byzantine ceramics, differences are determined in outer surface applications of the samples and samples are classified as Group 1 according to their body appearance. Therefore, Group 1 is classified into sub groups according to their outer surface applications, then classified according to decoration techniques and studied for problem.

Samples in Group 1 subgroups are similar according to their body structure and outer surface applications. Outer surface rims are coated with white-cream slip. Transparent yellow or green glaze covers the surface including the base bottom. Glaze is applied without slip part therefore yellow or green transparent glaze on outer surface

have brown or jade brown view. This group includes samples with Fine Sgraffito, Incised-Sgraffito, Incised and Champlévé type decorations, classified as open vessels. This group includes the samples, which belongs to well-known decoration repertoire within the Aegean Ware (1.1.1, 1.1.3, 1.1.7, 1.1.8.), also new entrants or will be new to the literature (1.1.4, 1.1.6). Also body structure of samples within the typical Fine Sgraffito (1.1.13) and Incised-Sgraffito decoration type (1.1.2, 1.1.10) are tried to be identified in order to determine similarity of provenance.

According to Dendrogram results of body part of samples;

Samples are classified into two main groups. In this classification determination of samples 1.1.2 (Incised-Sgraffito), 1.1.3 (Champlévé), 1.1.4 (Incised) in same group is an important result. Sample 1.1.6 (thought to belong wares with Aegean- type Incised decoration but different from the samples which have decorated with usage of multi-threaded tool in the form of scans¹) and 1.1.7 (with the well known form and decoration of Aegean-type) are grouped together.

Samples 1.1.10 (with classical Incised-Sgraffito decoration), 1.1.8 (Aegean type) and 1.1.13 (Fine Sgraffito) are classified into same group with low variation coefficient.

Sample 1.1.1 (Aegean- type Champlévé with animal figure² placed at the center of ware) classified in Group 2 refers to different production .

As a conclusion Aegean-type wares may originated from two different production centers. Body structure of Group 1 are used for production of open vessels with Fine Sgraffito, Incised-Sgraffito Aegean-type Incised, Aegean-type Champlévé decoration. Body classification made by naked eye is not sufficient in separation of samples slightly different from each other.

Group 1 Type 2; Samples of this group are similar according to body structures and outer surface applications. Outer surface rims are in white-cream colored slip. Transparent colorless glaze or yellow glaze (including the base bottom) applied irregularly. Surface have bright brown color at glazed parts, opaque brown color at

¹ Number of samples , with decoration in the form of vertical and horizontal waves, created with comb-like multi-threaded tool, are not so much. For some examples of this type of finds, location of production couldn't be detected, see Borisov 1989, 237, Fig.281 a,b.

² For similar figures like rabbit, female lion and panther see Morgan 1942, P1.LIII F Corinth); Sanders 1993, P1.24 (11 Sparta); BGC 1999, 65, cat.60 (Thebes), 156, 157, cat.187-188 (Castellorizo Shipwreck); Armstrong 1991, Fig.4-5; Benaki Museum 1999, 103, cat.200-202; B.Böhlendorf-Arslan 2004, Taf.68 (123 Istanbul); Yenişehirlioğlu 1989, Fig.3 (D27 Gülşehir); Doğer 2007, P1.XI f Smyrna Agora); Doğer 2010, 18, fig.3.c (Alabanda); Köroğlu 2004, 114, Fig.13 (Yumuktepe); Peduto 1993, 96, Tav.I (1 Ravello)

unglazed parts. For this group sample 1.2.5³ (with well-known decoration repertoire in scope of Aegean Wares) and 1.2.2 (with decoration which will be new in literature) are selected. Also Incised-Sgraffito⁴ (1.2.1) and Fine Sgraffito (1.2.3) wares' (with the typical decorations), body structures are tried to be characterized in order to answer the question of their provenance.

According to dendrogram samples 1.2.1 (Incised-Sgraffito) and 1.2.5 (Aegean-Type Champlevé, are classified in same group but the samples 1.2.2 (Incised (Aegean type ?)) and 1.2.3 (Fine Sgraffito) are classified in different groups.

As a conclusion, in spite of their different outer surface applications samples 1.2.1 and 1.2.5 are classified with the samples of *Group 1 Type 1*, and these two different decoration types have similar body composition. This result is an important information for these samples.

Group 1 Type 3; Samples of this group are similar according to body structures and outer surface applications. Outer surface rims are covered with white-cream colored slip. Slip thickness is high in rim part. Surface of samples is covered with transparent colorless, yellow or green glaze, have cream-brown moiré appearance. This group have relation with *Group 1 Type 2* samples. In this group Monochrome Plain Ware sample (1.3.1), Champlevé samples⁵ 1.3.4, 1.3.8 (in context of Aegean Ware samples with well-known decoration repertoire) and sample with little-known decoration (1.3.9) brought together. Also Fine Sgraffito samples (1.3.3 and 1.3.5) that have the decoration and drawing, slightly different from the classical repertoire. Body structures of samples are tested in order to determine whether the source used in their production is same or not.

According to Dendrogram Monochrome Plain Ware sample (1.3.4) and Champlevé sample (1.3.4) have similar properties⁶, also the sample 1.3.9 is in same group with these samples.

³ For the similar of lower part preserved Champlevé style samples, with typical running animal figure, see Footnote 1

⁴ On yellow glazed rim, there is band of pseudo Kufic ornamentation which is typical decoration of Incised-Sgraffito. For the finds bearing pseudo Cufic ornamentation, with triangle hook shaped ends, which is very common in 12th century ceramic samples see Doğer 1999, 150, 151 (Selçuk-Ayasuluk; Doğer 2001, Lev. 58, Fig. 3, (Izmir Archaeological Museum); Böhlendorf-Arslan 2004, Taf. 55 (62 Istanbul)

⁵ Part of two animal figure is preserved on the yellow glazed sample with low ring base. For similar finds see Morgan 1942, Fig. 142.a (Corinth)якобсон 1979, Puc. 82(6 Kherson); BGC 1999, 156, cat. 186 (Kastellorizo Shipwreck); Benaki Museum 1999, 92, cat. 174; 105, cat. 208, 209; Böhlendorf-Arslan 2004, Taf. 70 (127 Istanbul). Single or more animal figures on center can be encircled with Incised concentric bands (similar Sample 1.3.8).

⁶ For similar finds see Waksman and Wartburg 2006, 376, Fig. 4; 379, Fig. 5

As a conclusion samples in this group (1.3.1 and 1.3.9) provide information about the acceptance of Monochrome Plain Ware samples⁷ into Aegean Wares, and also identification of new decoration types. Grouping of 1.3.3, 1.3.5 and 1.3.8 samples, as well as classical Aegean Wares, prove that Fine Sgraffito samples, with slightly different scratch and decoration types, can be the product of same source.

Group 1 Type 4; Includes the samples with similar body structure and outer surface application. Covered with thick white-cream colored slip and transparent colorless glaze or yellow glaze (including the base bottom). Composed from the Fine Sgraffito⁸ (1.4.4, 1.4.10) and Aegean type Champlevé (1.4.11) samples.

According to dendrogram samples from the Fine Sgraffito (1.4.4, 1.4.10) and Aegean type Champlevé (1.4.11) samples have similar properties. This result is important to contribute for the question about the provenance of these samples with different decoration types.

Group 1 Type 5; Includes the samples with similar body structure and outer surface application. Although the decayed outer surfaces (except base bottom), glaze remains are determined at joining point of body and base. This group includes the Aegean Type Incised⁹ (1.5.1) and Champlevé (1.5.2) samples. As a conclusion, results proved that the both Incised and Champlevé decoration are applied to Aegean Type samples.

Group 1 Type 6; Includes the samples with similar body structure and outer surface application with different glaze colors. This group includes light green glazed sample¹⁰ (1.6.2) with well-known decoration repertoire, yellow glazed Fine Sgraffito

⁷ For finds from Daskyleion see Doğer 2012a, 118, Tab.5(20)

⁸ These samples carry fashion decoration of Fine-Sgraffito ceramics. Decoration composition of yellow glazed sample (1.4.4) with inward vertical rim is missing. For similar finds see Morgan 1942, 33, (Fig.22E Corinth); BGC 1999, 133, cat.148(Alonessos Shipwreck); Böhlendorf-Arslan, 2004, Taf.53 (55 Istanbul); Parman 1989, Fig.10a (Selçuk-Ayasuluk); Doğer 1999, 151 the middle picture; Doğer 2001, Lev.62, Fig.11 (Izmir Archaeological Museum); Hayes 1992, Pl.11a (Saraçhane). In sample 1.4.10 with medalion style composition, half of the decoration is preserved.

⁹ In yellow glazed sample with low ring base, part of composition formed from circles is preserved. For finds with similar decoration see BGC 1999, 152, cat. 179 (Kastellorizo Shipwreck), 54, cat. 43, 44 (Thebes); Böhlendorf-Arslan 2004, Taf.63 (107 Istanbul); Armstrong 1991, Fig.2-3; Armstrong 1989, Pl.4(47 Phokis); Fig.19 (43 Smixi); Fig.7 (43 Panagia); Doğer 2012, 113, cat.111 (Izmir Archaeological Museum), for finds with more richer interpretations see Doğer 2007, 117, Pl.17.d (Smyrna Agora); Doğer 2012a, 118, Tab.5 (16 Daskyleion).

¹⁰ For interlaced bands against background of scale pattern, Randall, 1968, pic. 60 (Baltimore, Walters Art Gallery); Hayes 1992, Pl. 10.d; Benaki Museum 1999, 65, cat. 105; BGC 1999, 141 (Alonessos Shipwreck) Morgan 1942, 120, Fig.94 (Corinth)

sample (1.6.3) with not well-known decoration repertoire and Aegean Type Champlevé¹¹ (1.6.4) samples.

According to dendrogram results Sample 1.6.2 (with Fine Sgraffito decoration and green glaze), and Sample 1.6.3 (with Fine sgraffito decoration and yellow glaze) determined as compatible. But the Sample 1.6.4 (Aegean Type Champlevé) is slightly different from the Samples 1.6.2 -1.6.3 and determined in different group. As a conclusion, two Fine Sgraffito samples with different glaze color have similar body compositions, new decoration type is recognized, in spite of the similarities based on the outer surface applications sample 1.6.4 (Aegean Type Champlevé) is slightly different from the 1.6.2 (Fine Sgraffito) and 1.6.3 (Fine Sgraffito) samples.

Group 2; Body properties of samples in this group are different from the *Group 1* samples. Differently from the Samples of Group 1, these samples are coated with pink slip on outer surface (including the base). Includes the sample 2.2 with classical Fine Sgraffito decoration (with different glaze color) and classical Aegean Type sample 2.3. According to the Dendrogram result, these samples with different decoration have similarity between them.

Group 3; Samples of this group is different from the samples of Group 1 and Group 2. Outer surface (including the base) is coated with thin and non-intensive slip layer. In rim part slip layer thickness is higher and only this part is covered with glaze. Glaze color is different for the samples and this group includes Fine Sgraffito, Incised, Incised-Sgraffito, and Champlevé samples.

For this group the samples in context of Aegean Wares with well-known decoration repertoire (3.4, 3.5, 3.7, 3.8, 3.10, 3.12, 3.15, 3.17, 3.18, 3.20, 3.21, 3.23, 3.24), little-known decoration repertoire (3.9, 3.25). Also the similar of Fine sgraffito samples, that is known generally as products of Corinth but also obtained in Pelagos Shipwreck and Kastellorizo Cargo, are bring together in this group. Also the samples with well-known repertoire (3.1, 3.6, 3.11, 3.14) and with unknown repertoire (3.3, 3.26) of Fine Sgraffito decoration, well-known repertoire of Incised-Sgraffito¹² decoration (3.13, 3.16, 3.19, 3.22) are bring together in order to determine similarities of them.

¹¹ Decoration is broken and missing

¹² For finds with similar decoration see Morgan 1942, 309, Fig.208 (Corinth); Doğer 1999, 149 bottom right picture (Selçuk-Ayasuluk); BGC 1999, 31, cat.10 (Athens); Benaki Museum 1999, 92, cat.174

According to the Dendrogram determination of Fine Sgraffito samples (3.1, 3.2, 3.14), Incised Sgraffito Samples (3.13, 3.19) and Aegean Type Champlevé (3.24) is an important result. Determination of Fine Sgraffito sample (3.6) with Aegean Type Incised sample (3.17) in same group is an important result. Determination of Aegean Type Incised sample (3.8, 3.18, 3.21), Incised-Sgraffito (3.22), samples in same group is another important result.

As a conclusion most crowded group of samples have dissimilarities, in spite of classification of these samples in same group according to eye determination. Incised-Sgraffito sample 3.25 (newly appeared fish style decoration) is different from other samples. Different style of fish figure from the classical samples is an engrossing detail for this sample.

4.6.1. General Estimation of Dendrogram

Samples (1.1.2, 1.1.3, 1.1.4, 1.1.6, 1.1.7, 1.2.1, 1.2.5, 1.3.1, 1.3.4, 1.3.9, 1.4.4, 1.4.10, 1.4.11, 1.5.1, 1.5.2, 1.6.2, 1.6.3) which classified into same group according to outer surface applications can be the product of same center, differences determined on outer surface of samples can be thought as the result of weak standardization.

Samples (2.2 and 2.3) have similar outer surface applications and body structures with different glaze color. These samples are not different too much from each other and have similarity with Group 1 and Group 3 samples according to their body composition.

Samples of Group 3 (3.1, 3.2, 3.8, 3.10, 3.11, 3.13, 3.14, 3.18, 3.19, 3.21, 3.22, 3.24) have main differences in body, slip and outer surface applications from the Samples 1.1.2, 1.1.3, 1.1.4, 1.1.6, 1.1.7, 1.2.1, 1.2.5, 1.3.1, 1.3.4, 1.3.9, 1.4.4, 1.4.10, 1.4.11, 1.5.1, 1.5.2, 1.6.2, 1.6.3 and, 2.2, 2.3 are classified in same group with these samples according to body composition. Differences on outer surface applications in this group, can be the result of the usage of same body composition by different workshops or products of different craftsman. This result support the opinion, Aegean Type Incised, Champlevé, Fine Sgraffito and Incised-Sgraffito samples can be the products of one or more workshops. Decorations determined for samples 1.1.4, 1.1.6 and 1.6.3 shows that there is personal trial decorations without the classical motifs.

Samples 1.1.8, 1.1.10, 1.1.13, 1.3.3, 1.3.5, 1.3.8, 1.6.4, which classified into same group according to outer surface applications, can be the product of same center, differences determined on outer surface of samples can be thought as the result of weak standardization.

Samples 3.5, 3.6, 3.17 have similar outer surface applications and body structures. These samples are not different too much from each other and have similarity with Group 1 and Group 3 samples according to their body composition. Samples 1.1.8, 1.1.10, 1.1.13, 1.3.3, 1.3.5, 1.3.8, 1.6.4 have similar structure with samples 3.5, 3.6, 3.17. Differences on outer surface applications in this group, can be the result of the usage of same body composition by different workshops or products of different craftsman. This result support the opinion, Aegean Type Incised, Champlevé, Fine Sgraffito samples can be the products of one or more workshops.

Sample 3.25 is a different sample with its composition. Fish figure on sample is different stylistically from the small-bodied fork tailed fish figure known from Kastellorizo Shipwreck. It has more coarser body and significant fish flakes¹³. This sample is similar to samples collected from Lebanon, Tell Arqa¹⁴, East Phokis (Valtesi)¹⁵, Istanbul (Constantinople)¹⁶, Pergamon¹⁷, Çamaltı Burnu I shipwreck¹⁸. Samples from Lebanon, Tell Arqa and Çamaltı Burnu I are characterized. According to results Tell Arqa Sample is similar to others but Çamaltı Burnu I sample is related stylistically to Aegean Wares but seem like another production sample. Similar results are obtained for Anaia sample. Decoration technique, head of fish constituting the decoration and the auxiliary motifs are in the style of Aegean Type Incised samples, new comment on body of fish shouldn't be missed. This situation, with analysis results, can be helpful for chronology problems.

Samples 1.1.1, 1.2.3 and 1.2.2 have similar outer surface applications and body structures. These samples improves that the workshop could produced Aegean Type Champlevé and Fine Sgraffito samples together. Also the sample 1.2.2 produced by scratching and decorated with herbal motif outside the usual repertoire, is helpful in recognition of some individual trials.

¹³ For some similar finds flakes are sometimes stylized with horizontal-vertical scratching

¹⁴ For find see Waksman and Wartburg 2006, 375, Fig.3(18)

¹⁵ For find see Armstrong 1989, 19, Fig.12(33)

¹⁶ For finds see Böhlendorf-Arslan 2004, Taf.120,121

¹⁷ For finds see Böhlendorf-Arslan 2004, Taf.96 (330)

¹⁸ For find see Günsenin 2003, 368, Fig.10a-b

4.6.2. General Archaeological Conclusion

Samples in first subgroups are related to each other with small variations. Differences in slip and outer surface applications are thought to be related with workshops using same clay source or craftsman of same workshop rather than the usage of different clay sources. As well as the Champlevé (3.24) and Incised samples (3.10) that are the favorite samples of Aegean Type, equivalents dating to 12th and second half of the 12th century, Fine Sgraffito (3.1,3.2) and Incised-Sgraffito (3.13,3.2) samples, with most recognizable decoration motifs of style, included in this table, this result is very important. This consequence demonstrate that this workshop produces the stylistic products of Komnenian Period of Corinth. Monochrome Plain Ware (1.3.1) determined in Anaia collection, this result is important for the determination of source of this little-known production. Small differences are obtained for the samples in 1A1 group in dendrogram, therefore it is thought that four different decoration type of samples are produced in this workshop or workshops. Small differences between the samples, can be the result of usage of clay from the different places of same source. Sample 3.25, considering its decoration style, Aegean Type Incised products can be the product of different geological region, or can be related with changes occurred in clay source during long production duration. Group 2 includes samples Aegean Type Incised, Champlevé and Fine Sgraffito samples that are slightly different from the samples of Group 1. According to Dendrogram Analysis result Anaia samples can be the product of two different workshop or a big workshop, with large scale production, using the two different clay source.

4.6.3. Comparison of Anaia Samples with Archaeological Samples

In this part of the study, the Middle Byzantine period pottery samples from different locations, that were studied by Waksman (Waksman et al. 2006), are compared with the Anaia samples (Table 4.10-4.11-4.12).

Table 4.10. Codes, decoration types and sources of Byzantine samples

Codes	Decoration types	Source
Byz 631	Fine Sgraffito Ware	Kouklia, Cyprus
Byz 353	Fine Sgraffito Ware	Cherson, Crimea
Byz 355	Fine Sgraffito Ware	Cherson, Crimea
Byz 629	Fine Sgraffito Ware	Paphos, Cyprus
Byz 354	Fine Sgraffito Ware	Cherson, Crimea
Byz 630	Fine Sgraffito Ware	Paphos, Cyprus
Byz 650	Incised-Sgraffito Ware	Kouklia, Cyprus
Byz 653	Incised-Sgraffito Ware	Kouklia, Cyprus
Byz 658	Incised-Sgraffito Ware	Paphos, Cyprus
Byz 649	Incised –Sgraffito Ware	Kouklia, Cyprus
Lev 359	Incised Ware	Tell Arqa, Lebanon
Lev 360	Incised Ware	Tell Arqa, Lebanon
Byz 632	Champlevé Ware	Paphos, Cyprus
Byz 651	Champlevé Ware	Kouklia, Cyprus
Byz 352	Champlevé Ware	Cherson,, Crimea

Table 4.11. Codes and decoration types of Anaia samples

Codes	Decoration Types	Codes	Decoration types	Codes	Decoration types
1.1.13	Fine Sgraffito Ware	3.14	Fine Sgraffito Ware	3.21	Incised-Sgraffito Ware
1.2.3	Fine Sgraffito Ware	1.1.4	Incised-Sgraffito Ware	3.25	Incised-Sgraffito Ware
1.3.3	Fine Sgraffito Ware	1.1.6	Incised-Sgraffito Ware	1.1.1	Champlevé
1.3.5	Fine Sgraffito Ware	1.1.7	Incised-Sgraffito Ware	1.1.3	Champlevé
1.4.4	Fine Sgraffito Ware	1.2.2	Incised-Sgraffito Ware	1.2.5	Champlevé
1.4.10	Fine Sgraffito Ware	1.3.9	Incised-Sgraffito Ware	1.3.4	Champlevé
1.6.2	Fine Sgraffito Ware	1.5.1	Incised-Sgraffito Ware	1.3.8	Champlevé
1.6.3	Fine Sgraffito Ware	2.3	Incised-Sgraffito Ware	1.4.1	Champlevé
2.2	Fine Sgraffito Ware	3.5	Incised-Sgraffito Ware	1.5.2	Champlevé
3.1	Fine Sgraffito Ware	3.8	Incised-Sgraffito Ware	1.6.4	Champlevé
3.2	Fine Sgraffito Ware	3.10	Incised-Sgraffito Ware	3.24	Champlevé
3.6	Fine Sgraffito Ware	3.17	Incised-Sgraffito Ware		
3.11	Fine Sgraffito Ware	3.18	Incised-Sgraffito Ware		

Waksman et.al. studied the chemical composition of the body part of the samples (see Table 4.10) by Wavelength Dispersive-X Ray Fluorescence (WD-XRF) in the Laboratoire de Ceramologie in Lyon, France. Results are given in Table 4.12..

Table 4.12. Chemical composition of the samples as determined by WD-XRF method (Waksman and Wartburg 2006). Major and minor elements are given in weight percent of oxides, trace elements are given in ppm.

Fine Sgraffito Ware	CaO	Fe ₂ O ₃	TiO ₂	K ₂ O	SiO ₂	Al ₂ O ₃	MgO	MnO	Na ₂ O	P ₂ O ₅	Zr	Sr	Rb	Zn	Cr	Ni	La	Ba	V	Ce	Pb	Cu
Byz 629	4.92	7.61	0.88	4.10	57.42	20.78	2.43	0.12	1.37	0.16	168	113	159	110	135	105	37	681	145	80	500	38
Byz 630	4.14	7.83	0.87	4.15	57.68	21.06	2.45	0.12	1.30	0.17	164	100	166	111	149	119	42	687	138	79	455	43
Byz 631	5.44	7.18	0.86	3.85	58.68	19.63	2.35	0.11	1.52	0.17	182	125	147	100	141	111	46	663	142	81	366	37
Byz 353	5.89	7.19	0.85	3.67	57.96	19.54	2.59	0.12	1.70	0.20	183	111	146	107	156	117	43	641	136	82	1176	44
Byz 354	5.45	7.58	0.86	3.82	57.19	20.51	2.45	0.12	1.43	0.15	167	97	151	111	144	111	44	709	138	84	2423	43
Byz 355	5.12	6.52	0.87	3.75	59.51	19.46	2.27	0.11	1.95	0.23	195	106	146	98	133	100	44	623	124	84	462	39
Incised Ware	CaO	Fe ₂ O ₃	TiO ₂	K ₂ O	SiO ₂	Al ₂ O ₃	MgO	MnO	Na ₂ O	P ₂ O ₅	Zr	Sr	Rb	Zn	Cr	Ni	La	Ba	V	Ce	Pb	Cu
Byz 649	5.52	7.55	0.84	3.95	57.26	20.42	2.52	0.12	1.29	0.16	156	138	150	103	142	106	36	714	144	79	1903	50
Byz 650	4.80	7.29	0.85	3.85	59.15	19.75	2.35	0.11	1.39	0.18	179	124	145	103	145	103	39	695	146	85	946	38
Byz 653	4.68	7.04	0.85	3.72	59.98	19.31	2.32	0.11	1.58	0.17	186	115	145	93	144	104	38	669	148	80	513	46
Byz 658	5.04	7.11	0.86	3.73	59.57	19.36	2.44	0.12	1.41	0.17	203	126	146	100	136	110	36	729	140	85	125	40
Lev 359	5.65	7.04	0.86	3.69	59.36	18.93	2.45	0.12	1.49	0.18	201	108	141	102	159	122	41	616	133	81	559	44
Lev 360	5.26	6.54	0.84	3.61	60.95	18.25	2.47	0.11	1.56	0.20	219	115	135	98	134	100	44	630	120	81	300	38
Champleve Ware	CaO	Fe ₂ O ₃	TiO ₂	K ₂ O	SiO ₂	Al ₂ O ₃	MgO	MnO	Na ₂ O	P ₂ O ₅	Zr	Sr	Rb	Zn	Cr	Ni	La	Ba	V	Ce	Pb	Cu
Byz 632	5.71	6.62	0.82	3.44	59.33	18.5	2.6	0.11	1.58	0.14	177	105	104	89	139	96	39	620	133	82	9896	64
Byz 651	4.90	7.23	0.85	3.92	59.11	19.64	2.39	0.12	1.4	0.16	187	121	147	105	151	103	37	644	139	86	1035	41
Byz 352	5.58	6.64	0.84	3.48	59.58	18.72	2.51	0.11	1.67	0.16	195	108	121	98	139	104	42	600	126	87	5410	44

A comparison of the two groups of samples was done by feeding the quantitative chemical analysis results into Hierarchical Clustering Analysis software. The purpose was to see if there were any relationships between the samples in two different studies (that is Waksman versus this study). Data was carefully selected to allow comparison of the samples with the same decoration types except the incised decorated samples. Results are given in Figures 4.15 to 4.17.

Dendrogram using Ward Method

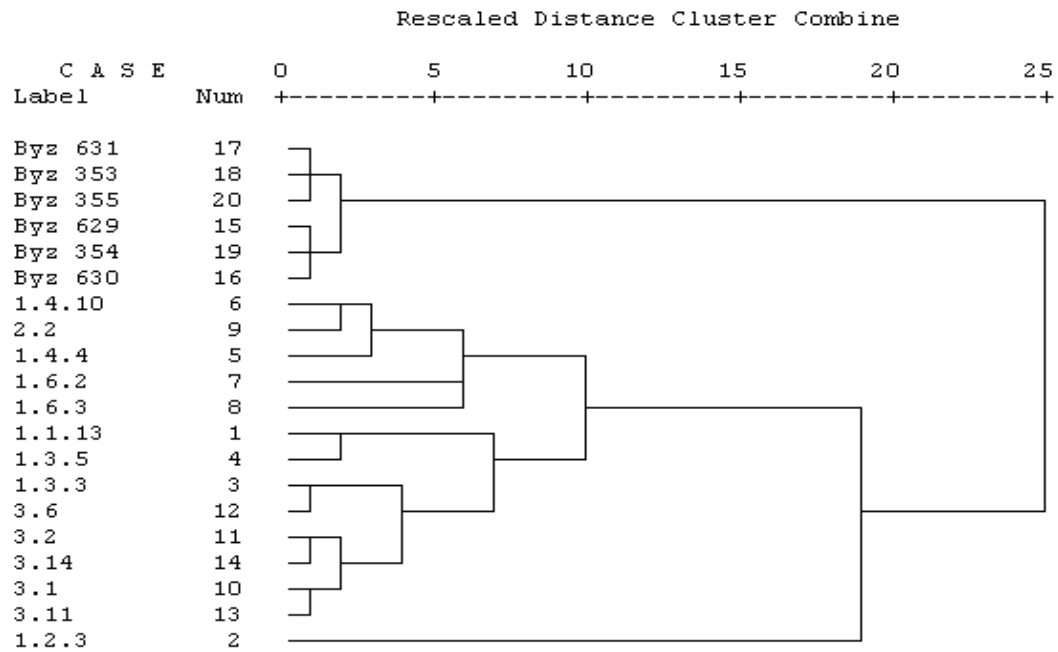


Figure 4.15. Comparison of fine sgraffito decorated Anaia and Byzantine samples

Dendrogram using Ward Method

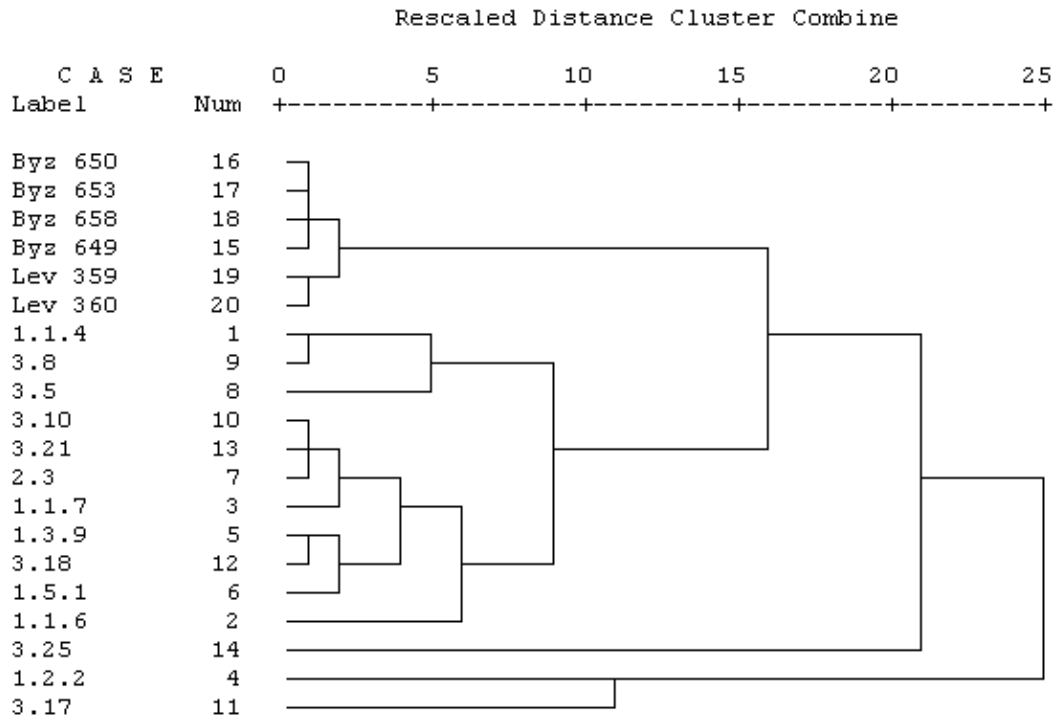


Figure 4.16. Comparison of incised decorated Aniaia samples with incised-sgraffito decorated Byzantine samples

Dendrogram using Ward Method

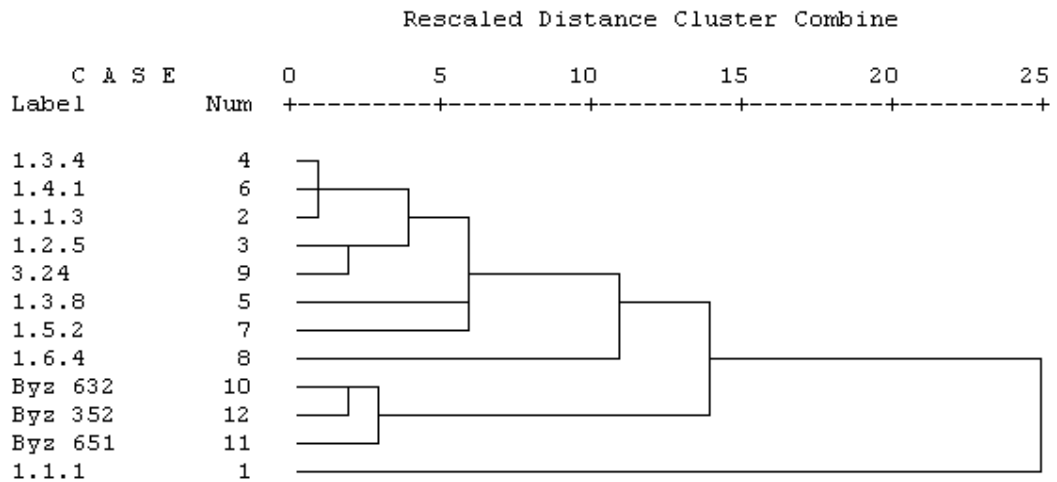


Figure 4.17. Comparison of champlévé decorated Aniaia and Byzantine samples

According to the dendrograms generated by the software, similarity between Aniaia samples and the samples from Cyprus, Crimea and Lebanon was very low. These samples could be the product of different workshops, or the clay used in production of

these samples could be different. Limited number of samples were used in these analysis, in order to obtain more reliable results the number of samples should be increased. Also the comparison of clay sources of these samples could give more information about the similarities.

4.6.4. General Interpretation and Discussion

Dendrograms generated via the software using Wards method showed that the ceramic samples collected from Anaia could be grouped into two categories A and B according to the chemical composition of the body. The group B consisted of three ceramic samples all glazed with sgraffito decoration. One of these samples was Champlévé and the other two were incised sgraffito. Interestingly, all these three samples had high alumina, iron oxide and potassium oxide percentage and comparatively low percentage of silica. The conclusion was that these three were very closely matched in their body compositions, possibly the same clay type or raw material mixture was used in their manufacture as they contained significantly higher amount of alumina. The dendrograms generated for data in this study and in the study by Waksman et.al. indicated that there was some minor similarity between the two groups of samples. But the degree of similarity was not decisive enough to make strong conclusions.

Chapter 5

Production and Characterization of Replicate Samples

Lead glazes are applied on ceramics to obtain colorless or colored finishing. They show high adherence to the clay body. Lead glazes melt between 700-1000°C depending on the composition and have been used since ancient times in the production of pottery.

In this part of the thesis lead glazed ceramic samples were produced and characterized by different methods. The aim was to produce replicate samples and to determine the interactions between body and glaze parts, by using different lead glaze compositions, different bodies, firing time, temperature and cooling rates.

5.1. Production and Characterization of Replicate Samples with Clay Body

In this part of the thesis replicate samples compatible with the original historic samples collected from Anaia Excavation, were tried to be produced. A set of experiments were designed for production of lead glazed ceramic samples in laboratory. In production of body part of samples, clay collected from SERANT A.Ş were used. The chemical composition of clay is given in Table 5.1.

Table 5.1. Composition of Clay (Menemen) determined by XRF method

	Composition (wt%)		Composition (wt%)
Na ₂ O	1.08	Fe ₂ O ₃	8.25
MgO	1.29	CoO	0.00
Al ₂ O ₃	18.73	NiO	0.01
SiO ₂	63.80	CuO	0.00
P ₂ O ₅	0.12	ZnO	0.01
K ₂ O	3.65	Rb ₂ O	0.02
CaO	1.66	SrO	0.03
PbO	0.01	ZrO ₂	0.03
TiO ₂	1.05	Ba	0.05
V ₂ O ₅	0.03	La	0.02
Cr ₂ O ₃	0.04	Ce	0.02
MnO	0.09	Sc	0.00

The body part of samples was formed by plaster mold which were produced in laboratory (Figure 5.1).



(a)

(b)

Figure 5.1. Plaster mold (a) and produced samples (b)

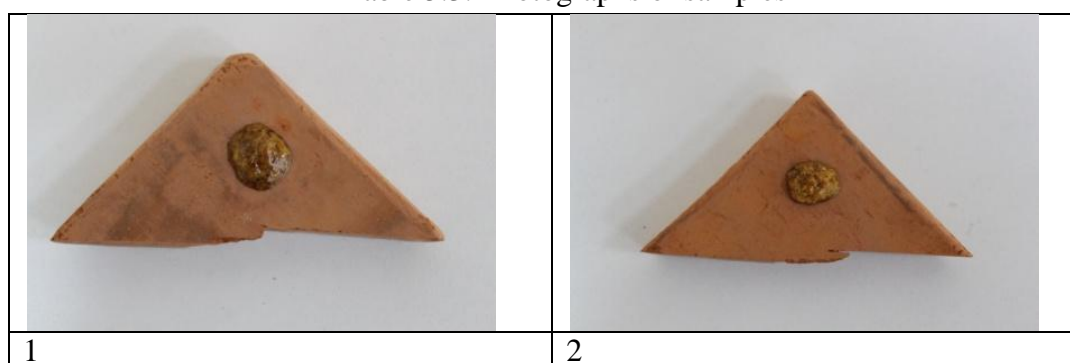
The prepared samples were removed from mold, dried to green body stage in oven. Heat treatment of samples was carried in kiln for one hour at 800°C with heating rate of 5°C/minute. Glazes were prepared in laboratory by mixing PbO (IRON Kimya) and SiO₂ (761-Kalemaden), Al₂O₃(Alcoa CT3000-SG), CaCO₃(012365-Alfa Aesar), Fe₂O₃ (012375-Alfa Aesar), MgOH (012367-Alfa Aesar) powders (with %98 purity). Pellets were prepared, with a diameter of 8mm, from this mixture and were left on the surface of body part. The samples were heat treated at 900°C, with a heating rate of

5°C/minute, during 20 minutes. Amounts of oxides used in preparation of glaze are given in Table 5.2 and Table 5.4. The photographs of samples after the heat treatment are given in Table 5.3 and Table 5.5.

Table 5.2. Amounts of oxides used in preparation of glaze layer











Mix	PbO	SiO ₂	Al ₂ O ₃	MgO	CaO	Fe ₂ O ₃	Na ₂ O
1	56.7	25.4	8.9	2.9	1.7	2	1.6
2	55	25	9	3	2	2	2
3	55	25	9	3	2	2	0
4	55	25	9	3	2	0	2
5	55	25	9	3	0	2	2
6	55	25	9	0	2	2	2
7	55	25	9	3	0	0	0
8	55	25	0	3	0	0	0
9	55	25	9	0	0	0	0
10	55	25	0	0	0	0	0
11	60	20	0	0	0	0	0
12	65	15	0	0	0	0	0
13	70	10	0	0	0	0	0
14	50	30	0	0	0	0	0
15	45	35	0	0	0	0	0
16	40	40	0	0	0	0	0

Table 5.3. Photographs of samples



(cont. on next page)

Table 5.3 (cont.)

	
3	4
	
5	6
	
7	8
	
9	10
	
11	12

(cont. on next page)

Table 5.3 (cont.)

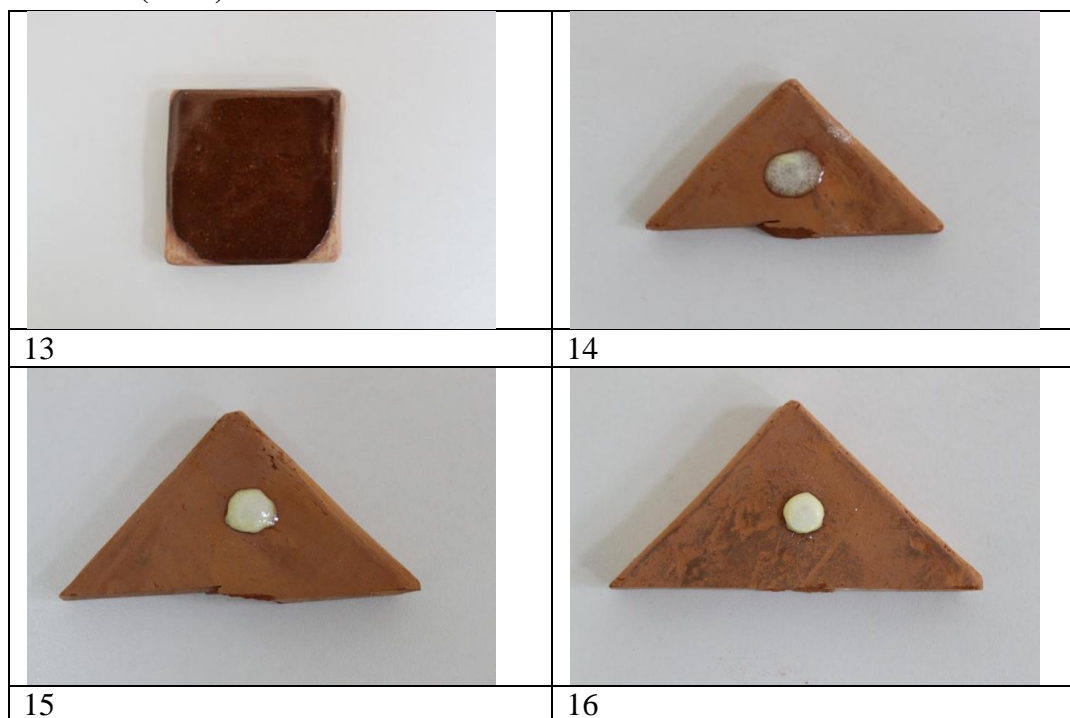










Table 5.4. Amounts of oxides used in preparation of glaze layer

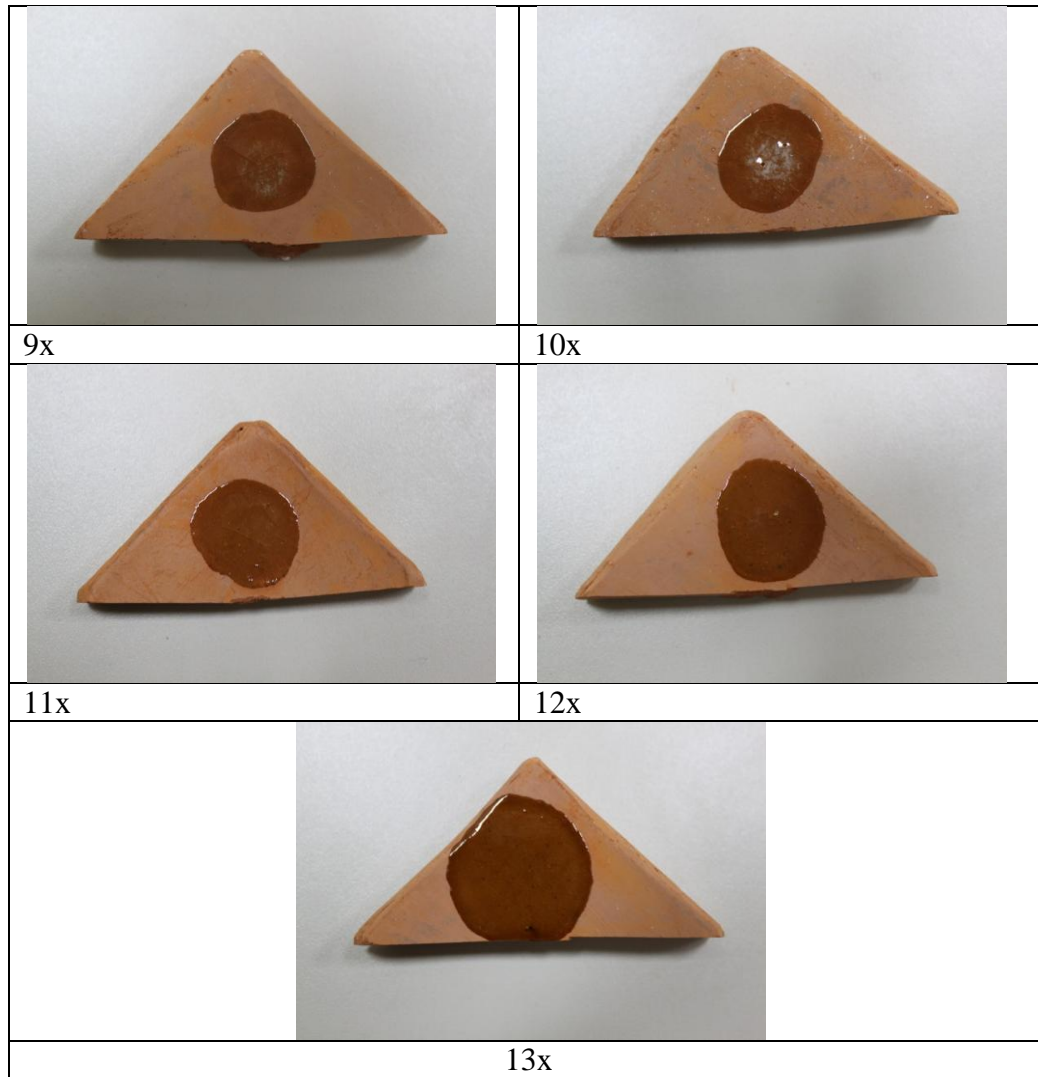
Mix	PbO	SiO₂	Al₂O₃	MgO	CaO	Fe₂O₃	Na₂O
1x	65	25	9	3	2	2	2
2x	65	25	9	3	2	2	0
3x	65	25	9	3	2	0	2
4x	65	25	9	3	0	2	2
5x	65	25	9	0	2	2	2
6x	65	25	9	3	0	0	0
7x	65	25	0	3	0	0	0
8x	65	25	9	0	0	0	0
9x	65	25	0	0	0	0	0
10x	70	30	0	0	0	0	0
11x	75	25	0	0	0	0	0
12x	80	20	0	0	0	0	0
13x	90	10	0	0	0	0	0

Table 5.5. Photographs of samples

	
1x	2x
	
3x	4x
	
5x	6x
	
7x	8x

(cont. on next page)

Table 5.5 (cont.)



The results indicated that the usage of high amount of lead (PbO) and low amount of quartz (SiO₂) in glaze composition resulted in the production of qualified samples (samples 11x, 12x, 13x). Addition of other oxides (Al₂O₃, MgO, CaO, Fe₂O₃, Na₂O) caused formation problems in glaze structure.

High lead content glazes melt at lower temperatures and react with body, lead diffuses to body and elements of body diffuses into glaze part. Interaction layer is formed between two layers. In order to determine the magnitude of interaction between the body and glaze parts, new set of samples were prepared in laboratory. Glazes were prepared from PbO (IRON Kimya), PbO+SiO₂(761-Kalemaden) and PbO+Clay(K-244-Kalemaden) mixtures, in PbO:SiO₂ (9:1) and PbO:K-244 (9:1) proportions. Chemical composition of Clay (K-244) is given in Table 5.6.

Table 5.6. Chemical composition of Clay (K-244) determined by XRF method

Oxides	% wt	Oxides	% wt
SiO ₂	59.361	NiO	0.015
Al ₂ O ₃	33.556	CuO	0.100
K ₂ O	2.362	ZnO	0.033
Na ₂ O	0.021	Rb ₂ O	0.018
MgO	0.697	SrO	0.057
Fe ₂ O ₃	1.896	ZrO ₂	0.024
CaO	0.490	PbO	0.006
TiO ₂	1.077	Elements	% wt
V ₂ O ₅	0.031	Sc	0.001
Cr ₂ O ₃	0.035	Ba	0.030
MnO	0.021	La	0.018
CoO	0.004	Ce	0.035






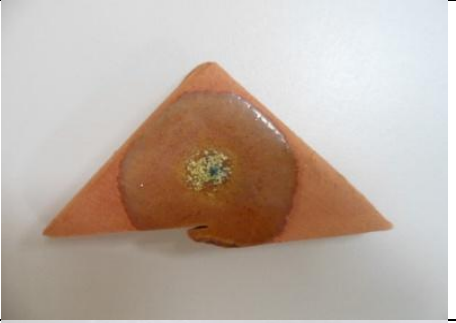


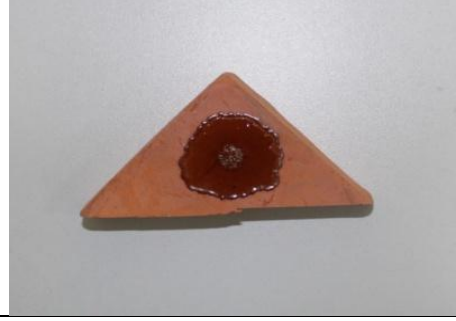

Glazes were applied on raw clay body or heat treated clay body (800°C, 1h with heating rate of 5°C/minute). Body part of the samples were produced from clay coded as Menemen (Serant A.Ş). Designed set of experiments and experimental conditions are given in Table 5.7.

Table 5.7. Codes, contents and heat treatment procedures of samples

Codes	Glaze Content	Cooling	Heat Treatment Temp., Soaking Time
S1	PbO	Slow Cooling	850 °C (20 min.)
S2	PbO	Rapid Cooling	850 °C (20 min.)
S3	PbO+SiO ₂	Slow Cooling	850 °C (20 min.)
S4	PbO+SiO ₂	Rapid Cooling	850 °C (20 min.)
S5	PbO+K ₂ O	Slow Cooling	850 °C (20 min.)
S6	PbO+K ₂ O	Rapid Cooling	850 °C (20 min.)
S7	PbO	Slow Cooling	900 °C (20 min.)
S8	PbO	Rapid Cooling	900 °C (20 min.)
S9	PbO+SiO ₂	Slow Cooling	900 °C (20 min.)
S10	PbO+SiO ₂	Rapid Cooling	900 °C (20 min.)
S11	PbO+K ₂ O	Slow Cooling	900 °C (20 min.)
S12	PbO+K ₂ O	Rapid Cooling	900 °C (20 min.)
S13	PbO	Slow Cooling	1000 °C (20 min.)
S14	PbO	Rapid Cooling	1000 °C (20 min.)
S15	PbO	Slow Cooling	1000 °C (1 h.)
S16	PbO	Slow Cooling	1000 °C (3 h.)
S17	PbO	Slow Cooling	1000 °C (20 min., raw body)
S18	PbO	Rapid Cooling	1000 °C (20 min., raw body)
S19	PbO+SiO ₂	Slow Cooling	1000 °C (20 min.)
S20	PbO+SiO ₂	Rapid Cooling	1000 °C (20 min.)
S21	PbO+K ₂ O	Slow Cooling	1000 °C (20 min.)
S22	PbO+K ₂ O	Rapid Cooling	1000 °C (20 min.)

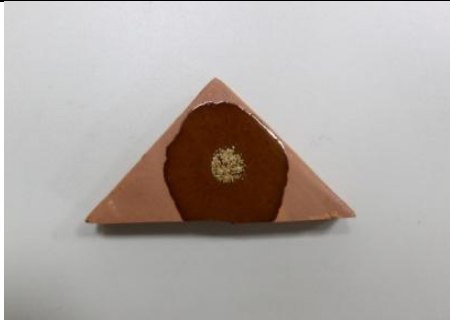
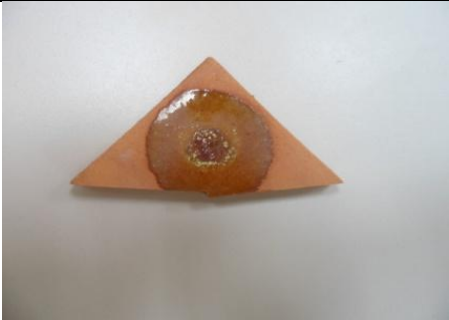







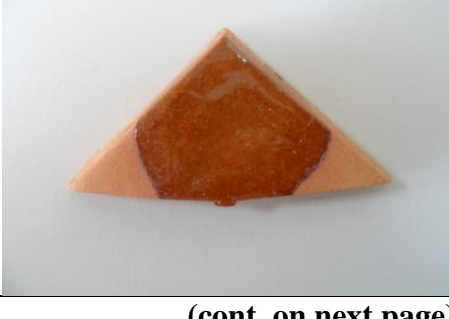
Photographs of the produced 22 samples are presented in Table 5.8. Glazes, containing high content of lead, melted and covered the surface of samples.

Table 5.8. Photographs of produced samples

Code	Photograph	Code	Photograph
S1		S2	
S3		S4	
S5		S6	
S7		S8	
S9		S10	

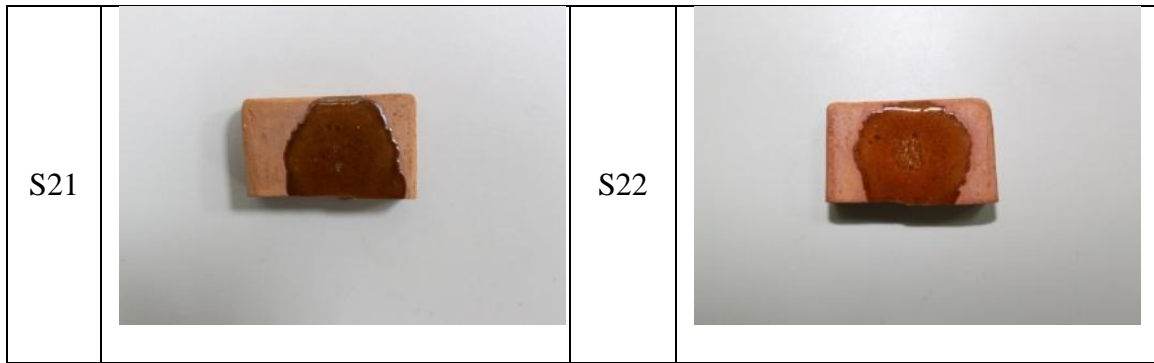
(cont. on next page)

Table 5.8 (cont.)

S11		S12	
S13		S14	
S15		S16	
S17		S18	
S19		S20	

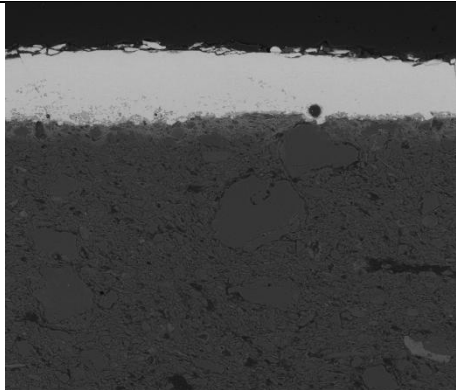
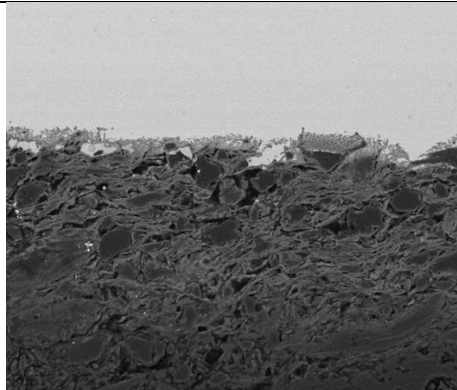

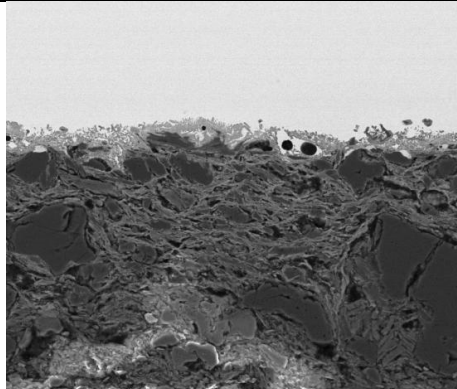
(cont. on next page)

Table 5.8 (cont.)



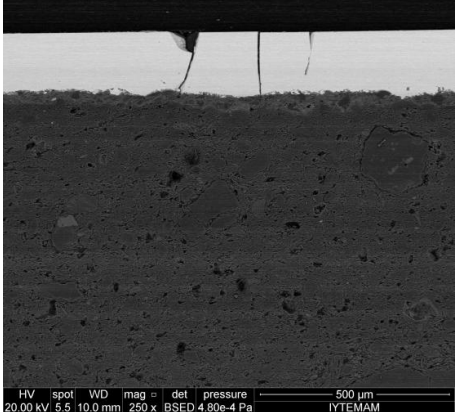
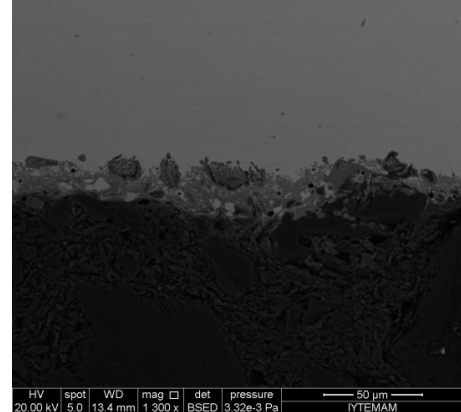
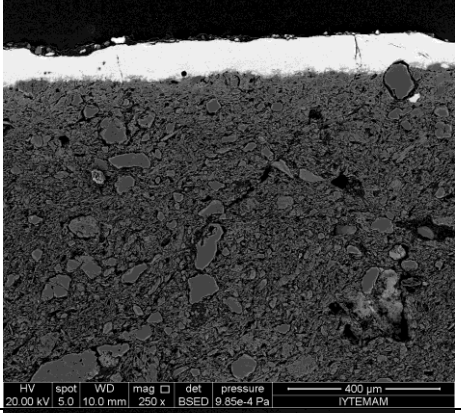
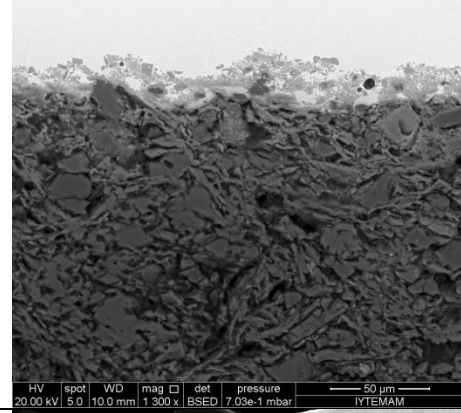
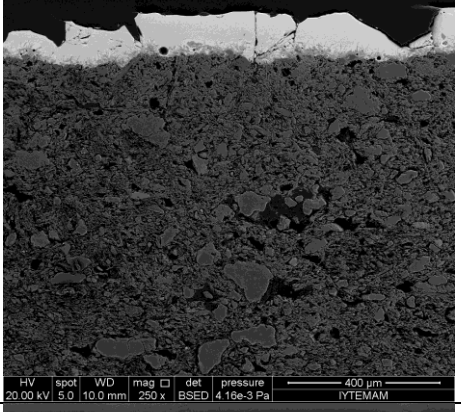
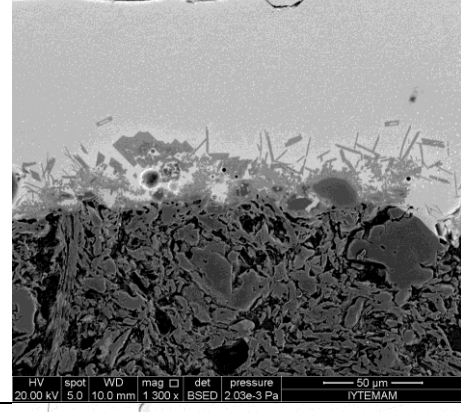
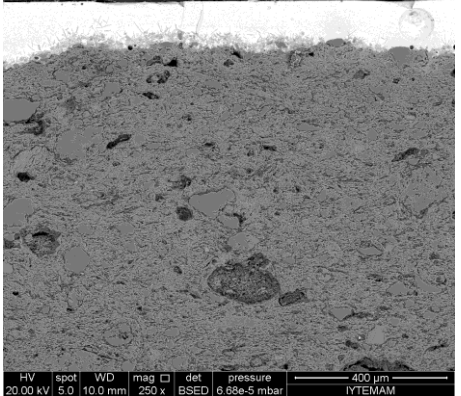
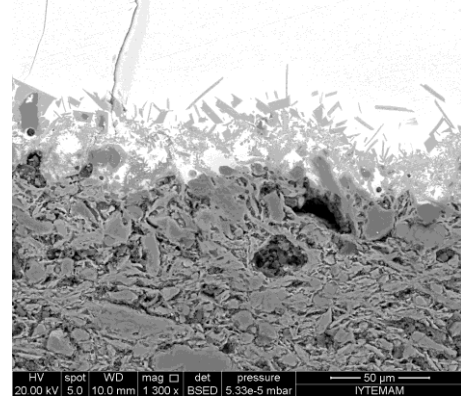
In order to determine the interaction between body and glaze parts, cross sections of samples were cut, polished and characterized by SEM-EDX analysis. In SEM analysis of samples different magnifications were used (250X and 1300 X). Results are given in Tables 5.9-5.14.

Table 5.9. SEM analysis results of samples glazed with PbO

Codes	250X	1300X
S1	 <p data-bbox="389 1384 847 1413">HV spot WD mag □ det pressure — 500 μm — 20.00 kV 5.0 10.1 mm 250 x BSED 50 Pa IYTEMAM</p>	 <p data-bbox="876 1384 1334 1413">HV spot WD mag □ det pressure — 50 μm — 20.00 kV 5.0 11.3 mm 1300 x BSED 1.00e-2 Pa IYTEMAM</p>
S2	 <p data-bbox="389 1800 847 1823">HV spot WD mag □ det pressure — 500 μm — 20.00 kV 5.0 10.0 mm 250 x BSED 50 Pa IYTEMAM</p>	 <p data-bbox="876 1800 1334 1823">HV spot WD mag □ det pressure — 50 μm — 20.00 kV 5.0 9.5 mm 1300 x BSED 7.99e-3 Pa IYTEMAM</p>

(cont. on next page)

Table 5.9 (cont.)

<p>S7</p>		
<p>S8</p>		
<p>S13</p>		
<p>S14</p>		

(cont. on next page)

Table 5.9 (cont.)

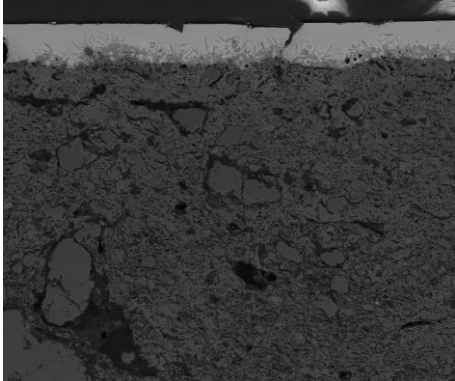
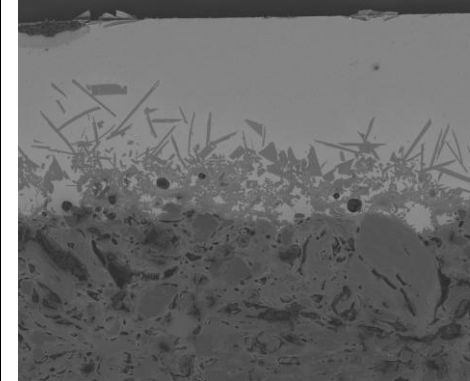

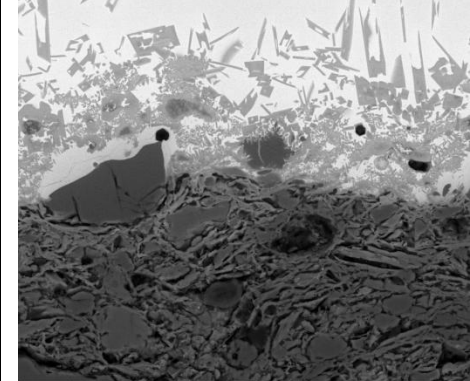
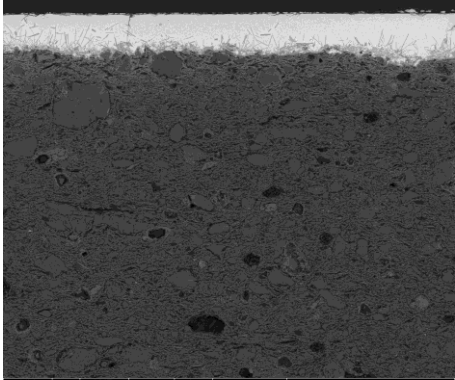
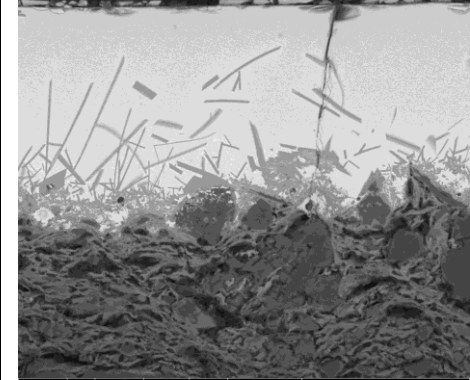
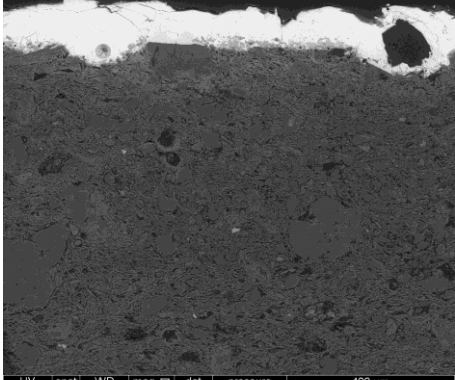
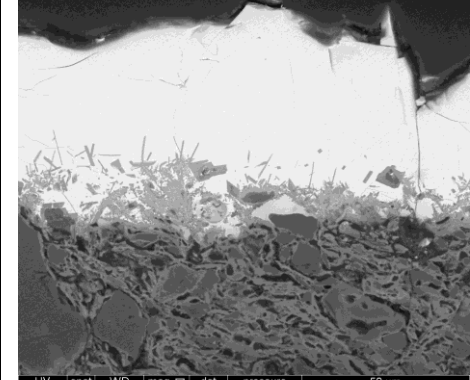
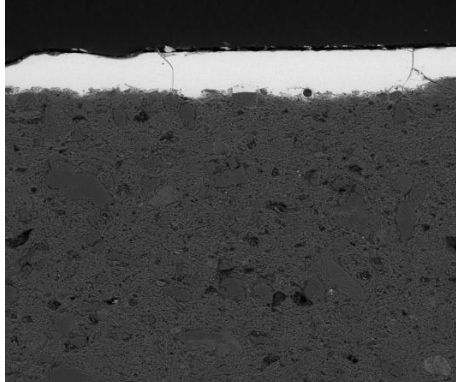

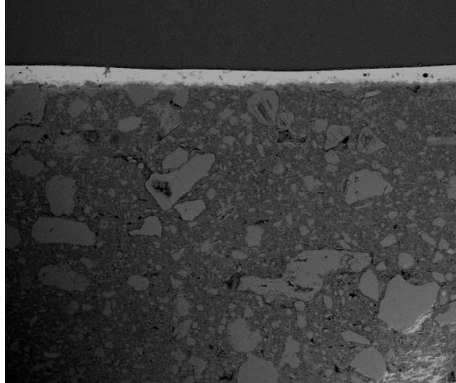
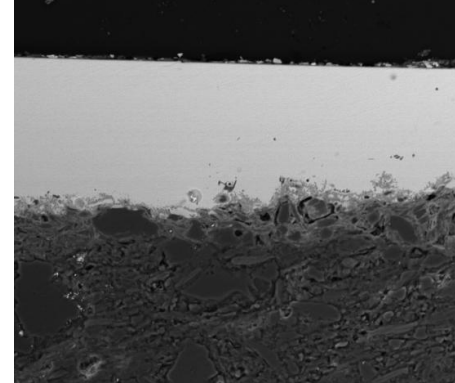
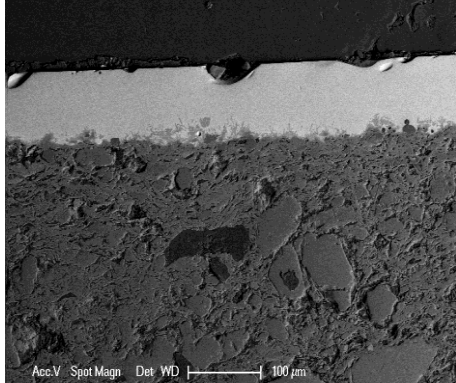
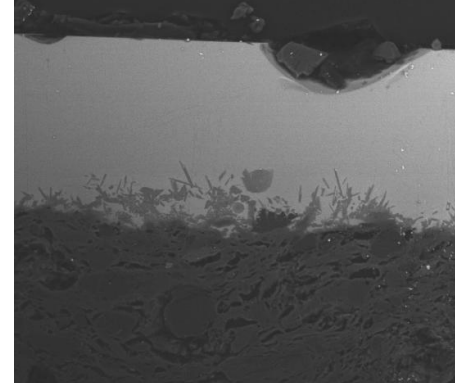
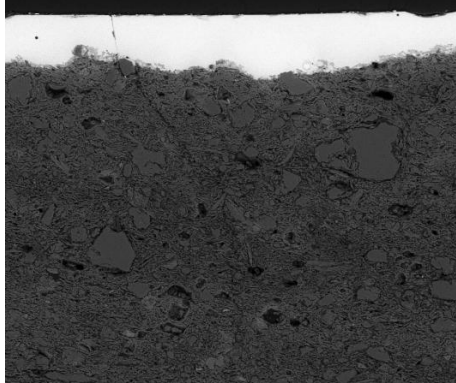
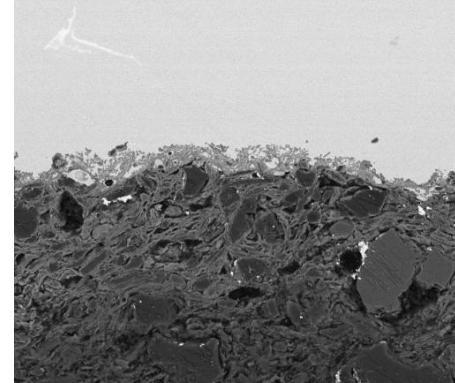
S15	 <p>HV 10.00 kV spot 5.0 WD 9.8 mm mag 250 x det BSED pressure 7.31e-5 mbar 400 μm IYTEMAM</p>	 <p>HV 10.00 kV spot 5.0 WD 9.6 mm mag 1300 x det BSED pressure 9.57e-5 mbar 50 μm IYTEMAM</p>
S16	 <p>HV 20.00 kV spot 5.0 WD 9.2 mm mag 250 x det BSED pressure 6.99e-1 mbar 400 μm IYTEMAM</p>	 <p>HV 20.00 kV spot 5.0 WD 10.0 mm mag 1500 x det BSED pressure 6.99e-1 mbar 50 μm IYTEMAM</p>
S17	 <p>HV 20.00 kV spot 5.0 WD 11.8 mm mag 250 x det BSED pressure 6.99e-1 mbar 400 μm IYTEMAM</p>	 <p>HV 20.00 kV spot 5.0 WD 11.8 mm mag 1500 x det BSED pressure 7.07e-1 mbar 50 μm IYTEMAM</p>
S18	 <p>HV 20.00 kV spot 5.0 WD 10.0 mm mag 250 x det BSED pressure 6.99e-1 mbar 400 μm IYTEMAM</p>	 <p>HV 20.00 kV spot 5.0 WD 10.0 mm mag 1500 x det BSED pressure 6.99e-1 mbar 50 μm IYTEMAM</p>

Table 5.10. EDX analysis results of samples glazed with PbO

Codes	Glaze Content	Cooling	Heat Treatment Temp.,		PbO	SiO ₂	Al ₂ O ₃	K ₂ O	CaO	MgO	FeO
			Soaking Time								
S1	PbO	Slow Cooling	850 oC (20 min.)		84.50	9.30	2.97	0.27	0.43	2.20	0.74
S2	PbO	Rapid Cooling	850 oC (20 min.)		86.86	9.09	2.37	0.04	0.15	1.39	0.20
S7	PbO	Slow Cooling	900 oC (20 min.)		79.35	11.20	6.03	0.40	0.55	0.43	2.05
S8	PbO	Rapid Cooling	900 oC (20 min.)		81.37	10.46	5.86	0.31	0.30	0.28	1.78
S13	PbO	Slow Cooling	1000 oC (20 min.)		56.81	28.10	8.54	1.46	1.83	0.78	2.58
S14	PbO	Rapid Cooling	1000 oC (20 min.)		59.61	25.77	8.46	1.30	1.20	0.95	2.60
S15	PbO	Slow Cooling	1000 oC (1 h.)		53.89	30.59	12.36	0.52	0.69	1.86	0.09
S16	PbO	Slow Cooling	1000 oC (3 h.)		51.76	32.71	12.76	1.03	0.30	1.42	0.00
S17	PbO	Slow Cooling	1000 oC (20 min., raw body)		54.89	29.56	9.31	1.01	1.33	1.05	2.84
S18	PbO	Rapid Cooling	1000 oC (20 min., raw body)		55.09	32.23	10.21	0.45	0.41	1.27	0.33

Considering the chemical composition, lead oxide content of glaze layer was affected by cooling procedure, slow cooling allowed the diffusion of lead oxide to body part and other oxides to glaze part, therefore the composition of lead oxide was decreased while other oxide contents were increased in glaze layer. Diffusion reaction was caused the formation of crystals at interface. The amount of diffusion was increased with temperature, at low temperatures diffusion was low. According to the SEM-EDX analysis results of samples at temperature of 850°C, interaction between glaze and body were small. Increment of heat treatment temperature was resulted to the extension of interface crystalline layer (lead-feldspar) developed between body and glaze parts. This reaction continues until the achievement of equilibrium between body and glaze parts. The application of glaze on raw or heat treated body was another important effect on formation of interaction layer. Considering the samples 13-14 and 17-18, application of lead glaze on raw body was caused the formation of thicker interaction zone (Table 5.9), raw body was more reactive than the heat treated body. Duration time also affected the thickness of interaction layer, considering the S15 and S16 samples, increment of duration time was caused the formation of thicker layer.

Table 5.11. SEM analysis results of samples glazed with PbO+SiO₂ (PbO:SiO₂, 9:1)

Codes	250X	1300X
S3	 <p>HV spot WD mag □ det pressure 20.00 kV 5.0 10.0 mm 250 x BSED 6.00e-1 mbar 400 μm IYTEMAM</p>	 <p>HV spot WD mag □ det pressure 20.00 kV 5.0 10.9 mm 1 300 x BSED 7.82e-3 Pa 50 μm IYTEMAM</p>
S4	 <p>HV spot WD mag □ det pressure 10.00 kV 3.0 9.5 mm 250 x BSED 6.98e-3 Pa 400 μm IYTEMAM</p>	 <p>HV spot WD mag □ det pressure 20.00 kV 5.0 8.8 mm 1 300 x BSED 4.55e-3 Pa 50 μm IYTEMAM</p>
S9	 <p>Acc.V Spot Magn Det WD 15.0 kV 4.0 200x BSE-3.1 IYTEMAM 400 μm</p>	 <p>HV spot WD mag □ det pressure 20.00 kV 5.0 9.9 mm 1 300 x BSED 7.64e-3 Pa 50 μm IYTEMAM</p>
S10	 <p>HV spot WD mag □ det pressure 20.00 kV 5.0 10.0 mm 250 x BSED 6.99e-1 mbar 400 μm IYTEMAM</p>	 <p>HV spot WD mag □ det pressure 20.00 kV 5.0 11.3 mm 1 300 x BSED 9.15e-3 Pa 50 μm IYTEMAM</p>

(cont. on next page)

Table 5.11 (cont.)

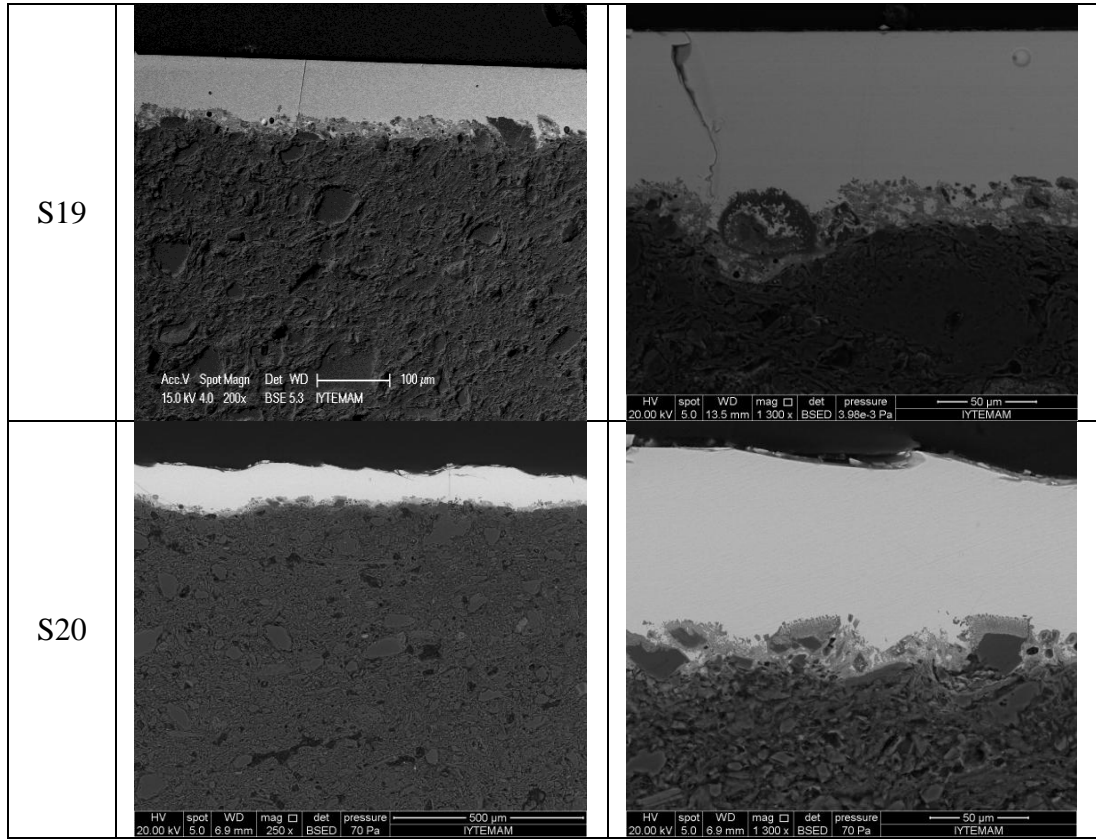


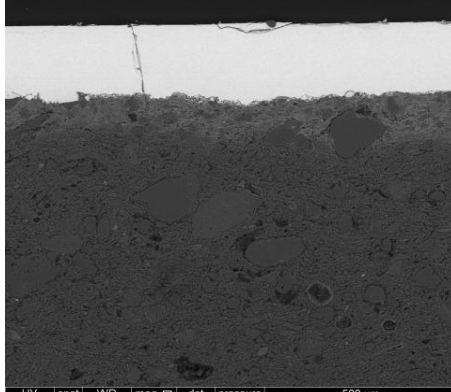
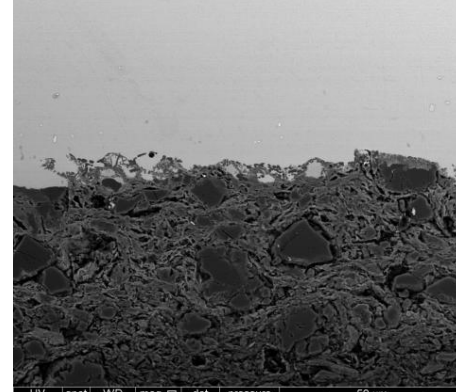
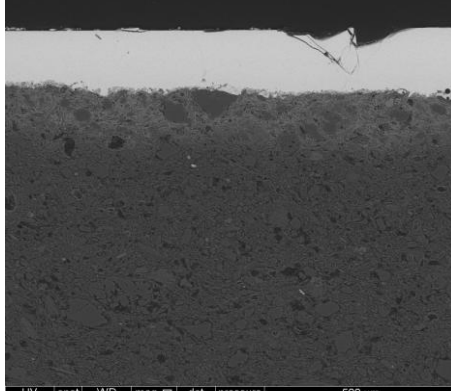
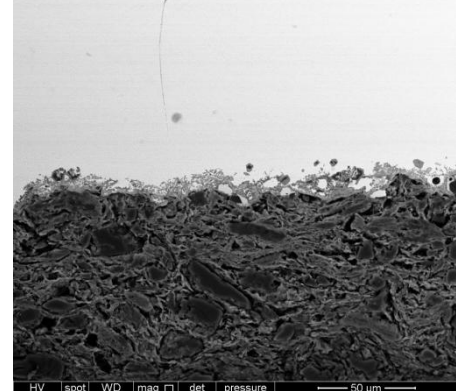
Table 5.12. EDX analysis results of samples glazed with PbO+SiO₂ (PbO:SiO₂, 9:1)

Codes	Glaze Content	Cooling	Heat Treatment Temp.,		PbO	SiO ₂	Al ₂ O ₃	K ₂ O	CaO	MgO	FeO
			Soaking Time								
S3	PbO+SiO ₂	Slow Cooling	850 oC	(20 min.)	74.00	20.70	3.11	0.27	0.29	0.90	0.74
S4	PbO+SiO ₂	Rapid Cooling	850 oC	(20 min.)	78.60	18.09	2.06	0.04	0.15	0.19	0.70
S9	PbO+SiO ₂	Slow Cooling	900 oC	(20 min.)	70.84	21.91	3.51	0.64	0.68	1.30	1.41
S10	PbO+SiO ₂	Rapid Cooling	900 oC	(20 min.)	75.47	19.35	2.61	0.18	0.35	0.60	1.45
S19	PbO+SiO ₂	Slow Cooling	1000 oC	(20 min.)	61.64	30.53	4.60	0.84	1.07	0.84	0.48
S20	PbO+SiO ₂	Rapid Cooling	1000 oC	(20 min.)	62.90	27.40	6.89	0.94	1.16	0.69	0.01

Considering the chemical composition, lead oxide content of glaze layer was affected by cooling procedure, slow cooling was provided time for diffusion of elements and was allowed the formation of interface layer between body and glaze parts. The amount of diffusion was increased with temperature, at low temperatures diffusion was low. Interaction layer thickness was increased with increment of temperature. These results were compatible with the results of glaze produced only from PbO, the main difference was the thickness of interaction layer formed for two different type of glaze. Decrement of PbO content and addition of SiO₂ to glaze composition had a negative

effect on thickness. Considering the SEM analysis results, S13 sample, coated with lead oxide glaze and heat treated at 1000°C, had 50 µm interface layer, but the S19 sample, coated with PbO+SiO₂ glaze and heat treated at 1000°C, had 30 µm interface layer. Lead oxide had a positive effect on the formation of interface layer.

Table 5.13. SEM analysis results of samples glazed with PbO+Clay(K-244) (PbO:Clay, 9:1)

Codes	250X	1300X
S5	 <p data-bbox="459 1003 911 1021">HV spot WD mag □ det pressure 500 µm 20.00 kV 5.0 10.8 mm 250 x BSED 50 Pa IYTEMAM</p>	 <p data-bbox="938 1003 1396 1021">HV spot WD mag □ det pressure 50 µm 20.00 kV 5.0 9.4 mm 1300 x BSED 1.07e-2 Pa IYTEMAM</p>
S6	 <p data-bbox="459 1417 911 1435">HV spot WD mag □ det pressure 500 µm 20.00 kV 5.0 10.0 mm 250 x BSED 50 Pa IYTEMAM</p>	 <p data-bbox="938 1417 1396 1435">HV spot WD mag □ det pressure 50 µm 20.00 kV 5.0 8.8 mm 1300 x BSED 7.14e-3 Pa IYTEMAM</p>

(cont. on next page)

Table 5.13 (cont.)

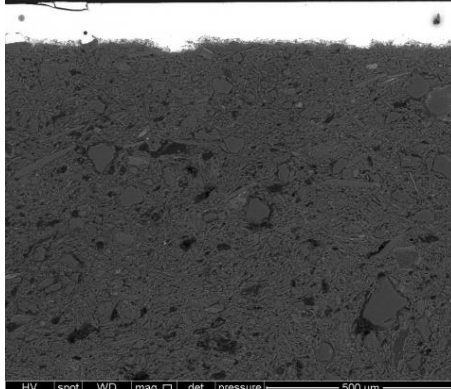
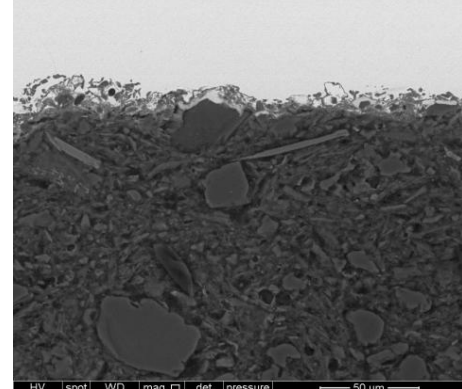
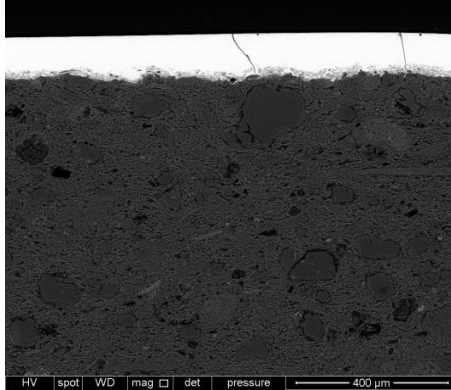
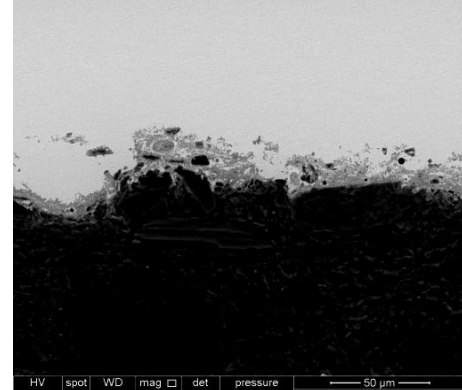
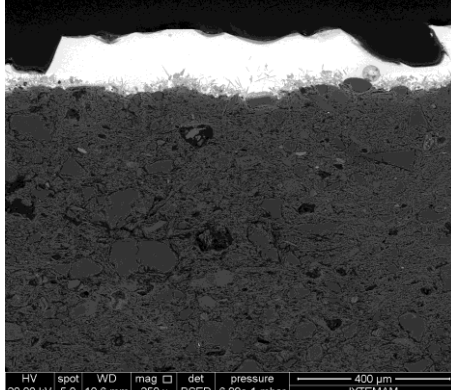
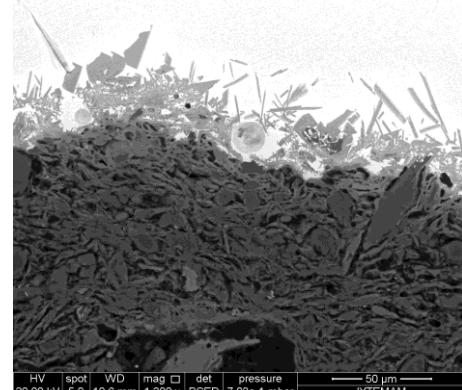
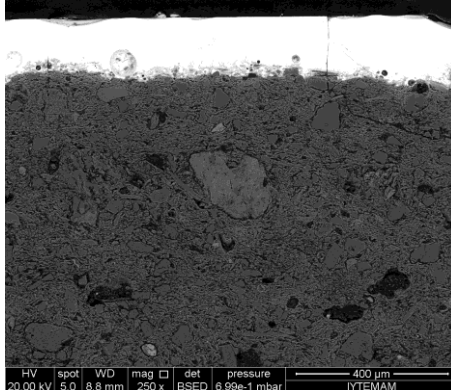
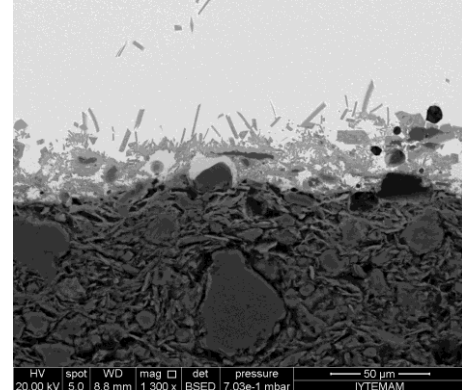
S11		
S12		
S21		
S22		

Table 5.14. EDX analysis results of samples glazed with PbO+Clay(K-244) (PbO:Clay)

Codes	Glaze Content	Cooling	Heat Treatment Temp., Soaking Time	PbO	SiO ₂	Al ₂ O ₃	K ₂ O	CaO	MgO	FeO
S5	PbO+K244	Slow Cooling	850 oC (20 min.)	77.37	15.55	4.51	0.38	0.65	0.60	0.65
S6	PbO+K244	Rapid Cooling	850 oC (20 min.)	82.78	11.27	4.25	0.35	0.21	0.54	0.50
S11	PbO+K244	Slow Cooling	900 oC (20 min.)	72.47	19.04	6.38	0.68	0.47	0.60	0.82
S12	PbO+K244	Rapid Cooling	900 oC (20 min.)	75.58	15.94	6.10	0.45	0.38	0.41	0.81
S21	PbO+K244	Slow Cooling	1000 oC (20 min.)	64.74	24.42	8.53	0.95	0.54	0.20	0.62
S22	PbO+K244	Rapid Cooling	1000 oC (20 min.)	69.06	18.82	8.45	0.93	1.34	0.86	0.54

Considering the cooling procedure, slow cooling were caused the formation of thicker interface layer between the body and the glaze parts. Interaction layer thickness also was increased with increment of temperature, because the amount of diffusion was increased with temperature. These results were compatible with the results of glaze produced only from PbO and mixture of PbO+SiO₂, the main difference was about the thickness of interaction layer formed between body and glaze layers. Addition of K-244 clay into PbO was caused the production of thinner interface layer, because aluminum in structure of clay act as stabilizer of glaze and decreases the diffusion of elements between body and glaze (Molera 2001). Lower degree of reaction between glaze and body was the result of stable glaze structure. According to SEM-EDX results S13 sample, which was coated with PbO glaze and heat treated at 1000°C, had 40 µm interface layer, the S19 sample, which was coated with PbO+SiO₂ glaze and heat treated at 1000°C, had 30 µm interface layer. The S22 sample, which was coated with PbO+Clay (K-244) glaze and heat treated at 1000°C, had 10 µm interface layer. Lead oxide had positive effect on formation of interface layer. Increment of PbO composition was caused the formation of thicker interface layer.

Interface layer was composed of the crystals, the chemical composition of these crystals were investigated by SEM-EDX analysis for sample S13 (Figure 5.2).

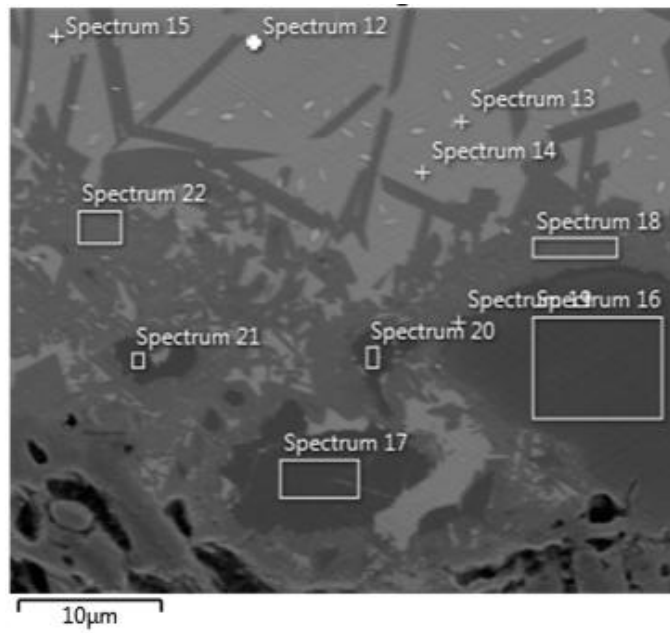


Figure 5.2. Crystals obtained at interface of S13 sample body and glaze part

According to the EDX results SiO_2 content was decreasing from dark colored crystal area to light colored glaze part and the PbO content was increasing from light colored glass area to dark colored crystal part (Figure 5.2, Table 5.15).

Table 5.15. EDX analysis of results of spectrums

Oxide	Oxide %										
	Spectrum 12	Spectrum 13	Spectrum 14	Spectrum 15	Spectrum 16	Spectrum 17	Spectrum 18	Spectrum 19	Spectrum 20	Spectrum 21	Spectrum 22
Na2O	1.45	0	1.18	1.78	3.44	3.65	2.33	6.05	4.5	4.14	1.56
MgO	1.43	2.15	1.48	1.6	2.66	1.07	0.51	1.41	2.61	0.57	2.15
Al2O3	18.07	8.74	17.58	17.55	32.67	14.86	27.68	34.47	36.74	26.55	20.84
SiO2	36	24.78	37.53	37.2	52.91	47.09	43.01	49.23	50.76	56.97	41.65
P2O5	0.12	0.47	0.36	0	0	0.46	0	0	0	0	0
K2O	1.27	0.54	0.92	1.05	2.41	1.31	0.58	0.46	0.31	1.51	0.38
CaO	0.33	0.55	0.39	0.48	0	0.02	0.08	0.02	0	0	0
TiO2	0.18	0.36	0.84	0	0	0.05	0	0.33	0.09	0.05	0
V2O5	0	0	0	0	0	0.16	0	0.08	0.15	0	0.01
Cr2O3	0.07	0.46	0	0.1	0.06	0	0	0	0	0.07	0
MnO	0	0.30	0	0	0.07	0	0	0.06	0.05	0	0.02
FeO	0	0	0	0	0	0.09	0	0	0	0	0.06
NiO	0.03	0	0	0.02	0	0.01	0	0	0	0.02	0.21
CuO	0.04	0.04	0	0	0	0.01	0.01	0.12	0	0.11	0.02
ZnO	0	0.10	0.03	0.03	0	0.07	0.11	0.07	0	0	0.13
Rb2O	0	0	0	0	0	0	0	1.26	0	0	0
SrO	0	0.13	0.61	0	0	0	0.25	0	0	0	0
ZrO2	0	0	0	0.07	1.7	0	0.02	0	1.58	1.19	0.25
SnO2	1.33	0.11	0	0	0.24	0.4	0	0.33	0.06	1.77	0
BaO	0	0	0.16	0.3	0	0	0.22	0.12	0	0	0
La2O3	0	0.11	0	0	0.07	0	0	0.38	0.17	0	0.3
Ce2O3	0.28	1.36	0	0	0.42	0.01	0	0.43	0.21	0.16	0
PbO	39.41	59.78	38.92	39.82	3.36	30.72	25.21	5.2	2.79	6.9	32.41

Calculated average formula of these crystals from their chemical compositions were represented in Table 5.16. Spectrum 17, 18, 19, 20, 21 and 22 was giving the chemical compositions of lead feldspars formed at glaze body interface. According to the results lead-feldspar crystals had the general chemical formula of $(K_a, Na_b, Pb_c)Al_xSi_yO_8$.

Table 5.16. Formula of the crystals obtained at interface

	Spectrum 12	Spectrum 13	Spectrum 14	Spectrum 15	Spectrum 16	Spectrum 17	Spectrum 18	Spectrum 19	Spectrum 20	Spectrum 21	Spectrum 22
O	0.88	0.43	0.91	0.88	8	8	8	8	8	8	8
Al	0.26	0.08	0.26	0.25	2.96	1.73	3.02	3.20	3.29	2.46	2.46
Si	0.46	0.21	0.49	0.47	4.23	4.84	4.15	4.04	4.01	4.67	4.35
Ca	0.01	0.01	0.01	0.01	0.00	0.00	0.01	0.00	0.00	0.00	0.00
Pb	1.00	1.00	1.00	1.00	0.53	6.28	4.83	0.85	0.44	1.12	6.72
Na	0.03	0.00	0.02	0.04	0.44	0.60	0.36	0.79	0.56	0.54	0.26
K	0.03	0.01	0.02	0.02	0.34	0.24	0.10	0.07	0.04	0.22	0.07

Feldspars are the group of aluminosilicate minerals, contain Na, Ca, K and Ba. The general chemical Formula of feldspar is $M[(Al, Si)_4O_8]$, M is alkali or alkali earth metal ions of large radius 0.09-0.15 nm, Na^+ , K^+ , Ca^{2+} , Ba^{2+} and other trace elements such as Li^+ , Rb^+ , Sr^{2+} and Pb^{2+} (Rui et.al. 2006).

Feldspars classified into two groups; alkali feldspars and plagioclase feldspars. Alkali feldspars include sanidine, microcline, orthoclase and anorthoclase. Plagioclase feldspars include the members of albite-anorthite solid solution series.

5.2. Production and Characterization of Replicate Samples with SiO_2 Body

In this part of thesis the body part of the replicate samples was produced from pure SiO_2 (761-Kalemaden) and the glaze part was produced from PbO (IRON Kimya). Body part was heat treated at 1600 °C. Pellet was prepared, with diameter of 8mm, from the PbO and left on surface of body part. Sample was heat treated at 900°C for 20 minutes. In order to determine the interaction between body and glaze parts, cross sections of samples were cut, polished and characterized by SEM-EDX analysis. Results are given in Figure 5.3- 5.4.

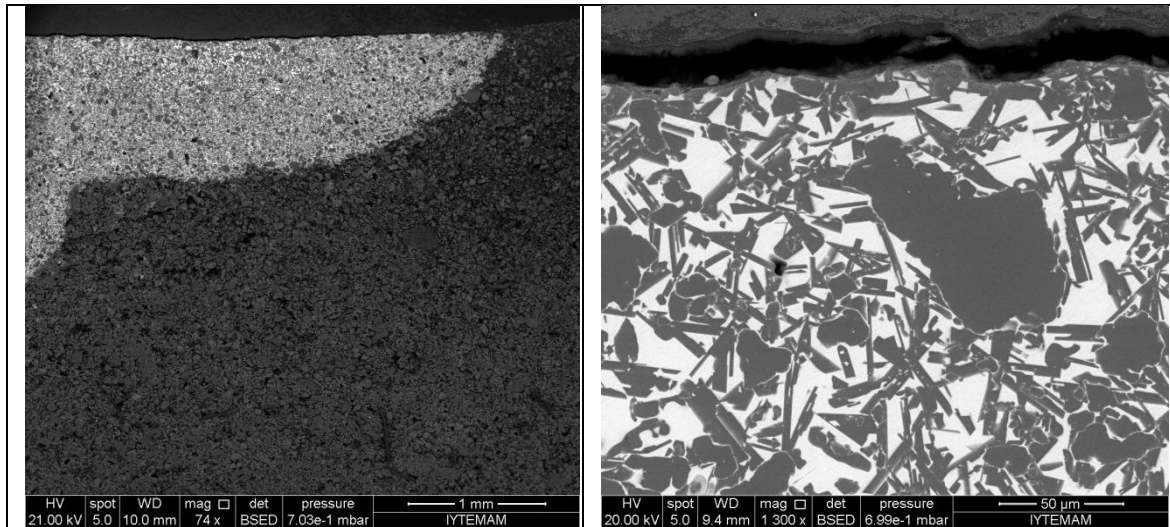


Figure 5.3. SEM analysis results of sample at different magnifications

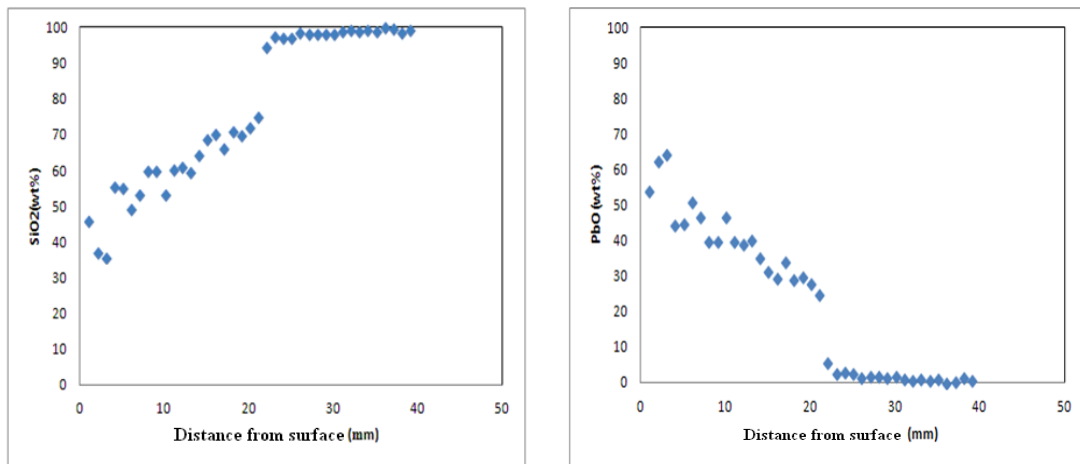


Figure 5.4. Line EDX analysis result of sample from glaze part(top) to body part(bottom)

Considering the SEM analysis result, the rate of reaction between body and glaze part was different from the archaeological samples or replicate samples produced from clay body and heat treated at same or higher temperatures. Amount of crystals produced at body glaze interface was very high. Crystals were reached to surface of glaze layer, which could not be obtained for the archaeological samples or replicate samples. This could be the result of usage of pure SiO₂ for body structure, reaction was increased therefore the amount of crystals were increased.

The distribution of elements in the structure determined by Mapping Method, is given in Figure 5.5. According to the results body part had high amount of Si element and glaze part had high amount of Pb element in their structure. SiO₂ body and PbO

glaze interaction was caused the formation of crystallites at interface. Diffusion of Si and Pb elements could be seen clearly in the glaze and the body parts due to the color change in photograph. This reaction continues until the achievement of equilibrium between body and glaze parts.

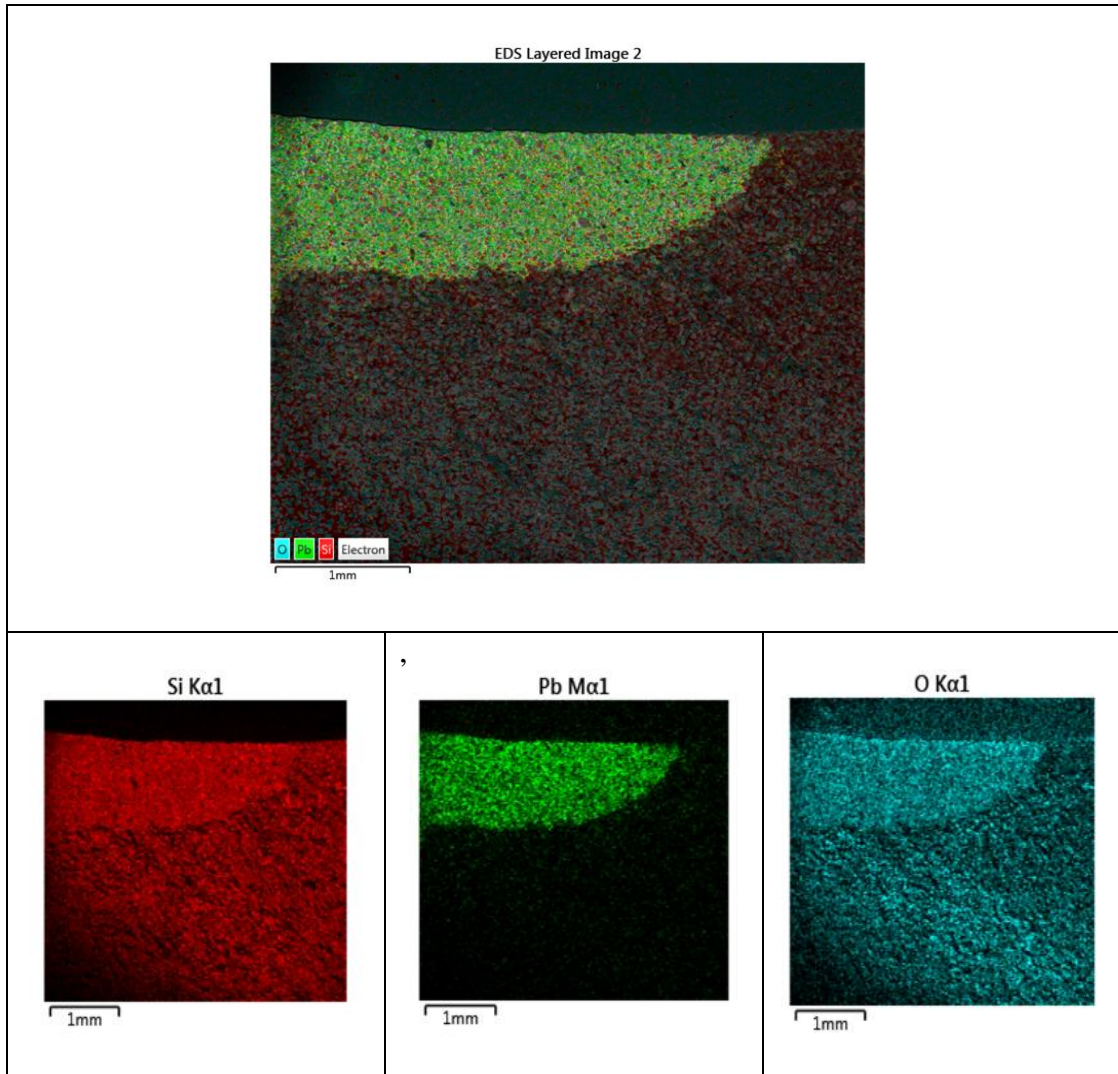


Figure 5.5. Mapping analysis results of sample heat treated at 1600°C

As it can be seen from the SEM analysis results interaction between body and glaze part was very high, crystals produced at interaction area were reached to surface of the glaze. Chemical compositions of crystals obtained at interaction zone are given in Figure 5.6.

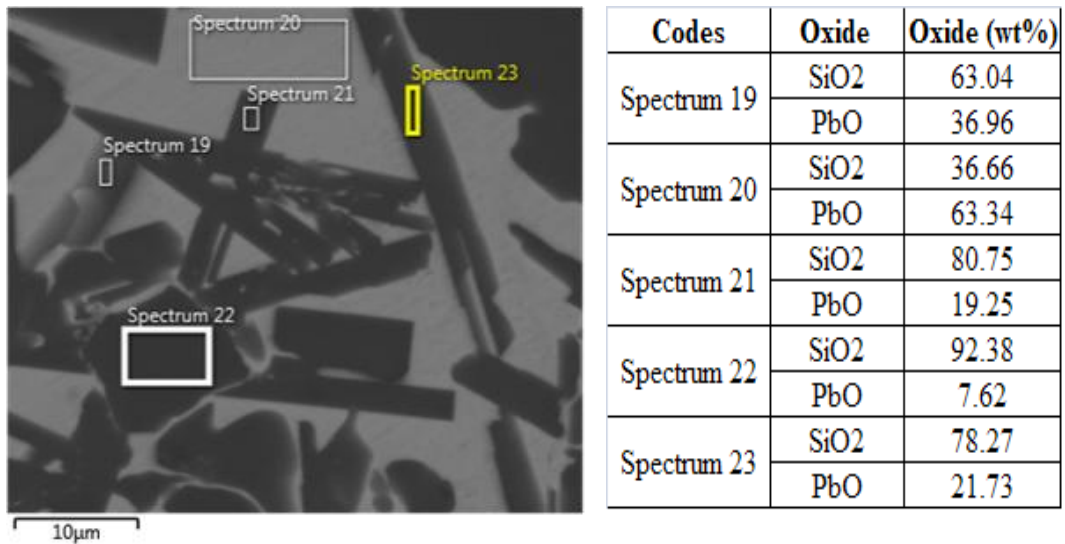


Figure 5.6. Chemical compositions of crystal determined by EDX analysis

Due to usage of pure SiO₂ body the crystals were in PbO-SiO₂ structure, different from the crystals produced between clay body and lead glaze. Dark areas had higher content of SiO₂ and lighter areas had higher content of PbO. Crystals close to body part had higher content of SiO₂ lower content of PbO in its structure.

CHAPTER 6

GENERAL INTERPRETATION and DISCUSSION

Characterization of pottery samples provides identification of their types and their classification. Raw materials used in production of potteries are chemical footprints which provide information about the provenance area (Gliozzo et al. 2008, Zuckerman et al. 2010). In this study 47 samples collected from Anaia with different decoration style, were characterized by different methods. Sample collection from the excavation site was done by Prof.Dr.Zeynep Mercangöz and sample classification based on visual characteristics was performed by Assoc.Prof.Dr. Lale Doğer, both of Ege University. All samples were red earthenware ceramics, covered with slip and lead glaze layers. These samples were characterized by Optical microscopy (OM), X-Ray diffraction (XRD), Scanning Electron Microscope (SEM-EDX) and X-Ray Fluorescence (XRF) methods. Optical microscopy analysis was used only in the determination of the thicknesses of the glaze and slip layers.

Mineralogical composition of the samples were determined by X-Ray Diffraction (XRD) method. Samples were composed of quartz, albite, muscovite, diopside, wollastonite, gehlenite and other less abundant minerals. Mineralogical properties of the raw materials, tempers, and newly formed minerals during heat treatment process affects the mineralogical composition of samples (Ortega et al. 2010). Endothermic and exothermic reactions which take place during heating depend on the firing temperature, soaking time, kiln atmosphere, particle size, chemistry and mineralogical properties of raw materials (Riccardi et al.1999, Cultrone et al.2011). Minerals determined in the structure are indicators of the temperature ranges reached during the firing process. Mineralogical composition of Anaia samples are compared with mineralogical composition of archaeological samples from those in literature for other samples (Cultrone et al. 2001, Maritan et al. 2005, Maritan et al. 2006, Jordan et al. 2009, Trindade et al. 2009, Tschegg et al. 2009). Samples were composed mainly of clay, during the firing process clay decomposes and produces new mineralogical phases. Considering the mineralogical composition of samples, firing temperature reached for these samples could be in the range of 800-900°C.

Chemical and microstructural properties of the body, slip and glaze layers of Anaia samples are determined by Scanning Electron Microscope (SEM-EDX) method. Body and slip layers are composed mainly from silica and alumina, however glaze part of samples have high amount of lead oxide. Considering the body and slip layers, silica content decreases, aluminum oxide increases from body to slip layer. This variation can be related with the removal of coarse quartz particles and the concentration of fine clay minerals during clay preparation which involves settling a clayey raw material suspension in large ponds and skimming the top parts which are naturally enriched by fine clay particles (Papachristodoulou et al.2010, Tite et al. 1982). Calcium and iron content also decreases from body to slip layer in order to enhance quality of slip layer and prevent from the red or black coloration (Maniatis et al. 1981, Papachristodoulou et al.2010, Mirti and David 2001). Glaze layer of Anaia samples are composed of high amount of lead oxide (37-56%wt). Therefore, they are classified as high lead glazes (Pace et al.2008). Glaze layer also includes important amount of aluminum oxide (~7%wt). Source of aluminum oxide is very important, it can diffuse from the slip part during firing or can be added to glaze in the form of clay (Tite et al. 1998, Molera et al. 1997). Aluminum oxide has important effect on viscosity and strength of glaze layer (Saad 2002). Lead glazes can be produced from lead oxide or mixture of lead oxide and silica (Tite et al.1998, Walton and Tite 2010). Which of these methods are used in the production of lead glaze can be determined by usage of equation explained in the study of Hurst and Freestone (1996). According to this classification all Anaia samples were covered with glaze layer that contained only lead oxide. This is very important information about the production procedure used in Anaia. Copper oxide and iron oxide were determined in the glaze layer of all samples. These oxides are colorants, green color of glazes are related with presence of Cu^{+2} or Fe^{+2} in the structure, although yellow to brown colors are related with Fe^{+3} oxides and complexes (Molera et al.1999, Molera et al. 1997, Hatcher et al.1994).

In scanning electron microscope (SEM) analysis by BSE images, an interaction layer was determined between the body and the glaze layers in all samples with variable thicknesses. During the heat treatment process glaze melts and lead in glaze reacts with clay minerals in the slip and the body layers. These minerals diffuse into the glaze layer and lead oxide diffuses into the ceramic body by counterdiffusion. New lead feldspar crystals precipitate along the interface between the slip and the glaze (Molera et al. 2001).

Chemical composition of pottery samples are strongly affected by the source of clay and other materials used in their production. Trace element concentrations reflect the geological variety of pottery samples (Hein et al. 2004, Padilla et al. 2006). In order to determine major and minor element compositions body part of pottery samples are characterized by X-Ray Fluorescence (XRF) Analysis. Body part of samples are composed mainly from silica and alumina. Alkalis have moderate concentration. During firing process alkalis can act as fluxes and can support the vitrification and sintering (Mirti and David 2001). Clays can be classified according to their CaO concentration. Clays containing CaO higher than 6%wt are classified as calcareous clays (Maniatis and Tite 1981). According to XRF results, calcareous and non-calcareous clays are used in the production of Anaia samples. Also decoration type was found to have no effect on the usage of calcareous clay in the production of these samples. XRF analysis results were used in the statistical treatment of these samples.

Samples were grouped with application of Hierarchical Cluster Analysis and Principal Component Analysis. Hierarchical Cluster Analysis results are represented in dendrograms that shows the relationship between samples. The resulting dendrogram structure in this study was, however, quite complex, in which samples with different decoration types were grouped in one cluster. These samples were expected to share different origins considering the visual examination. Also clay used in their production might have been collected from different sources or might be produced by mixture of different clays. Small differences were obtained between the samples.

Dendrograms generated via the software using Wards method showed that the ceramic samples collected from Anaia could be grouped into two categories A and B according to the chemical composition of the body. The group B consisted of three ceramic samples all glazed with sgraffito decoration. One of these samples was Champlévé and the other two were incised sgraffito. Interestingly, all these three samples had high alumina, iron oxide and potassium oxide percentage and comparatively low percentage of silica. The conclusion was that these three were very closely matched in their body compositions, possibly the same clay type or raw material mixture was used in their manufacture as they contained significantly higher amount of alumina. According to Dendrogram results Anaia samples can be product of two different workshops or a big workshop with large scale production, using two different clay sources.

The dendrograms generated for data in this study and in the study by Waksman et.al. was performed in order to compare the two studies to see if similarities could be identified. The results indicated that there was some minor similarity between the two groups of samples. But the degree of similarity was not decisive enough to make strong conclusions.

Principal component analysis was the second method used for determination of grouping pattern of samples. First two principal components described most of the total variance. They were used in the description of provenance of samples (Zhu et al. 2004). According to the results body part of all groups had similar Al_2O_3 and SiO_2 in their structure except the samples of Group 3. This group could be produced by clays from different source or different recipe could be used in production of this group. Slip compositions of samples were similar. Slip layer used in the production of these samples could be produced by clays from similar sources. Glaze layer of Anaia samples had high amount of lead in their structure. Groups had samples with different decoration types. Group 3 had a high amount of copper oxide, this could be the result of the application of different production recipe for this group, or this group could be the product of a different workshop.

Replicate samples were produced in order to determine the effect of firing temperature, glaze composition, cooling rate and firing duration on the microstructure of the samples. Three different types of glaze were applied on the clay body. Firing was done at different temperatures, with different soak time and cooling rates. Use of only lead oxide glaze increased the reaction rate and thickness of the interaction layer. Addition of SiO_2 or clay to lead glaze had negative effect on thickness of the interaction layer, because alumina from the clay acts as stabilizer and reduces the diffusion of elements. Increment of firing temperatures and application of slow cooling had positive effect on thickness of the interaction layer and the size of crystals. Usage of raw body instead of heat treated ones increased the degree of reaction between body and glaze, caused the formation of thicker interaction layer. In addition to these experiments, reaction between lead glaze and SiO_2 was also tested. Because of the porosity of the relatively pure silica pellet significant diffusion of lead from the glaze and almost complete invasion of the substrate silica pellet was observed. Abundant amount of the crystals of lead silicate were formed. As a conclusion production of crystals at the body-glaze interface depends on different factors. Under controlled conditions samples can be compared according to the properties of the interface layer.

CHAPTER 7

CONCLUSIONS

Pottery samples collected from Anaia were analyzed by different analytical techniques. Samples were analyzed to identify three distinct layers in cross sections: body, slip and glaze layers. Body was largely composed of SiO_2 , Al_2O_3 , CaO , Fe_2O_3 , Na_2O and K_2O along with other less abundant elements. Slip had similar chemistry but with less Fe_2O_3 due to the necessity to keep the color less red and more white to provide the proper background for sgraffito decoration which reveals the body layer during scratching with tools. The glaze was largely composed of lead oxide. It was found that no other additive was used in glaze formulation. Occasional pores were observed in the glaze layer. Between the glaze and the slip some new well formed crystals of lead feldspar were found to precipitate in dimensions of roughly 10-50 μm . There was nothing surprising in the body microstructure which contained large quartz particles, some feldspar minerals and lots of porosity. Replicate samples of earthenware pottery were manufactured in the laboratory using traditional clay and analytical grade lead oxide to mimic the formation of the pottery. Similar microstructural features were identified in these samples as well. Statistical analysis tools like HCA and PCA were used to see if any groupings were possible between the samples collected based on their chemical analysis. Dendrograms generated via HCA indicated a three sample group (samples 1.1.1., 1.2.2. and 1.2.3) which had similar body compositions leading to the conclusion that they were probably made from the same raw material. All other samples appeared to be made from a different clay. Therefore, most of these ceramics were made from one type of clay and a lesser fraction of these samples were made from another type of clay. Whether these may have been produced in the same shop is not in the scope of this thesis. Another HCA study was done to compare the data in this study with the data in Waksman's study in the literature. Dendrograms obtained showed some similarity. However, it was not possible to strongly and conclusively say that the two sample groups were related.

REFERENCES

- Armstrong, P. (1989). "Some byzantine and later settlements in eastern phokis" *The Annual of British School at Athens*, 84, 1-47
- Armstrong, P. 1991, "A group of byzantine bowls from skopelos", *Oxford Journal of Archaeology*, 10, 335-347
- Armstrong, P., Hatcher, H., 1997, "Byzantine and allied pottery, Phase 2", in book *Materials Analysis of Byzantine Pottery* edited by Henry Maguire, Dumbarton Oaks Research Library and Collection, Washington
- Armstrong, P., Hatcher H., Tite M., 1997b, "Changes in byzantine glazing technology from 9th to 13th centuries". In G. d'Archimbad (Ed) *LA Ceramique Medievale en Mediterranee*, Actes du 6e Congres de l'AICEM2, Aix-en-Provence
- Barone G., Lo Giudice A., Mazzoleni P., Pezzino A., Barilaro D., Crupi V., Triscari M., 2005, "Chemical characterization and statistical multivariate analysis of ancient pottery from messina", Catani, Lentini and Siracusa (Sicily), *Archaeometry* 47 (4), 745-762
- Baxter, M.J, 1994, "Exploratory multivariate analysis in archaeology", Edinburgh University
- Benedetto G.E. De, Laviano R., Sabbatini L., Zambonin P.G, 2002, "Infrared spectroscopy in the mineralogical characterization of ancient pottery", *Journal of Cultural Heritage*, 3 (3), 177-186
- Benedetto G.E, Fabbri B., Gualtieri S., Sabbatini L., Zambonin P.G., 2005, "FTIR-chemometric tools as aids for data reduction and classification of pre-Roman ceramics", *Journal of Cultural Heritage*, 6, 205-211
- Benedetto G.E, Acquafredda P., Masieri M, Quarta G., Sabbatini L., Zambonin P.G, Tite M., Walton M., 2004, "Investigation on roman lead glaze from canosa: results of chemical analyses" *Archaeometry*, 46 (4), 615-624
- Borisov, B.D., 1989, "Mediaeval settlement and necropolis (11th-12th century)" Djadova 1, Tokai University Press
- Bower N.W., Bromund R.H. and Smith R.H., 1975, "Atomic absorption for the archaeologist: an application to pottery from pella of the decapolis", *Journal of Field Archaeology*, 2 (4), 389-398
- Böhlendorf-Arslan, B., 2004, "Glasierte byzantinische keramik aus der türkei teil.III", İstanbul

- Buxeda J and Garrigós, I, 1999, "Alteration and contamination of archaeological ceramics: the perturbation problem", *Journal of Archaeological Science*, 26 (3), 295–313
- Buxeda J., Garrigós I, Kilikoglou V., Day P. M., 2001, "Chemical and mineralogical alteration of ceramics from A late bronze age kiln at kommos, crete: the effect on the formation of a reference group" *Archaeometry* 43 (3), 349-371
- Charalambous A.C., Skalis A.J, Kantiranis, Papadopoulou L.C., Tsirliganis N.C, Stratis J.A., 2010, "Cypriot byzantine glazed pottery: a study of paphos workshops" *Archaeometry*, 52, 628-643
- Casellato U., Fenzi F., Riccardi M.P, Osmida G.R, Vigato P.A, 2007, "Physico-chemical and mineralogical study of ceramic findings from mary city turkmenistan", *Journal of Cultural Heritage* 8, 412-422
- Chen M., 2006, "Physicochemical compositional analysis of ceramics: a case study in Kenting, Taiwan", *Archaeometry*, 48, 4, 565–580
- Daly G., 1995, "Glazes and glazing techniques", A&C Black, London
- Dark K., 2001, "Byzantine pottery", The History Press LTD
- Davoud A., Oliaiy P., Mohsenian M., Lamehi-Rachti M., Shokouhi F., 2009, "Provenance Study of Ancient Iranian Luster Pottery using PIXE Multivariate Statistical Analysis", *Journal of Cultural Heritage*, 10, 4, 487-492
- Doğer, L., 1999, "Kufi yazı taklidi motiflerle bezeli sgraffito, kazıma-sgraffito teknikli bizans seramikleri" *Antika Dekorasyon ve Sanat Dergisi*, 55,148-151
- Doğer, L., 2001, "İzmir arkeoloji müzesindeki bitkisel bezemeli sgraffito bizans kapları", *OLBA IV*: 209-223
- Doğer, L., 2007, "Byzantine ceramics:excavations at smyrna agora (1997-98 and 2002-2003)", *Çanak, BYZAS*, 7
- Doğer, L., 2010, "Kuşadası, Kadıkalesi/Anaia kazısı 2001-2007 yılı bizans ve çağdaşı diğer seramik buluntular üzerine bazı gözlemler", *Geçmişten Geleceğe Kuşadası Sempozyumu II*, Kuşadası Belediyesi Yayınları
- Doğer, L., (2012a)."Daskyleion II, hisartepe/daskyleion kazısı bizans seramikleri" Prof.Dr. Tomris Bakır'a Armağan, Ege Yayınları, İstanbul
- Eiland M.L. and Williams Q., 2001, "Investigation of islamic ceramics from tell tuneinir using x-ray diffraction", *geoarchaeology: An International Journal*, 16, 8, 875–903
- Everitt B.S., 1993, "Cluster Analysis", Hodder Education

- Farmer V.C., 1974, "The infrared spectra of minerals", Mineralogical Society Monograph 4
- Feliu, M.J. , Edreira M.C., Martin J., 2004, "Application of physical–chemical analytical techniques in the study of ancient ceramics", *Analytica Chimica Acta* 502, 241–250
- Fermo P., Delnevo E. , Lasagni M., Polla S., Vos M., 2008, "Application of chemical and chemometric analytical techniques to the study of ancient ceramics from Dougga (Tunisia)" *Microchemical Journal*, 88, 150–159
- Filho U.M.V., Latini R.M., Bellido A.V.B., Buarque A., Borges A.M., 2005, "Ancient ceramic analysis by neutron activation in association with multivariate methods" , *Brazilian Journal of Physics*, 35 (3B)
- Froh J., 2004, "Archaeological ceramics studied by scanning electron microscopy", *Hyperfine Interactions* 154, 159–176
- Gangas, N.-H.J., Sigalas, I., Moukarika, A., 1976. "Is the history of an ancient pottery ware correlated with its Mössbauer spectrum?", *Journal de Physique Colloque* C6,867-871
- Gebhard R., 2003, "Material Analysis in Archaeology", *Hyperfine Interactions*,150, 1-5
- Gliozzo, E., Vivacqua P., Memmi I.T, 2008, "Integrating archaeology, archaeometry and geology: local production technology and imports at Paola (Cosenza, Southern Italy), 35, 1074-1089
- González-García, Maniatis, Y., Simopoulos, A., Kostikas, A., 1981, " Moessbauer study of the effect of calcium content on iron oxide transformations in fired clays", *Journal of the American Ceramic Society* 64, 263-269
- Grifa C., Morra V., Langella A., Munzi P., 2009, "Byzantine ceramic production from cuma", *Archaeometry*, Volume 51, Number 1, 75-94
- Grimshaw, R.W., 1971, "Reactions at high temperatures, the chemistry and physics of Clays", Techbooks, India, 727
- Hall M., Maeda U., Hudson, M., 2002, 44, 213
- Hatcher H., Kaczmarczyk, A., Scherer, A., and Symonds, R. P., 1994, "Chemical classification and provenance of some Roman glazed ceramics", *American Journal of Archaeology*, 98, 431–56
- Hayes, J.W., 1992, "Excavations at saraçhane in istanbul, Volume 2, the pottery", Princeton University Press
- Heimann B.R., Magetti, M., "Experiments on Simulated Burial of Calcareous Terra Sigillata (Mineralogical Change) Preliminary Results, *British Museum Occasional Papers* No.19, *Scientific Studies in Ancient Ceramics* (ed. M.J. Hughes) 163-77

- Hein A., Kilikoglou V., 2007, "Modeling of Thermal Behavior of Ancient Metallurgical Ceramics", *J. Am. Ceram. Soc.*, 90 (3) 878–884
- Hein A., Müller N.S., Day P.M., Kilikoglou V., 2008 "Thermal conductivity of archaeological ceramics: The effect of inclusions, porosity and firing temperature", *Thermochimica Acta* 480, 35–42
- Hein A., Day P.M., Quinn P.S., Kilikoglou V., 2004, "The geochemical diversity of Neogene clay deposits in Crete and its implications for provenance studies of Minoan pottery", *Archaeometry*, 46 (3), 7–384
- Henderson J., 2000, "The Science and Archaeology of Materials", Routledge, London and New York
- Hill D.V, 2004, "Chemical and mineralogical characterization of sasanian and early islamic glazed ceramics from the deh luran plain, south-western iran", *Archaeometry* 46 (4), 585–605
- Ion R.M, Ion M.L., Fierascu R.C., Serban S., Dumitriu I., Radovici C., Bauman I., Cosulet S., Niculescu V.I.R., 2009, "Thermal analysis of romanian ancient ceramics", *J Therm Anal. Calorim.*
- Isphording W.C., 1974, "Combined thermal and x-ray diffraction technique for identification of ceramic ware temper and paste minerals" *American Antiquity*, 39 (3), 477-483
- İssi A., Kara A., Alp A.O., 2011, "An investigation of hellenistic period pottery production technology from harabebezikan/turkey", *Ceramics International*, 37 (7), 2575–2582
- Johnson W., Richard A. and Dean W., 1992, "Applied multivariate statistical analysis 3rd edition", Prentice Hall International Editions
- Jordan M.M., Martin-Martin J.D., Sanfeliu T., Gomez-Gras D, De La Fuente C., 2009, "Mineralogy and firing transformation of permo-triassic clays used in the manufacturing of ceramic tile bodies", *Applied Clay Science*, 44, 173-7
- Kilikoglou V., Grimanis P., Vassilaki-Grimani M., Grimanis A.P., 1991, "Comparison between two INAA methods applied to chemical characterization of ancient ceramics", *Journal of Radioanalytical and Nuclear Chemistry*, 152 (2), 469-477
- Kingery, W.D and Vandiver P.B., 1986, "Ceramic masterpieces, art, structure and technology", the Free Press, Division of Macmillan, Inc, Newyork
- Kingery W.D., Bowen H.K., Uhlman D.R., 1976, "Introduction to ceramics", Wiley Interscience
- Köroğlu, G., 2004, "Yumuktepe in the middle ages, mersin yumuktepe: a reappraisal", 103-132

- Krzanowski, W.J., 1993, "Principles of multivariate analysis, a user's perspective", Oxford Science Publications
- Lemerle Paul, 2004, "Bizans tarihi", İletişim Yayınları, İstanbul
- Lahlil S., Bouquillon A., Morin G., Galois L., and Lorre C., 2008, "Relationship between the coloration and the firing technology used to produce susa glazed ceramics of the end of the neolithic Period", *Archaeometry*, 50
- Maltoni S., Alberta S., Maritan L., Gianmario M., 2012, "The medieval lead-glazed pottery from Nogara(north-east Italy): multimethodological study", *Journal of Archaeological Science*, 39 (7), 2071-2078
- Maniatis Y., Tite M.S, 1981, "Technological examination of neolithic-bronze age pottery from central and southeast Europe and from near east", *J.Archaeol.Sci.*, 59-76
- Maniatis, Y., Simopoulos, A., Kostikas, A., Perdikatsis, V., 1983, "Effect of reducing atmosphere on minerals and iron oxides developed in fired clays: the role of Ca.", *Journal of the American Ceramic Society* 66, 773-781
- Maniatis Y., Simopoulos A., Kostikas A., 1981, "Moessbauer study of the effect of calcium content on iron oxide transformations in fired clays" *Journal of the American Ceramic Society*, 64, 263–269
- Maritan, L., C. Mazzoli, V. Michielin, D. M. Bonacossi, M. Luciani, and G. Molin, 2005, "The provenance and production technology of bronze age and iron age pottery from tell mishrifeh/qatna (syria)." *Archaeometry*, 47, 723-44
- Maritan L., Mazzoli C., Nodari L., Russo U., 2005, "Second iron age grey pottery Este (northeastern Italy): study of provenance and technology", *Applied Clay Science*, 29, 31-44
- Maritan L., Nodari L., Mazzoli C., Milano A., Russo U, 2006, "Influence of firing conditions on ceramic products: experimental study on clay rich in organic matter", *Applied Clay Science*, 31, 1-15
- McHale, A.E. 1994, "Phase equilibria diagrams: phase diagrams for ceramists", Westerville, Ohio: The American Ceramic Society
- McHale A., 1998, "Phase diagrams and ceramic processes", New York, Chapman&Hall
- Mercangöz Z., Doğer L., 2009, "Kuşadası, kadıkalesi/anaia bizans sırlı seramikleri", I. ODTÜ Arkeometri Çalıştay-Türkiye Arkeolojisi'nde Seramik ve Arkeometrik Çalışmaları-Prof. Dr. Ufuk Esin Anısına 7-9 Mayıs 2009, Ankara, 83-101
- Mirti P., Aceto M., Ancona M.C.P., 1998, "Campanian pottery from ancient bruttium (southern italy): scientific analysis of local and imported products", *Archaeometry*, 40, 2, 311-329

- Mirti P., Davit P., 2001, "Technological characterization of campanian pottery of type A, B and C and of regional products from ancient calabria (southern italy)" *Archaeometry*, 43 (1), pp. 19–33
- Molera J., Vendrell-Saz M., Garcia-Vallés M., Pradell T., 1997, "Technology and color development of hispano-moresque lead glazed pottery", *Archaeometry*, 39, 23–39
- Molera J., Pradell T., Vendrell-Saz M., 1998, "The colours of Ca-rich ceramic pastes: origin and characterization" *Applied Clay Science*, 13 (1998), 187–202
- Moropoulou A., Bakolas A., Bisbikou K., 1995, "Thermal analysis as a method of characterizing ancient ceramic technologies", *Thermochimica Acta* 2570, 743-753
- Moroni B., Conti C., 2006, "Technological features of renaissance pottery from deruta (umbria, italy): an experimental study", *Applied Clay Science*, 33, 230-246
- Morgan, H., 1942, "Corinth XI: the byzantine pottery", Cambridge
- Neff, H., 1994, "Rq-mode principal components analysis of ceramic compositional data", *Archaeometry* 36, 115
- Neff H., Bishop R.L., Sayre E.V., 1988, "A simulation approach to the problem of tempering in compositional studies of archaeological ceramics" *Journal of Archeological Science*, 15, 159
- Nodari L., Marcuz E., Maritan L., Mazzoli C., Russo U., 2007, "Hematite nucleation and growth in the firing of carbonate-rich clay for pottery production", *Journal of European Ceramic society*, 27, 4665-4673
- Ortega L.A., Zuluaga M.C., Alonso-Olazabal A., Murelaga X., Alday A., 2010, "Petrographic and geochemical evidence for long-standing supply of raw materials in Neolithic pottery (Mendandia Site, Spain)", *Archaeometry*, 52-6, 987-1001
- Pace M., Prevot A.B, Mirti P., Ricciardi R.V., 2008, "The technology of production of sasanian glazed pottery from Veh ardasir (central Iraq)" *Archaeometry*, 50, 591-605
- Padilla R., Van Espen P., Torres P.P.G, 2006, "The suitability of XRF analysis for compositional classification of archaeological ceramic fabric: a comparison with a previous NAA study", *Anal Chim Acta*, 558, 283–289
- Papachristodoulou C., Oikonomou A., Ioannides K., Gravani K., 2006, "A study of ancient pottery by means of X-ray fluorescence spectroscopy, multivariate statistics and mineralogical analysis", *Analytica Chimica Acta*, 573
- Papadopoulou D. N., Lalia-Kantouri M., Kantiranis N. and Stratis J. A., 2006, "Thermal and mineralogical contribution to the ancient ceramics and natural clays characterization", *Journal of Thermal Analysis and Calorimetry*, Vol. 84, 1, 39–45

- Papachristodoulou C., Gravani K., Oikonomou A., Ioannides K., 2010, "On the provenance and manufacture of red-slipped fine ware from ancient Cassope (NW Greece): evidence by X-ray analytical methods", *Journal of Archaeological Science*, 37 (9), 2146–2154
- Papanikola-Bakirtzi D, 1999, "Byzantine glazed ceramics, the art of sgraffito", *Archaeological Receipts Fund*, Athens
- Parman, E., (1989)." The pottery from st.john's basilica at ephesos" *BCH Suppl. XVIII: 277-289*
- Pillay A.E., Punyadeera C., Jacobson L. and Eriksen J., 2000, "Analysis of ancient pottery and ceramic objects using x-ray fluorescence spectrometry", *X-Ray Spectrom.* 29, 53–62
- Padilla R., Espen P.V, Torres P.P.G, 2006, "The suitability of xrf analysis for compositional classification of archaeological ceramic fabric: A comparison with a previous NAA study", *Analytica Chimica Acta* 558, 283–289
- Peduto, P., (1993)."Ceramica bizantina dalla campania" in S.Gelichi, *La ceramica nel mondo bizantino tra XI e XV secolo e i suoi rapporti con l'Italia*, *Atti del Seminario (certosa di Pontignano 1991)*, Firenze: 93-99
- Pollard M.A, Heron C., 2008, "Archaeological chemistry (RSC paperbacks)", *Royal Society of Chemistry, United Kingdom*
- Rathossi C, Tsolis-Katagas P., Katagas C., 2004, "Technology and composition of Roman pottery in northwestern peloponnese, greece", *Applied Clay Science* Volume 24, Issues 3-4, Pages 313-326
- Ramos S.S, Reig F.B, Adelantado J. V. G, Marco D. J. Y, Carbó A. D, 2002, "Application of XRF, XRD, thermal analysis, and voltammetric techniques to the study of ancient ceramics", *Anal Bioanal Chem* 373, 893–900
- Rhodes D., 1973, "Clay and Glazes for the Potter", *Chilton Book Company, Radnor, Pennsylvania*
- Rice, P.M., 1987, "Pottery Analysis", *The University of Chicago Press/Chicago and London*
- Riccardi M.P., Messiga B., Duminuco P., 1999, "An approach to the dynamics of clay firing", *Applied Clay Science*, 15, 393–409
- Riederer J., 2004, "Thin section microscopy applied to the study of archaeological ceramics" *Hyperfine Interact*, 154, 143–158
- Roberts J.P.,1963, "Determination of the firing temperature of ancient ceramics by measurement of thermal expansion", *Archaeometry* 6, 21–25

- Saad Z., 2002, "Chemical composition and manufacturing technology of collection of various types of islamic glazes excavated from jordan", *Journal of Archaeological Science*, 29, 803-810
- Sanders G.D.R., 1993, "Excavations at sparta:the roman stoa, 1988-91, preliminary report, part 1" *BSA* 88: 251-286
- Sciau P., Goudeau P., Tamura N., Dooryhee E., 2006, "Micro scanning x-ray diffraction study of gallo-roman terra sigillata ceramics", *Appl. Phys. A* 83, 219–224
- Scott J.A., Kamilli D., 1976, "Late byzantine glazed pottery from sardis", in *Actes du XVe Congrès international d'études byzantines*, Athènes, Vol. 2, 679-96
- Sena E.De., Landsberger S., Pena J.T., Wisseman S., 1995, "Analysis of ancient pottery from the palatine hill in rome", *Journal of Radioanalytical and Nuclear Chemistry*, 196, 2, 223-234
- Shenan Stephan, 1997, "Quantifying archaeology", University of Iowa Press, Iowa City
- Shoval S., Beck P., 2005, "Thermo-ftir spectroscopy analysis as a method of characterizing ancient ceramic technology", *Journal of Thermal Analysis and Calorimetry*, Vol. 82, 609–616
- Shepard, A.O., 1956, "Ceramics for the archaeologist", Carnegie Institute of Washington, Washington
- Siouris M.I, Walter J., 2006, "A neutron diffraction study of ancient greek ceramics", *Physica B* 385-386, 225–227
- Sterba J.H., Mommsen H., Steinhauser G., M.Bichler, 2009, "The influence of different tempers on the composition of pottery", *J.Archaeol.Sci.* 36, 1582-1589
- Tanevska V., Colomban P., Minčeva-Šukarova B., Grupče O., 2009, "Characterization of pottery from the Republic of Macedonia I: Raman analyses of Byzantine glazed pottery excavated from Prilep and Skopje (12th-14th century)", *Journal of Raman Spectroscopy*, 40(9), 1240-1248
- Technical Bulletin 1985-1E, *Infrared spectra of minerals, Reference guide to identification and characterization of minerals for the study of soils*, Canada
- Tiequan Z., Changsui W., Hongmin W., Zhenwei M., 2010, "The preliminary study on kiln identification of chinese ancient qingbai wares by ICP-AES", *Journal of Cultural Heritage*, 11, 4
- Tite M. S., Bimson M., and Freestone I. C., 1982, "An examination of the high gloss surface finishes on Greek Attic and Roman Samian wares", *Archaeometry*, 24, 117-26

- Tite M. S., Freestone, I., Mason, R., Molera, J., Vendrell-Saz, M., and Wood, N., 1998, "Lead glazes in antiquity-methods of production and reasons for use", *Archaeometry*, 40, 241–60
- Tite M.S., 1999, "Pottery Production, Distribution and Consumption-The contribution of Physical Science", *Journal of Archaeological Method and Theory*, 6 (3)
- Tite M.S., Kilikoglou V., Vekinis G., 2001, "Review article: strength, toughness and thermal shock resistance of ancient ceramics, and their influence on technological choice", *Archaeometry*, 43, 301-324
- Traoré K., Kabré T.S., Blanchart P., 2000, "Low temperature sintering of a pottery clay from Burkina Faso" *Applied Clay Science*, 17, 279–292
- Trezza M.A., Lavat A.E., 2001, "Analysis of the system $3\text{CaO}\cdot\text{Al}_2\text{O}_3\text{-CaSO}_4\cdot 2\text{H}_2\text{O}\text{-CaCO}_3\text{-H}_2\text{O}$ by FT-IR spectroscopy", *Cement and Concrete Research*, 31, 869-872
- Trindade M.J ., Dias M.I., Coroado J., Rocha F., 2009, "Mineralogical transformation of calcareous rich clays with firing: a comparative study between calcite and dolomite rich clays from Algarve, Portugal", *Applied Clay Science*, 42, 345-55
- Troja S.O, Cro A., Gueli M.A, Rosa V. La, Mazzoleni P., Pezzino A., Romeo M., 1996, "Characterization and thermoluminescence dating of prehistoric pottery sherds from milena", *Archaeometry*, 38, 1, 113-128
- Tschegg C., Ntaflos T, Hein I., 2009, "Thermally triggered two-stage reaction of carbonate and clay during ceramic firing- a case study on Bronze Age Cypriot ceramics", *Applied Clay Science*, 43, 69-78
- Tsolakidou A. and Kilikoglou V., 2002, "Comparative analysis of ancient ceramics by neutron activation analysis, inductively coupled plasma–optical-emission spectrometry, inductively coupled plasma–mass spectrometry, and X-ray fluorescence", *Anal Bioanal Chem* 374, 566–572
- Velde B., 1992, "Introduction to clay minerals", Chapman and Hall, London
- Velde B. and Druc, I.C., 1999, "Archaeological ceramics", Springer, Germany
- Wagner U., Wagner F.E., Häusler W., Shimada I., 2000, "The use of mössbauer spectroscopy in studies of archaeological ceramics", *Radiation in Art and Archeometry*, 417-443
- Wagner, F.E.,Wagner, U., 2004, "Moessbauer spectra of clays and ceramics", *Hyperfine Interactions*, 154, 35-82
- Waksman S.Y., Rossini I., Heitz C., 1994, " Byzantine pergamon: characterization of the ceramics production center", in *Proceedings of the 29th International Symposium on Archaeometry (Ankara, Turkey, May 9–14, 1994)*. METU Press, Ankara , Turkey, 209-218

- Waksman S.Y. and Spieser J.M., 1997, "Byzantine ceramics excavated in pergamon: archaeological classification and characterization of the local and imported productions by PIXE and INAA elemental analysis, mineralogy and petrography, in book *Materials Analysis of Byzantine Pottery* edited by Henry Maguire", *Dumbarton Oaks Research Library and Collection, Washington*
- Waksman S.Y., Wartburg M.L., 2006, "Fine-sgraffito ware, aegean ware and other wares: new evidence for a major production of byzantine ceramics", *Report of the Department of Antiquities Cyprus, 369-89*
- Waksman S.Y. and Teslenko I., 2010, "Novy svet ware, an exceptional cargo of glazed wares from a 13th-Century Shipwreck near sudak (Crimea, Ukraine)-morphological typology and laboratory investigations", *The International Journal of Nautical Archaeology, 39.2:357-375*
- Walton M.S, Tite M.S, 2010, "Production technology of roman lead glazed pottery and its continuance into late antiquity", *Archaeometry, 52,5,733-759*
- Yenişehirlioğlu, F., 1989, "La céramique glaçurée de gülpınar", *BCH Suppl. XVIII: 303-315*
- Zhang Z.Q, Cheng H.S, Xia H.N., Jiang J.C., Gao M.H., Yang F.J., 2002, "Trace element measurement by PIXE in the appraisal of ancient potteries", *Nuclear Instruments and Methods in Physics Research Section B: Beam Interactions with Materials And Atoms, Volume 190, Issue 1-4, 497-500*
- Zhu, J, Shan J., Qiu P., Qin Y., Wang C., He D., Sun B., Tong P., and Wu S., 2004, "The multivariate statistical analysis and xrd analysis of pottery at xigongqiao site." *Journal of Archaeological Science 31, 12, 1685-91*
- Zuckerman S., Ben-Shlomo D., Mountjoy P.A, Mommsen H., 2010, "A provenance study of mycenaean pottery from northern israel", *Journal of Archaeological Science, 37, 409-416*
- якобсон, А.Л.,(1979)." Керамика и кермическое ероизвдство средневековой таврики, ленинград"

VITA

Meral BUDAK ÜNALER

30.03.1979, İZMİR

EDUCATION

- B.Sc: (2002): Department of Chemical Engineering, Izmir Institute of Technology, Turkey.
- M.Sc: (2005): Department of Materials Science and Engineering, Izmir Institute of Technology, Turkey
- PhD: (2013): Department of Mechanical Engineering, Izmir Institute of Technology, Turkey

SELECTED PUBLICATIONS

Characterization of Middle Byzantine Ceramics from Kuşadası-Kadıkalesi/Anaia Excavation, Ulusal Kil Sempozyumu, Niğde, Eylül, 2012

Analysis of Byzantine fine sgraffito ware, incised ware and champlévé ware from Anaia, Turkey, European Meeting on Ancient Ceramics, 2013

Comparison Of Byzantine Fine Sgraffito And Incised-Sgraffito (Coarse Sgraffito) Ware From Kuşadası, Kadıkalesi/Anaia Excavation, 2013, in Book of “Byzantine Craftsmen - Latin Patrons. Reflections from the Anaian Commercial Production in the Light of the Excavations at Kadikalesi near Kuşadası”

Middle Byzantine Lead Glazed Pottery from Anaia: An Analytical Approach” Journal of Archaeological Science

SCHOLARSHIPS

Greek Ministry of Education scholarship in Technical University of Crete GREECE (6 Months)